UNIVERSITÀ
DEGLI STUDI
DI BRESCIA

DOTTORATO DI RICERCA IN INGEGNERIA MECCANICA E INDUSTRIALE

ICAR/08 Scienza delle Costruzioni

CICLO XXXIV

Finite strain chemo-thermo-electro-mechanics with applications in mechanobiology

Dottorando:
Matteo Arricca

Supervisore:
Prof. Alberto Salvadori, Università degli Studi di Brescia

Co-Supervisore:
Prof. Robert M. McMeeking, University of California, Santa Barbara

Abstract

La tesi proposta nasce da ben definite motivazioni biologiche, con lo scopo di fornire una caratterizzazione del comportamento delle cellule endoteliali nel processo di angiogenesi tumorale. Diversi framework multi-fisici vengono introdotti per applicazioni nel campo della meccanobiologia, così come in altre aree di ricerca.

L'angiogenesi è un noto processo progressivo, fisiologico o patologico, caratterizzato dalla formazione di nuovi vasi sanguigni che si originano da quelli pre-esistenti. Le cellule endoteliali, le quali rivestono le pareti interne dei vasi sanguigni, vengono influenzate da stimuli extra-cellulari rilasciati dalle cellule tumorali, e rispondono tramite rilocazione di recettori (proteine) sulla loro membrana, migrazione cellulare collettiva e riorganizzazione in nuovi vasi sanguigni. Il ruolo della dinamica recettoriale e della meccanica cellulare in risposta agli stimuli extra-cellulari è dunque oggetto di grande interesse, in quanto processi cruciali nelle fasi iniziali dell'angiogenesi. Le funzioni strutturali della cellula, le quali permettono l'avvenimento di processi ben noti come l'adesione e l'accasciamento cellulare, la motilità e la migrazione, sono attribuite alla generazione e la riorganizzazione della macchina contrattile citoscheletrica. Il citoscheletro è una rete interconnessa di proteine e polimeri filamentosi, soggetto ad un imponente riarrangiamento che permette la generazione di diverse strutture polimeriche, fornendo le forze e il supporto strutturale necessari per il movimento cellulare. Il ruolo della meccanica nei processi biologici è dunque di inconfutabile rilevanza, così come la responsabilità della meccanobiologia di fornire un supporto ad una caratterizzazione esaustiva dei sistemi viventi.

Modell multi-fisici con applicazioni in meccanobiologia richiedono di tener conto degli svariati fenomeni coinvolti nel processo sotto investigazione. La teoria della meccanica del continuo in grandi deformazioni rappresenta certamente il miglior candidato per descrivere la risposta strutturale delle cellule soggette a massicce deformazioni durante i processi di adesione cellulare, accasciamento e migrazione. Ciononostante, la sola meccanica è evidentemente insufficiente. Nonostante l'accoppiamento tra la meccanica in grandi deformazioni e la termodinamica sia alla base di innumerevoli modelli multi-fisici, è indubbia la necessità di considerare altri processi quali il trasporto di massa con appropriate leggi di diffusione, e di tenere conto delle reazioni chimiche. L'accoppiamento tra termodinamica, meccanica e chemo-diffusione conduce alla realizzazione dei così definiti chemo-transport-mechanical frameworks. Inoltre, e così come ben noto nel campo della termodinamica, la necessità di fornire una caratterizzazione statisticamente basata di alcuni fenomeni è frequente. È il caso della modellazione dei reticoli polimerici nel campo della fisica dei polimeri. Si presentano di conseguenza sfide aggiuntive nel tener conto di eventi multi-fisici a differenti scale spazio-temporali.

In questa tesi, i modelli teorici multi-fisici proposti trovano applicazioni che non sono puramente ristrette al campo della meccanobiologia. Termodinamica e meccanica in grandi deformazioni, meccanica dei continui statisticamente basata, e la teoria dell'elettromagnetismo Galileiano, rappresentano i principali temi investigati nella tesi e adottati per la realizzazione di diverse formulazioni multi-fisiche.

Abstract

The proposed thesis comes from well-defined biological motivations, aiming at providing a characterization of endothelial cell behavior in tumor angiogenesis. Several multi-physics frameworks are introduced for applications in the realm of mechanobiology, as well as in many other research areas.

Angiogenesis is a well known physiological or pathological multistep process that consists in the formation of new blood vessels from preexisting ones. Covering the inner walls of blood vessels, endothelial cells are affected by extracellular stimuli released by tumor cells, and respond via relocation of receptor proteins along their membrane, collective migration and reorganization in novel vessels. The role of receptor dynamics and cell mechanics in response to extracellular stimuli is therefore object of great interest, as they are pivotal processes at the early stages of angiogenesis. Cell structural functions, allowing the occurrence of well known processes such as cell adhesion and spreading, motility and migration, are ascribed to the generation and reorganization of the cytoskeletal contractile machinery. The cytoskeleton is an interconnected network of regulatory proteins and filamentous polymers that undergoes massive rearrangements to generate different biopolymer structures, providing the necessary forces and structural support for cell movements.
It is therefore of unquestionable relevance the role of mechanics in biological processes, as well as the responsibility of mechanobiology to provide a support for an exhaustive characterization of alive systems.

Multi-physics models with applications in mechanobiology require to account for several phenomena involved in the process under investigation. The finite strain theory in continuum mechanics certainly represents the best candidate to describe the structural response of cells undergoing massive deformations during cell adhesion, spreading, and migration. However, mechanics itself is evidently not sufficient. Despite the coupling between finite strain mechanics and thermodynamics stands for the basis of a countless amount of multi-physics models, the necessity to consider other processes such as mass transport with proper diffusion laws, and to account for chemical reactions, is beyond doubt. The coupling between thermo-mechanics and chemo-transport phenomena leads thus to design the so-termed chemo-transport-mechanical frameworks. Furthermore, and as well known in the realm of thermodynamics, insightful models often need to provide a statistically-based characterization of phenomena. It is the case of cross-linked polymer networks modeling in the field of polymer physics. Additional challenges therefore arise in accounting for multi-physics events that occur at different space-time scales.

In this thesis, general and theoretical multi-physics models are proposed for applications that are not only restricted to the realm of mechanobiology. Finite strain continuum thermo-mechanics, diffusion laws and phase segregation, chemical reactions with trapping, statistically-based continuum mechanics, and the Galilean electromagnetic theory, represent the main topics investigated in this thesis and adopted for designing several multi-physics formulations.

Contents

Chapter 1

Introduction

Biological motivation. Tumor neovascularization and angiogenesis-dependent diseases are strongly affected by the release of angiogenic growth factors, which can bind extracellular matrix components, leading to the formation of immobilized complexes [1]. Growth factor and adhesion receptors on endothelial cell membranes convey the extracellular signaling in a coordinate intracellular pathway, promoting cell migration and reorganization in novel active vessels [2].
The relocation of transmembrane receptor proteins along endothelial cell membranes has been object of great interest in biology, as it was recognized of pivotal role during the early stages of tumor angiogenesis. It is the case of the Vascular Endothelial Growth Factor Receptor 2 (VEGFR-2) - the main pro-angiogenic receptor - and of $\alpha_v\beta_3$ integrins, that respond to extracellular stimuli interacting with the Vascular Endothelial Growth Factor - a major pro-angiogenic ligand - or gremlins. Vascular Endothelial Growth Factors are released by tumor or inflammatory cells, and their accumulation in the extracellular matrix triggers the endothelial cell response via intracellular signaling cascades. Cellular responses may differ on the basis of the physical state of cells themselves. Attribution of such distinctive features has been assigned to the association of VEGFR-2 with several proteins, and the resulting generation of distinct multi-molecular complexes [1]. It is further proved the triggering role of Vascular Endothelial Growth Factors [3] or gremlins [4] in VEGFR-2 polarization, as well as the role of integrin receptors in VEGFR-2 activation, propagation, prolonging and strengthening of the intracellular signaling cascades, affecting the cell mechanical response.
The processes of cell motility and migration that drive cell reorganization in novel vessels are mostly dominated by the formation and reorganization of the cytoskeletal contractile machinery in several biopolymer structures. Among different cytoskeletal components, actin protein biopolymers appear to be the main responsible of such processes. Actin diffusion and polymerization into filamentous proteins, and successive branching and bundling processes, generate different biopolymer structures that fulfill several functions, as for the lamellipodium, filopodia, and lamellum filaments that either mature into the filopodia or merge with other bundles [5].

Designing mechanobiological frameworks to characterize receptor dynamics along cell membranes, and cell mechanical response to specific extracellular stimuli, thus represents a wide-complex, fascinating and multi-disciplinary task. Multi-physics models with applications in mechanobiology may have the potential to open new perspectives in highlighting key factors in angiogenesis-dependent diseases.

Multi-physics formulations. Chemo-transport-mechanical formulations have been designed in recent years [1, 2, 6, 7] to describe how the mechanical behavior of endothelial cells affects receptor recruitment and relocation along cell membranes during the early phases of tumor angiogenesis.
Characterization of endothelial cell behavior has been based upon *in-vitro* biological experiments of cell adhesion onto a rigid substrate coated with specific immobilized ligands, and VEGFR-2 dynamics on cell membranes was well captured despite initial strongly simplified assumptions on cell mechanics

[6]. Modeling receptor dynamics has been further broadened [1, 7] to account for the mutual interplay between growth factor and adhesion receptors, such as VEGFR-2 and $\alpha_v\beta_3$ integrins, with specific ligands, as for Vascular Endothelial Growth Factors or gremlins, and extracellular matrix proteins. Finite strain chemo-transport-mechanical models have been further designed [2] to better capture the mechanics of the cell, in a general framework for characterizing receptor dynamics along advecting cell membranes, cell adhesion and spreading, relocation and reaction of actin proteins to form biopolymer structures, and cell motility. However, modeling the cytoskeletal biopolymer structures, and their reorganization in response to external cues, still represents a huge challenge and open research work that currently has not yet been thoroughly accomplished.

Multi-physics frameworks are commonly designed to account for several phenomena and processes at different space-time scales, coupling effects arising from several physical activities. They undoubtedly find applications in multiple fields. The aforementioned receptor–ligand mediated cell adhesion and spreading, cell motility, and biopolymer structure formation and reorganization, in mechanobiology. Additionally, in the charge-discharge process of batteries in electro-chemo-mechanical energy storage, in exposition of metals to hydrogen gas in storage tanks, or in active soft materials with coexistent chemo-transport phenomena, among others.

In the proposed thesis, multi-physics models rooted in the realm of mechanobiology are introduced, encompassing finite strain and statistically-based continuum thermo-mechanics, mass transport and chemical reactions with trapping. Mass balance equations are properly augmented to account for chemical reactions. Finite strain thermo-mechanics follows a rigorous setting, stemming from the principles of conservation of linear and angular momentum, the laws of thermodynamics, and the method of Colemann and Noll [8] to derive thermodynamic prescriptions. Constitutive theory and resulting specifications, as well as the governing equations of the proposed frameworks, are lastly provided. Mechanobiological models are further accompanied by other general and theoretical formulations that have been designed beyond the well-defined biological motivations. It is the case of the Cahn-Hilliard theory for species diffusion and phase segregation, which has been coupled with a chemo-thermo-mechanical formulation, and the Galilean electromagnetic theory for moving end deformable bodies, re-phrased in Lagrangian formulation and coupled with finite-strain continuum thermo-mechanics.

Outline. Additionally to the current introductory section and final conclusions, the proposed thesis is organized in six manuscripts that can be summarized as follows.

Chapter 2. A general framework of finite strain continuum thermo-mechanics coupled with mass transport and chemical reaction with trapping is introduced. It extends a previous work [9] set in the field of small strain continuum mechanics. Within this formulation, kinematical specifications and strain decompositions are performed, finite strain continuum thermo-mechanics is widely covered following a rigorous treatment, and detailed constitutive prescriptions are provided to further establish proper specifications for mechanics, chemical potentials, heat and mass fluxes, and chemical kinetics. The structure of this chapter also works as basis for successive models presented in the thesis. It is indexed as [10] and often cited to allow a simplified exposition, motivate assumptions previously performed, and avoiding redundant steps in deriving equations.

Chapter 3. The general framework for protein relocation on advecting membranes, biopolymer formations within the cell, cell spreading and motility [2] is reproduced. Despite some modification with respect to the published paper, the structure of the original version has been taken unaltered. Equations are occasionally given without explicitly show the whole derivation, for which nonetheless reference can be made to [10], to which is assigned the explanation of all necessary steps to perform. This chapter provides a general framework in mechanobiology, accompanied by a comprehensive description of the biological processes that motivate the thesis.

Chapter 4. The review article on modeling receptor dynamics along advecting lipid membranes [11] is reproduced. Theoretical approaches and computational methodologies for modeling receptor relocation and recruitment along cell membranes are reviewed. An exhaustive biologically-based description of several receptors involved in different biological processes is provided. Appropriate multi-phyisics laws to model the mass flux of receptor along cell membranes and receptor-ligand chemical interactions, accounting for the cell structural response, are discussed for continuum models. Equations are here provided in the field of small strain continuum mechanics.

Chapter 5. A statistically-based continuum mechanical framework for polymer networks is introduced with the aim to model the generation and reorganization of actin cytoskeletal biopolymer structures within the cell. Statistical and finite strain continuum mechanics are coupled, and chemo-transport phenomena are accounted for. The resulting statistically-based chemo-transport-mechanical model represents a valid candidate for the non-trivial task of actin biopolymer behavior characterization. However, the framework introduced still requires in-depth analysis and developments with respect to the aim it has been designed for in this thesis. It represents a non-exhaustively accomplished part. Weaknesses of the proposed formulation are properly highlighted and discussed.

Chapter 6. Finite strain continuum thermo-mechanics is coupled with the Cahn-Hilliard theory for species diffusion and phase segregation, and chemical reaction with trapping, to design the proposed framework of this chapter. Beyond biological motivations, the model couples the classical Cahn-Hilliard theory with the general framework introduced in [10], which is here reproduced in a simplified version on behalf of a more detailed treatment of the *new* theory for species diffusion and phase segregation introduced. On the basis of previous studies, the a-priori requirement of free energy constitutive specifications by the Cahn-Hilliard equations are discussed, as well as the consistent thermodynamic setting of the model.

Chapter 7. A fully coupled non-relativistic theoretical framework of Galilean electromagnetism with finite strain continuum mechanics and thermodynamics is proposed. The electromagnetic theory is provided with an exhaustive treatment. The focus of the formulation introduced is kept on the non trivial coupling between the theories of Galilean electromagnetism for a convecting body and finite strain continuum thermo-mechanics. No other multi-physics processes are thus accounted for. The Lagrangian formulation of the principles of electromagnetism is provided, modifications to the laws of mechanics and thermodynamics are introduced, and the resulting electro-magneto-mechanical laws and quantities involved in the framework are discussed.

Chapter 2

A coupled model of transport-reaction-mechanics with trapping. Part II - Large strain analysis

Matteo Arricca[1,2], Mattia Serpelloni[1,2], Claudia Bonanno[1,3], Robert M. McMeeking[1,4,5,6] and Alberto Salvadori[1,2]

[1]The Mechanobiology Research Center, UNIBS, Italy
[2]Department of Mechanical and Industrial Engineering, University of Brescia, Italy
[3]Department of Civil, Environmental, Architectural Engineering and Mathematics, University of Brescia, Italy
[4]Materials and Mechanical Engineering Departments, University of California, Santa Barbara, USA
[5]School of Engineering, University of Aberdeen, King's College, Scotland, United Kingdom
[6]INM-Leibniz Institute for New Materials, Saarbruecken 66123, Germany

Abstract. A coupled finite strain chemo-transport-mechanical formulation with trapping is here proposed to extend a previous work set in the realm of small strain theory in continuum mechanics. The theory is rooted in non-equilibrium rational thermodynamics. The kinematics is based on a multiplicative decomposition of the deformation gradient to account for swelling and shrinking, thermal, elastic and inelastic contributions. Mass balance laws and balance of linear and angular momentum, as well as the laws of thermodynamics for a convecting body, are directly formulated in their material description, after specifications of some standard transformation rules between current and reference configuration. Thermodynamic restrictions are identified based on the functional dependence of the referential Helmholtz free energy density, which is chosen as the thermodynamic potential, and further subjected to a constitutive additive decomposition. Constitutive prescriptions for the chemical potentials, referential heat and mass fluxes, chemical kinetics and the generalized heat equation lead to the establishment of the governing equations.

2.1 Introduction

Multi-physics frameworks, by their own nature, account for several phenomena and model several processes at different scales, with the common need to couple effects arising from the different physical activities that contribute to each process. The proposed finite strain coupled model of transport-reaction-mechanics with trapping originates as a natural extension of a previous work [9] developed in the realm of small strain theory in continuum mechanics. Chemo-thermo-mechanics is usually coupled with mass transport, driven by a single effect like diffusion or migration (or a combination of both) and, less often, with trapping and/or a mass source term to account for mass conversion. The trapping process diminishes the availability of transported species that, once trapped, are usually assumed to stay immobilized. Heat fluxes and sources, mechanical surface and body forces, as standard in thermo-mechanics, complete the framework.

The coupling of chemo-thermo-mechanics with trapping allows the description of several multi-disciplinary applications. For instance, in the realm of mechanobiology, the conversion of free to trapped proteins [12, 13, 14, 15, 16, 17, 18] allows cell adhesion, mediated by chemical interactions between freely mobile receptors along a cell membrane and ligands located either on a substrate or onto another adjacent cell surface. Typically, the interaction of mobile high affinity integrins and specific proteins embedded in the extra-cellular matrix immobilize integrins in multi-molecular plaques termed focal adhesions [7, 19, 20, 21, 22, 23]. Similarly, the interplay between the Vascular Endothelial Growth Factor Receptor 2 (VEGFR2) along endothelial cell membranes and growth factor molecules released by cancer cells traps VEGFR2 [1, 6, 24]. In actin diffusion and polymerization to form cytoskeletal structures in the cell cytosol, the trapping process is associated with a change of phase of the actin protein, from globular to filamentous form [2].

Other multi-disciplinary applications of chemo-thermo-mechanics with trapping can be found in the exposure of metals to hydrogen gas. In storage tanks, hydrogen atoms diffuse within the crystalline structure of the metal and are trapped in defects [25, 26, 27, 28, 29, 30, 31, 32]. The batteries charge-discharge is due to the motion of ions, which are immobilized in active particles after their insertion into the electrodes [33, 34, 35, 36, 37, 38, 39, 40, 41, 42, 43]. Chemo-active soft materials with coexistent diffusion and reaction of species can induce a crosslinking mechanism or the inclusion of molecules in the polymer network (as in polymer gel membranes and/or hydrogels) [44, 45, 46, 47, 48, 49]. Further examples of chemo-thermo-mechanics with trapping are represented by vacancies and dendritic growth, solid propellant, bio-electrochemistry, solute solidification, moisture diffusion in polymer nanocomposites.

Following the same path of reasoning of [9], we use the network model proposed by Larche and Cahn [50]; it is therefore assumed that the freely diffusive species move in the network (lattice sites) of the hosting material, until immobilized via chemical reactions in specific trap sites, isolated from one another. The trapping process is commonly associated with a separation of phases, or a change of phase, and determined by species chemical interactions. The diffusion process of species is affected by the trapping process (and vice-versa) by means of a change in the concentration gradient.

The kinetic process of trapping, involving chemical reactions, is well described by appropriately modifying the *van't Hoff* mass action law to account for elastic and swelling contributions, and set in a well-established thermodynamic framework [51, 52]. A swelling phenomenon, due to the trapping process, may generate large mechanical stress and strain in the material, affecting all other processes due to a coupling with the chemo-thermo-mechanics; these interactions are accounted for, within a rigorous thermodynamic setting [53, 54], in the field of finite strain theory in continuum mechanics.

The manuscript is organized as follows. Section 2.2 provides some standard definitions to facilitate the exposition of the formulation in the field of finite strain mechanics. Assumptions on kinematics, in terms of multiplicative decomposition of the deformation gradient, and the resulting volumetric Jacobian and velocity gradient, are presented in Section 2.3. Mass balance equations and the laws of continuum mechanics are introduced in Section 2.4. Section 2.5 is dedicated to the laws of thermodynamics, and to exploiting thermodynamic prescriptions by means of the Coleman-Noll procedure [8], under the assumption of Curie's symmetry principles. Constitutive theory is discussed in Section 2.6, based on an additive decomposition of the referential Helmholtz free energy density, providing consistent phenomenological specifications for all contributions to the free energy, stress tensor, chemical potentials, heat and mass fluxes. Chemical kinetics and governing equations in Sections 2.7 and 2.8 complete the paper.

2.2 Definitions

2.2.1 Motion and deformation gradient

Let $\mathcal{B}_t \in \mathbb{R}^3$ denote the spatial description of an advecting volume, whose boundary is $\partial\mathcal{B}_t$. Let $\mathcal{B}_R$ and $\partial\mathcal{B}_R$ indicate their referential counterparts, as standard in finite strain mechanics [53, 54]. The transformation of a material point $\boldsymbol{X} \in \mathcal{B}_R$ into a spatial point $\boldsymbol{x} \in \mathcal{B}_t$, is described by means of a smooth function $\boldsymbol{\chi}(\boldsymbol{X}, t)$

$$\boldsymbol{x} = \boldsymbol{\chi}(\boldsymbol{X}, t) ,$$

which is a one-to-one map representing the motion of $\boldsymbol{X} \in \mathcal{B}_R$ at time t. We will also assume that $\mathcal{B}_t$ at $t = 0$ coincides with $\mathcal{B}_R$, *i.e.*, for all material points $\boldsymbol{X} = \boldsymbol{\chi}(\boldsymbol{X}, 0)$. The material velocity is given by $\dot{\boldsymbol{\chi}}(\boldsymbol{X}, t)$, whereas displacements write as $\boldsymbol{u} = \boldsymbol{\chi} - \boldsymbol{X}$.

At a fixed time t, we will name

$$\mathbf{F} = \boldsymbol{\nabla}_R \left[\, \boldsymbol{\chi}(\boldsymbol{X}, t) \,\right] , \tag{2.1}$$

the deformation gradient, *i.e.*, $\mathrm{F}_{ij} = \partial\chi_i / \partial X_j$. Only motions such that

$$J = \det\left[\, \mathbf{F} \,\right] > 0$$

are admissible, in order to avoid total material compaction (see [53]).

2.2.2 Transformation rules

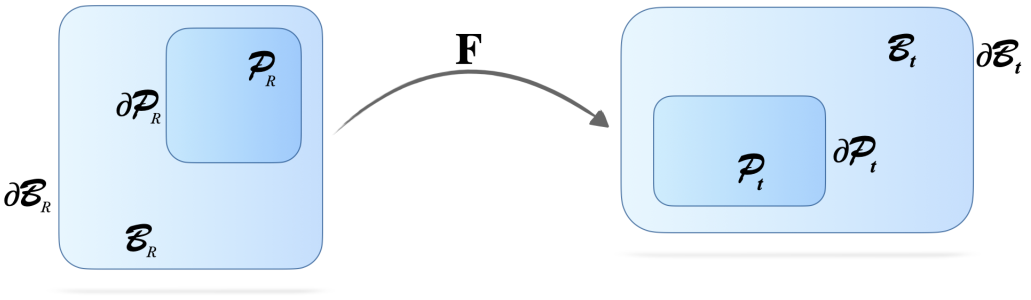

Figure 2.1: Schematic representation of the material and spatial configuration $\mathcal{B}_R$ and $\mathcal{B}_t$, with boundaries $\partial\mathcal{B}_R$ and $\partial\mathcal{B}_t$, and of a generic sub-part $\mathcal{P}_t \subset \partial\mathcal{P}_t$, image of $\mathcal{P}_R \subset \partial\mathcal{P}_R$, with boundaries $\partial\mathcal{P}_t$ and $\partial\mathcal{P}_R$, respectively.

Denote with $\mathcal{P}_t \subset \mathcal{B}_t$ an arbitrary region image of $\mathcal{P}_R \subset \mathcal{B}_R$, and with $\partial\mathcal{P}_t$ and $\partial\mathcal{P}_R$ their respective boundaries (see Figure 2.1). Let $f^{\mathcal{V}}(\boldsymbol{x}, t) \in \mathcal{P}_t$ and $f^{\mathcal{V}}_R(\boldsymbol{X}, t) \in \mathcal{P}_R$ be two generic tensorial functions of any order. If

$$\int_{\mathcal{P}_t} f^{\mathcal{V}}(\boldsymbol{x}, t)\, \mathrm{d}v = \int_{\mathcal{P}_R} f^{\mathcal{V}}_R(\boldsymbol{X}, t)\, \mathrm{d}\mathcal{V} , \tag{2.2}$$

then the following transformation rule applies

$$f^{\mathcal{V}}_R(\boldsymbol{X}, t) = J(\boldsymbol{X}, t)\, f^{\mathcal{V}}(\boldsymbol{x}(\boldsymbol{X}, t), t) . \tag{2.3}$$

Let $\boldsymbol{f}^{\mathcal{S}}(\boldsymbol{x}, t)$ be a spatial vector, and $\boldsymbol{x}$ a point on an oriented surface $\partial\mathcal{P}_t$ defined by the direction of the outward normal vector $\boldsymbol{n}$. Denote with $\boldsymbol{n}_R$ the outward normal vector to the oriented surface $\partial\mathcal{P}_R$. The referential counterpart $\boldsymbol{f}^{\mathcal{S}}_R(\boldsymbol{X}, t)$, with $\boldsymbol{X} \in \partial\mathcal{P}_R$, is defined by the identity

$$\int_{\partial\mathcal{P}_t} \boldsymbol{f}^{\mathcal{S}}(\boldsymbol{x}, t) \cdot \boldsymbol{n}\, \mathrm{d}a = \int_{\partial\mathcal{P}_R} \boldsymbol{f}^{\mathcal{S}}_R(\boldsymbol{X}, t) \cdot \boldsymbol{n}_R\, \mathrm{d}\mathcal{A} , \tag{2.4}$$

imposed on all $\partial\mathcal{P}_t \subset \partial\mathcal{B}_t$.

By recalling the Nanson's formula for area changes, $\boldsymbol{n}\,\mathrm{d}a = J\,\mathbf{F}^{-\mathrm{T}}\,\boldsymbol{n}_{R}\,\mathrm{d}\mathcal{A}$, Eq. (7.4) implies

$$\begin{aligned}
\int_{\partial\mathcal{P}_t} \boldsymbol{f}^{s}(\boldsymbol{x},t)\cdot\boldsymbol{n}\,\mathrm{d}a &= \int_{\partial\mathcal{P}_R} \boldsymbol{f}^{s}(\boldsymbol{x}(\boldsymbol{X},t),t)\cdot J(\boldsymbol{X},t)\,\mathbf{F}^{-\mathrm{T}}(\boldsymbol{X},t)\,\boldsymbol{n}_{R}\,\mathrm{d}\mathcal{A} \\
&= \int_{\partial\mathcal{P}_R} J(\boldsymbol{X},t)\,\mathbf{F}^{-1}(\boldsymbol{X},t)\,\boldsymbol{f}^{s}(\boldsymbol{x}(\boldsymbol{X},t),t)\cdot\boldsymbol{n}_{R}\,\mathrm{d}\mathcal{A} \qquad (2.5)\\
&= \int_{\partial\mathcal{P}_R} \boldsymbol{f}^{s}_{R}(\boldsymbol{X},t)\cdot\boldsymbol{n}_{R}\,\mathrm{d}\mathcal{A}\;,
\end{aligned}$$

and the the following transformation rule arises

$$\boldsymbol{f}^{s}_{R}(\boldsymbol{X},t) = J(\boldsymbol{X},t)\,\mathbf{F}^{-1}(\boldsymbol{X},t)\,\boldsymbol{f}^{s}(\boldsymbol{x}(\boldsymbol{X},t),t)\;. \qquad (2.6)$$

2.3 Kinematics

Following [55], we base the theory on the following multiplicative decomposition of the deformation gradient

$$\mathbf{F} = \mathbf{F}^{cte}\,\mathbf{F}^{p}\;, \qquad (2.7)$$

where $\mathbf{F}^{cte}$ is termed chemo-thermo-elastic deformation gradient, and represents the distorsion of the material in the neighborhood of $\boldsymbol{X}$ as a consequence of the combined effect of the chemical, temperature dependent and elastic mechanisms; $\mathbf{F}^{p}$ is termed inelastic distorsion and represents the irreversible deformations in the neighborhood of $\boldsymbol{X}$ due, for instance, to the flow of defects [53] in plasticity.

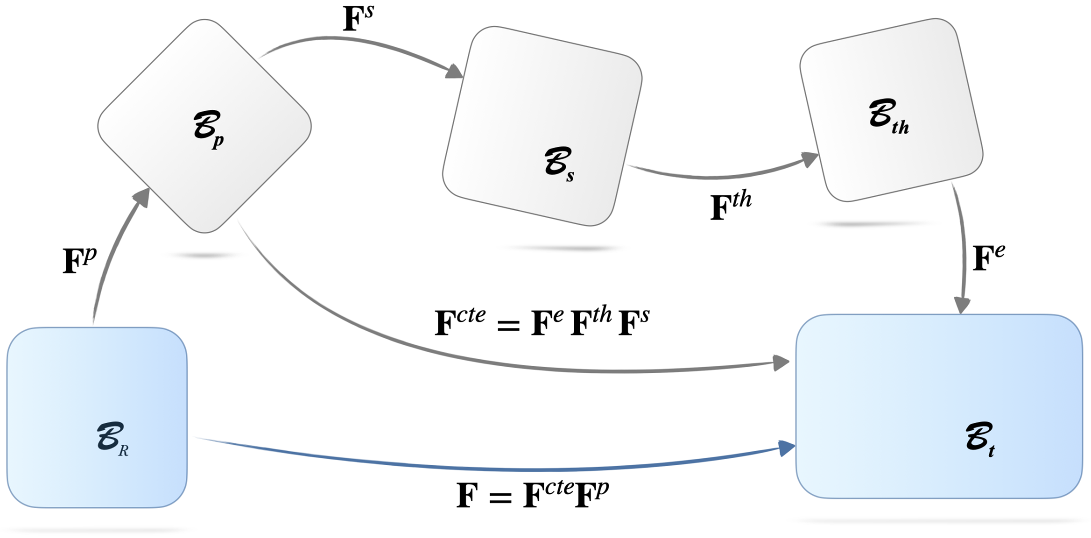

Figure 2.2: A schematic of the material $\mathcal{B}_{R}$, and spatial $\mathcal{B}_t$ configurations, and of the multiplicative decomposition of the deformation gradient in plasticity $\mathbf{F}^{p}$, from material to plastic configuration $\mathcal{B}_p$, and chemo-thermo-elastic $\mathbf{F}^{cte}$, from plastic to spatial configuration. The further multiplicative decomposition of $\mathbf{F}^{cte}$ entails the swelling contribution $\mathbf{F}^{s}$, from plastic to swelling $\mathcal{B}_s$, the thermal contribution $\mathbf{F}^{th}$, from swelling to thermal $\mathcal{B}_{th}$, and the elastic contribution $\mathbf{F}^{e}$, from $\mathcal{B}_{th}$ to $\mathcal{B}_t$.

The chemo-thermo-elastic deformation gradient $\mathbf{F}^{cte}$ is in turn subject to the further multiplicative decomposition

$$\mathbf{F}^{cte} = \mathbf{F}^{e}\,\mathbf{F}^{th}\,\mathbf{F}^{s}\;, \qquad (2.8)$$

with $\mathbf{F}^e$ the local reversible elastic distorsion, $\mathbf{F}^{th}$ the thermal contribution to the local distorsion, and $\mathbf{F}^s$ the local distorsion of the material due to volumetric swelling (shrinking) as a consequence of the trapping (extraction) of species in (from) the host material. A similar decomposition of the deformation gradient has been proposed in [2, 55], although the thermal contribution has not been accounted for. Bearing in mind the velocity gradient, $\mathbf{L} = \dot{\mathbf{F}}\,\mathbf{F}^{-1}$, and according to Eq. (2.7), the chemo-thermo-elastic and the inelastic velocity gradient will be defined by

$$\mathbf{L}^{cte} = \dot{\mathbf{F}}^{cte}\,\mathbf{F}^{cte^{-1}} \;, \tag{2.9a}$$

$$\mathbf{L}^{p} = \dot{\mathbf{F}}^{p}\,\mathbf{F}^{p^{-1}} \;, \tag{2.9b}$$

so that

$$\mathbf{L} = \dot{\mathbf{F}}\,\mathbf{F}^{-1} = \dot{\mathbf{F}}^{cte}\,\mathbf{F}^{p}\,\mathbf{F}^{p^{-1}}\,\mathbf{F}^{cte^{-1}} + \mathbf{F}^{cte}\,\dot{\mathbf{F}}^{p}\,\mathbf{F}^{p^{-1}}\,\mathbf{F}^{cte^{-1}} = \mathbf{L}^{cte} + \mathbf{F}^{cte}\,\mathbf{L}^{p}\,\mathbf{F}^{cte^{-1}} \;. \tag{2.10}$$

As standard in continuum mechanics, the decomposition of the velocity gradient into the symmetric stretch tensor $\mathbf{D}$ and the skew spin tensor $\mathbf{W}$, the chemo-thermo-elastic and the plastic velocity gradients can be expressed as

$$\mathbf{L}^{cte} = \mathbf{D}^{cte} + \mathbf{W}^{cte}, \qquad \mathbf{L}^{p} = \mathbf{D}^{p} + \mathbf{W}^{p} \;. \tag{2.11}$$

2.4 Balance laws

In the present framework, we maintain the same hypothesis assumed in [9]. Only isolated saturable and reversible trap sites are considered, since they are assumed to not form an extended continuous path for lattice species diffusion. For this reason, freely diffusive species through the host lattice network fill trap sites and, once in the trap, cease to diffuse. Species transport is therefore attributed solely to the lattice (interstitial) sites. Hence, the referential flux of species (number of moles of species α measured per unit reference area per unit time), here denoted with $\boldsymbol{h}_{\alpha_R}$, only has a purely interstitial lattice diffusion contribution, as in [50, 56].

2.4.1 Mass balance

Consider a generic species H at a point $\boldsymbol{X} \in \mathcal{P}_R$. The trapping process of H describes the conversion of mobile species to trapped species, and vice-versa, via the following one-component two-phases chemical reaction

$$\mathrm{H}_L \underset{k_R^-}{\overset{k_R^+}{\rightleftarrows}} \mathrm{H}_T \;, \tag{2.12}$$

where k_R^+ and k_R^- represent the referential positive rate factor for the forward reaction, yielding trapped species, and for the backward reaction, yielding free diffusive species, respectively. The reaction rate of Eq. (2.12) is denoted with $w_R^{(2.12)}$; specifications of $w_R^{(2.12)}$, k_R^+ and k_R^- will be provided in Section 2.7.

Let ρ_{α_R}, c_{α_R} and κ_α denote the referential density (mass per unit reference volume), the referential concentration (moles per unit reference volume) and the molar mass of species α, respectively. The three terms are linked to each other by means of the relation

$$\rho_{\alpha_R} = \kappa_\alpha\, c_{\alpha_R} \;. \tag{2.13}$$

Accordingly, mass balance equations for species $\alpha = L, T$ can be formulated either in terms of density or in terms of concentration of species, in the reference configuration

$$\dot{\overline{\int_{\mathcal{P}_R} c_{\alpha_R}(\boldsymbol{X},t)\;\mathrm{d}\mathcal{V}}} + \int_{\partial\mathcal{P}_R} \boldsymbol{h}_{\alpha_R}(\boldsymbol{X},t)\cdot\boldsymbol{n}_R\;\mathrm{d}\mathcal{A} \pm \int_{\mathcal{P}_R} w_R^{(2.12)}(\boldsymbol{X},t)\;\mathrm{d}\mathcal{V} = \int_{\mathcal{P}_R} s_{\alpha_R}(\boldsymbol{X},t)\;\mathrm{d}\mathcal{V} \;. \tag{2.14}$$

The right-hand side term s_{α_R} is the rate, in moles per unit reference volume per unit time, at which species α are generated by external sources, where a positive reaction rate $w_{R}^{(2.12)}$ refers to free species L.

After standard application of the divergence theorem, Eq. (2.14) takes the form

$$\int_{\mathcal{P}_R} \dot{c}_{\alpha_R}(\boldsymbol{X},t)\,\mathrm{d}\mathcal{V} + \int_{\mathcal{P}_R} \boldsymbol{\nabla}_R \cdot [\,\boldsymbol{h}_{\alpha_R}(\boldsymbol{X},t)\,]\,\mathrm{d}\mathcal{V} \pm \int_{\mathcal{P}_R} w_R^{(2.12)}(\boldsymbol{X},t)\,\mathrm{d}\mathcal{V} = \int_{\mathcal{P}_R} s_{\alpha_R}(\boldsymbol{X},t)\,\mathrm{d}\mathcal{V}\ , \tag{2.15}$$

for any region $\mathcal{P}_R \subset \mathcal{B}_R$.

It follows that, by means of the assumption of immobilized trapped species, which therefore provides no mass flux of H_T ($\boldsymbol{h}_{T_R} = \boldsymbol{0}$), the referential local form of the mass balance equations write as

$$\dot{c}_{L_R} + \boldsymbol{\nabla}_R \cdot [\,\boldsymbol{h}_{L_R}\,] + w_R^{(2.12)} = s_{L_R}\ , \tag{2.16a}$$

$$\dot{c}_{T_R} - w_R^{(2.12)} = s_{T_R}\ . \tag{2.16b}$$

The concentrations c_{α_R}, the reaction rate $w_R^{(2.12)}$ and the rate at which species are generated by sources s_{α_R}, being defined over a volume, transform according to Eq. (7.3),

$$c_{\alpha_R}(\boldsymbol{X},t) = J\,c_\alpha\ , \qquad w_R^{(2.12)}(\boldsymbol{X},t) = J\,w^{(2.12)}\ , \qquad s_{\alpha_R}(\boldsymbol{X},t) = J\,s_\alpha\ , \tag{2.17}$$

whereas the mass flux $\boldsymbol{h}_{L_R}$ follows the rule stated by Eq. (7.6), namely,

$$\boldsymbol{h}_{L_R}(\boldsymbol{X},t) = J\,\mathbf{F}^{-1}\,\boldsymbol{h}_L\ . \tag{2.18}$$

2.4.2 Balance of linear and angular momentum

Let

$$\boldsymbol{t}(\boldsymbol{x},t) = \mathbf{T}\,\boldsymbol{n} \tag{2.19}$$

define the current surface traction (force per unit current surface), with $\mathbf{T}$ the Cauchy stress tensor. By means of the Nanson's formula for the transformation of areas,

$$\begin{aligned}\int_{\partial\mathcal{P}_t} \boldsymbol{t}(\boldsymbol{x},t)\,\mathrm{d}a = \int_{\partial\mathcal{P}_t} \mathbf{T}(\boldsymbol{x},t)\,\boldsymbol{n}\,\mathrm{d}a = \int_{\partial\mathcal{P}_R} \mathbf{T}\,J\,\mathbf{F}^{-\mathrm{T}}\,\boldsymbol{n}_R\,\mathrm{d}\mathcal{A} &= \int_{\partial\mathcal{P}_R} \mathbf{T}_R(\boldsymbol{X},t)\,\boldsymbol{n}_R\,\mathrm{d}\mathcal{A} \\ &= \int_{\partial\mathcal{P}_R} \boldsymbol{t}_R(\boldsymbol{X},t)\,\mathrm{d}\mathcal{A}\ ,\end{aligned} \tag{2.20}$$

with $\boldsymbol{t}_R$ the referential surface traction (spatial force with material reference, *i.e.*, traction per unit reference surface [57]) and $\mathbf{T}_R$ the nominal, or first Piola-Kirchhoff, stress tensor, defined as

$$\mathbf{T}_R = J\,\mathbf{T}\,\mathbf{F}^{-\mathrm{T}}\ . \tag{2.21}$$

As in [9], inertia body forces are neglected and this implies that the referential balance of linear momentum takes the form

$$\int_{\partial\mathcal{P}_R} \boldsymbol{t}_R(\boldsymbol{X},t)\,\mathrm{d}\mathcal{A} + \int_{\mathcal{P}_R} \boldsymbol{b}_{0_R}(\boldsymbol{X},t)\,\mathrm{d}\mathcal{V} = \boldsymbol{0}\ , \tag{2.22a}$$

$$\int_{\partial\mathcal{P}_R} \boldsymbol{\chi} \times \boldsymbol{t}_R(\boldsymbol{X},t)\,\mathrm{d}\mathcal{A} + \int_{\mathcal{P}_R} \boldsymbol{\chi} \times \boldsymbol{b}_{0_R}(\boldsymbol{X},t)\,\mathrm{d}\mathcal{V} = \boldsymbol{0}\ , \tag{2.22b}$$

where $\boldsymbol{b}_{0_R}$ represents the referential body force (spatial body force density in the material reference configuration, *i.e.*, body force acting on a unit volume in the material configuration [57])

According to Eq. (2.20), after application of the divergence theorem and recognition that the resultant integral must hold for any arbitrary volume, the local form of the balance of linear momentum writes as

$$\boldsymbol{\nabla}_R \cdot [\,\mathbf{T}_R\,] + \boldsymbol{b}_{0_R} = \boldsymbol{0}\ , \tag{2.23a}$$

with $\boldsymbol{\nabla}_R \cdot [\,\mathbf{T}_R\,] = \partial \mathrm{T}_{Rij}/\partial X_j$, whereas the angular momentum localizes as

$$\mathbf{T}_R\mathbf{F}^{\mathrm{T}} = \mathbf{F}\,\mathbf{T}_R^{\mathrm{T}}\ . \tag{2.23b}$$

2.5 Thermodynamics

2.5.1 Energy balance

We augment the classical first law of thermodynamics, which provides the variation of the internal energy of a body as the sum of the power expended on it by external forces and the heat transferred in it, with the energy flow due to species transport. The first law of thermodynamics is therefore represented by the interplay among the internal energy of $\mathcal{P}_R$, the power expended on $\mathcal{P}_R$, the heat transferred in $\mathcal{P}_R$, and the power due to mass exchanged on $\mathcal{P}_R$. Electro-magnetic effects will be accounted for in a forthcoming publication, but are omitted here.

Denote with $\mathcal{U}$ the net internal energy, $\mathcal{W}_u$ the mechanical external power, $\mathcal{Q}_u$ the power due to heat transferred, and $\mathcal{T}_u$ the power due to mass transferred. The referential energy balance takes the form

$$\dot{\mathcal{U}}(\mathcal{P}_R) = \mathcal{W}_u(\mathcal{P}_R) + \mathcal{Q}_u(\mathcal{P}_R) + \mathcal{T}_u(\mathcal{P}_R) \; . \tag{2.24}$$

We point out that the assumption of negligible inertia forces implies that no kinetic energy is accounted for; on the same grounds, the mechanical external power is defined in terms of the conventional body forces.

The definition of the referential net internal energy can be provided either per unit reference mass or per unit reference volume, given that the referential mass density does not change in time ($\dot{\rho}_R = 0$) in view of the mass conservation for the hosting material. By defining u_R as the specific internal energy (per unit reference volume), we write the net internal energy of $\mathcal{P}_R$ as

$$\mathcal{U}(\mathcal{P}_R) = \int_{\mathcal{P}_R} u_R \; \mathrm{d}\mathcal{V} \; . \tag{2.25}$$

The individual contributions of Eq. (2.24) write as

$$\dot{\mathcal{U}}(\mathcal{P}_R) = \int_{\mathcal{P}_R} \dot{u}_R \; \mathrm{d}\mathcal{V} \; , \tag{2.26a}$$

$$\mathcal{W}_u(\mathcal{P}_R) = \int_{\partial\mathcal{P}_R} \dot{\boldsymbol{\chi}} \cdot \boldsymbol{t}_R \; \mathrm{d}\mathcal{A} + \int_{\mathcal{P}_R} \dot{\boldsymbol{\chi}} \cdot \boldsymbol{b}_{0R} \; \mathrm{d}\mathcal{V} \; , \tag{2.26b}$$

$$\mathcal{Q}_u(\mathcal{P}_R) = \int_{\mathcal{P}_R} s_{qR} \; \mathrm{d}\mathcal{V} - \int_{\partial\mathcal{P}_R} \boldsymbol{q}_R \cdot \boldsymbol{n}_R \; \mathrm{d}\mathcal{A} \; , \tag{2.26c}$$

$$\mathcal{T}_u(\mathcal{P}_R) = \int_{\mathcal{P}_R} {}^{u}\mu_L \, s_{LR} + {}^{u}\mu_T \, s_{TR} \; \mathrm{d}\mathcal{V} - \int_{\partial\mathcal{P}_R} {}^{u}\mu_L \, \boldsymbol{h}_{LR} \cdot \boldsymbol{n}_R \; \mathrm{d}\mathcal{A} \; . \tag{2.26d}$$

Terms in Eq.s (2.26) have the following meaning. The surface traction and the body force, $\boldsymbol{t}_R$ and $\boldsymbol{b}_{0R}$, have been defined in Section 2.4.2; s_{qR} and $\boldsymbol{q}_R$ represent the heat supplied by external agencies and the heat flux vector, respectively; the scalar ${}^{u}\mu_\alpha$ is the energy provided by a unit supply of moles of species $\alpha = L, T$, whereas $s_{\alpha R}$ and $\boldsymbol{h}_{LR}$ are the source term and the mass flux vector, respectively, as defined in the mass balance equation (2.14).

In view of the definition of the referential surface traction arising from Eq. (2.20), the power expenditure of external agencies $\mathcal{W}_u$ writes

$$\begin{aligned} \mathcal{W}_u(\mathcal{P}_R) &= \int_{\partial\mathcal{P}_R} \dot{\boldsymbol{\chi}} \cdot \mathbf{T}_R \, \boldsymbol{n}_R \; \mathrm{d}\mathcal{A} + \int_{\mathcal{P}_R} \dot{\boldsymbol{\chi}} \cdot \boldsymbol{b}_{0R} \; \mathrm{d}\mathcal{V} = \int_{\mathcal{P}_R} \boldsymbol{\nabla}_R \cdot [\, \dot{\boldsymbol{\chi}} \, \mathbf{T}_R \,] \; \mathrm{d}\mathcal{V} + \int_{\partial\mathcal{P}_R} \dot{\boldsymbol{\chi}} \cdot \boldsymbol{b}_{0R} \; \mathrm{d}\mathcal{A} \\ &= \int_{\mathcal{P}_R} \boldsymbol{\nabla}_R \, [\, \dot{\boldsymbol{\chi}} \,] : \mathbf{T}_R + \boldsymbol{\nabla}_R \cdot [\, \mathbf{T}_R \,] \cdot \dot{\boldsymbol{\chi}} \; \mathrm{d}\mathcal{V} + \int_{\mathcal{P}_R} \dot{\boldsymbol{\chi}} \cdot \boldsymbol{b}_{0R} \; \mathrm{d}\mathcal{V} \; , \end{aligned} \tag{2.27}$$

whence, making use of the balance of linear momentum (2.23a) to replace the vector $\boldsymbol{b}_{0R}$, Eq. (2.27) takes the form

$$\mathcal{W}_u(\mathcal{P}_R) = \int_{\mathcal{P}_R} \mathbf{T}_R : \boldsymbol{\nabla}_R \, [\, \dot{\boldsymbol{\chi}} \,] \; \mathrm{d}\mathcal{V} = \int_{\mathcal{P}_R} \mathbf{T}_R : \dot{\mathbf{F}} \; \mathrm{d}\mathcal{V} \; . \tag{2.28}$$

Application of the divergence theorem to the second term on the right-hand side of Eq. (2.26c) allows us to write the heat contribution to the energy balance as

$$\mathcal{Q}_u(\mathcal{P}_R) = \int_{\mathcal{P}_R} s_{qR} - \boldsymbol{\nabla}_R \cdot \left[\, \boldsymbol{q}_R \,\right] \mathrm{d}\mathcal{V} \tag{2.29}$$

where s_{qR} and $\boldsymbol{q}_R$ follow the transformation rules given by Eq.s (7.3) and (7.6), respectively.

The mass transfer contribution to the energy balance, after application of the divergence theorem and use of the localized mass balance equations (2.16) to substitute for the terms s_{LR} and s_{TR}, writes as

$$\begin{aligned}\mathcal{T}_u(\mathcal{P}_R) = & \int_{\mathcal{P}_R} {}^u\mu_L\, \dot{c}_{LR} + {}^u\mu_L\, \boldsymbol{\nabla}_R \cdot [\, \boldsymbol{h}_{LR} \,] + {}^u\mu_L\, w_R^{(2.12)} + {}^u\mu_T\, \dot{c}_{TR} - {}^u\mu_T\, w_R^{(2.12)}\, \mathrm{d}\mathcal{V} \\ & - \int_{\mathcal{P}_R} \boldsymbol{\nabla}_R\, [\, {}^u\mu_L \,] \cdot \boldsymbol{h}_{LR} + {}^u\mu_L\, \boldsymbol{\nabla}_R \cdot [\, \boldsymbol{h}_{LR} \,]\, \mathrm{d}\mathcal{V}\end{aligned}$$

therefore

$$\mathcal{T}_u(\mathcal{P}_R) = \int_{\mathcal{P}_R} {}^u\mu_L\, \dot{c}_{LR} + {}^u\mu_T\, \dot{c}_{TR} - \boldsymbol{\nabla}_R\, [\, {}^u\mu_L \,] \cdot \boldsymbol{h}_{LR} + ({}^u\mu_L - {}^u\mu_T)\, w_R^{(2.12)}\, \mathrm{d}\mathcal{V}\ . \tag{2.30}$$

Combining Eq.s (2.26a), (2.28), (2.29) and (2.30), we find that the referential form of the energy balance writes as

$$\begin{aligned}\int_{\mathcal{P}_R} \dot{u}_R\, \mathrm{d}\mathcal{V} = & \int_{\mathcal{P}_R} \mathbf{T}_R : \dot{\mathbf{F}}\, \mathrm{d}\mathcal{V} + \int_{\mathcal{P}_R} s_{qR} - \boldsymbol{\nabla}_R \cdot \left[\, \boldsymbol{q}_R \,\right] \mathrm{d}\mathcal{V} \\ & + \int_{\mathcal{P}_R} {}^u\mu_L\, \dot{c}_{LR} - \boldsymbol{h}_{LR} \cdot \boldsymbol{\nabla}_R\, [\, {}^u\mu_L \,] + {}^u\mu_T\, \dot{c}_{TR} + ({}^u\mu_L - {}^u\mu_T)\; w_R^{(2.12)}\, \mathrm{d}\mathcal{V}\ .\end{aligned} \tag{2.31}$$

Since it must hold for any arbitrary region $\mathcal{P}_R \subset \mathcal{B}_R$, Eq. (2.31) can be localized as

$$\dot{u}_R = \mathbf{T}_R : \dot{\mathbf{F}} + s_{qR} - \boldsymbol{\nabla}_R \cdot \left[\, \boldsymbol{q}_R \,\right] + {}^u\mu_L\, \dot{c}_{LR} - \boldsymbol{h}_{LR} \cdot \boldsymbol{\nabla}_R\, [\, {}^u\mu_L \,] + {}^u\mu_T\, \dot{c}_{TR} + ({}^u\mu_L - {}^u\mu_T)\; w_R^{(2.12)}\ . \tag{2.32}$$

2.5.2 Entropy imbalance

Similarly to the energy balance, we augment the second law of thermodynamics with a flux of entropy due to species transport. We further assume that the mechanics does not contribute directly to the total entropy flow [54, 51]. The second law of thermodynamics is therefore defined as the balance of the interplay among the internal entropy of $\mathcal{P}_R$ and the entropy transferred in $\mathcal{P}_R$ due to the mass and the heat transferred on $\mathcal{P}_R$.

Denote with $\mathcal{S}$ the net internal entropy of $\mathcal{P}_R$, with $\mathcal{S}_i$ the entropy produced inside $\mathcal{P}_R$, with $\mathcal{Q}_\eta$ and $\mathcal{T}_\eta$ the entropy per unit time due to the heat and mass transfer, respectively. Then

$$\dot{\mathcal{S}}(\mathcal{P}_R) - \dot{\mathcal{S}}_i(\mathcal{P}_R) = \mathcal{Q}_\eta(\mathcal{P}_R) + \mathcal{T}_\eta(\mathcal{P}_R)\ . \tag{2.33}$$

The second law of thermodynamics states

$$\dot{\mathcal{S}}_i(\mathcal{P}_R) \geq 0\ , \tag{2.34}$$

from which Eq. (2.33) can be re-written in the form

$$\dot{\mathcal{S}}(\mathcal{P}_R) - \mathcal{Q}_\eta(\mathcal{P}_R) - \mathcal{T}_\eta(\mathcal{P}_R) \geq 0\ . \tag{2.35}$$

We state the specific net internal entropy (per unit reference volume) η_R so that

$$\mathcal{S}(\mathcal{P}_R) = \int_{\mathcal{P}_R} \eta_R\, \mathrm{d}\mathcal{V}\ , \tag{2.36}$$

and the individual contributions of the entropy imbalance (2.35) write as

$$\dot{\mathcal{S}}(\mathcal{P}_R) = \int_{\mathcal{P}_R} \dot{\eta}_R \, \mathrm{d}\mathcal{V} \; , \tag{2.37a}$$

$$\mathcal{Q}_\eta(\mathcal{P}_R) = \int_{\mathcal{P}_R} \frac{1}{T} \, s_{qR} \, \mathrm{d}\mathcal{V} - \int_{\partial\mathcal{P}_R} \frac{1}{T} \, \boldsymbol{q}_R \cdot \boldsymbol{n}_R \, \mathrm{d}\mathcal{A} \; , \tag{2.37b}$$

$$\mathcal{T}_\eta(\mathcal{P}_R) = \int_{\mathcal{P}_R} {}^{\eta}\mu_L \, s_{LR} + {}^{\eta}\mu_T \, s_{TR} \, \mathrm{d}\mathcal{V} - \int_{\partial\mathcal{P}_R} {}^{\eta}\mu_L \, \boldsymbol{h}_{LR} \cdot \boldsymbol{n}_R \, \mathrm{d}\mathcal{A} \; , \tag{2.37c}$$

with ${}^{\eta}\mu_\alpha$ the change in specific entropy provided by a unit supply of moles of species $\alpha = L, T$.

Application of the divergence theorem leads to re-write Eq. (2.37b) in the form

$$\mathcal{Q}_\eta(\mathcal{P}_R) = \int_{\mathcal{P}_R} \frac{1}{T} \, s_{qR} - \boldsymbol{\nabla}_R \cdot \left[\frac{1}{T} \, \boldsymbol{q}_R \right] \mathrm{d}\mathcal{V} = \int_{\mathcal{P}_R} \frac{1}{T} \, s_{qR} - \frac{1}{T} \, \boldsymbol{\nabla}_R \cdot \left[\, \boldsymbol{q}_R \, \right] + \frac{1}{T^2} \, \boldsymbol{q}_R \cdot \boldsymbol{\nabla}_R \left[\, T \, \right] \mathrm{d}\mathcal{V} \; , \tag{2.38}$$

and the procedure performed to derive the mass contribution to the energy balance $\mathcal{T}_u(\mathcal{P}_R)$ given by Eq. (2.30) allows us to write Eq. (2.37c) as

$$\mathcal{T}_\eta(\mathcal{P}_R) = \int_{\mathcal{P}_R} {}^{\eta}\mu_L \, \dot{c}_{LR} + {}^{\eta}\mu_T \, \dot{c}_{TR} - \boldsymbol{\nabla}_R \left[\, {}^{\eta}\mu_L \, \right] \cdot \boldsymbol{h}_{LR} + \left({}^{\eta}\mu_L - {}^{\eta}\mu_T \right) w_R^{(2.12)} \, \mathrm{d}\mathcal{V} \; . \tag{2.39}$$

Combination of Eq.s (2.37a), (2.38) and (2.39) yields

$$\begin{aligned} & \int_{\mathcal{P}_R} \dot{\eta}_R \, \mathrm{d}\mathcal{V} - \int_{\mathcal{P}_R} \frac{1}{T} \, s_{qR} - \frac{1}{T} \, \boldsymbol{\nabla}_R \cdot \left[\, \boldsymbol{q}_R \, \right] + \frac{1}{T^2} \, \boldsymbol{q}_R \cdot \boldsymbol{\nabla}_R \left[\, T \, \right] \mathrm{d}\mathcal{V} \\ & \qquad - \int_{\mathcal{P}_R} {}^{\eta}\mu_L \, \dot{c}_{LR} + {}^{\eta}\mu_T \, \dot{c}_{TR} - \boldsymbol{h}_{LR} \cdot \boldsymbol{\nabla}_R \left[\, {}^{\eta}\mu_L \, \right] + \left({}^{\eta}\mu_L - {}^{\eta}\mu_T \right) w_R^{(2.12)} \, \mathrm{d}\mathcal{V} \geq 0 \; , \end{aligned} \tag{2.40}$$

on any arbitrary region $\mathcal{P}_R \subset \mathcal{B}_R$. Eq. (2.40) can be localized as

$$\begin{aligned} & T \, \dot{\eta}_R - s_{qR} + \boldsymbol{\nabla}_R \cdot \left[\, \boldsymbol{q}_R \, \right] - \frac{1}{T} \, \boldsymbol{q}_R \cdot \boldsymbol{\nabla}_R \left[\, T \, \right] - T \, {}^{\eta}\mu_L \, \dot{c}_{LR} - T \, {}^{\eta}\mu_T \, \dot{c}_{TR} + T \, \boldsymbol{h}_{LR} \cdot \boldsymbol{\nabla}_R \left[\, {}^{\eta}\mu_L \, \right] \\ & \qquad - T \, \left({}^{\eta}\mu_L - {}^{\eta}\mu_T \right) w_R^{(2.12)} \geq 0 \; , \end{aligned} \tag{2.41}$$

after multiplication by the temperature.

Taking advantage from Eq. (5.51) to replace the factor $-s_{qR} + \boldsymbol{\nabla}_R \cdot \left[\, \boldsymbol{q}_R \, \right]$ in Eq. (2.41), we can rephrase the second law of thermodynamics as

$$\begin{aligned} & T \, \dot{\eta}_R - \dot{u}_R + \mathbf{T}_R : \dot{\mathbf{F}} + {}^{u}\mu_L \, \dot{c}_{LR} - \boldsymbol{h}_{LR} \cdot \boldsymbol{\nabla}_R \left[\, {}^{u}\mu_L \, \right] + {}^{u}\mu_T \, \dot{c}_{TR} + \left({}^{u}\mu_L - {}^{u}\mu_T \right) w_R^{(2.12)} - \frac{1}{T} \, \boldsymbol{q}_R \cdot \boldsymbol{\nabla}_R \left[\, T \, \right] \\ & \qquad - T \, {}^{\eta}\mu_L \, \dot{c}_{LR} - T \, {}^{\eta}\mu_T \, \dot{c}_{TR} + T \, \boldsymbol{h}_{LR} \cdot \boldsymbol{\nabla}_R \left[\, {}^{\eta}\mu_L \, \right] - T \, \left({}^{\eta}\mu_L - {}^{\eta}\mu_T \right) w_R^{(2.12)} \geq 0 \; , \end{aligned} \tag{2.42}$$

whence,

$$\begin{aligned} & T \, \dot{\eta}_R - \dot{u}_R + \mathbf{T}_R : \dot{\mathbf{F}} + \left({}^{u}\mu_L - T \, {}^{\eta}\mu_L \right) \dot{c}_{LR} + \left({}^{u}\mu_T - T \, {}^{\eta}\mu_T \right) \dot{c}_{TR} - \boldsymbol{h}_{LR} \cdot \boldsymbol{\nabla}_R \left[\, {}^{u}\mu_L \, \right] \\ & \qquad - \frac{1}{T} \, \boldsymbol{q}_R \cdot \boldsymbol{\nabla}_R \left[\, T \, \right] + T \, \boldsymbol{h}_{LR} \cdot \boldsymbol{\nabla}_R \left[\, {}^{\eta}\mu_L \, \right] + \left({}^{u}\mu_L - T \, {}^{\eta}\mu_L \right) w_R^{(2.12)} - \left({}^{u}\mu_T - T \, {}^{\eta}\mu_T \right) w_R^{(2.12)} \\ & \qquad \geq 0 \; . \end{aligned} \tag{2.43}$$

By denoting

$$\mu_\alpha = {}^{u}\mu_\alpha - T \, {}^{\eta}\mu_\alpha \; , \tag{2.44}$$

$$A^{(2.12)} = \mu_T - \mu_L \; , \tag{2.45}$$

we can cast the entropy imbalance (2.43) in the form

$$
\begin{aligned}
&T\,\dot{\eta}_R - \dot{u}_R + \mathbf{T}_R : \dot{\mathbf{F}} + \mu_L\,\dot{c}_{L_R} + \mu_T\,\dot{c}_{T_R} - \boldsymbol{h}_{L_R} \cdot \boldsymbol{\nabla}_R\,[\,{}^{u}\mu_L\,] - \frac{1}{T}\,\boldsymbol{q}_R \cdot \boldsymbol{\nabla}_R\,[\,T\,] + T\,\boldsymbol{h}_{L_R} \cdot \boldsymbol{\nabla}_R\,[\,{}^{\eta}\mu_L\,] \\
&\quad - A^{(2.12)}\,w_R^{(2.12)} \geq 0\ .
\end{aligned}
\tag{2.46}
$$

By noting that

$$
T\,\boldsymbol{h}_{L_R} \cdot \boldsymbol{\nabla}_R\,[\,{}^{\eta}\mu_L\,] = \boldsymbol{h}_{L_R} \cdot \boldsymbol{\nabla}_R\,[\,T\,{}^{\eta}\mu_L\,] - \boldsymbol{h}_{L_R} \cdot {}^{\eta}\mu_L\,\boldsymbol{\nabla}_R\,[\,T\,]\ , \tag{2.47}
$$

and according to definition (2.44), it holds

$$
\begin{aligned}
-\frac{1}{T}\,\boldsymbol{q}_R \cdot \boldsymbol{\nabla}_R\,[\,T\,] - \boldsymbol{h}_{L_R} \cdot \boldsymbol{\nabla}_R\,[\,{}^{u}\mu_L\,] + T\,\boldsymbol{h}_{L_R} \cdot \boldsymbol{\nabla}_R\,[\,{}^{\eta}\mu_L\,] =& \frac{1}{T}\left(\boldsymbol{q}_R + T\,{}^{\eta}\mu_L\,\boldsymbol{h}_{L_R}\right) \cdot \boldsymbol{\nabla}_R\,[\,T\,] \\
&- \boldsymbol{h}_{L_R} \cdot \boldsymbol{\nabla}_R\,[\,\mu_L\,]\ .
\end{aligned}
$$

Following [9], we introduce a new referential heat flux as

$$
\boldsymbol{q}\!\!\!\boldsymbol{-}_R = \boldsymbol{q}_R + T\,{}^{\eta}\mu_L\,\boldsymbol{h}_{L_R}\ , \tag{2.48}
$$

which leads to the alternative localized referential form of the entropy imbalance

$$
T\,\dot{\eta}_R - \dot{u}_R + \mathbf{T}_R : \dot{\mathbf{F}} - \frac{1}{T}\,\boldsymbol{q}\!\!\!\boldsymbol{-}_R \cdot \boldsymbol{\nabla}_R\,[\,T\,] + \mu_L\,\dot{c}_{L_R} + \mu_T\,\dot{c}_{T_R} - \boldsymbol{h}_{L_R} \cdot \boldsymbol{\nabla}\,[\,\mu_L\,] - A^{(2.12)}\,w_R^{(2.12)} \geq 0\ . \tag{2.49}
$$

2.5.2.1 Stress measures

The multiplicative decomposition of the deformation gradient performed in Eq. (2.7) leads to the splitting of the mechanical contribution to the entropy imbalance (5.56) into two separate terms, following the same path of reasoning of [55].

By means of Eq. (2.7), and the definition of the first Piola-Kirchhoff stress tensor (2.21), it holds that

$$
\mathbf{T}_R : \dot{\mathbf{F}} = J\,\mathbf{T}\,\mathbf{F}^{-\mathrm{T}} : \dot{\mathbf{F}} = J\,\mathbf{T}\,\mathbf{F}^{{cte}^{-\mathrm{T}}}\,\mathbf{F}^{{p}^{-\mathrm{T}}} : \dot{\mathbf{F}}^{cte}\,\mathbf{F}^{p} + J\,\mathbf{T}\,\mathbf{F}^{{cte}^{-\mathrm{T}}}\,\mathbf{F}^{{p}^{-\mathrm{T}}} : \mathbf{F}^{cte}\,\dot{\mathbf{F}}^{p}\ . \tag{2.50}
$$

The first term on the right-hand side of Eq. (2.50) can be manipulated in order to obtain

$$
J\,\mathbf{T}\,\mathbf{F}^{{cte}^{-\mathrm{T}}}\,\mathbf{F}^{{p}^{-\mathrm{T}}} : \dot{\mathbf{F}}^{cte}\,\mathbf{F}^{p} = J^{cte}\,J^{p}\,\mathbf{T}\,\mathbf{F}^{{cte}^{-\mathrm{T}}} : \dot{\mathbf{F}}^{cte} = J^{p}\,\mathbf{T}_R^{cte} : \dot{\mathbf{F}}^{cte} \tag{2.51}
$$

which represents the chemo-thermo-elastic part of the mechanical contribution to the entropy imbalance, and where the chemo-thermo-elastic first Piola-Kirchhoff stress tensor is defined as

$$
\mathbf{T}_R^{cte} = J^{cte}\,\mathbf{T}\,\mathbf{F}^{{cte}^{-\mathrm{T}}}\ . \tag{2.52}
$$

Another stress measure commonly used in finite strain theory in continuum mechanics is the second Piola-Kirchhoff stress tensor, here denoted with $\mathbf{S}$ and related to the first Piola-Kirchhoff stress tensor via the standard relation $\mathbf{T}_R = \mathbf{F}\,\mathbf{S}$. It is therefore possible to define the chemo-thermo-elastic second Piola-Kirchhoff stress tensor $\mathbf{S}^{cte}$ as

$$
\mathbf{S}^{cte} = \mathbf{F}^{{cte}^{-1}}\,\mathbf{T}_R^{cte} = J^{cte}\,\mathbf{F}^{{cte}^{-1}}\,\mathbf{T}\,\mathbf{F}^{{cte}^{-\mathrm{T}}}\ , \tag{2.53}
$$

whence, Eq. (2.51) can be cast in the form

$$
J^{p}\,\mathbf{T}_R^{cte} : \dot{\mathbf{F}}^{cte} = J^{p}\,\mathbf{F}^{cte}\,\mathbf{F}^{{cte}^{-1}}\mathbf{T}_R^{cte} : \dot{\mathbf{F}}^{cte} = J^{p}\,\mathbf{F}^{{cte}^{-1}}\mathbf{T}_R^{cte} : \mathbf{F}^{{cte}^{\mathrm{T}}}\dot{\mathbf{F}}^{cte} = J^{p}\,\mathbf{S}^{cte} : \mathbf{F}^{{cte}^{\mathrm{T}}}\dot{\mathbf{F}}^{cte}\ . \tag{2.54}
$$

We further define the chemo-thermo-elastic right Cauchy-Green and Green-Lagrange strain tensors as

$$
\mathbf{C}^{cte} = \mathbf{F}^{{cte}^{\mathrm{T}}}\mathbf{F}^{cte}\ , \tag{2.55a}
$$

$$
\mathbf{E}^{cte} = \frac{1}{2}\left(\mathbf{C}^{cte} - \mathbf{1}\right)\ . \tag{2.55b}
$$

The time derivative of $\mathbf{C}^{cte}$ simply writes

$$\dot{\mathbf{C}}^{cte} = \dot{\mathbf{F}}^{cte^{\mathrm{T}}} \mathbf{F}^{cte} + \mathbf{F}^{cte^{\mathrm{T}}} \dot{\mathbf{F}}^{cte} \ , \tag{2.56}$$

whereas[1], the time derivative of $\mathbf{E}^{cte}$ writes

$$\dot{\mathbf{E}}^{cte} = \frac{1}{2}\, \dot{\mathbf{C}}^{cte} = \operatorname{sym}\left[\mathbf{F}^{cte^{\mathrm{T}}} \dot{\mathbf{F}}^{cte} \right] \ . \tag{2.57}$$

By noting that the symmetry of $\mathbf{T}$ implies the symmetry of $\mathbf{S}^{cte}$, we write the chemo-thermo-elastic contribution (2.54) in the form

$$\begin{aligned} J^p\, \mathbf{T}^{cte}_{R} : \dot{\mathbf{F}}^{cte} &= J^p\, \mathbf{S}^{cte} : \mathbf{F}^{cte^{\mathrm{T}}} \dot{\mathbf{F}}^{cte} = J^p\, \mathbf{S}^{cte} : \operatorname{sym}\left[\mathbf{F}^{cte^{\mathrm{T}}} \dot{\mathbf{F}}^{cte} \right] = J^p\, \mathbf{S}^{cte} : \dot{\mathbf{E}}^{cte} \\ &= J^p\, \mathbf{S}^{cte} : \frac{1}{2}\, \dot{\mathbf{C}}^{cte} \ . \end{aligned} \tag{2.58}$$

according to Eq. (2.57).

The second right-hand side term of Eq. (2.50) represents the inelastic contribution to the entropy imbalance (5.56), and can be re-written as

$$J\, \mathbf{T}\, \mathbf{F}^{cte^{-\mathrm{T}}}\, \mathbf{F}^{p^{-\mathrm{T}}} : \mathbf{F}^{cte}\, \dot{\mathbf{F}}^{p} = J^{cte}\, J^p\, \mathbf{F}^{cte^{\mathrm{T}}}\, \mathbf{T}\, \mathbf{F}^{cte^{-\mathrm{T}}} : \dot{\mathbf{F}}^{p}\, \mathbf{F}^{p^{-1}} = J^p\, \mathbf{M}^{cte} : \mathbf{L}^p \ , \tag{2.59}$$

with $\mathbf{M}^{cte}$ chemo-thermo-elastic Mandel stress tensor,

$$\mathbf{M}^{cte} = J^{cte}\, \mathbf{F}^{cte^{\mathrm{T}}}\, \mathbf{T}\, \mathbf{F}^{cte^{-\mathrm{T}}} = \mathbf{C}^{cte}\, \mathbf{S}^{cte} \ , \tag{2.60}$$

according to Eq.s (2.53) and (2.55a).

Combining Eq. (2.58) with Eq. (2.59), we find that the mechanical contribution to the second law of thermodynamics takes the following final form

$$\mathbf{T}_{R} : \dot{\mathbf{F}} = \frac{1}{2}\, J^p\, \mathbf{S}^{cte} : \dot{\mathbf{C}}^{cte} + J^p\, \mathbf{M}^{cte} : \mathbf{L}^p \ . \tag{2.61}$$

2.5.3 Clausius-Duhem inequality

From the definition of the Helmholtz free energy density (per unit referential volume),

$$\psi_{R} = u_{R} - T\, \eta_{R} \ , \tag{2.62}$$

the first two terms of the localized referential form of the entropy imbalance (5.56) can be re-written as

$$T\, \dot{\eta}_{R} - \dot{u}_{R} = -\dot{\psi}_{R} - \dot{T}\, \eta_{R} \ . \tag{2.63}$$

According to Eq.s (2.61) and (2.63), the localized referential second law of thermodynamics (5.56) can be expressed in the form

$$\begin{aligned} &-\dot{\psi}_{R} - \dot{T}\, \eta_{R} - \frac{1}{T}\, \boldsymbol{q}_{R} \cdot \boldsymbol{\nabla}_{R} \left[\, T \,\right] + \frac{1}{2}\, J^p\, \mathbf{S}^{cte} : \dot{\mathbf{C}}^{cte} + J^p\, \mathbf{M}^{cte} : \mathbf{L}^p + \mu_L\, \dot{c}_{L_R} + \mu_T\, \dot{c}_{T_R} \\ &\quad - \boldsymbol{h}_{L_R} \cdot \boldsymbol{\nabla}_{R} \left[\, \mu_L \,\right] - A^{(2.12)}\, w^{(2.12)}_{R} \geq 0 \ . \end{aligned} \tag{2.64}$$

We take the referential Helmholtz free energy density as a function of temperature T, concentrations of species c_{α_R}, chemo-thermo-elastic right Cauchy-Green strain tensor $\mathbf{C}^{cte}$, and of

---

[1] Recall that

$$\mathbf{A} = \frac{1}{2}\left(\mathbf{A} + \mathbf{A}^{\mathrm{T}} \right) + \frac{1}{2}\left(\mathbf{A} - \mathbf{A}^{\mathrm{T}} \right) = \operatorname{sym}\left[\, \mathbf{A} \,\right] + \operatorname{skw}\left[\, \mathbf{A} \,\right] \ ,$$

for any tensor $\mathbf{A}$, and set $\mathbf{A} = \mathbf{F}^{cte^{\mathrm{T}}} \dot{\mathbf{F}}^{cte}$.

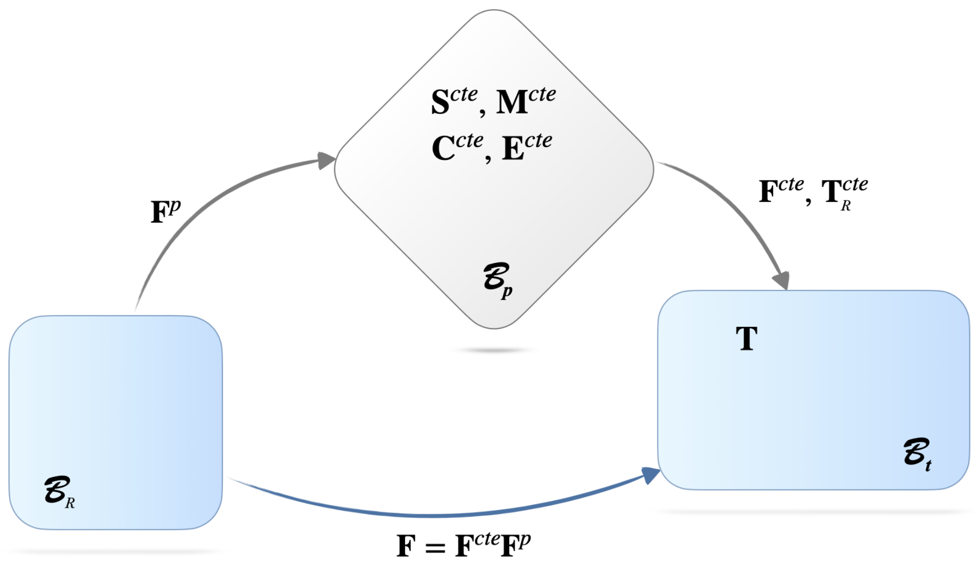

Figure 2.3: Schematic of the material $\mathcal{B}$, intermediate $\mathcal{B}_p$, and spatial $\mathcal{B}_t$ configurations, and of the stress and strain tensors in their domains. The chemo-thermo-elastic second Piola-Kirchhoff and Mandel stress tensors, $\mathbf{S}^{cte}$ and $\mathbf{M}^{cte}$, the chemo-thermo-elastic right Cauchy-Green and Green-Lagrange strain tensors, $\mathbf{C}^{cte}$ and $\mathbf{E}^{cte}$, from intermediate $\mathcal{B}_p$ to itself; the chemo-thermo-elastic first Piola-Kirchhoff stress tensor $\mathbf{T}_R^{cte}$, from intermediate $\mathcal{B}_p$ to spatial $\mathcal{B}_t$; the Cauchy stress tensor $\mathbf{T}$ from spatial $\mathcal{B}_t$ to itself.

a kinematic tensorial internal variable $\boldsymbol{\Xi}$ having the usual meaning in inelastic constitutive laws [53, 54, 58, 59, 60, 61]

$$\psi_R = \psi_R\left(T, c_{L_R}, c_{T_R}, \mathbf{C}^{cte}, \boldsymbol{\Xi}\right) \, . \tag{2.65}$$

The selection of $\mathbf{C}^{cte}$ as the strain internal variable appears here to be the most suitable choice in view of the multiplicative decomposition of the deformation gradient (2.7), which underpins the proposed framework. It is worth pointing out that alternative choices for the strain could be taken. A suitable choice is represented by the total right Cauchy-Green tensor, since the mechanical contribution in the Clausius-Duhem inequality would be solely represented in terms of total stress and strain tensors, *e.g.*, $\frac{1}{2}\,\mathbf{S} : \dot{\mathbf{C}}$, by following the same path of reasoning which led to Eq. (2.58).

In view of the selected functional dependence of the referential Helmholtz free energy density shown in Eq. (2.65), the time derivative of ψ_R writes as

$$\dot{\psi}_R = \frac{\partial \psi_R}{\partial \mathbf{C}^{cte}} : \dot{\mathbf{C}}^{cte} + \frac{\partial \psi_R}{\partial c_{L_R}}\, \dot{c}_{L_R} + \frac{\partial \psi_R}{\partial c_{T_R}}\, \dot{c}_{T_R} + \frac{\partial \psi_R}{\partial T}\, \dot{T} + \frac{\partial \psi_R}{\partial \boldsymbol{\Xi}} : \dot{\boldsymbol{\Xi}} \, . \tag{2.66}$$

By denoting the inelastic stress tensor conjugate to $\boldsymbol{\Xi}$ as

$$\mathbf{X} = -\frac{\partial \psi_R}{\partial \boldsymbol{\Xi}} \, , \tag{2.67}$$

we are able to combine Eq.s (2.49), (2.61), (2.66) and (2.67) in the Clausius-Duhem inequality in the form

$$\begin{aligned} &\left(\frac{1}{2}\, J^p\, \mathbf{S}^{cte} - \frac{\partial \psi_R}{\partial \mathbf{C}^{cte}}\right) : \dot{\mathbf{C}}^{cte} + \left(\mu_L - \frac{\partial \psi_R}{\partial c_{L_R}}\right) \dot{c}_{L_R} + \left(\mu_T - \frac{\partial \psi_R}{\partial c_{T_R}}\right) \dot{c}_{T_R} - \left(\eta_R + \frac{\partial \psi_R}{\partial T}\right) \dot{T} \\ &\quad + \mathbf{X} : \dot{\boldsymbol{\Xi}} + J^p\, \mathbf{M}^{cte} : \mathbf{L}^p - \frac{1}{T}\, \boldsymbol{q}_R \cdot \boldsymbol{\nabla}_R\, [\, T\,] - \boldsymbol{h}_{L_R} \cdot \boldsymbol{\nabla}_R\, [\, \mu_L\,] - A^{(2.12)}\, w_R^{(2.12)} \geq 0 \, . \end{aligned} \tag{2.68}$$

According to the method of Coleman and Noll [8], inequality (2.68) must hold for any value of the time derivative of the strain tensor $\mathbf{C}^{cte}$, of the concentrations of lattice and trapped species c_{L_R} and c_{T_R}, and of the temperature T.

The following thermodynamic restrictions thus arise

$$\mathbf{S}^{cte} = 2\, J^{p^{-1}} \left. \frac{\partial \psi_R}{\partial \mathbf{C}^{cte}} \right|_{T,\, c_{L_R},\, c_{T_R},\, \mathbf{\Xi}} , \tag{2.69a}$$

$$\eta_R = - \left. \frac{\partial \psi_R}{\partial T} \right|_{c_{L_R},\, c_{T_R},\, \mathbf{C}^{cte},\, \mathbf{\Xi}} , \tag{2.69b}$$

$$\mu_L = \left. \frac{\partial \psi_R}{\partial c_{L_R}} \right|_{T,\, c_{T_R},\, \mathbf{C}^{cte},\, \mathbf{\Xi}} , \tag{2.69c}$$

$$\mu_T = \left. \frac{\partial \psi_R}{\partial c_{T_R}} \right|_{T,\, c_{L_R},\, \mathbf{C}^{cte},\, \mathbf{\Xi}} . \tag{2.69d}$$

What remains of the Clausius-Duhem inequality (2.68) establishes irreversible processes. As we cannot place any restriction on the values of $\mathbf{C}^{cte}$, c_{α_R}, and T, the same applies for $\mathbf{L}^p$, $\mathbf{\Xi}$, $\boldsymbol{\nabla}_{\!R}\, [\, \mu_L \,]$, $\boldsymbol{\nabla}_{\!R}\, [\, T \,]$, and $w_R^{(2.12)}$. As a consequence, restrictions on $\mathbf{X}\!\!\!|$, $\mathbf{M}^{cte}$, $\boldsymbol{h}_{L_R}$, $\boldsymbol{q}_R$, and $A^{(2.12)}$ are determined. The internal entropy production (multiplied by T), can be written with the usual dissipative structure [62], namely

$$\underbrace{J^p\, \mathbf{M}^{cte} : \mathbf{L}^p + \mathbf{X}\!\!\!| : \dot{\mathbf{\Xi}}}_{\text{inelastic}} - \underbrace{\boldsymbol{h}_{L_R} \cdot \boldsymbol{\nabla}_{\!R}\, [\, \mu_L \,]}_{\text{diffusive}} - \underbrace{\frac{1}{T}\, \boldsymbol{q}_R \cdot \boldsymbol{\nabla}_{\!R}\, [\, T \,]}_{\text{thermal}} - \underbrace{w_R^{(2.12)}\, A^{(2.12)}}_{\text{chemical}} \geq 0 \, . \tag{2.70}$$

No coupling between fluxes and thermodynamic forces of different tensorial order is imposed in view of the assumption of Curie's symmetry principles [51]. Therefore the the following three conditions arise from the internal entropy production (2.70)

$$J^p\, \mathbf{M}^{cte} : \mathbf{L}^p + \mathbf{X}\!\!\!| : \dot{\mathbf{\Xi}} \geq 0 \, , \tag{2.71a}$$

$$\boldsymbol{h}_{L_R} \cdot \boldsymbol{\nabla}_{\!R}\, [\, \mu_L \,] + \frac{1}{T}\, \boldsymbol{q}_R \cdot \boldsymbol{\nabla}_{\!R}\, [\, T \,] \leq 0 \, , \tag{2.71b}$$

$$w_R^{(2.12)}\, A^{(2.12)} \leq 0 \, . \tag{2.71c}$$

Inequalities (2.71) restrict the values that thermodynamic fluxes can assume.

In view of thermodynamic restrictions (2.69c) and (2.69d), the scalars μ_α declared in Eq. (2.44) are seen to be chemical potentials[2], whereas $A^{(2.12)}$ is the affinity of the chemical reaction (2.12).

2.5.4 Specifications for ${}^u\mu_\beta$ and ${}^\eta\mu_\beta$

Thermodynamic restriction (2.69b) allows to express the specific net internal entropy η_R as a function of temperature T, concentration of species c_{L_R} and c_{T_R}, chemo-thermo-mechanical strain tensor $\mathbf{C}^{cte}$, and kinematic tensorial internal variable $\mathbf{\Xi}$. Being the net internal energy u_R function of η_R, it can be defined as a function of the same thermodynamic variables, namely

$$u_R = u_R(\eta_R\, (T, \mathbf{C}^{cte}, c_{L_R}, c_{T_R}, \mathbf{\Xi}),\, \mathbf{C}^{cte}, c_{L_R}, c_{T_R}, \mathbf{\Xi}) \, . \tag{2.72}$$

---

[2] It is perhaps worth to point out that the chemical potential μ_α has the same material and spatial description, in that the derivative of ψ with respect to c_α and the derivative of ψ_R with respect to c_{α_R} are the same. This arises from the fact that, in defining the referential Helmholtz free energy,

$$\int_{\mathcal{P}_t} \psi \; \mathrm{d}v = \int_{\mathcal{P}_t} \rho\, \psi_m \; \mathrm{d}v = \int_{\mathcal{P}_R} \rho\, \psi_m\, J \; \mathrm{d}\mathcal{V} = \int_{\mathcal{P}_R} \rho_R\, \psi_m \; \mathrm{d}\mathcal{V} \, ,$$

hence, being $\rho_{\alpha_R} = \kappa_\alpha\, c_{\alpha_R}$, both the derivative of ψ with respect to c_α and the derivative of ψ_R with respect to c_{α_R} result in the Helmholtz free energy per unit mass ψ_m. The same applies to ${}^u\mu_\alpha$ and ${}^\eta\mu_\alpha$ with respect to the net internal energy and the entropy, respectively.

Taking advantage of the thermodynamic restrictions (2.69c), (2.69d) and of the definition (2.62) of the referential Helmholtz free energy density, the chemical potential of species α can be derived in the form

$$\begin{aligned}\mu_\alpha(T, \mathbf{C}^{cte}, c_{\alpha_R}, \boldsymbol{\Xi}) &= \frac{\partial}{\partial c_{\alpha_R}} \psi_{_R}(T, \mathbf{C}^{cte}, c_{\alpha_R}, \boldsymbol{\Xi}) = \frac{\partial u_{_R}}{\partial c_{\alpha_R}} + \frac{\partial u_{_R}}{\partial \eta_{_R}} \frac{\partial \eta_{_R}}{\partial c_{\alpha_R}} - T \, \frac{\partial \eta_{_R}}{\partial c_{\alpha_R}} \\ &= \frac{\mathrm{d} u_{_R}}{\mathrm{d} c_{\alpha_R}} - T \, \frac{\partial \eta_{_R}}{\partial c_{\alpha_R}} \; ,\end{aligned} \tag{2.73}$$

at fixed entropy. In view of definition (2.44) we compute the entropy per mole ${}^{\eta}\mu_\alpha$ as

$${}^{\eta}\mu_\alpha = \frac{\partial \eta_{_R}}{\partial c_{\alpha_R}} = - \frac{\partial}{\partial c_{\alpha_R}} \frac{\partial \psi_{_R}}{\partial T} = - \frac{\partial}{\partial T} \frac{\partial \psi_{_R}}{\partial c_{\alpha_R}} = - \frac{\partial}{\partial T} \, \mu_\alpha(T, \mathbf{C}^{cte}, c_{\alpha_R}, \boldsymbol{\Xi}) \; . \tag{2.74}$$

The following specification for the energy per mole ${}^{u}\mu_\alpha$ arises from Eq. (2.73)

$${}^{u}\mu_\alpha = \mu_\alpha + T \, {}^{\eta}\mu_\alpha = \mu_\alpha + T \, \frac{\partial \eta_{_R}}{\partial c_{\alpha_R}} \; . \tag{2.75}$$

Eqs (2.44), (2.69c), (2.69d) and (2.73) allow eventually to state

$${}^{\eta}\mu_\alpha = - \frac{\partial^2 \psi_{_R}}{\partial c_{\alpha_R} \partial T} \; , \tag{2.76a}$$

$${}^{u}\mu_\alpha = \frac{\partial \psi_{_R}}{\partial c_{\alpha_R}} - T \, \frac{\partial^2 \psi_{_R}}{\partial c_{\alpha_R} \partial T} \; . \tag{2.76b}$$

Remark. The identifications of the energetic and entropic contributions to the chemical potential given by Eq.s (2.76) provide a neat formulation for the entropy production inequality (2.71b). Recalling the definition of the new referential heat flux $\boldsymbol{\mathchar'26\mkern-9mu q}_{_R}$ (2.48), we find that

$$\begin{aligned}\boldsymbol{h}_{L_R} \cdot \boldsymbol{\nabla}_{_R} [\, \mu_L \,] + \frac{1}{T} \, \boldsymbol{\mathchar'26\mkern-9mu q}_{_R} \cdot \boldsymbol{\nabla}_{_R} [\, T \,] &= \boldsymbol{h}_{L_R} \cdot \boldsymbol{\nabla}_{_R} [\, \mu_L \,] + \frac{1}{T} \, \boldsymbol{q}_{_R} \cdot \boldsymbol{\nabla}_{_R} [\, T \,] + {}^{\eta}\mu_L \, \boldsymbol{h}_{L_R} \cdot \boldsymbol{\nabla}_{_R} [\, T \,] \\ &= \boldsymbol{h}_{L_R} \cdot (\, \boldsymbol{\nabla}_{_R} [\, \mu_L \,] + {}^{\eta}\mu_L \, \boldsymbol{\nabla}_{_R} [\, T \,] \,) + \frac{1}{T} \, \boldsymbol{q}_{_R} \cdot \boldsymbol{\nabla}_{_R} [\, T \,] \; .\end{aligned} \tag{2.77}$$

In addition, Eq. (2.76a) establishes the independence of the vector $\boldsymbol{\nabla}_{_R} [\, \mu_L \,] + {}^{\eta}\mu_L \, \boldsymbol{\nabla}_{_R} [\, T \,]$ from the temperature gradient. Indeed, simple algebra collected in Appendix A.1 leads to

$$\begin{aligned}\boldsymbol{\nabla}_{_R} [\, \mu_L \,] + {}^{\eta}\mu_L \, \boldsymbol{\nabla}_{_R} [\, T \,] = \; & \frac{\partial^2 \psi_{_R}}{\partial c_{L_R}^2} \, \boldsymbol{\nabla}_{_R} [\, c_{L_R} \,] + \frac{\partial^2 \psi_{_R}}{\partial c_{L_R} \partial c_{T_R}} \, \boldsymbol{\nabla}_{_R} [\, c_{T_R} \,] + \frac{\partial^2 \psi_{_R}}{\partial c_{L_R} \partial \mathbf{C}^{cte}} : \boldsymbol{\nabla}_{_R} \left[\, \mathbf{C}^{cte} \,\right] \\ & + \frac{\partial^2 \psi_{_R}}{\partial c_{L_R} \partial \boldsymbol{\Xi}} : \boldsymbol{\nabla}_{_R} [\, \boldsymbol{\Xi} \,] \; .\end{aligned} \tag{2.78}$$

2.5.5 Strain Decomposition

The current Section provides the specifications for both the swelling (de-swelling) contribution and the thermal contribution to the deformation gradient, and the resulting velocity gradients, as performed in [2] to describe the chemo-thermo-mechanics of cells, and following the path of reasoning of [55].

Recall the multiplicative decomposition of the $\mathbf{F}^{cte}$ given by Eq. (2.8). The swelling (de-swelling) distorsion $\mathbf{F}^{s}$ due to the conversion of mobile to trapped species (and vice-versa), and the thermal distorsion $\mathbf{F}^{th}$, are henceforth assumed to have a spherical form, hence

$$\mathbf{F}^{s} = \lambda_s \, \mathbf{1} \; , \tag{2.79a}$$

$$\mathbf{F}^{th} = \lambda_{th} \, \mathbf{1} \; , \tag{2.79b}$$

with λ_s and λ_{th} positive coefficients termed chemical swelling and thermal stretch, respectively.

The swelling volumetric Jacobian and its evolution in time write as

$$J^s = \det\left[\,\mathbf{F}^s\,\right] = \lambda_s^3 \;, \tag{2.80a}$$

$$\dot{J}^s = 3\,\lambda_s^2\,\dot{\lambda}_s \;, \tag{2.80b}$$

and the velocity gradient

$$\mathbf{L}^s = \dot{\mathbf{F}}^s\,\mathbf{F}^{s^{-1}} = \frac{\dot{\lambda}_s}{\lambda_s}\,\mathbf{1} = \frac{1}{\lambda_s}\,\frac{1}{3}\,\frac{\dot{J}_s}{\lambda_s^2}\,\mathbf{1} = \frac{1}{3}\,\frac{\dot{J}_s}{\lambda_s^3}\,\mathbf{1} = \frac{1}{3}\,\frac{\dot{J}^s}{J^s}\,\mathbf{1} \;. \tag{2.81}$$

Having the same spherical form of $\mathbf{F}^s$, the thermal distorsion $\mathbf{F}^{th}$, given by Eq. (2.79b), leads to results of the same form. Hence, with regard to the thermal volumetric Jacobian, it holds

$$J^{th} = \det\left[\,\mathbf{F}^{th}\,\right] = \lambda_{th}^3 \;, \tag{2.82a}$$

$$\dot{J}^{th} = 3\,\lambda_{th}^2\,\dot{\lambda}_{th} \;, \tag{2.82b}$$

whereas the thermal velocity gradient writes as

$$\mathbf{L}^{th} = \dot{\mathbf{F}}^{th}\,\mathbf{F}^{th^{-1}} = \frac{\dot{\lambda}_{th}}{\lambda_{th}}\,\mathbf{1} = \frac{1}{3}\,\frac{\dot{J}^{th}}{J^{th}}\,\mathbf{1} \;. \tag{2.83}$$

We further assume that the skew-symmetric part of both the swelling velocity gradient and the thermal velocity gradient are negligible, therefore $\mathbf{W}^s = 0$ and $\mathbf{W}^{th} = 0$, from which descends

$$\mathbf{L}^s \equiv \mathbf{D}^s \;, \qquad \mathbf{L}^{th} \equiv \mathbf{D}^{th} \;. \tag{2.84}$$

2.5.5.1 Assumptions on $\mathbf{L}^s$

To specify the swelling velocity gradient (2.81) in terms of concentrations of diffusive and trapped species, c_{L_R} and c_{T_R}, take a function $f^s(c_{L_R}, c_{T_R})$, and define the swelling volumetric Jacobian as

$$J^s = f^s(c_{L_R}, c_{T_R}) = f_L^s(c_{L_R})\, f_T^s(c_{T_R}) \;. \tag{2.85}$$

Furthermore, denote with $\omega_L^s > 0$ and $\omega_T^s > 0$ the chemical expansion coefficients of species L and T, obtained as the derivative of Eq. (2.85) with respect to c_{L_R} and c_{T_R}, respectively. Then

$$\omega_L^s(c_{L_R}, c_{T_R}) = \frac{\partial f_L^s(c_{L_R})}{\partial c_{L_R}}\, f_T^s(c_{T_R}) \;, \tag{2.86a}$$

$$\omega_T^s(c_{L_R}, c_{T_R}) = \frac{\partial f_T^s(c_{T_R})}{\partial c_{T_R}}\, f_T^s(c_{L_R}) \;. \tag{2.86b}$$

According to Eq.s (2.86), the evolution in time of J^s (2.85) can be re-written as

$$\begin{aligned} \dot{J}^s = \dot{f}^s(c_{L_R}, c_{T_R}) &= \dot{f}_L^s(c_{L_R})\, f_T^s(c_{T_R}) + f_L^s(c_{L_R})\, \dot{f}_T^s(c_{T_R}) = \frac{\partial f_L^s}{\partial c_{L_R}}\, \dot{c}_{L_R}\, f_T^s + f_L^s\, \frac{\partial f_T^s}{\partial c_{T_R}}\, \dot{c}_{T_R} \\ &= \omega_L^s\, \dot{c}_{L_R} + \omega_T^s\, \dot{c}_{T_R} \;. \end{aligned} \tag{2.87}$$

Denote with Θ_L^s, Θ_T^s the ratio between Eq.s (2.86a), (2.86b) and Eq. (2.85), namely

$$\Theta_L^s(c_{L_R}) = \frac{\omega_L^s(c_{L_R}, c_{T_R})}{f^s(c_{L_R}, c_{T_R})} = \frac{1}{f_L^s(c_{L_R})\, f_T^s(c_{T_R})}\, \frac{\partial f_{L_R}^s}{\partial c_{L_R}}\, f_T^s(c_{T_R}) = \frac{1}{f_L^s}\, \frac{\partial f_{L_R}^s}{\partial c_{L_R}} \;, \tag{2.88a}$$

$$\Theta_T^s(c_{T_R}) = \frac{\omega_T^s(c_{L_R}, c_{T_R})}{f^s(c_{L_R}, c_{T_R})} = \frac{1}{f_L^s(c_{L_R})\, f_T^s(c_{T_R})}\, \frac{\partial f_{T_R}^s}{\partial c_{T_R}}\, f_L^s(c_{L_R}) = \frac{1}{f_T^s}\, \frac{\partial f_{T_R}^s}{\partial c_{T_R}} \;. \tag{2.88b}$$

Accordingly, the swelling velocity gradient $\mathbf{L}^s$ shown in Eq. (2.81) takes the form

$$\begin{aligned} \mathbf{L}^s &= \frac{1}{3}\,\frac{\dot{J}^s}{J^s}\,\mathbf{1} = \frac{1}{3}\,\frac{1}{f_L^s\,f_T^s}\,(\,\omega_L^s\,\dot{c}_{L_R} + \omega_T^s\,\dot{c}_{T_R}\,)\,\mathbf{1} = \frac{1}{3}\,\frac{1}{f_L^s\,f_T^s}\left(\frac{\partial f_L^s}{\partial c_{L_R}}\,f_T^s\,\dot{c}_{L_R} + \frac{\partial f_T^s}{\partial c_{T_R}}\,f_L^s\,\dot{c}_{L_R}\right)\mathbf{1} \\ &= \frac{1}{3}\left(\frac{1}{f_L^s}\,\frac{\partial f_L^s}{\partial c_{L_R}}\,\dot{c}_{L_R} + \frac{1}{f_T^s}\,\frac{\partial f_T^s}{\partial c_{T_R}}\,\dot{c}_{L_R}\right)\mathbf{1} = \frac{1}{3}\,(\,\Theta_L^s\,\dot{c}_{L_R} + \Theta_T^s\,\dot{c}_{T_R}\,)\,\mathbf{1}\;. \end{aligned} \tag{2.89}$$

A classical specification for the functions $f_L^s(c_{L_R})$ and $f_T^s(c_{T_R})$ is represented by the relations

$$f_L^s(c_{L_R}) = 1 + \left(c_{L_R} - c_{L_R}^0\right)\,\omega_{L_R}^s\;, \qquad f_T^s(c_{T_R}) = 1 + \left(c_{T_R} - c_{T_R}^0\right)\,\omega_{T_R}^s\;, \tag{2.90a}$$

with $c_{\alpha_R}^0$ reference (datum) value of the concentration of species. Eq.s (2.88) take the form

$$\Theta_L^s(c_{L_R}, c_{T_R}) = \frac{\omega_L^s}{1 + \left(c_{L_R} - c_{L_R}^0\right)\,\omega_{L_R}^s}\;, \qquad \Theta_T^s(c_{L_R}, c_{T_R}) = \frac{\omega_T^s}{1 + \left(c_{T_R} - c_{T_R}^0\right)\,\omega_{T_R}^s}\;. \tag{2.91a}$$

2.5.5.2 Assumptions on $\mathbf{L}^{th}$

Specifications for the thermal velocity gradient are given hereafter with the same structure used in the previous section. Hence, by defining with $f^{th}(T)$, the function which identifies the thermal volumetric Jacobian,

$$J^{th} = f^{th}(T)\;, \tag{2.92}$$

its time derivative writes as

$$\dot{J}^{th} = \frac{\partial f^{th}(T)}{\partial T}\,\dot{T} = \gamma\,\dot{T}\;, \tag{2.93}$$

where γ denotes the thermal expansion coefficient,

$$\gamma = \frac{\partial f^{th}}{\partial T}\;. \tag{2.94}$$

Following the same path of reasoning of Eq.s (2.88), we find that the ratio $\Theta^{th}(T)$ writes as

$$\Theta^{th}(T) = \frac{\gamma}{J^{th}} = \frac{\gamma}{f^{th}(T)}\;, \tag{2.95}$$

from which descends the thermal velocity gradient $\mathbf{L}^{th}$ as

$$\mathbf{L}^{th} = \frac{1}{3}\,\frac{\dot{J}^{th}}{J^{th}}\,\mathbf{1} = \frac{1}{3}\,\frac{1}{f^{th}}\,\gamma\,\dot{T}\,\mathbf{1} = \frac{1}{3}\,\Theta^{th}\,\dot{T}\,\mathbf{1}\;. \tag{2.96}$$

in accordance with Eq.s (2.83), (2.92), (2.93), (2.95).

A classical choice for the function $f^{th}(T)$ is given by the relation

$$f^{th}(T) = 1 + \gamma\,\left(T - T_0\right)\;, \tag{2.97}$$

with T_0 the reference (datum) temperature, whence

$$\Theta^{th}(T) = \frac{\gamma}{1 + \gamma\,\left(T - T_0\right)}\;. \tag{2.98}$$

2.5.5.3 Definition of $\mathbf{C}^e$

To make explicit the elastic part of $\mathbf{C}^{cte}$, recall the multiplicative decomposition of $\mathbf{F}^{cte}$ given by Eq. (2.8), and the definitions of the swelling and thermal deformation gradients, $\mathbf{F}^s$ and $\mathbf{F}^{th}$, shown in Eq.s (2.79).

The chemo-thermo-elastic deformation gradient can be therefore re-written as

$$\mathbf{F}^{cte} = \mathbf{F}^e\,\mathbf{F}^{th}\,\mathbf{F}^s = \mathbf{F}^e\,\lambda_{th}\,\lambda_s\;. \tag{2.99}$$

It follows that, the elastic right Cauchy-Green strain tensor takes the form

$$\mathbf{C}^e = \mathbf{F}^{e^{\mathrm{T}}}\mathbf{F}^e = \lambda_s^{-1}\,\lambda_{th}^{-1}\,\mathbf{F}^{cte^{\mathrm{T}}}\,\lambda_s^{-1}\,\lambda_{th}^{-1}\,\mathbf{F}^{cte} = \lambda_s^{-2}\,\lambda_{th}^{-2}\,\mathbf{C}^{cte} = J^{s^{-\frac{2}{3}}}\,J^{th^{-\frac{2}{3}}}\,\mathbf{C}^{cte}\;. \tag{2.100}$$

2.6 Constitutive theory

2.6.1 Helmholtz free energy

The referential Helmholtz free energy density ψ_R is additively decomposed as

$$\begin{aligned}\psi_R(T, c_{L_R}, c_{T_R}, \mathbf{C}^{cte}, \Xi) = \psi_0 + \psi_R^{th}(T, c_{L_R}, c_{T_R}) + \psi_R^{diff}(T, c_{L_R}, c_{T_R}, \mathbf{C}^{cte}, \Xi) \\ + \psi_R^{el}(T, c_{L_R}, c_{T_R}, \mathbf{C}^{cte}) + \psi_R^{in}(T, c_{L_R}, c_{T_R}, \Xi) \; .\end{aligned} \tag{2.101}$$

Terms in Eq. (2.101), a detailed analysis of which can be found in [63], have the following meaning. ψ_0 is a datum value; ψ_R^{th} represents the thermal contribution, ψ_R^{diff} the diffusive contribution, ψ_R^{el} the elastic contribution, and ψ_R^{in} is the inelastic counterpart of ψ_R.

Compared to the small strain analysis [9], the material description of Eq. (2.101) entails a dependence of the diffusive contribution upon the strain, as is better reasoned hereinafter.

The thermal contribution $\psi_R^{th}(T, c_{L_R}, c_{T_R})$ is taken of the form

$$\psi_R^{th}(T, c_{L_R}, c_{T_R}) = - \sum_{\alpha = H,L,T} c_{\alpha_R} \, {}^{\eta}\mu_\alpha^0 \, (T - T_0) + \frac{1}{2} \frac{c_{v\,\alpha}^0 \, c_{\alpha_R}}{T_0} \, (T - T_0)^2 \; . \tag{2.102}$$

Symbols in Eq. (2.102) have the following meaning: the subscript H is used to designate the host material, whose concentration, in moles per unit reference volume, is denoted with c_{H_R}; c_{vH}^0, c_{vL}^0, and c_{vT}^0 represent the specific heats of the host material, the diffusive and the trapped species, respectively. The specific heat of each species is taken to be constant and, being (conventionally) energy per mole per degree Kelvin, it multiplies the referential concentration of their respective species, to be converted to energy per unit reference volume. Lastly, to allow for entropy exchange through thermal fluctuations, the terms ${}^{\eta}\mu_H^0$, ${}^{\eta}\mu_L^0$, and ${}^{\eta}\mu_T^0$ appear in Eq. (2.102).

The transport contribution $\psi_R^{diff}(T, c_{L_R}, c_{T_R}, \mathbf{C}^{cte}, \Xi)$ is the referential free energy density of mobile interstitial species that interact with the host material. In the continuum approximation of mixing, it is here described by a regular solution model [55, 52] which accounts for the entropy of mixing as well as the enthalpic interactions. It has the form

$$\psi_R^{diff}(T, c_{L_R}, c_{T_R}, \mathbf{C}^{cte}, \Xi) = \mu_L^0 \, c_{L_R} - T \, \eta_{L_R}^{diff} + \mu_T^0 \, c_{T_R} - T \, \eta_{T_R}^{diff} - T \, \eta_{L_R}^{\chi} \; . \tag{2.103}$$

The terms μ_L^0 and μ_T^0 represent reference values of chemical potentials that specify the free energy in the absence of interaction and entropic contributions. Furthermore, by means of μ_L^0 and μ_T^0 it is possible to define the trap energy ΔE_T, *i.e.*, the negative of the Gibbs free energy change, as

$$\Delta E_T = \mu_L^0 - \mu_T^0 = R \, T \ln \left[K_{eq} \right] \; , \tag{2.104}$$

where K_{eq} represents the equilibrium constant of the chemical reaction (2.12).

The entropy of mixing $\eta_{L_R}^{diff}$ and $\eta_{T_R}^{diff}$ is provided by statistical mechanics, in terms of the density of states Ω_α, by means of the Boltzmann's equation,

$$\eta_{\alpha_R}^{diff} = k_B \ln \left[\Omega_{\alpha_R} \right] \; , \tag{2.105}$$

with k_B the Boltzmann constant. In the case of a two-state system [64],

$$\Omega_{\alpha_R} = \left(\vartheta_{\alpha_R}^{\vartheta_{\alpha_R}} \, (1 - \vartheta_{\alpha_R})^{1 - \vartheta_{\alpha_R}} \right)^{-N_A \, c_{\alpha_R}^{max}} \; , \tag{2.106}$$

with N_A Avogadro's number, $c_{\alpha_R}^{max}$ the referential saturation for species α, and ϑ_{α_R} defined by the ratio

$$\vartheta_{\alpha_R}(\boldsymbol{X}, t) = \frac{c_{\alpha_R}}{c_{\alpha_R}^{max}} \; . \tag{2.107}$$

We here assume that, $c_{\alpha_R}^{max}$ being defined on the volume $\mathcal{P}$, it behaves in accordance with the transformation rule (7.3), and therefore in the same way as the referential concentration defined by Eq. $(2.17)_1$ (see Figure 2.4*a*). It follows that,

$$c_{\alpha_R}^{max}(\boldsymbol{X},t) = J\, c_{\alpha}^{max} \; . \tag{2.108}$$

Eq. (2.108) implies that $c_{\alpha_R}^{max}$ is not a constant value, therefore leading to the dependence of the transport contribution $\eta_{\alpha_R}^{diff}$ upon $\mathbf{C}^{cte}$ by means of the Jacobian J.

On the contrary, according to Eq.s $(2.17)_1$ and (2.108), the ratio θ_{α_R} (2.107) is configuration invariant, *i.e.*

$$\vartheta_{\alpha_R}(\boldsymbol{X},t) = \vartheta_{\alpha}(\boldsymbol{x},t) \; . \tag{2.109}$$

By entering Eq. (2.106) into the Boltzmann's equation (2.105), and recalling the definition of the universal gas constant, $R = k_B N_A$, one finds

$$\eta_{L_R}^{diff} = -R\, c_{L_R}^{max} \; \left(\vartheta_L \ln\left[\, \vartheta_L \,\right] + (1-\vartheta_L) \ln\left[\, 1-\vartheta_L \,\right] \right) \; . \tag{2.110}$$

The specification for $\eta_{T_R}^{diff}$ has the same form stated by Eq. (2.110). However, by noting that the saturation limit for trapped species may change in time due to inelastic deformations of the host material, we select a dependence of $c_{T_R}^{max}$ upon $\boldsymbol{\Xi}$. Then

$$\eta_{T_R}^{diff} = -R\, c_{T_R}^{max}(\boldsymbol{\Xi}) \; \left(\vartheta_T(\boldsymbol{\xi}) \ln\left[\, \vartheta_T(\boldsymbol{\Xi}) \,\right] + (1-\vartheta_T(\boldsymbol{\xi})) \ln\left[\, 1-\vartheta_T(\boldsymbol{\Xi}) \,\right] \right) \; . \tag{2.111}$$

Lastly, the excess Gibbs energy writes as

$$-T\, \eta_{L_R}^{\chi} = R\, T\, c_{L_R}^{max}\, \chi\, \vartheta_L\, (1-\vartheta_L) \tag{2.112}$$

where the Flory interaction parameter χ , also termed the exchange parameter [64], allows us to characterize the energy of interaction between diffusive species and insertion sites of the host material. Eq. (2.112) endows the free energy density with a nonconvex behavior with respect to c_{L_R} for $\chi > 2$, which in turn may lead to phase segregation [65, 39, 66]. If all interactions between mobile species and host sites are the same, then $\chi = 0$ and there is no enthalpy of mixing, therefore implying an ideal, purely entropic mixing.

Combining Eq.s (2.110), (2.111) and (2.112), the referential diffusive contribution to the Helmholtz free energy re-writes as

$$\begin{aligned} \psi_R^{diff}(T, c_{L_R}, c_{T_R}, \mathbf{C}^{cte}, \boldsymbol{\Xi}) = {} & R\, T\, c_{L_R}^{max}\, \chi\, \vartheta_L\, (1-\vartheta_L) \\ & + \sum_{\alpha=L,T} \mu_\alpha^0\, c_{\alpha_R} + R\, T\, c_{\alpha_R}^{max} \; \left(\vartheta_\alpha \ln\left[\, \vartheta_\alpha \,\right] + (1-\vartheta_\alpha) \ln\left[\, 1-\vartheta_\alpha \,\right] \right) \end{aligned} \tag{2.113}$$

The elastic contribution to the free energy can be written in many possible ways, with material parameters changing with concentrations and temperature. In [55] it is taken in the form

$$\psi_R^{el}(\mathbf{E}^e, c_{L_R}, c_{T_R}) = \frac{1}{2}\, \mathbf{E}^e : \mathbb{C} : \mathbf{E}^e \; , \tag{2.114}$$

with $\mathbf{E}^e = \frac{1}{2}(\mathbf{C}^e - \mathbf{1})$ elastic Green-Lagrange strain tensor and $\mathbb{C}$ a fourth-order tensor given by

$$\mathbb{C} = 2\, G(c_{L_R}, c_{T_R})\, \mathbf{1}^4 + \left(K(c_{L_R}, c_{T_R}) - \frac{2}{3}\, G(c_{L_R}, c_{T_R}) \right) \, \mathbf{1}^2 \otimes \mathbf{1}^2 \; , \tag{2.115}$$

where $G(c_{L_R}, c_{T_R})$ and $K(c_{L_R}, c_{T_R})$ represent the bulk and shear modulus, respectively. *Mooney-Rivlin* materials would be written, instead, as

$$\psi_R^{el}(\mathbf{C}^e, c_{L_R}, c_{T_R}) = C_1(c_{L_R}, c_{T_R}) \; [I_1(\mathbf{C}^e) - 3] + C_2(c_{L_R}, c_{T_R}) \; [I_2(\mathbf{C}^e) - 3] \tag{2.116}$$

with $C_1(c_{L_R}, c_{T_R})$ and $C_2(c_{L_R}, c_{T_R})$ material constants to be empirically determined, and $I_j(\mathbf{C}^e)$ j-th invariant of $\mathbf{C}^e$. *Compressible Neo-Hookean* materials would instead be written in the form [59]

$$\psi_R^{el}(\mathbf{C}^e, c_{L_R}, c_{T_R}) = \psi_R^{el,iso}(\mathbf{C}^e, c_{L_R}, c_{T_R}) + \psi_R^{el,vol}(J^e, c_{L_R}, c_{T_R}) \tag{2.117}$$

with $\psi_R^{el,iso}(\mathbf{C}^e, c_{L_R}, c_{T_R})$ the deviatoric, or isochoric, contribution to the elastic free energy density, usually taken as

$$\psi_R^{el,iso}(\mathbf{C}^e, c_{L_R}, c_{T_R}) = \frac{1}{2}\, G(c_{L_R}, c_{T_R}) \left[J^{e^{-\frac{2}{3}}}\, I_1(\mathbf{C}^e) - 3 \right] \,, \tag{2.118}$$

and $\psi_R^{el,vol}(J^e, c_{L_R}, c_{T_R})$ the volumetric part of the elastic free energy density, which can be assumed to have the forms [67]

$$\psi_R^{el,vol}(J^e, c_{L_R}, c_{T_R}, T) = \frac{1}{2}\, K(c_{L_R}, c_{T_R})\, \ln^2 [\, J^e \,] \,, \tag{2.119a}$$

$$\psi_R^{el,vol}(J^e, c_{L_R}, c_{T_R}, T) = \frac{1}{4}\, K(c_{L_R}, c_{T_R}) \left[\ln^2 [\, J^e \,] + (J^e - 1)^2 \right] \,. \tag{2.119b}$$

All these free energies depend upon concentrations intrinsically, *i.e.*, material parameters as the shear and bulk moduli change with the concentration and temperature.

Remark. The ratio ϑ_{α_R} (2.107) accounts for the saturation limit $c_{\alpha_R}^{max}$ of the species involved in the chemical reaction (2.12).

The assumption (2.108) leads to the configurational invariance of the ratio ϑ_{α_R}, as specified by Eq. (2.109). In other words, the number of moles occupying a convecting volume is invariant with time, *i.e.*, it does not change from $\mathcal{B}$ to $\mathcal{B}_t$. The saturation concentration $c_{\alpha_R}^{max}$, on the other hand, is time dependent according to the transformation rule (2.17). This case is depicted in Figure 2.4*a*.

Conversely, Figure 2.4*b* shows another case in which species can relocate to occupy an eventual volume expansion of the hosting material. The maximum number of moles per unit volume $c_{\alpha_R}^{max}$ is therefore time invariant, *i.e.*, $c_{\alpha_R}^{max}(\boldsymbol{X}) = c_{\alpha}^{max}(\boldsymbol{x})$. It descends that

$$\vartheta_{\alpha_R}(\boldsymbol{X}, t) = J\, \vartheta_\alpha(\boldsymbol{x}, t) \,.$$

2.6.2 Contributions to the second Piola-Kirchhoff stress tensor

The additive decomposition of ψ_R performed in Eq. (2.101), and the stated functional dependence of each contribute, in addition to the thermodynamic restriction (2.69a), allow to state the dependence of the chemo-thermo-elastic second Piola-Kirchhoff stress tensor $\mathbf{S}^{cte}$ upon two contributions. It holds that

$$\mathbf{S}^{cte} = 2\, J^{p^{-1}}\, \frac{\partial}{\partial \mathbf{C}^{cte}}\, \psi_R(T, c_{L_R}, c_{T_R}, \mathbf{C}^{cte}, \boldsymbol{\Xi}) = 2\, J^{p^{-1}}\, \frac{\partial \psi_R^{diff}}{\partial \mathbf{C}^{cte}} + 2\, J^{p^{-1}}\, \frac{\partial \psi_R^{el}}{\partial \mathbf{C}^{cte}} \,. \tag{2.120}$$

To compute the first term, recall that ψ_R^{diff} depends upon $\mathbf{C}^{cte}$ by means of J^{cte}. Therefore, making use of the chain rule (the proof is collected in Appendix A.2), we find

$$\frac{\partial \psi_R^{diff}}{\partial \mathbf{C}^{cte}} = \frac{\partial \psi_R^{diff}}{\partial J^{cte}}\, \frac{\partial J^{cte}}{\partial \mathbf{C}^{cte}} = \frac{\partial \psi_R^{diff}}{\partial J^{cte}}\, \frac{J^{cte}}{2}\, \mathbf{C}^{cte^{-1}} \,, \tag{2.121}$$

which is a volumetric term induced by the change of the saturation concentration. Furthermore, ψ_R^{el} depends upon $\mathbf{C}^{cte}$ by means of the elastic right Cauchy-Green strain tensor $\mathbf{C}^e$. Indeed, recalling Eq. (2.100) and the chain rule, one gets

$$\frac{\partial \psi_R^{el}}{\partial \mathbf{C}^{cte}} = \frac{\partial \psi_R^{el}}{\partial \mathbf{C}^e}\, \frac{\partial \mathbf{C}^e}{\partial \mathbf{C}^{cte}} = \frac{\partial \psi_R^{el}}{\partial \mathbf{C}^e}\, J^{s^{-\frac{2}{3}}}\, J^{th^{-\frac{2}{3}}}\, \mathbf{1} \,. \tag{2.122}$$

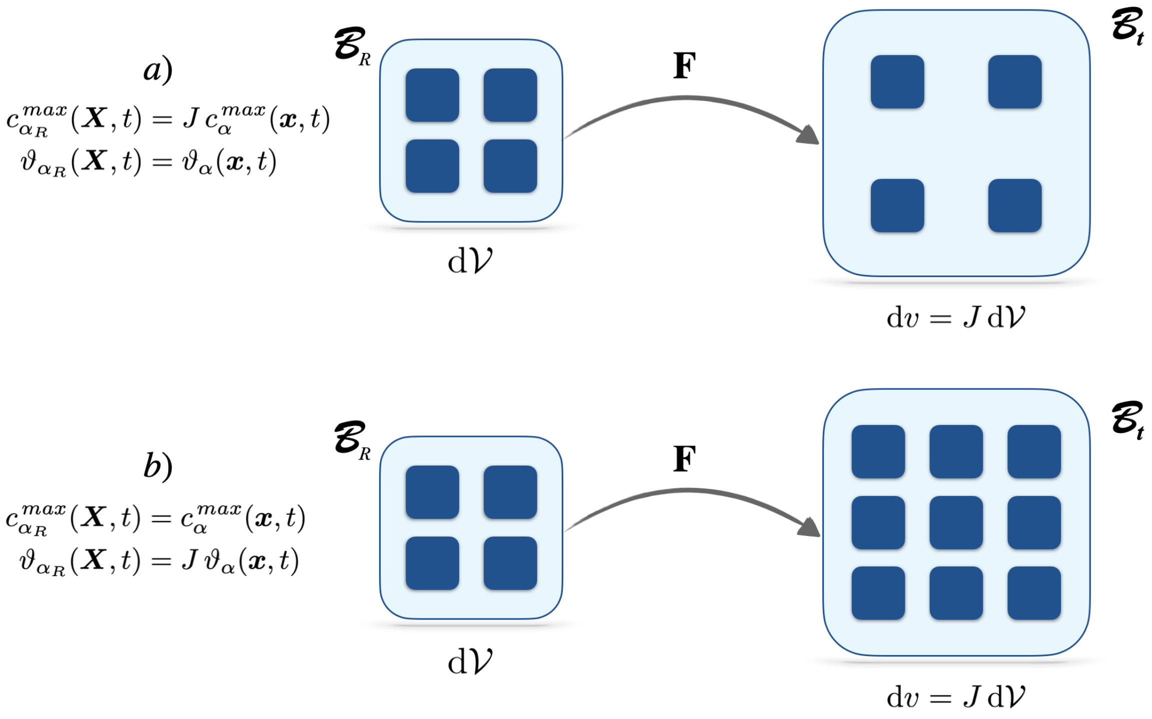

Figure 2.4: Depiction of two cases that are paradigms in which *a*) the maximum number of moles per unit volume varies with the volumetric Jacobian J, and *b*) the maximum number of moles per unit volume is invariant.

Eventually,

$$\mathbf{S}^{cte} = 2\, J^{p^{-1}} \frac{\partial \psi_R^{diff}}{\partial J^{cte}}\, J^{cte}\, \mathbf{C}^{cte^{-1}} + 2\, J^{p^{-1}} \frac{\partial \psi_R^{el}}{\partial \mathbf{C}^e}\, J^{s^{-\frac{2}{3}}}\, J^{th^{-\frac{2}{3}}} \,, \tag{2.123}$$

Recalling Eq.s (2.110), (2.111), (2.112) and (2.113), we find

$$J^{cte} \frac{\partial \psi_R^{diff}}{\partial J^{cte}} = -T\, \eta_{L_R}^{diff} - T\, \eta_{T_R}^{diff} - T\, \eta_{L_R}^{\chi} \,, \tag{2.124}$$

where $-T\,\eta_{L_R}^{\chi}$ describes an enthalpic contribution of interactions, whereas the two terms $-T\,\eta_{L_R}^{diff}$ and $-T\,\eta_{T_R}^{diff}$ represent an entropic contribution to the stress.

In conclusion, combining Eq.s (2.122) and (2.124), we find that the chemo-thermo-elastic second Piola-Kirchhoff stress tensor writes as

$$\mathbf{S}^{cte} = -T\, J^{p^{-1}} \left(\eta_{L_R}^{diff} + \eta_{T_R}^{diff} + \eta_{L_R}^{\chi} \right) \mathbf{C}^{cte^{-1}} + 2\, J^{p^{-1}} \frac{\partial \psi_R^{el}}{\partial \mathbf{C}^e}\, J^{s^{-\frac{2}{3}}}\, J^{th^{-\frac{2}{3}}} \,. \tag{2.125}$$

2.6.3 Chemical potential

Recalling Eq.s (2.102) and (2.113), one finds that the chemical potential of species α can be constitutively defined via the relation

$$\mu_\alpha = \frac{\partial \psi_R^{diff}}{\partial c_{\alpha_R}} + \frac{\partial \psi_R^{th}}{\partial c_{\alpha_R}} + \frac{\partial \psi_R^{el}}{\partial c_{\alpha_R}} + \frac{\partial \psi_R^{in}}{\partial c_{\alpha_R}} \tag{2.126}$$

whence, according to Eqs (2.102) and (2.113), for $\alpha = L, T$, it holds that

$$\begin{aligned}\mu_L = \mu_L^0 + R\,T\,\chi\,(1 - 2\,\vartheta_L) + R\,T \ln\left[\frac{\vartheta_L}{1-\vartheta_L}\right] - {}^{\eta}\mu_L^0\,(T - T_0) - \frac{1}{2}\,\frac{c_{v\,L}^0}{T_0}\,(T-T_0)^2 \\ + \frac{\partial \psi_{R}^{el}}{\partial c_{L_R}} + \frac{\partial \psi_{R}^{in}}{\partial c_{L_R}} \;,\end{aligned} \tag{2.127a}$$

$$\mu_T = \mu_T^0 + R\,T \ln\left[\frac{\vartheta_T}{1-\vartheta_T}\right] - {}^{\eta}\mu_T^0\,(T - T_0) - \frac{1}{2}\,\frac{c_{v\,T}^0}{T_0}\,(T-T_0)^2 + \frac{\partial \psi_{R}^{el}}{\partial c_{T_R}} + \frac{\partial \psi_{R}^{in}}{\partial c_{T_R}} \;. \tag{2.127b}$$

In view of Eqs (2.76a) and (2.127), the change in specific entropy provided by a unit supply of moles of species L and T writes as

$$\begin{aligned}{}^{\eta}\mu_L &= -\frac{\partial^2 \psi_{R}}{\partial c_{L_R} \partial T} = -\frac{\partial \mu_L}{\partial T} \\ &= -R\,\chi\,(1 - 2\,\vartheta_L) - R \ln\left[\frac{\vartheta_L}{1-\vartheta_L}\right] + {}^{\eta}\mu_L^0 + \frac{c_{v\,L}^0}{T_0}\,(T-T_0) - \frac{\partial^2 \psi_{R}^{el}}{\partial T \partial c_{L_R}} - \frac{\partial^2 \psi_{R}^{in}}{\partial T \partial c_{L_R}} \;,\end{aligned} \tag{2.128a}$$

and

$$\begin{aligned}{}^{\eta}\mu_T = -\frac{\partial^2 \psi_{R}}{\partial c_{T_R} \partial T} = -\frac{\partial \mu_T}{\partial T} = \\ - R \ln\left[\frac{\vartheta_T}{1-\vartheta_T}\right] + {}^{\eta}\mu_T^0 + \frac{c_{v\,T}^0}{T_0}\,(T-T_0) - \frac{\partial^2 \psi_{R}^{el}}{\partial T \partial c_{T_R}} - \frac{\partial^2 \psi_{R}^{in}}{\partial T \partial c_{T_R}} \;,\end{aligned} \tag{2.128b}$$

respectively.

2.6.4 Heat and mass fluxes

The thermodynamic restriction (2.71b) may be satisfied in many possible ways. A classical strategy is to model the flux of interstitial species $\boldsymbol{h}_{L_R}$ by Fick's law, and the new heat flux $\boldsymbol{\not{q}}_{R}$ via Fourier's law, by means of positive definite mobility and heat conductivity tensors, $\mathbf{M}_{L_R}$ and $\mathbb{K}$, respectively,

$$\boldsymbol{h}_{L_R} = -\mathbf{M}_{L_R}(c_{L_R})\,\boldsymbol{\nabla}_{R}\left[\,\mu_L\,\right] \;, \qquad \boldsymbol{\not{q}}_{R} \;= -\mathbb{K}\,\boldsymbol{\nabla}_{R}\left[\,T\,\right] \;. \tag{2.129}$$

As done in [9], we relate the ordinary heat flux $\boldsymbol{q}_{R}$ to the temperature gradient $\boldsymbol{\nabla}_{R}\left[\,T\,\right]$ via Fourier's law, and the mass flux to the remaining gradients, in view of Eq. (2.78) and in a consistent way with the thermodynamic restriction (2.71b). Therefore

$$\boldsymbol{h}_{L_R} = -\mathbf{M}_{L_R}(c_{L_R})\,\left(\boldsymbol{\nabla}_{R}\left[\,\mu_L\,\right] + {}^{\eta}\mu_L\,\boldsymbol{\nabla}_{R}\left[\,T\,\right]\right) \;, \tag{2.130a}$$

$$\boldsymbol{q}_{R} = -\mathbb{K}\,\boldsymbol{\nabla}_{R}\left[\,T\,\right] \;. \tag{2.130b}$$

To account for saturation and to satisfy the physical requirement that both the pure and the saturated phases, $c_{L_R} = 0$ and $c_{L_R} = c_{L_R}^{max}$, lead to vanishing mobility, the mobility tensor $\mathbf{M}_{L_R}(c_{L_R})$ is chosen in the following isotropic non linear form [55]

$$\mathbf{M}_{L_R}(c_{L_R}) = \mathbb{u}_L\, c_{L_R}^{max}\,\vartheta_L\,(1 - \vartheta_L)\,\mathbf{1} \;, \tag{2.131}$$

with $\mathbb{u}_L > 0$ the mobility of interstitial chemical species, and $c_{L_R}^{max}$ and ϑ_L defined by Eq.s (2.108) and (2.107), respectively.

To formulate Fick's law (2.130a), recall how the vector $\boldsymbol{\nabla}_{R}\left[\,\mu_L\,\right] + {}^{\eta}\mu_L\,\boldsymbol{\nabla}_{R}\left[\,T\,\right]$ has been defined in Eq (2.78). Then

$$\begin{aligned}\boldsymbol{h}_{L_R} = &- \mathbf{M}_{L_R}(c_{L_R})\,\left(\frac{\partial^2 \psi_{R}}{\partial c_{L_R}^2}\,\boldsymbol{\nabla}_{R}\left[\,c_{L_R}\,\right] + \frac{\partial^2 \psi_{R}}{\partial c_{L_R} \partial c_{T_R}}\,\boldsymbol{\nabla}_{R}\left[\,c_{T_R}\,\right] \frac{\partial^2 \psi_{R}}{\partial c_{L_R} \partial \mathbf{C}^{cte}} : \boldsymbol{\nabla}_{R}\left[\,\mathbf{C}^{cte}\,\right]\right. \\ &\left. + \frac{\partial^2 \psi_{R}}{\partial c_{L_R} \partial \boldsymbol{\Xi}} : \boldsymbol{\nabla}_{R}\left[\,\boldsymbol{\Xi}\,\right]\right) \;.\end{aligned} \tag{2.132}$$

The first term in brackets of Eq. (2.132) writes as

$$\begin{aligned}\frac{\partial^2\psi_{R}}{\partial c_{L_R}^2}\,\boldsymbol{\nabla}_{R}\left[\,c_{L_R}\,\right] = R\,T\,\frac{1}{c_{L_R}^{max}}\left(-2\,\chi+\frac{1}{\vartheta_L(1-\theta_L)}\right)\boldsymbol{\nabla}_{R}\left[\,c_{L_R}\,\right]+\frac{\partial^2\psi_{R}^{el}}{\partial c_{L_R}^2}\,\boldsymbol{\nabla}_{R}\left[\,c_{L_R}\,\right]\\ +\frac{\partial^2\psi_{R}^{in}}{\partial c_{L_R}^2}\,\boldsymbol{\nabla}_{R}\left[\,c_{L_R}\,\right]\ ,\end{aligned} \tag{2.133}$$

whereas the last three terms in brackets of Eq. (2.132) take the form

$$\frac{\partial^2\psi_{R}}{\partial c_{L_R}\partial c_{T_R}}\,\boldsymbol{\nabla}_{R}\left[\,c_{T_R}\,\right]=\frac{\partial^2\psi_{R}^{el}}{\partial c_{L_R}\partial c_{T_R}}\,\boldsymbol{\nabla}_{R}\left[\,c_{T_R}\,\right]+\frac{\partial^2\psi_{R}^{in}}{\partial c_{L_R}\partial c_{T_R}}\,\boldsymbol{\nabla}_{R}\left[\,c_{T_R}\,\right]\ , \tag{2.134a}$$

$$\frac{\partial^2\psi_{R}}{\partial c_{L_R}\partial\mathbf{C}^{cte}}:\boldsymbol{\nabla}_{R}\left[\,\mathbf{C}^{cte}\,\right]=\frac{\partial^2\psi_{R}^{el}}{\partial c_{L_R}\partial\mathbf{C}^{cte}}:\boldsymbol{\nabla}_{R}\left[\,\mathbf{C}^{cte}\,\right]\ , \tag{2.134b}$$

$$\frac{\partial^2\psi_{R}}{\partial c_{L_R}\partial\boldsymbol{\Xi}}:\boldsymbol{\nabla}_{R}\left[\,\boldsymbol{\Xi}\,\right]=\frac{\partial^2\psi_{R}^{in}}{\partial c_{L_R}\partial\boldsymbol{\Xi}}:\boldsymbol{\nabla}_{R}\left[\,\boldsymbol{\Xi}\,\right]\ . \tag{2.134c}$$

Taking advantage of the definition of the mobility tensor $\mathbf{M}_{L_R}(c_{L_R})$ given by Eq. (2.131), and by defining the interstitial diffusivity according to Einstein's equation, we deduce that

$$\mathbb{D}_L=\mathbb{u}_L\,R\,T\ ,$$

and simple algebra allows us to re-write the Fick's law (2.130a) as

$$\begin{aligned}\boldsymbol{h}_{L_R}=&-\mathbb{D}_L\left[1-2\,\chi\,\vartheta_L(1-\vartheta_L)\right]\boldsymbol{\nabla}_{R}\left[\,c_{L_R}\,\right]\\ &-\mathbf{M}_{L_R}\left(\frac{\partial^2\psi_{R}^{el}}{\partial c_{L_R}^2}\,\boldsymbol{\nabla}_{R}\left[\,c_{L_R}\,\right]+\frac{\partial^2\psi_{R}^{el}}{\partial c_{L_R}\partial c_{T_R}}\,\boldsymbol{\nabla}_{R}\left[\,c_{T_R}\,\right]+\frac{\partial^2\psi_{R}^{el}}{\partial c_{L_R}\partial\mathbf{C}^{cte}}:\boldsymbol{\nabla}_{R}\left[\,\mathbf{C}^{cte}\,\right]\right)\\ &-\mathbf{M}_{L_R}\left(\frac{\partial^2\psi_{R}^{in}}{\partial c_{L_R}^2}\,\boldsymbol{\nabla}_{R}\left[\,c_{L_R}\,\right]+\frac{\partial^2\psi_{R}^{in}}{\partial c_{L_R}\partial c_{T_R}}\,\boldsymbol{\nabla}_{R}\left[\,c_{T_R}\,\right]+\frac{\partial^2\psi_{R}^{in}}{\partial c_{L_R}\partial\boldsymbol{\Xi}}:\boldsymbol{\nabla}_{R}\left[\,\boldsymbol{\Xi}\,\right]\right)\ .\end{aligned} \tag{2.135}$$

2.7 Chemical kinetics

For an ideal system, in which the solvent does not take part in reactions, the kinetics of reaction (2.12) is well modeled via the following law of mass action [51]

$$w_{R}^{(2.12)}(\boldsymbol{X},t)=k_{R}^{+}\,\frac{\vartheta_L}{1-\vartheta_L}-k_{R}^{-}\,\frac{\vartheta_T}{1-\vartheta_T}\ . \tag{2.136}$$

In agreement with the transformation $(2.17)_2$ of $w_{R}^{(2.12)}$ defined by Eq. (7.3), the rate factors for both the forward and reverse reaction, k_{R}^{+} and k_{R}^{-}, transform according to

$$k_{R}^{\pm}(\boldsymbol{X},t)=J\,k^{\pm}\ , \tag{2.137}$$

therefore both k_{R}^{+} and k_{R}^{-} are not constant values, rather they evolve with the deformation of the body by means of J.

Furthermore, following what is proposed in [9], the variation in time of $k_{R}^{\pm}(\boldsymbol{X},t)$ is related to the stress and to the concentration of species via elastic parameters. Consequently, the referential rate factor which describes the reverse reaction is taken as

$$\begin{aligned}k_{R}^{-}=\tilde{k}_{R}^{-}\,\exp\left(\frac{1}{R\,T}\,\frac{\partial\psi_{R}^{el}}{\partial c_{T_R}}\right)\,\exp\left(\frac{1}{R\,T}\,\frac{\partial\psi_{R}^{in}}{\partial c_{T_R}}\right)\,\exp\left(-\frac{{}^{\eta}\mu_T^0\,(T-T_0)}{R\,T}\right)\\ \exp\left(-\frac{c_{v\,T}^0(T-T_0)^2}{2\,R\,T\,T_0}\right)\ ,\end{aligned} \tag{2.138a}$$

whereas the referential factor providing the description of the forward reaction has the form

$$\begin{aligned} k^{+}_{R} = \tilde{k}^{+}_{R} \, \exp\left(\frac{1}{RT} \frac{\partial \psi^{el}_{R}}{\partial c_{L_R}} \right) \exp\left(\frac{1}{RT} \frac{\partial \psi^{in}_{R}}{\partial c_{L_R}} \right) \exp\left(- \frac{{}^{\eta}\mu^0_L \, (T - T_0)}{RT} \right) \\ \exp\left(- \frac{c^0_{v\,L} (T - T_0)^2}{2\,RT\,T_0} \right) \exp\left(\chi \, (1 - 2\,\vartheta_L) \right) \; . \end{aligned} \tag{2.138b}$$

Therefore, the factors k^{+}_{R} and k^{-}_{R}, with respect to both the small strain analysis prescriptions [9] and the spatial description they would have, are no longer constants, given that they follow the same transformation rule for $k^{\pm}_{R}(\boldsymbol{X}, t)$ shown in Eq. (6.71) and defined by Eq. (7.3). This new formulation is consistent with the usual mass action law described by the *van't Hoff* relation [64], which is recovered when elastic, swelling, and interaction contributions vanish.

The condition of null affinity, $A^{(2.12)} = 0$, can be solved for the Gibbs free energy change, $\mu^0_L - \mu^0_T$, in order to obtain the equilibrium constant K_{eq} of the chemical reaction (2.12). According to the definition (2.45) of the affinity $A^{(2.12)}$, and re-writing Eq. (2.104) to obtain K_{eq}, we find

$$K_{eq} = \exp\left(\frac{\Delta E_\tau}{RT} \right) = \exp\left(\frac{\mu^0_L - \mu^0_T}{RT} \right) \; , \tag{2.139}$$

The terms μ^0_L and μ^0_T can be derived by means of the constitutive definition of the chemical potentials (2.127a) and (2.127b), respectively. Accordingly, the term $\mu^0_L - \mu^0_T$ of Eq. (2.139) writes at equilibrium as

$$\begin{aligned} \mu^0_L - \mu^0_T = & - RT\,\chi \, \left(1 - 2\,\vartheta^{eq}_L\right) + RT \left(\ln\left[\frac{\vartheta^{eq}_T}{1 - \vartheta^{eq}_T} \right] - \ln\left[\frac{\vartheta^{eq}_L}{1 - \vartheta^{eq}_L} \right] \right) + \left({}^{\eta}\mu^0_L - {}^{\eta}\mu^0_T \right) \left(T^{eq} - T_0 \right) \\ & + \frac{1}{2} \left(\frac{c^0_{v\,L} - c^0_{v\,T}}{T_0} \right) \left(T^{eq} - T_0 \right)^2 + \left(\frac{\partial \psi^{el}_{R}}{\partial c_{T_R}} - \frac{\partial \psi^{el}_{R}}{\partial c_{L_R}} \right) + \left(\frac{\partial \psi^{in}_{R}}{\partial c_{T_R}} - \frac{\partial \psi^{in}_{R}}{\partial c_{L_R}} \right) \; , \end{aligned}$$

whence, the equilibrium constant K_{eq} of the chemical reaction (2.12) writes as

It descends that, the equilibrium constant K_{eq} (2.139) of the chemical reaction (2.12) writes

$$\begin{aligned} K_{eq} = & \frac{\vartheta^{eq}_T}{1 - \vartheta^{eq}_T} \, \frac{1 - \vartheta^{eq}_L}{\vartheta^{eq}_L} \, \exp\left[- \chi \, \left(1 - 2\,\vartheta^{eq}_L \right) \right] \\ & \exp\left[\frac{{}^{\eta}\mu^0_L - {}^{\eta}\mu^0_T}{RT} \left(T^{eq} - T_0 \right) \right] \exp\left[\frac{1}{2} \frac{c^0_{v\,L} - c^0_{v\,T}}{RT\,T_0} \left(T^{eq} - T_0 \right)^2 \right] \\ & \exp\left[\frac{1}{RT} \left(\frac{\partial \psi^{el}_{R}}{\partial c_{T_R}} - \frac{\partial \psi^{el}_{R}}{\partial c_{L_R}} \right) \right]^{eq} \exp\left[\frac{1}{RT} \left(\frac{\partial \psi^{in}_{R}}{\partial c_{T_R}} - \frac{\partial \psi^{in}_{R}}{\partial c_{L_R}} \right) \right]^{eq} \; . \end{aligned} \tag{2.140}$$

An alternative way to derive K_{eq} is by imposing $w^{(2.12)}_{R} = 0$ in Eq. (2.136). In this instance, the equilibrium constant of reaction (2.12) writes as

$$K_{eq} = \frac{\tilde{k}^{+}_{R}}{\tilde{k}^{-}_{R}}$$

and Eq. (2.140) is recovered by taking advantage of Eq.s (2.138) to express $\tilde{k}^{+}_{R}$ and $\tilde{k}^{-}_{R}$.

The thermodynamic restriction

$$w^{(2.12)}_{R} \, A^{(2.12)} \leq 0$$

is satisfied by means of Eq.s (2.138). Furthermore, a classical way to enforce thermodynamic restrictions for the chemical reaction (2.12) is to select a positive phenomenological coefficient, usually termed $L^{(2.12)}$, which linearly relates the affinity, $A^{(2.12)}$, to the reaction rate, $w^{(2.12)}_{R}$, via the relation

$$w^{(2.12)}_{R} = - L^{(2.12)} \, A^{(2.12)} \; .$$

The proof of these two last statements is not influenced by finite strains and can be found in [9].

2.8 Governing equations

The governing equations are obtained by incorporating the constitutive prescriptions of the chemo-thermo-elastic second Piola-Kirchhoff stress tensor $\mathbf{S}^{cte}$ (2.125), the referential heat and mass flux vectors, $\boldsymbol{q}_{_R}$ and $\boldsymbol{h}_{L_R}$, given by Eq.s (2.130b) and (2.135), respectively, and the mass action law (2.136) with specifications (2.138), into the balance equations (2.16), (2.23a), and (2.141d). Governing equations are written in term of the state variables c_{L_R}, c_{T_R}, $\boldsymbol{u}$, and T. They read

$$\dot{c}_{L_R} + \boldsymbol{\nabla}_{_R} \cdot \left[\, \boldsymbol{h}_{L_R}(c_{L_R}, c_{T_R}, T, \mathbf{C}^{cte}, \boldsymbol{\Xi}) \,\right] + w_{_R}^{(2.12)}(c_{L_R}, c_{T_R}, T, \mathbf{C}^{cte}, \boldsymbol{\Xi}) = s_{L_R} \ , \tag{2.141a}$$

$$\dot{c}_{T_R} - w_{_R}^{(2.12)}(c_{L_R}, c_{T_R}, T, \mathbf{C}^{cte}, \boldsymbol{\Xi}) = s_{T_R} \ , \tag{2.141b}$$

$$\boldsymbol{\nabla}_{_R} \cdot \left[\, \mathbf{T}_{_R} \left(\mathbf{S}^{cte}, \mathbf{C}^{cte}, c_{L_R}, c_{T_R}, T\right) \,\right] + \boldsymbol{b}_{0_R} = \mathbf{0} \ , \tag{2.141c}$$

$$\begin{aligned} -T \, \frac{\partial^2 \psi_{_R}}{\partial T^2} \, \dot{T} - \boldsymbol{\nabla}_{_R} \cdot [\, \mathbf{K}\!\!\!| \; \boldsymbol{\nabla}_{_R} \, [\, T \,] \,] = {} & T \, \frac{\partial^2 \psi_{_R}}{\partial T \partial \mathbf{C}^{cte}} : \dot{\mathbf{C}}^{cte} + J^p \, \mathbf{M}^{cte} : \mathbf{L}^p + s_{qR} \\ & + \left(\mathbf{X}\!\!\!| \; + T \, \frac{\partial^2 \psi_{_R}}{\partial T \partial \boldsymbol{\Xi}} \right) : \dot{\boldsymbol{\Xi}} \\ & + \mathbf{M}_{L_R}(c_{L_R}) \; (\boldsymbol{\nabla}_{_R} \, [\, \mu_L \,] + {}^{\eta}\mu_L \, \boldsymbol{\nabla}_{_R} \, [\, T \,]) \cdot \boldsymbol{\nabla}_{_R} \, [\, {}^{u}\mu_L \,] \\ & + ({}^{u}\mu_L - {}^{u}\mu_T) \, w_{_R}^{(2.12)} \ . \end{aligned} \tag{2.141d}$$

Details of the derivation of Eq. (2.141d) have been collected in Appendix A.3.

The boundary conditions

$$\boldsymbol{h}_{L_R} \cdot \boldsymbol{n}_{_R} = \overline{h}_{_R} \qquad \boldsymbol{X} \in \partial^N \mathcal{V} \ , \tag{2.142a}$$

$$\boldsymbol{q}_{_R} \cdot \boldsymbol{n}_{_R} = \overline{q}_{_R} \qquad \boldsymbol{X} \in \partial^N \mathcal{V} \ , \tag{2.142b}$$

$$\mathbf{T}_{_R} \, \boldsymbol{n}_{_R} = \overline{\boldsymbol{t}}_{_R} \qquad \boldsymbol{X} \in \partial^N \mathcal{V} \ , \tag{2.142c}$$

are imposed along Neumann boundaries $\partial^N \mathcal{V}$. To ensure solvability of the problem, Dirichlet boundary conditions have to be enforced along the complementary boundary $\partial^D \mathcal{V}$, hence

$$T = \overline{T} \qquad \boldsymbol{X} \in \partial^D \mathcal{V} \ , \tag{2.143a}$$

$$\boldsymbol{u} = \overline{\boldsymbol{u}} \qquad \boldsymbol{X} \in \partial^D \mathcal{V} \ . \tag{2.143b}$$

Initial conditions are usually imposed for the concentration of interstitial species, $c_{L_R}(\boldsymbol{X}, t = 0)$, as well as of trapped species $c_{T_R}(\boldsymbol{X}, t = 0)$ and temperature, $T(\boldsymbol{X}, t = 0)$. To comply with equilibrium thermodynamics these conditions are chosen to be uniform in the material and to ensure equilibrium with external species. Balance of momentum, together with boundary conditions, provide the necessary and sufficient equations and conditions to solve for $\boldsymbol{u}$ at $t = 0$.

2.9 Concluding remarks

A general framework that couples mass transport, chemical reactions with trapping, and finite strain thermo-mechanics has been presented. The formulation describes interstitial motion of free diffusive species in a hosting material; once trapped, species stay immobile, ceasing to contribute to mass transport and potentially inducing the swelling of the material. Elasto-plastic effects, as well as thermal evolution, are accounted for.

Kinematics is designed by means of a suitable multiplicative split of the deformation gradient. Mass balance equations are augmented with the rate of the chemical reaction, which portrays the conversion of mobile guest species to trapped species, and vice-versa, and a source term to describe injection or removal of mass. The enthalpy and the entropy contributions due to mass flux for the two laws of thermodynamics lead to the definition of the chemical potential as the sum of enthalpic and entropic contributions. In accordance with the multiplicative decomposition of the deformation gradient, the mechanical contribution to the entropy imbalance is additively split into chemo-thermo-elastic and inelastic parts, conveniently defined as a function of the chemo-thermo-elastic second Piola-Kirchhoff and Mandel stress tensors, respectively. The standard method of Coleman and Noll, and the assumption of Curie's symmetry principles, determine all thermodynamic prescriptions. The referential Helmholtz free energy density is chosen as a thermodynamic potential, and constitutively subjected to an additive decomposition to account for all processes involved in the material behavior. Such splitting drives the constitutive specifications of chemical potentials, heat and mass fluxes, and chemical kinetics. Governing equations, with associated Neumann and Dirichlet boundary conditions, are derived to complete the full coupling of the finite strain chemo-thermo-mechanics with trapping.

Appendix A

A.1 Proof of Eq. (2.78)

The independence of the vector $\boldsymbol{\nabla}_R\left[\,\mu_L\,\right] + {}^{\eta}\mu_L\,\boldsymbol{\nabla}_R\left[\,T\,\right]$ upon the temperature gradient ca be shown be re-writing the chemical potential gradient of species L in the form

$$\begin{aligned}
\boldsymbol{\nabla}_R\left[\,\mu_L\,\right] &= \boldsymbol{\nabla}_R\left[\frac{\partial\psi_R}{\partial c_{L_R}}\right] = \frac{\partial}{\partial c_{L_R}}\,\boldsymbol{\nabla}_R\left[\,\psi_R\left(T, c_{L_R}, c_{T_R}, \mathbf{C}^{cte}, \boldsymbol{\Xi}\right)\,\right] \\
&= \frac{\partial}{\partial c_{L_R}}\left(\frac{\partial\psi_R}{\partial T}\,\boldsymbol{\nabla}_R\left[\,T\,\right] + \frac{\partial\psi_R}{\partial c_{L_R}}\,\boldsymbol{\nabla}_R\left[\,c_{L_R}\,\right] + \frac{\partial\psi_R}{\partial c_{T_R}}\,\boldsymbol{\nabla}_R\left[\,c_{T_R}\,\right] + \frac{\partial\psi_R}{\partial\mathbf{C}^{cte}} : \boldsymbol{\nabla}_R\left[\,\mathbf{C}^{cte}\,\right]\right. \\
&\quad \left. + \frac{\partial\psi_R}{\partial\boldsymbol{\Xi}} : \boldsymbol{\nabla}_R\left[\,\boldsymbol{\Xi}\,\right]\right) \\
&= \frac{\partial^2\psi_R}{\partial c_{L_R}\partial T}\,\boldsymbol{\nabla}_R\left[\,T\,\right] + \frac{\partial^2\psi_R}{\partial c_{L_R}^2}\,\boldsymbol{\nabla}_R\left[\,c_{L_R}\,\right] + \frac{\partial^2\psi_R}{\partial c_{L_R}\partial c_{T_R}}\,\boldsymbol{\nabla}_R\left[\,c_{T_R}\,\right] \\
&\quad + \frac{\partial^2\psi_R}{\partial c_{L_R}\partial\mathbf{C}^{cte}} : \boldsymbol{\nabla}_R\left[\,\mathbf{C}^{cte}\,\right] + \frac{\partial^2\psi_R}{\partial c_{L_R}\partial\boldsymbol{\Xi}} : \boldsymbol{\nabla}_R\left[\,\boldsymbol{\Xi}\,\right]\ ,
\end{aligned} \tag{A.1}$$

and the term ${}^{\eta}\mu_L\,\boldsymbol{\nabla}_R\left[\,T\,\right]$, according to the definition shown in Eq. (2.76a), as

$${}^{\eta}\mu_L\,\boldsymbol{\nabla}_R\left[\,T\,\right] = -\frac{\partial^2\psi_R}{\partial c_{\alpha_R}\partial T}\,\boldsymbol{\nabla}_R\left[\,T\,\right]\ . \tag{A.2}$$

Combination of Eq.s (A.1) and (A.2) yields

$$\begin{aligned}
\boldsymbol{\nabla}_R\left[\,\mu_L\,\right] + {}^{\eta}\mu_L\,\boldsymbol{\nabla}_R\left[\,T\,\right] = &\frac{\partial^2\psi_R}{\partial c_{L_R}^2}\,\boldsymbol{\nabla}_R\left[\,c_{L_R}\,\right] + \frac{\partial^2\psi_R}{\partial c_{L_R}\partial c_{T_R}}\,\boldsymbol{\nabla}_R\left[\,c_{T_R}\,\right] + \frac{\partial^2\psi_R}{\partial c_{L_R}\partial\mathbf{C}^{cte}} : \boldsymbol{\nabla}_R\left[\,\mathbf{C}^{cte}\,\right] \\
&+ \frac{\partial^2\psi_R}{\partial c_{L_R}\partial\boldsymbol{\Xi}} : \boldsymbol{\nabla}_R\left[\,\boldsymbol{\Xi}\,\right]\ .
\end{aligned} \tag{A.3}$$

A.2 Proof of Eq. (2.121)

To compute the term,

$$\frac{\partial\psi_R^{diff}}{\partial\mathbf{C}^{cte}} = \frac{\partial\psi_R^{diff}}{\partial J^{cte}}\,\frac{\partial J^{cte}}{\partial\mathbf{C}^{cte}}\ , \tag{A.4}$$

recall $J = \det\left[\,\mathbf{F}\,\right]$ and the following properties of the determinant

$$\det\left[\,\mathbf{A}\,\right] = \det\left[\,\mathbf{A}^{\mathrm{T}}\,\right]\ , \tag{A.5a}$$

$$\det\left[\,\mathbf{A}\,\right]^2 = \det\left[\,\mathbf{A}\,\mathbf{A}\,\right] = \det\left[\,\mathbf{A}\,\right]\,\det\left[\,\mathbf{A}\,\right]\ , \tag{A.5b}$$

$$\frac{\partial\det\left[\,\mathbf{A}\,\right]}{\partial\mathbf{A}} = \det\left[\,\mathbf{A}\,\right]\,\mathbf{A}^{-\mathrm{T}}\ , \tag{A.5c}$$

for any square tensor $\mathbf{A}$.

Let K denote the square of the volumetric Jacobian,

$$K = J^2 = \det[\,\mathbf{F}\,]^2 \ . \tag{A.6}$$

whence, by means of the definition of the right Cauchy-Green tensor, $\mathbf{C} = \mathbf{F}^{\mathrm{T}}\,\mathbf{F}$, and according to Eq.s (A.5a) and (A.5b), it holds

$$K = J^2 = \det[\,\mathbf{F}\,\mathbf{F}\,] = \det[\,\mathbf{F}\,]\,\det[\,\mathbf{F}\,] = \det\left[\,\mathbf{F}^{\mathrm{T}}\,\right]\,\det[\,\mathbf{F}\,] = \det\left[\,\mathbf{F}^{\mathrm{T}}\,\mathbf{F}\,\right] = \det[\,\mathbf{C}\,] \ . \tag{A.7}$$

From Eq. (A.5c), and taking advantage from the symmetry of $\mathbf{C}$, it is possible to write

$$\frac{\partial K}{\partial \mathbf{C}} = \frac{\partial \det[\,\mathbf{C}\,]}{\partial \mathbf{C}} = \det[\,\mathbf{C}\,]\;\mathbf{C}^{-\mathrm{T}} = \det[\,\mathbf{C}\,]\;\mathbf{C}^{-1} \ . \tag{A.8a}$$

The derivative of K with respect to $\mathbf{C}$ can also be written, making use of the chain rule, as

$$\frac{\partial K}{\partial \mathbf{C}} = \frac{\partial K}{\partial J}\,\frac{\partial J}{\partial \mathbf{C}} = 2\,J\,\frac{\partial J}{\partial \mathbf{C}} \ , \tag{A.8b}$$

Combination of Eq.s (A.8a) and (A.8b) yields

$$\frac{\partial J}{\partial \mathbf{C}} = \frac{1}{2\,J}\,\frac{\partial K}{\partial \mathbf{C}} = \frac{1}{2\,J}\det[\,\mathbf{C}\,]\;\mathbf{C}^{-1} \tag{A.9}$$

whence, taking advantage from Eq. (A.7) to re-write $\det[\,\mathbf{C}\,]$,

$$\frac{\partial J}{\partial \mathbf{C}} = \frac{1}{2\,J}\,K\,\mathbf{C}^{-1} = \frac{1}{2\,J}\,J^2\,\mathbf{C}^{-1} = \frac{J}{2}\,\mathbf{C}^{-1} \ . \tag{A.10}$$

By means of Eq. (A.10), Eq. (A.4) writes

$$\frac{\partial \psi_{R}^{diff}}{\partial \mathbf{C}^{cte}} = \frac{\partial \psi_{R}^{diff}}{\partial J^{cte}}\,\frac{\partial J^{cte}}{\partial \mathbf{C}^{cte}} = \frac{\partial \psi_{R}^{diff}}{\partial J^{cte}}\,\frac{J^{cte}}{2}\,\mathbf{C}^{cte^{-1}} \ , \tag{A.11}$$

A.3 The generalized heat equation

To derive the generalized heat equation, recall the referential localized energy balance (5.51), and the split of the mechanical contribution $\mathbf{T}_{R} : \dot{\mathbf{F}}$ into chemo-thermo-elastic and inelastic terms given by Eq. (2.61). It holds that

$$\begin{aligned} \dot{u}_{R} = {} & \frac{1}{2}\,J^p\,\mathbf{S}^{cte} : \dot{\mathbf{C}}^{cte} + J^p\,\mathbf{M}^{cte} : \mathbf{L}^p + s_{q_R} - \boldsymbol{\nabla}_{R} \cdot \left[\,\boldsymbol{q}_{R}\,\right] + {}^{u}\mu_L\,\dot{c}_{L_R} - \boldsymbol{h}_{L_R} \cdot \boldsymbol{\nabla}_{R}\,[\,{}^{u}\mu_L\,] \\ & + {}^{u}\mu_T\,\dot{c}_{T_R} + ({}^{u}\mu_L - {}^{u}\mu_T)\;w_{R}^{(2.12)} \ . \end{aligned} \tag{A.12}$$

By means of Eq.s (2.63) and (2.66), and taking advantage of the definition of the inelastic stress (2.67), and from thermodynamic prescriptions (2.69),

$$T\,\dot{\eta}_R - \dot{u}_{R} = -\dot{\psi}_{R} - \dot{T}\,\eta_R = -\frac{1}{2}\,J^p\,\mathbf{S}^{cte} : \dot{\mathbf{C}}^{cte} - \mu_L\,\dot{c}_{L_R} - \mu_T\,\dot{c}_{T_R} + \mathbf{X}\!\!\!\!| : \dot{\boldsymbol{\Xi}} \ . \tag{A.13}$$

Taking advantage of Eq. (A.12) to replace $\dot{u}_{R}$, Eq. (A.13) can be cast in the form

$$\begin{aligned} T\,\dot{\eta}_R = -T\,\frac{\partial \dot{\psi}_{R}}{\partial T} = {} & J^p\,\mathbf{M}^{cte} : \mathbf{L}^p + s_{q_R} - \boldsymbol{\nabla}_{R} \cdot \left[\,\boldsymbol{q}_{R}\,\right] + ({}^{u}\mu_L - \mu_T)\;\dot{c}_{L_R} - \boldsymbol{h}_{L_R} \cdot \boldsymbol{\nabla}_{R}\,[\,{}^{u}\mu_L\,] \\ & + ({}^{u}\mu_T - \mu_T)\;\dot{c}_{T_R} + ({}^{u}\mu_L - {}^{u}\mu_T)\,w_{R}^{(2.12)} + \mathbf{X}\!\!\!\!| : \dot{\boldsymbol{\Xi}} \ . \end{aligned} \tag{A.14}$$

whence, by means of the time derivative of the Helmholtz free energy in view of its functional dependence (2.66),

$$
\begin{aligned}
-T\,\frac{\partial\dot{\psi}_{R}}{\partial T} &= -T\,\frac{\partial}{\partial T}\left(\frac{\partial\psi_{R}}{\partial\mathbf{C}^{cte}} : \dot{\mathbf{C}}^{cte} + \frac{\partial\psi_{R}}{\partial c_{L_R}}\,\dot{c}_{L_R} + \frac{\partial\psi_{R}}{\partial c_{T_R}}\,\dot{c}_{T_R} + \frac{\partial\psi_{R}}{\partial T}\,\dot{T} + \frac{\partial\psi_{R}}{\partial\boldsymbol{\Xi}} : \dot{\boldsymbol{\Xi}}\right) \\
&= -T\,\left(\frac{\partial^2\psi_{R}}{\partial T\partial\mathbf{C}^{cte}} : \dot{\mathbf{C}}^{cte} + \frac{\partial^2\psi_{R}}{\partial T\partial c_{L_R}}\,\dot{c}_{L_R} + \frac{\partial^2\psi_{R}}{\partial T\partial c_{T_R}}\,\dot{c}_{T_R} + \frac{\partial^2\psi_{R}}{\partial T^2}\,\dot{T} + \frac{\partial^2\psi_{R}}{\partial T\partial\boldsymbol{\Xi}} : \dot{\boldsymbol{\Xi}}\right)\ .
\end{aligned}
\tag{A.15}
$$

Equating Eq.s (A.14) and (A.15) to re-write the terms

$$
-T\,\frac{\partial^2\psi_{R}}{\partial T^2}\,\dot{T} + \boldsymbol{\nabla}_{R}\cdot\left[\,\boldsymbol{q}_{R}\,\right]
$$

it follows that

$$
\begin{aligned}
-T\,\frac{\partial^2\psi_{R}}{\partial T^2}\,\dot{T} + \boldsymbol{\nabla}_{R}\cdot\left[\,\boldsymbol{q}_{R}\,\right] = {} & J^p\,\mathbf{M}^{cte} : \mathbf{L}^p + s_{qR} + \left({}^{u}\mu_L - \mu_L + T\,\frac{\partial^2\psi_{R}}{\partial T\partial c_{L_R}}\right)\,\dot{c}_{L_R} \\
& - \boldsymbol{h}_{L_R}\cdot\boldsymbol{\nabla}_{R}\left[\,{}^{u}\mu_L\,\right] + \left({}^{u}\mu_T - \mu_T + T\,\frac{\partial^2\psi_{R}}{\partial T\partial c_{T_R}}\right)\,\dot{c}_{T_R} \\
& + \left({}^{u}\mu_L - {}^{u}\mu_T\right)w_{R}^{(2.12)} + \left(\mathbb{X} + T\,\frac{\partial^2\psi_{R}}{\partial T\partial\boldsymbol{\Xi}}\right) : \dot{\boldsymbol{\Xi}} + T\,\frac{\partial^2\psi_{R}}{\partial T\partial\mathbf{C}^{cte}} : \dot{\mathbf{C}}^{cte}\ ,
\end{aligned}
\tag{A.16}
$$

In respect of the definition of μ_α given by Eq. (2.44), and according to the specification for ${}^{\eta}\mu_\alpha$ defined in Eq. (2.76a), the two parenthetical terms that multiply $\dot{c}_{\alpha_R}$ in Eq. (C.8) are null, hence

$$
T\,\frac{\partial^2\,\psi_{R}}{\partial c_{\alpha_R}\partial T} + {}^{u}\mu_\alpha - \mu_\alpha = 0\ .
\tag{A.17}
$$

Therefore

$$
\begin{aligned}
-T\,\frac{\partial^2\psi_{R}}{\partial T^2}\,\dot{T} + \boldsymbol{\nabla}_{R}\cdot\left[\,\boldsymbol{q}_{R}\,\right] = {} & T\,\frac{\partial^2\psi_{R}}{\partial T\partial\mathbf{C}^{cte}} : \dot{\mathbf{C}}^{cte} + J^p\,\mathbf{M}^{cte} : \mathbf{L}^p + s_{qR} - \boldsymbol{h}_{L_R}\cdot\boldsymbol{\nabla}_{R}\left[\,{}^{u}\mu_L\,\right] \\
& + \left(\mathbb{X} + T\,\frac{\partial^2\psi_{R}}{\partial T\partial\boldsymbol{\Xi}}\right) : \dot{\boldsymbol{\Xi}} + \left({}^{u}\mu_L - {}^{u}\mu_T\right)w_{R}^{(2.12)}\ .
\end{aligned}
\tag{A.18}
$$

Lastly, by means of the constitutive prescriptions for the Fick's and Fourier's laws (2.130a) and (2.130b), respectively, the following generalized heat equation arises

$$
\begin{aligned}
-T\,\frac{\partial^2\psi_{R}}{\partial T^2}\,\dot{T} - \boldsymbol{\nabla}_{R}\cdot\left[\,\mathbb{K}\,\boldsymbol{\nabla}_{R}\left[\,T\,\right]\right] = {} & T\,\frac{\partial^2\psi_{R}}{\partial T\partial\mathbf{C}^{cte}} : \dot{\mathbf{C}}^{cte} + J^p\,\mathbf{M}^{cte} : \mathbf{L}^p + s_{qR} \\
& + \left(\mathbb{X} + T\,\frac{\partial^2\psi_{R}}{\partial T\partial\boldsymbol{\Xi}}\right) : \dot{\boldsymbol{\Xi}} \\
& + \mathbf{M}_{L_R}(c_{L_R})\,\left(\boldsymbol{\nabla}_{R}\left[\,\mu_L\,\right] + {}^{\eta}\mu_L\,\boldsymbol{\nabla}_{R}\left[\,T\,\right]\right)\cdot\boldsymbol{\nabla}_{R}\left[\,{}^{u}\mu_L\,\right] \\
& + \left({}^{u}\mu_L - {}^{u}\mu_T\right)w_{R}^{(2.12)}
\end{aligned}
\tag{A.19}
$$

with ${}^{u}\mu_L$ and ${}^{u}\mu_T$ defined by Eq. (2.76b).

Chapter 3

A framework for modeling cell spreading, motility, and receptor dynamics

Mattia Serpelloni[1,2], Matteo Arricca[1,2], Claudia Bonanno[1,3] and Alberto Salvadori[1,2]

[1]The Mechanobiology Research Center, UNIBS, Italy
[2]Department of Mechanical and Industrial Engineering, University of Brescia, Italy
[3]Department of Civil, Environmental, Architectural Engineering and Mathematics, University of Brescia, Italy

Abstract. The response of cells during spreading and motility is dictated by several multi-physics events, which are triggered by extracellular cues and occur at different time-scales. For this sake, it is not completely appropriate to provide a cell with classical notions of the mechanics of materials, as for "rheology" or "mechanical response". Rather, a cell is an alive system with constituents that show a reproducible response, as for the contractility for single stress fibers or for the mechanical response of a biopolymer actin network, but that reorganize in response to external cues in a non-exactly predictable and reproducible way. Aware of such complexity, in this note we aim at formulating a multi-physics framework for modeling cell spreading and motility, accounting for the relocation of proteins on advecting lipid membranes.

3.1 Introduction

Receptor dynamics along cell membrane is a key factor in several biological phenomena, as for angiogenesis, tumor metastasis, endocytosis and exocytosis. Angiogenesis is a multistep process in which endothelial cells are affected by several extracellular stimuli, including growth factors, extracellular matrix, and parenchymal and stromal cells. In this process, growth factor receptors as well as adhesion receptors convey the extracellular signaling in a coordinate intracellular pathway promoting cell proliferation, migration, and reorganization in active vessels [68]. Integrins are a family of cell adhesion receptors that support and modulate several cellular functions required for tumor metastasis. They can directly contribute to the control and progress of metastatic dissemination. During tumor development, changes in this family of receptors impact upon the ability of tumor cells to interact with their environment and enable metastatic cells to convert to a migratory and invasive phenotype. Integrins regulate each step of the metastasis, and affect tumor cell survival and interaction with changing environments in transit from the primary tumor to distant target organs [69]. Receptor-mediated endocytosis is a process by which cells absorb metabolites, hormones, proteins –

and, in some cases, viruses – by the inward budding of the plasma membrane (invagination). This process forms vesicles containing the absorbed substances and is strictly mediated by receptors on the surface of the cell [70].

Whereas uncountable papers have been published on the biology of cell spreading, motility and the relocation of proteins on advecting lipid membranes, the mathematical modeling definitely lags behind experiments and overall received much less attention. Although nowadays a widespread literature in mechanobiology exists [71], the protein relocation and interaction with the reorganizing cytoskeleton in the biological phenomena mentioned above is still an ongoing research topic, let alone the formulation of efficient algorithms and computational solvers for three-dimensional simulations [72].

In this note, we attempt at defining a multi-physics scheme for the modeling of cell spreading, motility and the receptor dynamics along advecting lipid membranes, framing the mathematical setting within the mechanics and thermodynamics of continua [53], stemming from seminal works [14, 15, 73] and accounting for recent literature, either connected to the endocytosis of virus in human and animal cells [74, 75, 76] or ligand-receptor mediated raft formation [77], chemotaxis [78], surface-associated caveolae mechanotransduction [79]. The general framework illustrated in this note applies to growth and remodeling, too, falling within the category of *theory of finite growth* according to the terminology defined in [80].

The paper is designed as follows. After a nomenclature of the main symbols and the definition of operators in a Lagrangian setting, the paper focuses in Section 3.3 upon receptor relocation and reaction on a lipid membrane that advects. The topic is purposely presented in a broad sense, in order to be applicable to several possible receptor-ligand interactions. Section 3.3 includes the equations that rule protein transport on an advecting lipid membrane, and receptors-ligand interactions in form of chemical reactions that take place concurrently with relocation. A rather similar approach has been taken in section 3.4, which concerns the relocation and reaction of actin to form biopolymers within the cytosol. The mechanical evolution of the cell is discussed afterwards in Section 3.5. Besides stating the classical laws of mechanics, the section is accompanied by an extensive discussion on boundary conditions, aimed at showing that Neumann type of conditions, due to electrostatic interactions, are most likely not responsible for cell spreading and motion, in view of the modest amount of energy involved in those interactions compared to the bulk energy of a cell. We therefore concluded that spreading is a result of extensional and contractile forces exerted by pseudopodia and the cytoskeleton machinery [81]. Those forces have been investigated in Section 3.6, where the thermodynamics of receptor motion on the membrane was studied at first up to the constitutive theory and the receptor-ligand interaction kinetics. The analysis of the thermo-chemo-mechanics of cells is the last section of this work. In it, we highlight the role of strain and stress decompositions in order to model cell adhesion, protrusion, and contractility. A bibliographic review is presented in a rather extensive paragraph, showing various approaches pursued in the literature to cover the multiscale scenario of cell viscoelasticity and identifying missing pieces within the theoretical framework that we set in the present note.

3.2 Definitions

Denote with $\mathcal{B}_t$ a volume that advects, and with $\partial\mathcal{B}_t$ its surface. A point $\boldsymbol{x} \in \mathcal{B}_t$ is defined as the image of a point $\boldsymbol{X}$ in the reference configuration $\mathcal{B}_{\scriptscriptstyle R}$ through a smooth function $\boldsymbol{\chi}(\boldsymbol{X}, t)$ termed *motion*. Following [53], we will name *deformation* the snapshot of a motion at a fixed time t

$$\boldsymbol{\chi}_t(\boldsymbol{X}) = \boldsymbol{\chi}(\boldsymbol{X}, t) \; .$$

The deformation is assumed to be a one-to-one map. In addition, denoting the deformation gradient with

$$\mathbf{F} = \boldsymbol{\nabla}_{\scriptscriptstyle R} \left[\boldsymbol{\chi}_t \right] ,$$

the requirement $J = \det\left[\, \mathbf{F} \,\right] > 0$ holds.

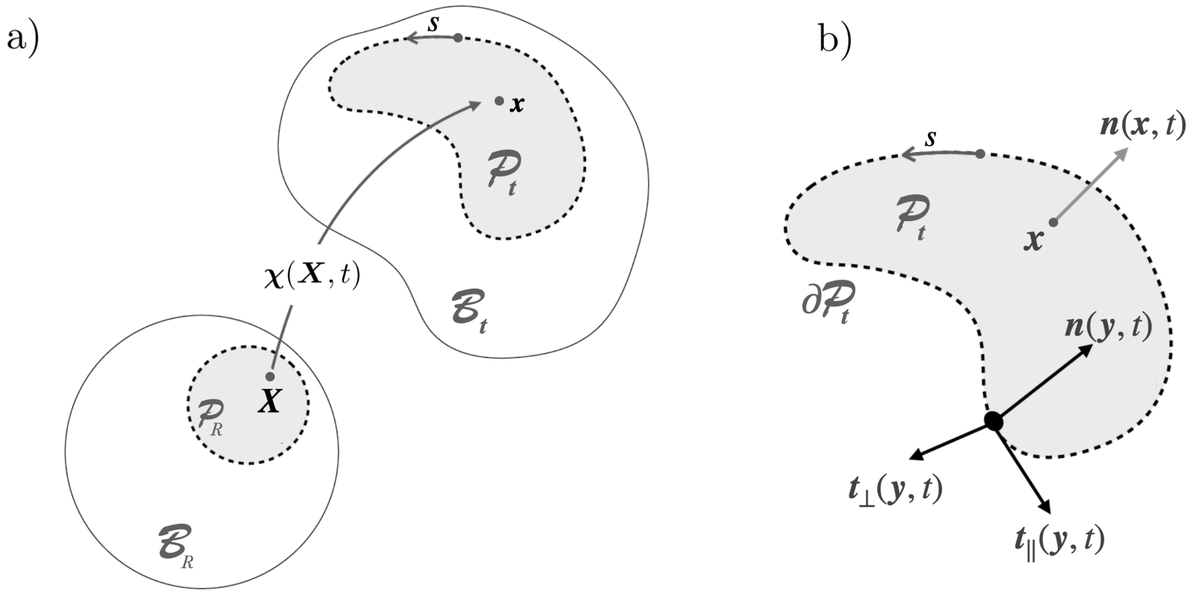

Figure 3.1: Notation. a) The reference body $\mathcal{B}_R$ and the deformed body $\mathcal{B}_t$. A material point $\boldsymbol{X} \in \mathcal{P}_R \subset \mathcal{B}_R$ is mapped into a spatial point $\boldsymbol{x} \in \mathcal{P}_t \subset \mathcal{B}_t$. b) Frenet frame at point $\boldsymbol{y} \in \partial\mathcal{P}_t$ and the normal vector $\boldsymbol{n}$ at point $\boldsymbol{x} \in \mathcal{P}_t$.

Define $\partial\mathcal{P}_t \subset \partial\mathcal{B}_t$ as in Fig. 3.1, and consider a scalar function $f(\boldsymbol{x},t)$, with $\boldsymbol{x} \in \mathcal{P}(t)$. The *Frenet-Serret* reference frame at a generic point $\boldsymbol{y} \in \partial\mathcal{P}_t$ is defined in Fig. 3.1, in terms of the two unit vectors $\boldsymbol{t}_{\parallel}(\boldsymbol{y},t)$ (tangent) and $\boldsymbol{t}_{\perp}(\boldsymbol{y},t)$ (normal). The vector $\boldsymbol{n}(\boldsymbol{y},t)$ (binormal) is here taken of non-unit length, being the imagine in $\mathcal{B}_t$ of a unit vector $\boldsymbol{n}_R$ in the reference configuration $\mathcal{B}_R$, by means of the contravariant transformation

$$\boldsymbol{n} = \mathbf{F}^{-\mathrm{T}}\,\boldsymbol{n}_R \ .$$

On the other hand, the following covariant transformations hold

$$\boldsymbol{t}_{\parallel R} = \mathbf{F}^{-1}\,\boldsymbol{t}_{\parallel} \ , \qquad \boldsymbol{t}_{\perp R} = \mathbf{F}^{-1}\,\boldsymbol{t}_{\perp} \ ,$$

with the obvious implication that $\boldsymbol{t}_{\parallel R}$ and $\boldsymbol{t}_{\perp R}$ are not unit vectors.

The *projected divergence operator* of a vector field $\boldsymbol{v}_R$, whose image is $\boldsymbol{v}$ with arbitrary direction on $\partial\mathcal{P}_t$, writes

$$\boldsymbol{\nabla}_{\mathcal{S}_R} \cdot [\,\boldsymbol{v}_R\,] = \boldsymbol{\nabla}_R \cdot [\,\boldsymbol{v}_R\,] - \boldsymbol{n}_R \cdot \boldsymbol{\nabla}_R\,[\,\boldsymbol{v}_R\,]\,\boldsymbol{n}_R \ , \tag{3.1}$$

with $\boldsymbol{\nabla}_R \cdot [\ ]$ *standard* divergence operator defined on $\mathcal{P}_R$.

Provided sufficient smoothness, the divergence theorem holds also for advecting membranes, in the form

$$\int_{\partial\mathcal{P}_R} \boldsymbol{\nabla}_{\mathcal{S}_R} \cdot [\,\boldsymbol{v}_R\,]\,\mathrm{d}\mathcal{A} = \int_{\mathcal{C}_R} \boldsymbol{v}_R \cdot \boldsymbol{t}_{\perp R}\,\mathrm{d}\mathcal{L} \ . \tag{3.2}$$

For an exhaustive definition of the surface nabla operator $\boldsymbol{\nabla}_{\mathcal{S}_R}$ see [82]. Proof of theorem (3.2), as well as other theorems not explicitly stated in this manuscript can be found in [7]. A more comprehensive definition of Frenet formulae and operators on a surface have been exposed in the original paper [2].

3.3 Relocation and reaction of receptors on a lipid membrane that advects

3.3.1 Mass transport on a surface that advects

Consider a generic species a at a point $\boldsymbol{x}$ on the surface $\partial\mathcal{P}_t$, and let c_a define its concentration (moles or molecules per unit surface). Species a convects with velocity $\boldsymbol{v}_a(\boldsymbol{x},t)$. The latter entails the dragging, or advection, velocity $\boldsymbol{v}_{adv}(\boldsymbol{x},t)$ and another velocity that is due to many possible physics, as for diffusion or migration. The mass flux vector of species a, denoted with $\boldsymbol{h}_a$ hereinafter, is the product of the surface concentration c_a times the net velocity of species a, hence $\boldsymbol{h}_a = c_a\,(\boldsymbol{v}_a - \boldsymbol{v}_{adv})$.

Take a surface $\partial\mathcal{P}_R \subset \partial\mathcal{B}_R$ bounded by $\mathcal{C}_R$, as the referential descriptions of $\partial\mathcal{P}_t \subset \partial\mathcal{B}_t$ bounded by $\mathcal{C}_t$. The flux of species a across the boundary $\mathcal{C}_R$ writes

$$\int_{\mathcal{C}_R} \boldsymbol{h}_{a_R} \cdot \boldsymbol{t}_{\perp_R}\,\mathrm{d}\mathcal{L}\,.$$

where $\boldsymbol{h}_{a_R}$ denotes the referential mass flux,

$$\boldsymbol{h}_{a_R} = j(\boldsymbol{X},t)\,\mathbf{F}^{-1}(\boldsymbol{X},t)\,\boldsymbol{h}_a\,(\,\boldsymbol{x}(\boldsymbol{X},t\,),t\,)\;, \tag{3.3}$$

with $j(\boldsymbol{X},t)$ areal Jacobian defined by the relation [53, 58]

$$j(\boldsymbol{X},t) = J\,|\mathbf{F}^{-T}\boldsymbol{n}_R| = J\,\sqrt{\boldsymbol{n}_R \cdot \mathbf{C}^{-1}\boldsymbol{n}_R}\;, \tag{3.4}$$

with $\mathbf{C}$ right Cauchy-Green tensor.

Mass balance of species a in $\partial\mathcal{P}_R$ writes

$$\dot{\overline{\int_{\partial\mathcal{P}_R} c_{a_R}(\boldsymbol{X},t)\,\mathrm{d}\mathcal{A}}} + \int_{\mathcal{C}_R} \boldsymbol{h}_{a_R} \cdot \boldsymbol{t}_{\perp_R}\,\mathrm{d}\mathcal{L} = \int_{\partial\mathcal{P}_R} s_{a_R}(\boldsymbol{X},t)\,\mathrm{d}\mathcal{A}\;, \tag{3.5}$$

where c_{a_R} is the referential concentration of species, and s_{a_R} is the reference mass supply[1]. It holds

$$c_{a_R} = j(\boldsymbol{X},t)\,c_a(\,\boldsymbol{x}(\boldsymbol{X},t\,),t\,) \qquad s_{a_R} = j(\boldsymbol{X},t)\,s_a(\,\boldsymbol{x}(\boldsymbol{X},t\,),t\,)\;. \tag{3.6}$$

After application of the divergence theorem (3.2) and recognition that the resultant integrals must hold for any arbitrary surface $\partial\mathcal{P}_R \subset \partial\mathcal{B}_R$, Eq. (3.5) eventually localizes as

$$\dot{c}_{a_R} + \boldsymbol{\nabla}_{\mathcal{S}_R} \cdot [\,\boldsymbol{h}_{a_R}\,] = s_{a_R}\;. \tag{3.7}$$

After definitions of the net velocity and the flux of species a in $\partial\mathcal{P}_t$, equations have been here introduced in Lagrangian formulation, following [10]. Statement of all equations in spatial setting, with subsequent rephrasing in reference configuration, have been here omitted and can be found in the original version [2] and in [7].

3.3.2 Relocation and reaction

The association and formation of a protein complex follow a two-steps mechanism: the formation of an encounter complex, in which previously free proteins show few specific interactions and assume many orientations, and the evolution of the encounter complex in the final complex. The binding-unbinding interaction

$$\mathrm{R} + \mathrm{L} \underset{k_R^f}{\overset{k_R^b}{\rightleftarrows}} \mathrm{C} \tag{3.8}$$

---

[1] As an example, in biology cells may produce proteins that move to the lipid membranes from the cytosol.

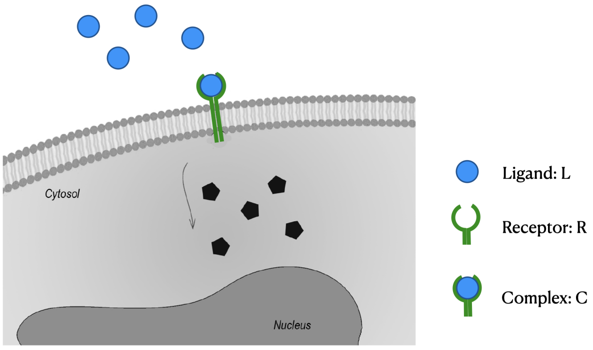

Figure 3.2: Schematic representation of receptor-ligand interaction and complex formation on the cell membrane modeled via Eq. (3.8).

accounts for both mechanisms [12].

Coefficients k^f_R and k^b_R are the kinetic constants of the forward and backward reaction, respectively. The rate of reaction (3.8), denoted with $w^{(3.8)}_R$ and measured in $[mol/m^2 s]$, quantifies the net formation of C on the advecting membrane as the difference between the forward and backward reactions. Eq. (3.7) shall be extended to account for reaction (3.8) and tailored to species $a = \mathrm{R}, \mathrm{L}, \mathrm{C}$.

Receptors (either free or bound into the complex) are distributed along the membrane together with other lipid species and proteins. They are assumed to freely move laterally, and effects due to steric hindrance are not accounted for. The amount of proteins per unit area that can be placed at a membrane is thus limited by the actual size of the protein itself. This evidence ushers the definition of a concentration saturation limit $c^{max}_a(\boldsymbol{X}, t)$, representing the maximum number of moles or molecules per unit area for any species a.

During their life, cells and their membranes undergo major *macroscopic* mechanical deformations. Studies on the red blood cell [83] suggest that the membrane deformation occur at constant area, but this evidence does not appear to be supported by experiments in endothelial cells during spreading [81]. Individual protein and phospholipid can easily move laterally within the membrane, which results in a very low shear stiffness. The mechanisms that are in charge of areal expansion during cell spreading are complex and involve the micro-structural topology[2] of the membrane. It is the case, for instance, of invaginated membrane domains flattening [84], *i.e.* the role of caveolae as membrane surface repositories that readily made available for fast geometrical evolution, as during filopodia extension.

Given that the area occupied by each unit species is invariant, we consider species relocations to occupy areal expansions of the hosting material. Therefore, accounting for the fact that the maximum amount of moles or molecules on the membrane increases with areal expansions leads to take a constant value of the concentration saturation limit (moles or molecules per unit surface), hence

$$c^{max}_{a_R}(\boldsymbol{X}, t) = c^{max}_a(\boldsymbol{x}, t) \; , \tag{3.9}$$

oppositely to [10].

Accordingly, the value of the non-dimensional ratio between the concentration of species a and its amount at saturation

$$\vartheta_a(\boldsymbol{X}, t) = \frac{c_{a_R}}{c^{max}_{a_R}} \; , \tag{3.10}$$

is subjected to the transformation

$$\vartheta_{a_R}(\boldsymbol{X}, t) = j(\boldsymbol{X}, t) \, \vartheta_a(\boldsymbol{x}(\boldsymbol{X}, t), t) \; , \tag{3.11}$$

---

[2] Multiscale investigations, however, fall out of the scope of the present work.

according to Eq.s $(3.6)_1$, (3.9) and (3.10).

The kinetics of reaction (3.8) is modeled as for ideal systems via the law of mass action [51]

$$w_{_R}^{(3.8)} = k^f \, \frac{\vartheta_{\mathrm{R}_R}}{(1-\vartheta_{\mathrm{R}_R})} \, \frac{\vartheta_{\mathrm{L}_R}}{(1-\vartheta_{\mathrm{L}_R})} - k^b \, \frac{\vartheta_{\mathrm{C}_R}}{(1-\vartheta_{\mathrm{C}_R})} \; , \tag{3.12}$$

where the configuration invariance of the kinetic coefficients,

$$k_{_R}^f(\boldsymbol{X},t) = k^f(\boldsymbol{x},t) \qquad k_{_R}^b(\boldsymbol{X},t) = k^b(\boldsymbol{x},t) \; , \tag{3.13}$$

descends from the transformation rule

$$w_{_R}^{(3.8)}(\boldsymbol{X},t) = j(\boldsymbol{X},t) \, w^{(3.8)}(\boldsymbol{x}(\boldsymbol{X},t),t) \; , \tag{3.14}$$

and the consideration of Eq. (3.11).

At chemical equilibrium $w_{_R}^{(3.8)} = 0$, and concentrations obey the relation

$$\frac{k^f}{k^b} = \frac{\vartheta^{\mathrm{eq}}_{\mathrm{C}_R}}{(1-\vartheta^{\mathrm{eq}}_{\mathrm{C}_R})} \, \frac{(1-\vartheta^{\mathrm{eq}}_{\mathrm{R}_R})}{\vartheta^{\mathrm{eq}}_{\mathrm{R}_R}} \, \frac{(1-\vartheta^{\mathrm{eq}}_{\mathrm{L}_R})}{\vartheta^{\mathrm{eq}}_{\mathrm{L}_R}} = K^{(3.8)}_{\mathrm{eq}} \tag{3.15}$$

which defines the constant of equilibrium $K^{(3.8)}_{\mathrm{eq}}$ of reaction (3.8).

Far from the saturation limit, $(1-\vartheta_{a_R}) \sim 1$ for all a. Accordingly, the mass action law (3.12) re-writes in the form

$$w_{_R}^{(3.8)} = k^f \, \vartheta_{\mathrm{R}_R} \, \vartheta_{\mathrm{L}_R} - k^b \, \vartheta_{\mathrm{C}_R} \; . \tag{3.16}$$

according to Eq. (3.13).

The diffusion of receptors and the viscous evolution of the cell during adhesion and migration appear to be much slower than the interaction kinetics, *i.e.* the time required to reach chemical equilibrium is orders of magnitude smaller than the time-scale of other processes. For this reason, thermodynamic equilibrium may be invoked in place of a transient evolution, thus inferring the constraint $w_{_R}^{(3.8)} = 0$ to the concentrations of species at all times. Far from saturation, equating (3.16) to zero yields

$$\vartheta_{\mathrm{C}_R} = \frac{k^f}{k^b} \, \vartheta_{\mathrm{R}_R} \, \vartheta_{\mathrm{L}_R} \; . \tag{3.17}$$

Making use of definition of (3.10), Eq. (3.17) can be cast in the form

$$c_{\mathrm{C}_R} = \frac{k^b}{k^f} \, \frac{c^{max}_{\mathrm{R}} \, c^{max}_{\mathrm{L}}}{c^{max}_{\mathrm{C}}} c_{\mathrm{R}_R} \, c_{\mathrm{L}_R} \; , \tag{3.18}$$

In vivo experiments show that complex molecules usually have a much smaller mobility than receptors, perhaps induced by their size. For in vitro experiments [6, 1, 24], ligands are prevented to flow onto the substrate. Given that complex molecules result from the interaction with immobile ligands, they are macroscopically steady as well. Since receptors move along the membrane, reaction (3.8) traps mobile receptors, and vice-versa [9]. In this work, analogously to [16], ligands and complex are assumed to be motionless, therefore

$$\boldsymbol{h}_{\mathrm{L}_R} = \boldsymbol{h}_{\mathrm{C}_R} = \boldsymbol{0} \; . \tag{3.19}$$

In view of considerations made so far, the local form of the mass balance (3.7) specifies as

$$\dot{c}_{\mathrm{R}_R} + \boldsymbol{\nabla}_{\mathcal{S}_R} \cdot [\, \boldsymbol{h}_{\mathrm{R}_R} \,] + w_{_R}^{(3.8)} = s_{\mathrm{R}_R} \tag{3.20a}$$

$$\dot{c}_{\mathrm{L}_R} + w_{_R}^{(3.8)} = 0 \; , \tag{3.20b}$$

$$\dot{c}_{\mathrm{C}_R} - w_{_R}^{(3.8)} = 0 \; , \tag{3.20c}$$

Eq. (3.20a) is defined on the membrane $\partial\mathcal{P}_{R}$, where receptors flow. The supply s_{R_R} accounts for internalization or generation of proteins, thus representing the amount of receptors that are generated within the cell and reach the membrane or that internalize. It can be related to the time derivative of the areal jacobian $j(\boldsymbol{X},t)$, thus representing the change in membrane area, through a parameter κ_{R_R}. It holds

$$s_{\mathrm{R}_R}(\boldsymbol{X},t) = \kappa_{\mathrm{R}_R}\left[|\mathbf{F}^{-\mathrm{T}}\,\boldsymbol{n}_{R}|\, J\,\mathrm{tr}\,[\,\mathbf{L}\,] - \frac{J}{2}\,\frac{1}{|\mathbf{F}^{-\mathrm{T}}\,\boldsymbol{n}_{R}|}\,\boldsymbol{n}_{R}\cdot\mathbf{C}^{-1}\,\dot{\mathbf{C}}\,\mathbf{C}^{-1}\,\boldsymbol{n}_{R}\right] \,, \tag{3.21}$$

with $\mathbf{L}=\dot{\mathbf{F}}\,\mathbf{F}^{-1}$ velocity gradient and $\mathbf{C}$ right Cauchy-Green strain tensor.

At all points at which ligands and receptors do not interact, the reaction rate $w_{R}^{(3.8)}$ vanishes. Eq. (3.20b) is rather defined in the location where ligands stand. In vitro, a given amount of ligands (which can be thought of as the initial condition of Eq. (3.20b) are spread upon a microscope slide. Finally, Eq. (3.20c) is defined in the contact zone between the cell and the slide where reaction (3.8) takes place.

It is convenient to rephrase Eq. (3.20b) in terms of the "ligands made available for the reaction" in place of the "ligands spread on the slide". The former ligands are the ones "felt" at a point on the membrane as the distance from such point and the substrate, where ligands are spread out, becomes sufficiently small. Such distance can be understood as a cutoff within which the formation of an encounter complex becomes possible, as made clear in [12, 85, 86, 87]. Despite the size of the cutoff distance remains inaccurately estimated, it was established to be on the order of tens nanometers [14, 12]. It arises form the interplay of attractive and repulsive forces between either two cells or a cell and a substrate. Indeed, negative electrical charge carried by cells generates repulsive electrostatic forces - *repulsive barrier* - which is further enriched by an additional resistance provided by the compression of the glycocalyx proteins. Rather, electrodynamic van der Waals forces are expected to be attractive [12]. Both van der Waals and compressive forces are characterized as non-specific long ranged forces, whereas cell adhesion is generally mediated by the specific short ranged receptor-ligand interactions, which can cause cell adhesion much more tightly than the non-specific electrical forces [12, 16]. Cells separated by a distance less than, or equal to, the cutoff distance should form a zone of adhesion with the substrate by means of local fluctuations in receptors density, so that small regions of increased density can penetrate through the resisting potential to react with the source of ligands on substrate [14].

This point of view, which corresponds to the picture of tight receptor-ligand bond as a set of weak non covalent physical interactions [88], is made explicit by a supply function s_{L_R} that vanishes at long ranges and rapidly reaches the initial concentration of ligands available for the reaction at short distances. We therefore re-write Eq. (3.20b) in the form

$$\dot{c}_{\mathrm{L}_R} + w_{R}^{(3.8)} = s_{\mathrm{L}_R} \;. \tag{3.22}$$

The ligand supply $s_{\mathrm{L}_R}(\boldsymbol{X},t)$ becomes available for the reaction during the spreading of the cell. It seems to be logically related to *i*) a gap function between the substrate rich in ligands and the cell membrane, and *ii*) a lag in time, a point-wise function of an internal variable that activates when the gap function is below some threshold and is related to the chemical kinetics of the binding-unbinding reaction (3.8). In this form, all three equations (3.20a), (3.20c), (3.22) can be written on the membrane $\boldsymbol{X}\in\partial\mathcal{P}_{R}$.

Assuming that the time scale of the chemical reaction is much faster than other processes, the concentrations of species may be governed by thermodynamic equilibrium at all times. The concentration of complex c_{C_R} relates then to the others by the equation $w_{R}^{(3.8)}=0$. Therefore, according to Eq. (3.18), the two concentrations c_{R_R} and c_{L_R} fully describe the problem in the assumption of infinitely fast kinetics, whereas the concentration of the complex can be deduced a posteriori. The two governing equations descend from Eq. (3.20) and write

$$\dot{c}_{\mathrm{R}_R} + \dot{c}_{\mathrm{C}_R} + \boldsymbol{\nabla}_{\mathcal{S}_R}\cdot[\,\boldsymbol{h}_{\mathrm{R}_R}\,] + w_{R}^{(3.8)} = s_{\mathrm{R}_R} \;, \quad \boldsymbol{X}\in\partial\mathcal{P}_{R} \;, \tag{3.23a}$$

$$\dot{c}_{\mathrm{L}_R} + \dot{c}_{\mathrm{R}_R} + w_{R}^{(3.8)} = s_{\mathrm{L}_R} \;, \quad \boldsymbol{X}\in\partial\mathcal{P}_{R} \;, \tag{3.23b}$$

after recognition of Eq. (3.22).

Relocation of receptors that undergo binding-unbinding reactions on a membrane that advects is thus described by Eq.s (3.23a), (3.23b) and (3.18), with associated initial conditions

$$c_{\mathrm{R}_R}(\boldsymbol{X},0) = c^0_{\mathrm{R}_R}(\boldsymbol{X}) \ , \qquad c_{\mathrm{L}_R}(\boldsymbol{X},0) = 0 \ , \qquad c_{\mathrm{C}_R}(\boldsymbol{X},0) = 0 \ ,$$

and Dirichlet-Neumann boundary conditions. These equations are coupled to the mechanical evolution of the cell (*i.e.* adhesion, spreading, migration) through the function $s_{\mathrm{L}_R}(\boldsymbol{X},t)$, which "transfers" ligands on the membrane according to the geometry of the cell.

3.4 Relocation and reaction of actin to form biopolymers

The mathematical description made in Section 3.3 will guide the modeling of the relocation and reaction of actin to form biopolymers in the cytosol, which will be summarized here in a shorter shape.

Biopolymers are composed of actin, a protein termed globular or G-actin in its monomeric form, and F-actin when it forms filamentous polymers - see Fig. 3.3 a). Actin filaments can in turn bundle to form stress fibers, or cross-link to form polymer networks that allow the movement of the cell - see Fig. 3.3 b). Polymerization is usually triggered by extracellular signals, denote with $\mathcal{C}(\boldsymbol{X},t)$ hereinafter. In the case of cell locomotion, *e.g.*, the cell extends finger-like protrusions to "feel" the surrounding surface. The precise details of the signaling pathways are nonetheless here ignored.

The transduction of the signal results in the polymerization of actin filaments and their cross-linking or bundling. The formation of single actin filaments can be modeled as a bimolecular reaction [89]. In this note, the biopolymer turn-over will be described at a larger scale, involving the interplay between fundamental units and stress-fibers or pseudopodia, in the form

$$\mathrm{G} \underset{k^-_R}{\overset{k^+_R}{\rightleftarrows}} \mathrm{F} \tag{3.24}$$

with F denoting either one of the two biopolymers, G globular actin, k^+_R and k^-_R forward and backward kinetic constants representing the polymerization and depolymerization of actin, respectively.

The network or fiber formation rate of reaction (3.24), denoted with $w^{(3.24)}_R$, is influenced by mechanical stresses. Stress fiber stability is favored by tension, for instance. For this reason, the stress tensor enters the chemical potential and the dissociation reaction of biopolymers.

The kinetics of reaction (3.24) is modeled via the law of mass action, properly extended to account for signaling,

$$w^{(3.24)}_R(\boldsymbol{X},t) = \mathcal{C}(\boldsymbol{X},t)\, k^+_R \,\frac{\vartheta_{\mathrm{G}}}{(1-\vartheta_{\mathrm{G}})} - \mathcal{D}(\boldsymbol{X},t)\, k^-_R \,\frac{\vartheta_{\mathrm{F}}}{(1-\vartheta_{\mathrm{F}})} \ , \tag{3.25}$$

with function $\mathcal{D}$ accounting for the role of the stress in the dissociation of biopolymers (see for instance [19]).

Note that Eq. (3.25) is written in accordance with

$$w^{(3.24)}_R(\boldsymbol{X},t) = J(\boldsymbol{X},t)\, w^{(3.24)}_R(\boldsymbol{x}(\boldsymbol{X},t),t) \ , \qquad \vartheta_a(\boldsymbol{X},t) = \vartheta_a(\boldsymbol{x}(\boldsymbol{X},t),t) \ , \tag{3.26}$$

with $J(\boldsymbol{X},t) = \det[\,\mathbf{F}\,]$, having assumed for the bulk of the cell

$$c^{max}_{a_R}(\boldsymbol{X},t) = J(\boldsymbol{X},t)\, c^{max}_a(\boldsymbol{x}(\boldsymbol{X},t),t) \ , \tag{3.27}$$

differently to what performed in Section 3.3.2.

The invariance of ϑ_a with the configuration implies that "constants" k^+_R and k^-_R are not constants, hence

$$k^+_R(\boldsymbol{X},t) = J(\boldsymbol{X},t)\, k^+(\boldsymbol{x}(\boldsymbol{X},t),t) \ , \qquad k^-_R(\boldsymbol{X},t) = J(\boldsymbol{X},t)\, k^-(\boldsymbol{x}(\boldsymbol{X},t),t) \ . \tag{3.28}$$

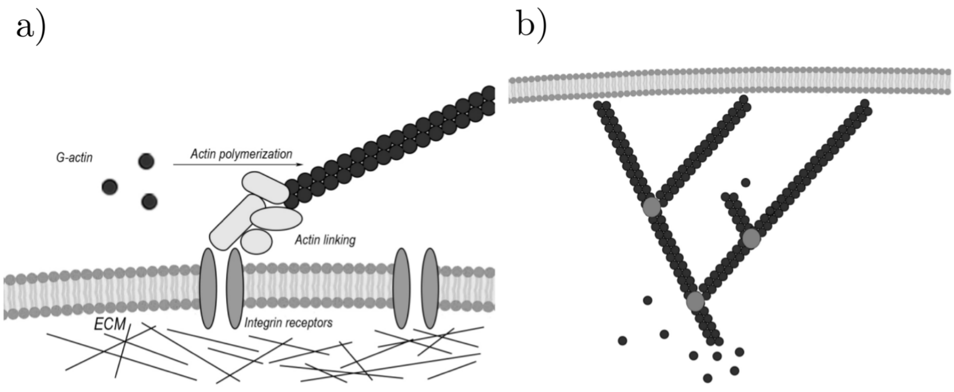

Figure 3.3: Biopolymers schematics. a) F-actin polymerization, triggered by integrin activity. b) Schematic of the biopolymer network at the leading edge of a cell.

3.4.1 Mass transport in the cytosol

Take a volume $\mathcal{P}_R \subset \mathcal{B}_R$, whose surface is $\partial\mathcal{P}_R \subset \partial\mathcal{B}_R$, and consider species $a = \mathrm{G}, \mathrm{F}$. The mass balance of species a writes

$$\dot{\overline{\int_{\mathcal{P}_R} c_{a_R} \, \mathrm{d}\mathcal{V}}} + \int_{\partial\mathcal{P}_R} \boldsymbol{h}_{a_R} \cdot \boldsymbol{n}_R \, \mathrm{d}\mathcal{A} \pm \int_{\mathcal{P}_R} w_R^{(3.24)} \, \mathrm{d}\mathcal{V} = \int_{\mathcal{P}_R} s_{a_R} \, \mathrm{d}\mathcal{V} \, , \tag{3.29}$$

with

$$c_{a_R}(\boldsymbol{X}, t) = J(\boldsymbol{X}, t) \, c_a(\, \boldsymbol{x}(\boldsymbol{X}, t\,), t\,) \tag{3.30}$$

reference molarity of species a,

$$\boldsymbol{h}_{a_R}(\boldsymbol{X}, t) = J(\boldsymbol{X}, t) \, \mathbf{F}^{-1}(\boldsymbol{X}, t) \, \boldsymbol{h}_a(\, \boldsymbol{x}(\boldsymbol{X}, t\,), t\,) \, , \qquad s_{a_R}(\boldsymbol{X}, t) = J(\boldsymbol{X}, t) \, s_a(\, \boldsymbol{x}(\boldsymbol{X}, t\,), t\,) \, , \tag{3.31}$$

reference flux vector $\boldsymbol{h}_{a_R}(\boldsymbol{X}, t)$ and the reference mass supply $s_{a_R}(\boldsymbol{X}, t)$, respectively, and $w_R^{(3.24)}$ defined by Eq. $(3.26)_1$.

As for the complex molecules, filaments usually have a much smaller mobility than monomers, and might be therefore assumed to be motionless. Then

$$\boldsymbol{h}_{\mathrm{F}_R} = \mathbf{0} \, . \tag{3.32}$$

Accordingly, after application of the divergence theorem and recognition that the resultant integrals must hold for any $\mathcal{P}_R \subset \mathcal{B}_R$, Eq. (3.29) specializes as

$$\dot{c}_{\mathrm{G_R}} + \boldsymbol{\nabla}_R \cdot [\, \boldsymbol{h}_{\mathrm{G}_R} \,] + w_R^{(3.24)} = s_{\mathrm{G}_R} \, , \tag{3.33a}$$

$$\dot{c}_{\mathrm{F_R}} - w_R^{(3.24)} = s_{\mathrm{G}_R} \, . \tag{3.33b}$$

The diffusion of monomers appears to be much slower than the interaction kinetics, and the concentrations of species may be therefore governed by thermodynamic equilibrium at all times [22]. The concentration of filaments c_{F_R} relates then to the monomers by the equation $w_R^{(3.24)} = 0$, mediated by the local amount of signaling and stress. Eq.s (3.33), with associated initial conditions

$$c_{\mathrm{G}_R}(\boldsymbol{X}, 0) = c^0_{\mathrm{G}_R}(\boldsymbol{X}) \, , \qquad c_{\mathrm{F}_R}(\boldsymbol{X}, 0) = c^0_{\mathrm{F}_R}(\boldsymbol{X}) \, ,$$

and Dirichlet-Neumann boundary conditions, define the relocation of monomers that undergo polymerization reactions.

3.5 Mechanical evolution of the cell

Based upon the selection of the mechanisms that are supposed to govern the structural response of the cell, the balance laws of linear and angular momentum come out. Literature provides two basic approaches, whether the structural functions are demanded entirely to the cell membrane [90, 91, 92, 93, 94] or to the development of a cytoskeletal structure within the bulk of the cell [19, 20, 73, 95, 21, 96, 97, 98, 99]. The influence of curvature on the membrane elastic stiffness appears to be related to the size of the cell [17], and seems to be negligible for endothelial cells of diameter $\sim 10\mu$m. These two evidences lead to consider the reorganization of the cytoskeleton the main responsible for the mechanical response of endothelial cells [100], coupled to a passive behavior dictated by the viscosity of the cytosol [73, 19, 99]. Accordingly, balance of linear and angular momentum will be formulated for the bulk of the cell rather than the membrane.

Forces in continuum mechanobiology are described by *contact* forces between adjacent regions (as for the forces exchanged by the substrate and the cell during adhesion), *surface* forces exerted on the boundary of the cell by the environment (as for the receptor-ligand attractive and repulsive electrostatic interactions [12, 101]), *body* forces exerted on interior points by the environment (as for the gravity or pseudopodia forces that preside migration). Contact and surface forces will be denoted henceforth with $\boldsymbol{t}_{R}$, whereas body forces will be denoted with $\boldsymbol{b}_{R}$.

Throughout the rest of the paper we will neglect inertia forces, although some authors [102] pinpointed the role of inertia forces during migration. Accordingly, the balance of linear and angular momentum,

$$\int_{\partial \mathcal{P}_R} \boldsymbol{t}_R(\boldsymbol{X},t) \, \mathrm{d}\mathcal{A} + \int_{\mathcal{P}_R} \boldsymbol{b}_{0_R}(\boldsymbol{X},t) \, \mathrm{d}\mathcal{V} = \boldsymbol{0} \; , \tag{3.34a}$$

$$\int_{\partial \mathcal{P}_R} \boldsymbol{\chi} \times \boldsymbol{t}_R(\boldsymbol{X},t) \, \mathrm{d}\mathcal{A} + \int_{\mathcal{P}_R} \boldsymbol{\chi} \times \boldsymbol{b}_{0_R}(\boldsymbol{X},t) \, \mathrm{d}\mathcal{V} = \boldsymbol{0} \; , \tag{3.34b}$$

with $\boldsymbol{b}_{0_R}$ conventional body force, not encompassing inertial effects.

Let $\boldsymbol{t} = \mathbf{T}\,\boldsymbol{n}$ define the current surface traction, with $\mathbf{T}$ Cauchy stress, and $\boldsymbol{t}_R = \mathbf{T}_R\,\boldsymbol{n}_R$ its referential counterpart, with $\mathbf{T}_R$ first Piola stress tensor. Application of the divergence theorem to Eq.s (3.34) and recognition that the resultant integrals must hold for any arbitrary volume yield

$$\boldsymbol{\nabla}_R \cdot [\, \mathbf{T}_R \,] + \boldsymbol{b}_{0_R} = \boldsymbol{0} \; , \tag{3.35a}$$

$$\mathbf{T}_R \, \mathbf{F}^{\mathrm{T}} = \mathbf{F} \, \mathbf{T}_R^{\mathrm{T}} \; . \tag{3.35b}$$

with and $\boldsymbol{\nabla}_R \cdot [\, \mathbf{T}_R \,] = \partial \mathrm{T}_{Rij} / \partial X_j$ and

$$\mathbf{T}_R = J(\boldsymbol{X},t) \, \mathbf{T}(\boldsymbol{x}(\boldsymbol{X},t),t) \, \mathbf{F}^{-\mathrm{T}}(\boldsymbol{X},t) \; ,$$

according to the definition of surface tractions, whereas the following transformation for the conventional body force holds

$$\boldsymbol{b}_{0_R}(\boldsymbol{X},t) = J(\boldsymbol{X},t) \; \boldsymbol{b}_0(\boldsymbol{x}(\boldsymbol{X},t),t) \; .$$

Contact and surface forces are boundary conditions for problem (3.35a). They emanate from electrostatic long or short range interactions, from receptor-ligand adhesion forces, as well as from contact tractions after adhesion. A vast literature [89, 103, 104] has been devoted to quantify the forces involved in these interaction mechanisms. It emerges that uncertainties remain in the establishment of realistic values for attraction forces, not surprisingly due to the complexity of the required experimental tasks.

3.6 Thermodynamics

The quest of the right principles of thermodynamics in mechanobiology is, on one hand, far from being understood and, from a wider perspective, it paves the way to boundless questions of philosophical and ethical nature, as for the establishment of a thermodynamics of life [105], which fall completely out of the scope of present paper. Major accomplishments have been recently achieved [106] in formulating fresh concepts that deviate from classical results of thermodynamics of non equilibrium. In this scientific area, which is nowadays flourishing, new fundamentals assertions are expected in the years to come.

Being aware that classical formulations of non equilibrium thermodynamics [51] may not be able to capture some principles of mechanobiology that rule receptor dynamics - as for the homeostatic constraint [107], we are prone to deepen our formulation in future studies.

3.6.1 Thermodynamics of receptor motion on the membrane

Following [10, 9], receptor dynamics on the lipid membrane is thermodynamically described by energy and entropy balances, imposing as usual that the internal production of entropy cannot be negative. After the definition of the referential specific Helmholtz free energy per unit volume $\psi_{_R}$, taken as a function of temperature and concentrations, $\psi_{_R}\left(T, c_{\mathrm{R}_R}, c_{\mathrm{L}_R}, c_{\mathrm{C}_R}\right)$ the entropy imbalance in the Clausius-Duhem form is derived. The method of Coleman and Noll [8] finally allows to identify the following thermodynamic restrictions

$$\mu_{\mathrm{R}} = \frac{\partial \psi_{_R}}{\partial c_{\mathrm{R}_R}}, \qquad \mu_{\mathrm{L}} = \frac{\partial \psi_{_R}}{\partial c_{\mathrm{L}_R}}, \qquad \mu_{\mathrm{C}} = \frac{\partial \psi_{_R}}{\partial c_{\mathrm{C}_R}}, \qquad \eta_{_R} = -\frac{\partial \psi_{_R}}{\partial T} \; , \tag{3.36}$$

for chemical potentials μ_α and entropy $\eta_{_R}$. Furthermore, assuming that receptor relocations take place in thermal equilibrium conditions, the so called Clausius-Plank inequalities apply

$$\boldsymbol{h}_{\mathrm{R}_R} \cdot \boldsymbol{\nabla}_{\mathcal{S}_R} \left[\, \mu_{\mathrm{R}} \, \right] \leq 0 \; , \tag{3.37a}$$

$$A^{(3.8)} \, w_{_R}^{(3.8)} \leq 0 \; , \tag{3.37b}$$

with $A^{(3.8)}$ chemical affinity of reaction (3.8). A strategy to meet the thermodynamic restriction (3.37a) is to model the flux of receptors by Fickian-diffusion, which linearly correlates $\boldsymbol{h}_{\mathrm{R}_R}$ to the gradient of its chemical potential μ_{R}

$$\boldsymbol{h}_{\mathrm{R}_R} = -\mathbf{M}_{\mathrm{R}}(c_{\mathrm{R}_R}) \, \boldsymbol{\nabla}_{\mathcal{S}_R} \left[\, \mu_{\mathrm{R}} \, \right] \; , \tag{3.38}$$

by means of a positive definite mobility tensor $\mathbf{M}_{\mathrm{R}}(c_{\mathrm{R}_R})$. The following isotropic non linear specialization for the mobility tensor $\mathbf{M}_{\mathrm{R}}(c_{\mathrm{R}_R})$ is chosen [55]

$$\mathbf{M}_{\mathrm{R}}(c_{\mathrm{R}_R}) = \mathbb{u}_{\mathrm{R}} \, c_{\mathrm{R}}^{max} \; \vartheta_{\mathrm{R}_R} \; (1 - \vartheta_{\mathrm{R}_R}) \; \mathbf{1} \; , \tag{3.39}$$

with c_{R}^{max} and $\mathbb{u}_{\mathrm{R}} > 0$ saturation limit for receptors and mobility of receptors, respectively.

Definition (3.39) represents the physical requirement that both the pure ($c_{\mathrm{R}_R} = 0$) and the saturated ($c_{\mathrm{R}_R} = c_{\mathrm{R}}^{max}$) phases have vanishing mobilities. Neither the mobility $\mathbb{u}_{\mathrm{R}}$ nor the saturation concentration c_{R}^{max} are assumed to change in time. Whereby experimental data indicate an influence of temperature, stresses, or concentrations, such a limitation can be removed without altering the conceptual picture. Noting that

$$\boldsymbol{\nabla}_{\mathcal{S}_R} \left[\, \mu_{\mathrm{R}} \, \right] = \frac{R \, T}{c_{\mathrm{R}}^{max}} \, \frac{1}{\vartheta_{\mathrm{R}_R} (1 - \vartheta_{\mathrm{R}_R})} \, \boldsymbol{\nabla}_{\mathcal{S}_R} \left[\, c_{\mathrm{R}_R} \, \right] \; ,$$

with R universal gas constant, Fick's Law (3.38) specializes as

$$\boldsymbol{h}_{\mathrm{R}_R} = -\mathbb{D}_{\mathrm{R}} \, \boldsymbol{\nabla}_{\mathcal{S}_R} \left[\, c_{\mathrm{R}_R} \, \right] \; , \tag{3.40}$$

where $\rlap{|}D_{\mathrm{R}} = \rlap{|}u_{\mathrm{R}} \, R \, T$ is the receptor diffusivity.

The chemical kinetics of reaction (3.8) is modeled via the law of mass action (3.12). Experimental evidences [6] show that *i*) the equilibrium constant (3.15) is high, thus favoring the formation of ligand-receptor complexes and the depletions of both receptors and ligands, *ii*) the diffusion of receptors on the cell membrane is much slower than interaction kinetics. Accordingly, it can be assumed that the reaction kinetics is infinitely fast, in the sense that the time required to reach chemical equilibrium is orders of magnitude smaller than the time-scale of other processes. For these reasons we assume that the concentrations of species are ruled by thermodynamic equilibrium at all times, and the concentration of complex c_{C_R} is related to the others by Eq. (3.18). This very same equation could be derived imposing

$$A^{(3.8)} = 0 \; .$$

Simple algebra allows deriving Eq. (3.18), provided that to the equilibrium constant $K_{\mathrm{eq}}^{(3.8)}$ the alternative definition

$$K_{\mathrm{eq}}^{(3.8)} = \exp\left(- \frac{\Delta G^0}{R \, T} \right) \tag{3.41}$$

is given, where $\Delta G^0 = \mu^0_{\mathrm{C}} - \mu^0_{\mathrm{L}} - \mu^0_{\mathrm{R}}$ is the standard Gibbs free energy.

3.6.2 Thermo-chemo-mechanics of cells

Endothelial cells show two main paradigmatic mechanical attitudes, active and passive. Active response is related to the cell ability to change its own cytoskeletal conformation, as a result of external cues, *i.e.* to reorganize the morphology of biopolymers that provides the structural resistance during adhesion (to the ECM or to other cells), migration [108] (*e.g.* chemotaxis [109], mechanotaxis, and durotaxis [110]) and division (*e.g.* mitosis). Passive, instead, refers to the mechanical response that each component of the cell has inasmuch material bodies, in accordance with their own internal structure and as a result of external actions.

Following [10, 9], the thermo-chemo-mechanics of endothelial cells can be stated stemming from energy and entropy balances. The referential specific Helmholtz free energy per unit volume is taken as a function of temperature, strain $\mathbf{C}$, concentrations c_{G_R} and c_{F_R}, and of some kinematic internal variables $\boldsymbol{\Xi}$ that compare with the usual meaning in inelastic constitutive laws [53, 58, 59, 54, 60, 61], hence $\psi_R \left(T, c_{\mathrm{G}_R}, c_{\mathrm{G}_R}, \mathbf{C}, \boldsymbol{\Xi} \right)$. The method of Coleman and Noll [8] allow identifying the following thermodynamic restrictions

$$\mathbf{S} = 2 \, \frac{\partial \psi_R}{\partial \mathbf{C}} \; , \qquad \eta_R = - \frac{\partial \psi_R}{\partial T} \; , \qquad \mu_{\mathrm{G}} = \frac{\partial \psi_R}{\partial c_{\mathrm{G}_R}} \; , \qquad \mu_{\mathrm{F}} = \frac{\partial \psi_R}{\partial c_{\mathrm{F}_R}} \; , \tag{3.42a}$$

with $\mathbf{S} = \mathbf{F}^{-1} \, \mathbf{T}_R$ second Piola-Kirchhoff stress. The internal stress, conjugate to $\boldsymbol{\Xi}$, will be denoted with the symbol $\rlap{|}\mathbf{X}$,

$$\rlap{|}\mathbf{X} = - \frac{\partial \psi_R}{\partial \boldsymbol{\Xi}} \; . \tag{3.42b}$$

Eq.s (3.42a) yields to the Clausius-Plank inequality. Under the assumptions of Curie symmetry principle [51] and thermal equilibrium,

$$\begin{aligned} \rlap{|}\mathbf{X} : \dot{\boldsymbol{\Xi}} \; & \geq 0 \; , & (3.43a) \\ \boldsymbol{h}_{\mathrm{G}_R} \cdot \boldsymbol{\nabla}_R \left[\, \mu_{\mathrm{G}_R} \right] \; & \leq 0 \; , & (3.43b) \\ A^{(3.24)}_R \, w^{(3.24)}_R \; & \leq 0 \; . & (3.43c) \end{aligned}$$

The flow of actin monomers is linearly related to the gradient of their chemical potential by Fick's assumption, consistently with the thermodynamic restriction (3.43b),

$$\boldsymbol{h}_{\mathrm{G}_R} = - \mathbf{M}_{\mathrm{G}}(c_{\mathrm{G}_R}) \; \boldsymbol{\nabla}_R \left[\, \mu_{\mathrm{G}} \, \right] \; . \tag{3.44a}$$

The following positive definite, isotropic non linear specialization for the mobility tensor $\mathbf{M}_{\mathrm{G}}$ is chosen [55]

$$\mathbf{M}_{\mathrm{G}}(c_{\mathrm{G}_R}) = \psi_{\mathrm{G}}\, c^{max}_{\mathrm{G}_R}\, \vartheta_{\mathrm{G}}\ (1-\vartheta_{\mathrm{G}})\ \mathbf{1}\ , \tag{3.45}$$

where $c^{max}_{\mathrm{G}_R}$ and $\psi_{\mathrm{G}} > 0$ are the saturation limit and the mobility of actin monomers. Assuming that the trapped species F has vanishing mobility is an alternative view of modeling the absence of their flux.

3.6.2.1 Decompositions

The stress field $\mathbf{S}$ will be additively decomposed in the sum of the active and passive contributions,

$$\mathbf{S} = \mathbf{S}^{act} + \mathbf{S}^{pas}\ , \tag{3.46}$$

analogously to generalized Maxwell models. Active response is related to cytoskeletal reorganization in stress fibers and pseudopodia, whereas the passive response reflects the mechanical behavior that each component of the cell has inasmuch material bodies.

We base the theory for pseudopodia on a multiplicative decomposition of the deformation gradient

$$\mathbf{F} = \mathbf{F}^{e}\, \mathbf{F}^{s}\ . \tag{3.47}$$

Tensor $\mathbf{F}^{s}$, named swelling distortion is the local distortion of the material neighborhood of a point due to a volumetric swelling (de-swelling) due to the phase change of actin, from monomeric to a network of filaments, and vice-versa. Its representation will be taken as $\mathbf{F}^{s} = \lambda^{s}\,\mathbf{1}$, assuming therefore that a dense network of actin filaments form in pseudopodia. This approach conforms well for lamellipodia filament networks, although it might result inappropriate for slender and highly oriented microstructures seen in filopodia, which might be better captured by protrusion-contraction uniaxial tensors presented in [102, 111] or [112]. The following identities can be easily assessed

$$\det\left[\,\mathbf{F}^{s}\,\right] = J^{s} = {\lambda_{s}}^{3}\ , \qquad \frac{\dot{J}^{s}}{J^{s}} = 3\,\frac{\dot{\lambda}_{s}}{\lambda_{s}}\ , \qquad \mathbf{L}^{s} = \dot{\mathbf{F}}^{s}\,\mathbf{F}^{s-1} = \frac{1}{3}\frac{\dot{J}^{s}}{J^{s}}\mathbf{1}\ . \tag{3.48}$$

We assume that changes in J^{s} occur because of changes in filaments $J^{s} = J^{s}(c_{\mathrm{F}_R})$, with the form

$$\dot{J}^{s} = \omega_{s}(c_{\mathrm{F}_R})\,\dot{c}_{\mathrm{F}_R}\ , \tag{3.49}$$

with $\omega_{s}\,(c_{\mathrm{F}_R})$ partial molar volume of the pseudopodia (see [10] for details).

The decomposition (3.47) leads to a multiplicative decomposition for the right Cauchy-Green tensor,

$$\mathbf{C} = \mathbf{C}^{e}\,\mathbf{C}^{s}\ , \tag{3.50}$$

with $\mathbf{C}^{s} = J^{s\,2/3}\,\mathbf{1}$ swelling factor, and $\mathbf{C}^{e} = J^{s\,-2/3}\,\mathbf{C}$ elastic factor.

A classical specification of $J^{s}(c_{\mathrm{F}_R})$ is the affine map [55]

$$J^{s}(c_{\mathrm{F}_R}) = 1 + (c_{\mathrm{F}_R} - c^{0}_{\mathrm{F}_R})\,\omega_{s}\ , \tag{3.51}$$

with a constant partial molar volume $\omega_{s} > 0$.

In the realm of viscoelasticity, it is also common to perform a multiplicative decomposition of the deformation gradient $\mathbf{F}^{e}$ into volumetric $\mathbf{F}^{e,vol}$ and isochoric $\mathbf{F}^{e,iso}$ factors

$$\mathbf{F}^{e} = \mathbf{F}^{e,vol}\,\mathbf{F}^{e,iso}\ . \tag{3.52}$$

The volumetric factor $\mathbf{F}^{e,vol} = J^{e\,1/3}\,\mathbf{1}$ turns out to be completely identified by the determinant of $\mathbf{F}^{e}$, whereas the isochoric factor $\mathbf{F}^{e,iso} = J^{e\,-1/3}\,\mathbf{F}^{e}$ obeys to the constraint $\det[\,\mathbf{F}^{e,iso}\,] = 1$. The decomposition (3.52) leads to a multiplicative decomposition for the elastic factor $\mathbf{C}^{e}$. Accordingly

$$\mathbf{C}^{e} = \mathbf{C}^{e,vol}\,\mathbf{C}^{e,iso}\ , \tag{3.53}$$

with $\mathbf{C}^{e,vol} = J^{e\,2/3}\,\mathbf{1}$ volumetric factor, and $\mathbf{C}^{e,iso} = J^{e\,-2/3}\,\mathbf{C}^{e}$ isochoric factor.

3.6.2.2 Constitutive theory

The Helmholtz free energy density ψ_R is modeled by decomposition into a thermal contribution ψ_R^{th}, a diffusive contribution ψ_R^{diff}, an elastic contribution ψ_R^{el}, and an inelastic counterpart ψ_R^{in}. Then

$$\psi_R(T, c_{\mathrm{G}_R}, c_{\mathrm{F}_R}, \mathbf{C}, \boldsymbol{\Xi}) = \psi_R^{th}(T) + \psi_R^{diff}(c_{\mathrm{G}_R}, c_{\mathrm{F}_R}, \mathbf{C}) + \psi_R^{el}(c_{\mathrm{F}_R}, \mathbf{C}) + \psi_R^{in}(c_{\mathrm{F}_R}, \boldsymbol{\Xi}) \, . \tag{3.54}$$

This splitting is here taken for granted without motivation. Furthermore, we will not indulge in the description of ψ_R^{th} and ψ_R^{in}, and we briefly summarize terms ψ_R^{diff} and ψ_R^{el} on the basis of [10, 9]. All contributions of Eq. (3.54) have been exhaustively detailed in [63].

The diffusive contribution to the Helmholtz free energy density writes

$$\begin{aligned} \psi_R^{diff}(c_{\mathrm{G}_R}, c_{\mathrm{F}_R}) = {} & \mu_{\mathrm{G}}^0 \, c_{\mathrm{G}_R} + R T c_{\mathrm{G}_R}^{max} \left[\vartheta_{\mathrm{G}} \ln \vartheta_{\mathrm{G}} + (1 - \vartheta_{\mathrm{G}}) \ln(1 - \vartheta_{\mathrm{G}}) \right] \\ & + \mu_{\mathrm{F}}^0 \, c_{\mathrm{F}_R} + R T c_{\mathrm{F}_R}^{max} \left[\vartheta_{\mathrm{F}} \ln \vartheta_{\mathrm{F}} + (1 - \vartheta_{\mathrm{F}}) \ln(1 - \vartheta_{\mathrm{F}}) \right] \, . \end{aligned} \tag{3.55}$$

Following [59] and according to the multiplicative decomposition (3.53),

$$\psi_R^{el}(c_{\mathrm{F}_R}, \mathbf{C}) = \psi_R^{el,vol}(c_{\mathrm{F}_R}, \mathbf{C}^{e,vol}) + \psi_R^{el,iso}(c_{\mathrm{F}_R}, \mathbf{C}^{e,iso}) \, . \tag{3.56}$$

The volumetric part of the elastic free energy is defined through J^e, highlighting the role of the swelling tensor and of the concentration of pseudopodia, since

$$\mathbf{C}^{e,vol} = J^{e\,2/3} \, \mathbf{1} = J^{2/3} \, J^{s\,-2/3} \, \mathbf{1} = \left[\frac{J}{1 + (c_{\mathrm{F}_R} - c_{\mathrm{F}_R}^0) \, \omega_s} \right]^{\frac{2}{3}} \mathbf{1} \, , \tag{3.57}$$

in view of Eq. (3.51). On the other end, it holds

$$\mathbf{C}^{e,iso} = \mathbf{C}^e \, J^{e\,-2/3} = \mathbf{C} \, J^{s\,-2/3} \, J^{e\,-2/3} = \mathbf{C} \, J^{-2/3} \, , \tag{3.58}$$

therefore $\mathbf{C}^{e,iso}$ depends merely upon the state of deformation and not upon the concentration of species.

The selection for ψ_R^{el} and ψ_R^{in}, shall be different in modeling the passive behavior or the active response of pseudopodia and stress fibers. The elastic, reversible, behavior that occurs once the viscous effects vanish is captured by ψ_R^{el}. The inelastic free energy accounts for the non-equilibrium response due to viscosity, termed dissipation potential. By means of thermodynamic restrictions (3.42) and identity (3.42b),

$$\mathbf{X}\mkern-10mu| = - \frac{\partial \psi_R^{in}}{\partial \boldsymbol{\Xi}} \tag{3.59a}$$

$$\mathbf{S} = 2 \, \frac{\partial \psi_R^{diff}}{\partial \mathbf{C}} + 2 \, \frac{\partial \psi_R^{el}}{\partial \mathbf{C}} \, . \tag{3.59b}$$

Inelastic internal entropy production (3.43a) has been described by the internal flux variables $\boldsymbol{\Xi}$ and by their energy-conjugate stress $\mathbf{X}\mkern-10mu|$. A simple way to satisfy constraint (3.43a) is choosing a positive definite operator $\mathbb{L}$ such that

$$\mathbf{X}\mkern-10mu| = \mathbb{L} \, \dot{\boldsymbol{\Xi}} \, . \tag{3.60}$$

In case of isotropy, the fourth order operator $\mathbb{L}$ restricts to the scalar viscosity ν times the identity operator. Eq.s (3.59a) and (3.60) provide evolution equations for $\mathbf{X}\mkern-10mu|$ that allow the algorithmic integration of the constitutive law once a selection for the free energy ψ_R^{in} is made.

The chemical potential of G-actin monomers and of F-actin networks descends from thermodynamic prescriptions (3.42a), in the form

$$\mu_{\mathrm{G}} = \frac{\partial \psi_R^{diff}}{\partial c_{\mathrm{G}_R}} \tag{3.61a}$$

$$\mu_{\mathrm{F}} = \frac{\partial \psi_R^{diff}}{\partial c_{\mathrm{F}_R}} + \frac{\partial \psi_R^{el,vol}}{\partial c_{\mathrm{F}_R}} + \frac{\partial \psi_R^{el,iso}}{\partial c_{\mathrm{F}_R}} + \frac{\partial \psi_R^{in}}{\partial c_{\mathrm{F}_R}} \, . \tag{3.61b}$$

While the chemical potential of actin monomers has merely an entropic nature, mechanical contributions enter the definition of the chemical potential of actin networks. Specifically, mechanics affects $\mu_{\rm F}$ in the volumetric contribution $\psi_R^{el,vol}$ through the swelling tensor $\mathbf{C}^{e,vol}$ (3.57), whereas the isochoric tensor $\mathbf{C}^{e,iso}$ was proven to be independent upon the concentration of species in Eq. (3.58). Nonetheless, the parameters of the viscoelastic loading-unloading law are expected to depend upon the extent of the polymerization reaction by means of the network concentration $c_{{\rm F}_R}$ in all terms of the mechanical free energy.

The mechanical effect on the chemical potential does not propagate into the mass flux because the mobility of actin network is assumed to be negligible. Mechanics however enters the affinity of polymerization reaction (3.24). The stress state is expected to favor polymerization nearby the lipid membrane and depolymerization towards the nucleus.

3.6.2.3 The multiscale scenario of cell viscoelasticity

Although the free energy scenario is rather clear, a specialization of the constitutive equations has not been attempted here and in many cases (as for the lamellipodia filament network) it has not been attempted in the literature, to the best of our knowledge. The hindrance stands in the multiscale scenario of cell viscoelasticity. Despite the mechanical behavior and properties of the main cytoskeletal biopolymer components (actin filaments, intermediate filaments, and microtubules) has been nowadays quite clarified, at least in terms of relative stiffness and strengths, bundles of the filaments, their response, polymerization, shape and time evolution, are hard to be captured by comprehensive models at the "macroscopic" scale through appropriate free energies. As a consequence, the ability of models to capture the mechanics of fundamental cellular processes (as chemotaxis, cell sprouting, junction and differentiation [113], endocytosis [114] and exocytosis, to cite a few) still requires abundant research before gaining predicting capabilities in simulations.

The cytoskeleton, an interconnected network of regulatory proteins and filamentous biological polymers depicted schematically in Fig. 3.4, undergoes massive reorganization during cell deformation, especially after cell rolling and adhesion [89, 115] and in mediating, sensing and transduction of mechanical cues from the micro-environment [116]. Homogenized models for the mechanical response of a cell shall condense in effective properties the *i*) polymerization and de-polimerization of filaments, *ii*) the cross-linking process that determine the architecture of cytoskeletal filaments, *iii*) the passive mechanical properties of the cytosol. The thermodynamics of statistically-based continuum theories for polymers with transient networks [117, 118, 119, 120] appear to be a valuable candidate for the selection of free energies $\psi_R^{el}(c_{{\rm F}_R}, \mathbf{C})$ and $\psi_R^{in}(c_{{\rm F}_R}, \Xi)$. At present, such a comprehensive model has not yet been proposed for the pseudopodia driven cell motion. Classical models as hyperelastic Saint-Venant [102] or newtonian viscous fluids [121] eventually surrounded by a hyperelastic, zero-thickness membrane [122], have been used for pseudopodia, whereas a very large amount of literature concerns pseudopod dynamics (see for instance [123] and the large literature therein) or ameboid motion [124]. Different approaches to cell motility, as for active gel theory coupled to the classical theory of thin elastic shells, are also widely used [125], but are not discussed in this work. The framework described herein, including myosin dynamics, phase transformations between G-actin and F-actin, has been depicted in a set of publications by the group of H. Gomez [126, 127]. The flow of the F-actin network was treated as a Newtonian fluid and directed by its velocity. A one dimensional yet comprehensive model has been proposed in [128].

The multiscale scenario is invoked also for cell contractility. There are evidences [129] that the interaction among filaments, motors, and cross-linkers is mechanically stimulated. As reported in [116], myosin binding to actin fibers occurs in a force-dependent manner, as well as the contractile response of actomyosin to extracellular stiffness. According to [130], force feedback controls motor activity and increases density and mechanical efficiency of self-assembling branched actin networks, thus suggesting that those feedbacks could allow migratory cells adjusting their viscoelastic properties to favor migration. Mass transport and cell contractility have been accounted for in several publications with different degree of complexity [99, 112, 119]. To the best of our knowledge, however, the

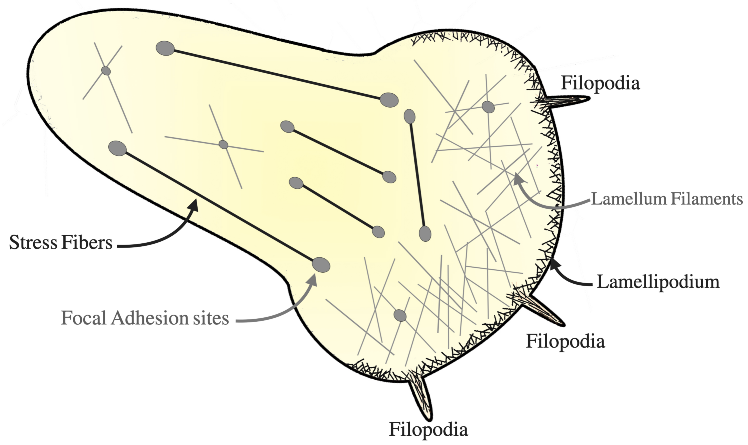

Figure 3.4: A schematic picture of some cytoskeletal biopolymers.

force transmission has always been modeled stemming from the similarity between the sarcomeric structure of stress fibers and the actin-myosin interactions in muscle cells. In [19] a multi-dimensional network of stress fibers was built on the notion of a representative volume element, in which stress fibers can form in any direction with equal probability. An average macroscopic stress is then recovered from the fiber tension, which in turn is generated by cross-bridging cycles and described by a Hill-like relation [131] of viscoelastic nature.

Experimental evidences, however, seem to show that such a resemblance might be questionable in the dynamics and mechanics of endothelial cell spreading [81], and hence that the predictive capability of this family of models might be poor for this family of cells.

Finally, the passive response of the cytosol, mainly provided by the intermediate filaments attached to the nuclear and plasma membranes, has been modeled by several authors by means of classical models as linear elasticity [119], the finite strain generalization of Hooke's law [19], or a Neo-Hookean potential energy.

3.7 Concluding remarks

In this note, a multi-physics framework of protein relocation on advecting lipid membranes during cell spreading and motion has been put forward. It sets the (continuum) thermodynamic background for simulations of receptor recruitment during migration. Simulations carried out in [6] stem from a simplified form of the framework and described the limiting factors in vascular endothelial growth factor receptor relocation. Similarly, we discussed in [1] the relocation of integrins on the membrane and their interactions with growth factor receptors. Those simulations may have a significant impact in biology and in the pharmacological treatment of cancer, both in view of their predictive nature in virtual experiments and by clearly identifying the sequence of processes that limit the relocation of targeted proteins during in vitro experiments.

The present work still has significant limitations, yet by illustrating a complex and rigorous scenario it might be a cornerstone to account for several further processes. To cite a major phenomenon that has been insufficiently discussed here, the protein transport on the membrane is crucially coupled to the cytoskeleton reorganization, which is related to the motion of integrins on the membrane. The formation of focal adhesion sites is preliminary to the generation of stress fibers, and contractility. Internalization of complexes is another occurrence not included in this work. Further publications, therefore, will be devoted to extend this framework to these and others challenging tasks.

We also aimed in this paper at recollecting recent publications from several schools on cell mechanics, encasing them in a unified framework, being aware that a comprehensive account of publications is significantly hard in view of the broadness of the literature in the field. We clarified that for some processes, as for contractility and protrusion, either a thermodynamically consistent formulation has not been devised yet or it stems upon simplistic models that do not account for the microstructural evolution of biopolymers. Even in this fascinating field, the last word is far from being spoken.

Acknowledgements. This work has been supported by grants from the company *Ferriera Valsabbia* through a liberal donation to fund studies in the field of Mechanobiology, and from *Fondazione Berlucchi* to Mattia Serpelloni. We gratefully acknowledge pleasant scientific discussions with S. Mitola, E. Grillo, and C. Ravelli from the DMMT at the University of Brescia.

Chapter 4

Modeling receptor motility along advecting lipid membranes

Matteo Arricca[1,2], Alberto Salvadori[1,2], Claudia Bonanno[1,3], Mattia Serpelloni[1,2]

[1]The Mechanobiology Research Center, UNIBS, Italy
[2]Department of Mechanical and Industrial Engineering, University of Brescia, Italy
[3]Department of Civil, Environmental, Architectural Engineering and Mathematics, University of Brescia, Italy

Abstract. This work aims to overview multiphysics mechanobiological computational models for receptor dynamics along advecting cell membranes. Continuum and statistical models of receptor motility are the two main modeling methodologies identified in reviewing the state of the art. Within the former modeling class, a further subdivision based on different biological purposes and processes of proteins' motion is recognized; cell adhesion, cell contractility, endocytosis, and receptor relocations on advecting membranes are the most relevant biological processes identified in which receptor motility is pivotal. Numerical and/or experimental methods and approaches are highlighted in the exposure of the reviewed works provided by the literature, pertinent to the topic of the present manuscript. With a main focus on the continuum models of receptor motility, we discuss appropriate multiphyisics laws to model the mass flux of receptor proteins in the reproduction of receptor relocation and recruitment along cell membranes to describe receptor–ligand chemical interactions, and the cell's structural response. The mass flux of receptor modeling is further supported by a discussion on the methodology utilized to evaluate the protein diffusion coefficient developed over the years.

4.1 Introduction

The present manuscript focuses on the multiphysics modeling of protein motility along advecting animal cell membranes, overviewing the state of the art and proposing suitable physical laws to couple receptor relocation on membranes with cellular mechanical deformation. From a conceptual point of view, physical theories and mathematical tools allow us to relate the mechanical principles with the behavior of living matter: thermo-mechanics of continua [53, 54] is the ideal framework to model nature's laws. Due to its intrinsic interdisciplinarity, a multi-physics approach to biological phenomena may have the potential to highlight key and limiting factors, providing innovative pathways for analysis and interpretation.

Receptor motility along cell membranes is involved in several biological processes, such as cell, bacteria, and virus adhesion and motility, as well as endocytosis and exocytosis, to cite a few

[132, 133, 134, 135, 136, 137]. The cell membrane plays a crucial role in cellular protection, in the control and transport of nutrients [138], and in regulating the interchange of different substances in the cell [139]. Its structure facilitates directional or Brownian diffusion of receptors, internalization, and segregation. Acting as a barrier between the extra-cellular and intra-cellular environments, the cell membrane controls the flux of matter across and along its surface [140]. Being constituted of two sheets of phospholipid (amphoteric) molecules, cell membranes in aqueous environments acquire the conformation of a phospholipid bilayer, with the hydrophobic end inside the bilayer and the hydrophilic outside. Such a conformation, including the various embedded proteins (receptors, ion channels, transporters, and other proteins), constitutes the so-called *fluid-mosaic* model [141]. Membrane fluidity represents one of the most critical membrane properties [138], and it is still the object of several studies [138, 142, 139, 143, 144, 145, 140, 146]. Among numerous molecules relocating along the plasma membrane, we focus here on the motility of receptor proteins. For the sake of generality, and due to the aim of this manuscript, we do not distinguish among the different types of receptors in terms of structure and second-messenger systems.

The paper is organized as follows. Continuum models of receptor motility along advecting membranes are illustrated in Section 4.2; in it, we will collect and discuss publications on receptor–ligand-mediated cell adhesion, cell contractility, protein relocation on advecting membranes, receptor-mediated endocytosis, and a few other subjects. Statistical models of receptor dynamics are shortly recapitulated in Section 4.3. In view of the huge number of publications in this realm, we cannot aim at being exhaustive. In the following Section 4.4, we discuss some specific thermodynamic prescriptions for the mass flux of receptors and the kinetics of receptor-ligand interactions. The summary in Section 4.5 completes the manuscript.

4.2 Continuum models of receptor motility

4.2.1 Receptor–ligand-mediated cell adhesion

Receptor–ligand-mediated cell adhesion is one of the most common and widely studied mechanobiological processes. In it, receptor motility plays a significant role. To the best of our knowledge, the pioneering studies of Bell [12] and co-workers [101] paved the way in developing multi-physics models in mechanobiology. The receptor density in receptor–ligand-mediated cell–cell adhesion was analyzed in a thermodynamic framework, investigating the competition between attractive receptor–ligand and repulsive electrostatic forces. The former was proven to be of greater influence [12]. An increment of receptor concentration in the adhesion zone was further proposed as a transduction mechanism for triggering different cellular responses. Similarly, the redistribution of receptors is viewed as a signal for cell polarization. Phase transitions occur in cell adhesion, and the stabilization of the cell–cell contact is achieved via cooperative rearrangements of the internal components of the cells [101] (Bell and co-workers [101] used *internal variables* literally, instead of *internal components* . As for other terminology such as *plasticity*, this example displays how very similar words have completely different meanings in mechanics and biology. Such an outcome of the cultural and historical evolution of the disciplines is a further challenge in mechanobiology). Goldstein et al. [147] published a theoretical study of the interaction of low-density lipoprotein (LDL) receptors with coated pits (specialized cell surface structures in which receptors aggregate). They evaluated the diffusion limits for the forward rate constant of the receptor–ligand chemical interaction on a human fibroblast, as well as the average time that LDL receptors spend on the cell surface before being trapped in a coated pit. The obtained results, in agreement with the experiments, led them to conclude that if LDL receptors are inserted at a random position in the cell membrane, their motion is driven by pure diffusion before being trapped in coated pits. A further study [148] found that the way in which coated pits return to the surface does not affect the average time that receptors spend on the membrane, the forward rate constant or the fraction of receptors aggregated in coated pits at high values of the diffusion coefficient, whereas the effect is substantial for “immobile” receptors.

To mimic cell–tissue interaction, the kinetics of cell adhesion due to the bonding between $\alpha_{\mathrm{II}b}\beta_3$

integrins and ligands, gravitation, and Helfrich repulsion were studied in [13] for a single giant vesicle on a solid substrate. The analysis of the growth of the adhesion front revealed the prominent role of the receptor–ligand pairs: at high concentrations, the kinetics of ligand–receptor formation drives the propagation of the front of (tight) adhesion at constant velocity, whereas small ligand densities entail a diffusion-limited growth with a square root dependence on the time. The role of receptor motility in the process of adhesive contact was analyzed in the transient growth of the adhesion zone by Freund and Lin [14]. They assumed the flow of receptors to be proportional to the local gradient in chemical potential and formulated a continuum model of the adhesion of an initially uniformly curved elastic plate to a flat substrate. For very large plates, they solved the problem in closed form, whereas the necessity of numerical methods emerged for those of a limited size. Using the same model, Shenoy and Freund [15] investigated the expansion of a circular adhesion zone when binder (ligand) density is insufficient to overcome the repulsive barrier that resists cell adhesion. They explained the cross-over effect observed in [13] when the densities of ligands and receptors are equal. Indeed, the growth of the adhesion front radius with a time square root dependence observed experimentally in [13] was recovered

$$R(t) = 2\,a\,\sqrt{\mathbb{D}_{\rm L}\, t}\;, \tag{4.1}$$

with t meaning time, $\mathbb{D}_{\rm L}$ ligand diffusivity and a coefficient depending on the ratio between the ligand and receptor concentrations, $c_{\rm L}$ and $c_{\rm R}$; particularly, a assumes finite values for $c_{\rm L}/c_{\rm R} < 1$, whereas the square-root growth regime breaks off for $c_{\rm L}/c_{\rm R} \simeq 1$.

Liu et al. [16] extended the former framework [14, 15] and introduced a so-called traction–separation relation to model cell–substrate interaction. They provided an additional contribution to the flux of receptors, otherwise governed by the classic Fick's law, proportional to the traction component tangent to the membrane surface, to account for the role of non-specific force as driving force for the recruitment of receptors towards the adhesion front. Numerical simulations via finite-element methods shown that the advancing adhesion front might be stable or unstable if exposed to small perturbations, as a function of the membrane shear modulus, the adhesive tractions, and the receptor density. Instability occurs at high adhesive tractions, soft membranes or high ligand–receptor concentration ratios. The traction–separation model [16] was extended in [23], performing simulations of biotin receptor-streptavidin ligand binding-mediated attachment–detachment of a red blood cell to a substrate. A surface diffusion model described receptor motility. The governing equations were implemented in a finite element scheme, providing results in agreement with experimental data.

Golestaneh and Nadler [17] introduced a spontaneous area dilation to account for the influence of receptors on cell deformation and adhesion. Similar to the adhesion–traction model [16, 23], a non-linear receptor–ligand binding force replicated the charge-induced dipole interactions, while Fick's law governed the diffusion of the receptors on the membrane. This study examined the nature of the coupling between electrostatic adhesive forces and the deformation of particle [149] via a non-linear continuum model. A strong coupling was found for small and moderate membrane deformations.

4.2.2 Cell contractility

Deshpande and co-workers proposed a bio-mechanical model, widely used later on, to couple cell contractility with focal adhesions (FAs) [20]. The mechano-sensitive properties of FAs were modeled in a continuum framework, wherein the cytoskeletal contractile forces generated by stress fibers (SFs) drive and stabilize the assembly of the FA complexes. The model accounts for the diffusion of low-affinity integrins along the cell membrane and predicts different levels of concentration of FAs. Simulations replicated high concentration of FAs around the periphery of the cell, the increment of FAs at decreasing cell sizes, and the decrease in intensity of FAs if cell contractility is curtailed. Stemming from this framework, a signaling model was devised based on the generation of IP$_3$ molecules during the FA growth [96], predicting the range of IP$_3$ diffusivities at which the SF activation signal is spatially uniform. The model [20] was also employed for investigating the role of actin cytoskeleton in compression and cell adhesion [97, 98], and to account for the feedback between intracellular signaling, FA formation, and SF contractility in the osteoblast response on a grooved substrate [150]. Simulations revealed the presence of stretched SFs dominant bundles during compression for polarized and axisymmetric spread cells. Round cells were predicted to have fewer SFs and a lower compressive strength. Highly contractile cells were revealed to provide greater resistance to compression by means of dominant circumferential SFs [97]. Supported by experimental observations, the substrate-dependent response of contractile cells with no predefined SF or FA arrangement was predicted. SF contractility was found to affect the substrate-dependent response of cells, including changes in nuclear stress and cell tractions. An increment in SF and FA formation was numerically predicted for stiffer substrates [98]. In [150], it was shown that the cell orientation is governed by the diffusion of signaling proteins activated at FA sites on the ridges. The responsiveness of osteoblasts to the topography of substrates was rationalized by the model. Broadening [20, 150], a non-local finite element setting, was implemented in [95] to study the competition between cytoskeletal and passive elastic-free energies as a driving mechanism in cell spreading. As experimentally observed, a high concentration of aligned SFs along free edges corresponds to a state with low free energy. McMeeking and Deshpande [151], while summarizing previous models [73, 19], presented a bio-chemo-mechanical model implemented in a finite element code for simulating in vitro cell behavior. They targeted contractility, adhesion, signaling, cytoskeleton formation and remodeling.

A coupled formulation of chemo-diffusive integrins with the cytoskeleton, underlying cell contraction and spreading, was proposed in [22]. In agreement with experimental observations, numerical simulations suggested that substrate stiffness and chemistry strongly affect cellular contraction and spreading. The relevant role of mechanics in contraction, adhesion, and spreading of adherent cells was highlighted.

4.2.3 Protein relocation on advecting membranes

Mikucki and Zhou [152], using an energetic variational principle on advecting membranes, derived a curvature-driven transport equation, relating molecule concentrations to a gradient flow governed by a drift-diffusion equation. They predicted the molecular localization on static membrane surfaces at locations with preferred mean curvatures, and that the molecular localization is in turn driven by the generation of preferred mean curvature.

Carotenuto et al. [77] developed a multi-physics approach to investigate how ligand–receptor interactions along the cell membrane trigger raft formation. Diffusion and kinetics of binding and unbinding were studied. Understanding how transporters and active receptors trigger raft formation and clustering is of paramount relevance in membrane-mediated phenomena such as COVID-19 virus–cell interaction.

A discrete model of chemotaxis, which takes into account possible alterations in cellular motility, was presented in [78]. A derivation of the Patlak–Keller–Segel (PKS) model as a continuum limit from the discrete model was shown. Comparisons between numerical simulations of the discrete model and numerical solutions of the PKS model were performed, showing an excellent agreement between the two models.

The authors of this review studied the relocation of transmembrane receptors along advecting cell membranes, like for Vascular Endothelial Growth Factor Receptors 2 (VEGFR2) and $\alpha_v \beta_3$ integrins, by designing chemo-transport-mechanical multi-physics formulations [6, 1, 7, 2] to describe how the mechanical behavior of an endothelial cell (EC) affects receptor dynamics during the early phases of tumor angiogenesis. VEGFR2 dynamics on cell membranes was studied in [6] for EC adhesion onto a rigid substrate coated with specific immobilized ligands, on the basis of the established role as activator of the angiogenic process of the chemical interactions between soluble non-canonical ligands, as gremlins [153, 154], released by cancer cells. Although strongly simplified assumptions on cell mechanics were made, VEGFR2 dynamics was well captured and validated against co-designed experimental investigations [155]. The emergence of three different phases of VEGFR2 relocation and complex generation was unveiled and related to distinct mechanisms, including: (*i*) the initial cell–substrate contact interaction and the VEGFR2–gremlin high chemical reaction rate, (*ii*) the mechanical deformation, (*iii*) the VEGFR2 relocation on EC membrane due to diffusion. The mathematical description of the model was detailed in a companion paper [24]. The model, framed in the mechanics and thermodynamics of continua, follows a general description proposed in [9], and takes advantage of successful descriptions of physically similar systems [156, 157, 41]. The model has been broadened [1, 7] to account for the interplay between VEGFR2 and VEGF-A or the gremlin, $\alpha_v\beta_3$ integrin and the glycoprotein fibronectin embedded in extracellular matrix, and the experimentally revealed interaction between $\alpha_v\beta_3$ integrin and the VEGFR2–gremlin complex [158]. The induced receptor polarization was identified in cell protrusions and in the basal aspect of ECs. Relocation and reaction of $\alpha_v\beta_3$ receptors along cell membranes were also included in a general framework for cell spreading, motility, and receptor dynamics [2, 7]. The mechanics of the cell was accounted for in the field of finite strain theory in continuum mechanics and in a consistent (continuum) thermodynamic setting, together with the modeling of relocation and reaction of actin proteins to form biopolymer structures.

4.2.4 Receptor mediated endocytosis

Based on [14, 15], Gao, Shi and Freund [75] presented a receptor-mediated endocytosis study, considering the role of mobile receptors in wrapping the cell membrane around a cylindrical or spherical particle coated with immobile and uniformly distributed ligands. They showed the existence of a minimum value of both particle radius and receptor density below which wrapping cannot take place. An estimation of the size of the smallest and the largest particle that can be successfully wrapped was given.

A similar study was performed by Decuzzi and Ferrari [159]. They considered both elliptical and cylindrical particles, showing how the internalization is affected by size and aspect ratio.

The same model proposed in [75] allowed us to develop a framework for modeling uptake and release of nanoparticles in human and animal cells. In that paper, the mechanics of cell–nanomaterial interactions was investigated, showing how nanoparticles enter cells by receptor-mediated endocytosis. Coarse-grained molecular dynamics was implemented to perform simulations of nanoparticles interacting with cell membranes [74].

Further works on receptor-driven endocytosis were presented by Wiegold, Klinge, Gilbert, and Holzapfel [76, 160]. They considered viruses as a substrate with fixed receptors, whereas receptors of the host cell could relocate on its membrane. Numerical simulations performed via finite difference methods showed a rapid variation in receptor density at the early stage, while approaching a steady state as the time progresses.

4.2.5 Protein motility miscellanea

Lee et al. [161] proposed a finite-difference mathematical model to describe charged receptor transport on the cell membrane, showing the importance of cell shape in receptor diffusion and in the response to an extracellular sinusoidal electric field. They illustrated how the distribution of receptors may alter transmembrane potential and highlighted the prominence of cell shape (i.e., of the mechanics that rules its evolution) in governing interactions between alternating current electric fields and receptors.

Mac Gabhann and Popel [162] modeled the effect of placental growth factor (PlGF) on the response of VEGF ligands in pathological angiogenesis. A set of coupled reaction–diffusion equations described secretion, transport, binding, and internalization of ligands. The presence of PIGF was established to determine a change in the formation of endothelial surface growth factor–VEGFR1 complexes, and a less significant increment in the number of VEGFR2 complexes. Similar equations were used in [163] to study the binding kinetics and signaling pathways of basic fibroblast growth factor (FGF-2) through a reaction–diffusion model of in vitro FGF-2 transport and receptor–ligand binding. Based on experimental results that included degradation of the internalized cell surface species, formation of double triads, and dimerization of FGF-2 ligands, the role of the low-affinity heparan sulfate proteoglycans (HSPGs), the identity of the minimal signaling complex leading to FGF-2 activity, and the importance of FGF-2 dimerization were pointed out.

Rattanakul, Crooke et al. [164] modeled the signal transduction pathways involving G-proteins by including reaction–diffusion equations of various reactants both inside and on the extra-cellular surface membrane. They investigated the dynamic and steady-state properties of the model via weakly nonlinear stability analysis, showing the robust formation of Turing-type patterns under different system parameters, and discussing theoretical predictions against reported experimental evidence.

As an extension of [165], Earnshaw and Bresslof used reaction–diffusion equations to describe the trafficking of α-amino-3-hydroxy-5-methyl-4-isoxazolepropionic acid receptors (AMPA-Rs) and to evaluate how lateral diffusion contributes to the strength of a synapse [166]. They calculated the distribution of synaptic receptor numbers across the population of spines, determining the effect of lateral diffusion on the strength of a synapse.

Daniels [167] deduced a mathematical expression, in the perturbative deformation regime, to describe the diffusion-limited reaction rate. The coupling between the deformation of a curved membrane and the chemical activities along it was accounted for. The reduction of 20% of the receptor–ligand reaction rate due to the locally induced membrane curvature was theoretically derived.

4.3 Statistical models of receptor motility

Kusumi et al. [168] studied the relocation of E-cadherin and transferrin receptors along mouse keratinocyte cell membranes. A compartmentalization of the cell membrane in small domains, wherein receptors are confined, was suggested as a consequence of the detection of four types of receptor motion (stationary mode, simple Brownian diffusion, and directed and confined diffusion). This conjecture arose from the development of a mean-square displacement (MSD)-based method and the experimental comparison between single-particle tracking (SPT) and fluorescence photobleaching recovery (FPR).

In investigating the non-Brownian diffusion of molecules on membranes by the STP method, Monte Carlo simulations on particles undergoing short-term confined and long-term hop diffusion within a compartment were performed. This simulation strategy detects and characterizes the anomalous diffusion by systematically varying the frame time and rate [169].

By means of a coarse-grained triangular element model, Atilgan and Sun [170] developed a Monte-Carlo methodology, examining the changes in free energy during membrane shape transitions. They showed how a critical value of the concentration of proteins may bring to the formation of small vesicles, therefore influencing the topology of the plasma membrane.

A bimolecular fluorescence complementation (BiFC)-based approach combined with fluorescence correlation spectroscopy (FCS) was used to monitor the diffusion of G-protein-coupled receptor oligomers in the plasma membrane [171]. The approach was used for the first time to measure the membrane diffusional characteristics of adenosine A_1 and A_{2A} receptor homo- and heterodimers in Chinese hamster ovary cells, demonstrating the differences in diffusivity between adenosine receptor homo- and heterodimers.

Paszek et al. [172] developed a chemo-mechanical model in which integrin diffusion, changes in integrin activation status, and integrin–ligand interactions were simulated via kinetic Monte Carlo (KMC) algorithms. The results show the mediator role of glycocalyx in integrin–ligand interactions, which was found to be sufficient to drive integrin clustering even in the absence of cytoskeletal crosslinking or homotypic integrin–integrin interactions.

Receptor dynamics was also accounted by Duke and Graham [173] in reviewing statistical mechanical models for receptors clustering. They accounted for cluster generation and discussed the equilibrium thermodynamics of receptors, ligands, and cytosolic adaptor proteins. The role of adaptor proteins in permitting cells to exert control on cluster formation and to target clustering at specific locations on the cell surface was highlighted.

A nano-meter scale mathematical model that couples membrane bending and long surface molecules (LSMs) compression was presented in [174] to reproduce the lateral mobility of LSMs by drift–diffusion equations. Size-based segregation of LSMs from a receptor–ligand complex was proposed as the mechanism of receptor triggering. Supra-diffusive segregation of LSMs from a single receptor–ligand complex was found.

The reduced mobility of receptors after aggregation processes on the membrane was modeled via both standard and density-dependent diffusion equations in [175]. Critical values of the mobility were compared with numerical simulations, showing that the formation of the aggregate is quite influenced by density-dependent diffusion.

Martini et al. [176] studied the kinetics of a membrane-integrated protein that locates at specific binding sites on the genome, and also acts as a transcriptional activator. Mathematical analysis and KMC simulations of lattice models were combined with fluorescence-microscopy experiments. CadC (the pH receptor of the acid stress response Cad system in E. coli) diffusion along the membrane and conformational fluctuations of the genomic DNA were accounted for. They found that diffusion and captured mechanisms are potentially sufficient for bacterial membrane proteins to establish functional contacts with cytoplasmic targets.

4.4 Discussion

4.4.1 Modeling the mass flux of receptors

Most continuum models described in Section 4.2 account for the protein transport. The mass flux of receptors, $\boldsymbol{h}_{\rm R}$, is usually described via Fick's law,

$$\boldsymbol{h}_{\rm R} = -\mathbb{D}_{\rm R} \, \boldsymbol{\nabla}_{\mathcal{S}} \left[\, c_{\rm R} \, \right] \; , \tag{4.2}$$

with diffusivity $\mathbb{D}_{\rm R}$ and surface gradient operator $\boldsymbol{\nabla}_{\mathcal{S}} [\;]$.

Other authors [16, 23] reformulated Eq. (4.2) for $\boldsymbol{h}_{\rm R}$, assuming that receptors are attracted by ligands by means of a traction force function of the receptor-ligand distance - within a certain cutoff distance - and concentrations. In this case, in addition to Fick's law concentration gradient, a further flux term

$$\boldsymbol{h}^{T}_{\rm R} = u_{\rm R} \, \boldsymbol{t} \cos \beta \tag{4.3}$$

shall be accounted for, where $u_{\rm R}$ is the receptor mobility under ligand attractive forces and $\boldsymbol{t} \cos \beta$ represents the tangential component of the traction (see Figure 4.1).

The influence of non-specific traction forces exerted by ligands on receptor motility and cell adhesion has to be related to the cell size and/or the stage of adhesion considered. Studies performed on different time scales and cell sizes, for the spreading of a mouse embryonic fibroblasts on a matrix-coated surface [177], or for a bovine aortic EC on polyacrylamide gels [178], confer an influence of such forces mostly related to the early stages of adhesion. The adhesion–traction model predicts the isotropic early stage of cell adhesion [16] well, essentially independent to cytoskeleton remodeling and strongly dependent on high ligand densities. This was made even more clear in [23], where a micropipette-manipulated red blood cell attachment–detachment model showed, for an analysis of ≈ 50 ms, a level-off of the adhesion–traction forces after approximately a third of the adhesion-spreading time, and a consequent need for receptor diffusion from remote areas of the cell to fuel the spreading. Moreover, at lower densities of ligands, the spreading becomes strongly dependent on cytoskeletal structures, and cells tend to spread anisotropically by randomly extending pseudopodia [178]. Furthermore, studies on charged flexible particles that adhere to an oppositely charged rigid substrate due to electrostatic attraction forces [149] established that surface forces drive small particle adhesion. The underformed cell radius was considered in the micron/sub-micron range 1 μm [178], or even smaller, 12.5 nm [17]. It follows that, in dealing with cells of radius 10 μm or higher (such as ECs), receptor motility and cell adhesion can be considered unaffected by short-range surface tractions, since their energetic contribution appears to be insufficient in cell spreading without accounting for pseudopodia migration mechanisms.

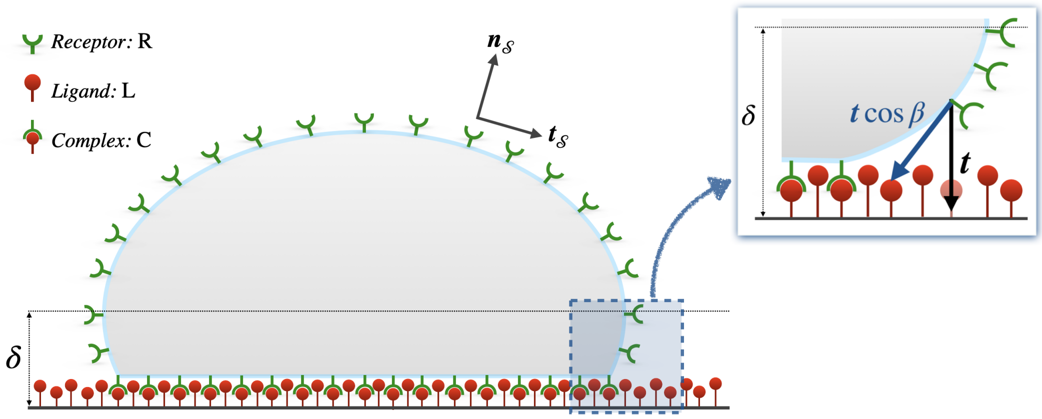

Figure 4.1: Schematic of an adherent cell onto an enriched ligands substrate, inspired by [16, 23]. The image depicts the concept formulated within the adhesion traction model. Vectors $\boldsymbol{n}_{\mathcal{S}}$ and $\boldsymbol{t}_{\mathcal{S}}$ represent the normal and the tangent vector at a certain location on the cell membrane, respectively. Within the cutoff limit δ, the tangential component $\boldsymbol{t}\cos\beta$ of the traction exerted by ligands (vertical traction $\boldsymbol{t}$), attracts the receptors on the cell membrane, generating an additive flux term, $\boldsymbol{h}_{\mathrm{R}}^{T}$, appearing in Eq. (4.3). β is the angle with respect to the vertical defined by $\boldsymbol{t}$.

4.4.2 Evaluation of the protein diffusion coefficient

The diffusive motion of a particle α is predicted by the well-known Einstein–Smoluchowski relation,

$$\mathbb{D}_\alpha = \mathbb{\mu}_\alpha \, k_{_B} \, T \tag{4.4}$$

with $k_{_B}$ as the Boltzmann constant, $\mathbb{\mu}_\alpha$ mobility coefficient and T temperature. To the best of our knowledge, the first model to evaluate the diffusivity was proposed by Saffman and Delbrück (SD) [179], describing the diffusion of a particle due to Brownian motion in biological membranes, and demonstrating a weak logarithmic dependence of the lateral diffusivity on the particle radius r_α,

$$\mathbb{D}_\alpha \propto \ln\left[\, r_\alpha \,\right] \; . \tag{4.5}$$

Several experiments have been devoted to investigating the parameters that influence the diffusivity of proteins on the membrane, such as the membrane's thermal fluctuations [180], the bending rigidity and surface tension [181], the change in the membrane shape [182], and the hydrophobic mismatch between protein length and membrane thickness [183, 184]. The Saffmann theory [185] of membrane hydrodynamics was extended to investigate the correlated Brownian motion of protein pairs [186, 187]. The influence of protein concentration on the motion was accounted for in deriving expressions for the diffusion coefficients as a function of concentrations for small protein size [186]; the effect of the immobile inclusions on the membrane was studied in [187].

The Saffman–Delbrück theory [179] was questioned when investigating the dependence of $\mathbb{D}_\alpha$ on the protein radius [188], because a non-hydrodynamic primary source of protein drag was found after experimental observations. A numerical framework to predict the diffusivity of arbitrarily shaped objects embedded in lipid bilayer membranes was proposed [189], and the influence of finite-size effects in molecular simulations was investigated [190]. An underestimation of diffusion constants due to the sizes of the simulation was predicted via coarse-grained Martini and all-atom CHARMM36 (C36) force fields [191]. By measuring the lateral mobility of transmembrane peptides via fluorescence correlation spectroscopy (FCS), the SD theory was confirmed for low protein-to-lipid ratios, whereas a linear dependence between the diffusion coefficient and the protein radius was found for higher protein-to-lipid ratios [192], further accounting for the influence of the peptide structure by comparison between experimental data and coarse-grained molecular dynamics (MD) simulations [193]. How peptide–membrane lipid interactions generate mechanisms that drive membrane deformations and lead to the curvatures necessary in membrane remodeling processes was examined in [194]. The surface chemistry adaptability of peptides via side chain rearrangements in response to the environment, the amplification of their activity by means of hydrophobicity and cationic charge, and the pivotal role of their shape-changing properties in interacting with membranes was demonstrated [195]. The collective diffusion coefficient in deformable bilayer membranes hosting transmembrane proteins that diffuse collectively was studied, revealing the resistance exerted by the presence of proteins on monolayer sliding [196]. Via fluorescence correlation spectroscopy, diffusion coefficients of transmembrane proteins in different types of membrane were estimated in [197], and a linear decreasing trend of membrane-bound protein diffusivities with the increase in membrane coverage proteins was proved in [198].

The discrepancies in the evaluation of the diffusion coefficient with that predicted by the SD model results were analyzed in [199]. However, the mobility of a rigid spherical particle of radius r_α in a 3D solvent with viscosity ν has an inverse dependence on the particle radius, as found by the SD theory [179] and expressed by the well-known Stokes–Einstein relation,

$$\psi_\alpha = 6\pi \, \nu \, r_\alpha \; , \tag{4.6}$$

The mobility of the same particle when embedded in a 2D fluid membrane is further elaborated. Complexities arise from the coupling between the 2D fluid and the surrounding 3D solvent, with the constraint of no slip at the interfaces. Such hydrodynamic coupling introduces an inherent length scale into membrane hydrodynamics, $\zeta = \nu_{\mathcal{S}}/\nu$, where $\nu_{\mathcal{S}}$ is the 2D membrane viscosity. It was therefore proposed to evaluate the mobility of a diffusive particle on a membrane according to [199]:

$$\psi_\alpha = \frac{1}{4\pi \, \nu_{\mathcal{S}}} \, f(\zeta / r_\alpha) \qquad \text{with} \qquad f(\zeta / r_\alpha) = \begin{cases} \pi \zeta / 4 \, r_\alpha & \text{for } \zeta \ll r_\alpha \\ \ln \left[\, \zeta / r_\alpha \, \right] - \gamma_E & \text{for } \zeta \gg r_\alpha \end{cases} \tag{4.7}$$

with γ_E is the Euler–Mascheroni constant.

In conclusion, the results show that the weak logarithmic dependence (see Eq. (4.5)) of the diffusivity on r_α in fluid membranes holds particles much smaller than ζ. For proteins, the applicable limit is $\zeta / r_\alpha \gg 1$, suggesting that all membrane-bound proteins, and even the constituent lipids of the membrane, should have approximately the same diffusion constant [199].

4.4.3 Modeling receptor–ligand kinetics

The chemical reaction

$$\mathrm{R} + \mathrm{L} \underset{k^b}{\overset{k^f}{\rightleftarrows}} \mathrm{C} \tag{4.8}$$

portrays the conversion of freely diffusive receptors on the membrane to trapped receptors, and vice versa. k^f and k^b are the forward and reverse rate factors for the formation, or dissociation, of the complex C from free receptors and ligands, R and L.

The authors of this review modeled the reaction rate w of the chemical reaction (4.8) through the following law of mass action [51]

$$w = k^f \, \frac{\vartheta_{\mathrm{R}}}{1 - \vartheta_{\mathrm{R}}} \, \frac{\vartheta_{\mathrm{L}}}{1 - \vartheta_{\mathrm{L}}} - k^b \, \frac{\vartheta_{\mathrm{C}}}{1 - \vartheta_{\mathrm{C}}} \; , \tag{4.9a}$$

where ϑ_α is defined as $\vartheta_\alpha = c_\alpha / c_\alpha^{max}$, with c_α meaning concentration (molecules per unit area) and c_α^{max} concentration saturation limit, for $\alpha = \mathrm{R}, \mathrm{L}, \mathrm{C}$.

Another common way to write Eq. (4.9a), as in [12, 23], for instance, is

$$w = k^f \; (c_{\mathrm{R}} - c_{\mathrm{C}}) \; (c_{\mathrm{L}} - c_{\mathrm{C}}) - k^b \, c_{\mathrm{C}} \; . \tag{4.9b}$$

Eq. (4.9b) appears in [12, 23] written in terms of densities (number of species per unit area) instead of concentrations. The relation which links the density of species, ρ_α, to the concentration is

$$\rho_\alpha = \kappa_\alpha \, c_\alpha \ ,$$

with κ_α molecular density.

Considering that external forces may cause the unfolding or disruption of receptor–ligand complexes [12, 101, 200, 201], it was proposed in [23] to augment the law of mass action (4.9b) by two exponential terms. The first exponent multiplies the forward reaction term of the equation and depends on the receptor–ligand separation distance (within the cutoff limit). The latter, multiplying the backward reaction term, is assumed to be dependent on the ligand–receptor traction force. Eq.s (4.9) arise considering only short-range receptor–ligand interactions, which lead to strong adhesion, much more than non-specific forces [12, 16].

The chemical reaction (4.8) descends from a more general relation that describes the generation of a protein complex via a two-step mechanism in which the formation of an encounter complex R|L precedes either the generation of the final complex C or the recovery of free proteins [85, 86]:

$$\mathrm{R} + \mathrm{L} \underset{k^b_*}{\overset{k^f_*}{\rightleftarrows}} \mathrm{R|L} \underset{k^b}{\overset{k^f}{\rightleftarrows}} \mathrm{C}\,, \tag{4.10}$$

where the coefficients k^f_* and k^b_* represent the rate of formation and dissolution of the encounter complex.

In the formation of R|L , proteins change their orientations, leading either to evolution into C, when R and L proteins match to each other, or to dissociation into free proteins. Geometry, in terms of inter-protein distances and rotation angles with respect to the orientation of C, is relevant in achieving the final step of association. In a certain range of distances and angles, an electrostatic steering region determines the directional diffusion mobility of protein(s) instead of Brownian motion [86].

If the concentration of R|L is smaller than the concentration of both the free proteins and the final complexes, it is a good approximation [12] to neglect the variation in time of R|L in Eq. (4.10), leading to the most commonly used relation (4.8). Accordingly, the generation of a receptor–ligand complex can be considered to occur immediately once the receptor–ligand distance is sufficiently small. This allows us to disregard the dependence upon the cutoff distance and the predominant rotational Brownian motion of receptors in the R|L state [179]. Tight cell–substrate adhesion allows us to consider complexes as immobilized to the substrate once generated, leading to the mass action law in the form of Eq. (4.9a).

Lastly, as introduced in Section 4.2, receptor motility is commonly associated to cell adhesion and spreading, therefore requiring a description of the cell by means of the laws of mechanics. Cell mechanical response can be assigned either to the bulk of the cell or to the cell membrane. The former choice, supported by [73, 19, 20, 96, 97, 98, 95, 151, 99, 7, 2], for instance, implies the assignment of the cell structural response to the cytoskeleton remodeling; alternatively, other authors demand the structural functions to the cell membrane, for instance [91, 90, 93, 94, 92]. Despite studies on red blood cells providing a description of the cell membrane deformation at a constant area [83], the influence of curvature on the membrane elastic stiffness is related to cell dimensions. The link among curvature, elastic stiffness and cell dimension was highlighted in [17] in studying a small cell of the radius 12.5 nm.

We are persuaded that the attribution of the structural response to the cell membrane and the importance of binding forces on the mechanical response of cells stated in [17] do not match with cells with larger dimensions, as ECs.

4.5 Summary

In this article, we summarized theoretical approaches and computational methodologies developed since the late 1970s, in modeling protein motion along advecting membranes for different biological processes. It has been our aim to collect some of the most emblematic mathematical and computational methodologies, providing a broad introduction to a scientific topic that is in great development nowadays.

Multi-physics methodologies applied to receptor motility along cell membranes may provide a rationale to the evolution in time of quantities of interest for the protein dimerization processes observed experimentally, identifying limiting factors with significant accuracy. Receptor dynamics and receptor–ligand chemical interactions are coupled with cell mechanics. Mechanobiology provides the description of the evolution of cells, with the potential to predict protein dynamics and cell behavior in biological processes. Co-designing theoretical multi-physics frameworks, numerical simulations, and experimental outcomes may allow us to identify the laws that regulate receptor activation, relocation and recruitment, therefore opening new perspectives to support biological and medical research.

Acknowledgements. This work has been supported by grants from the company *Ferriera Valsabbia* through a liberal donation to fund studies in the field of mechanobiology. It falls into the activity of the international research center *The Mechanobiology Research Center, UNIBS*: we acknowledge the support of companies *Antares Vision* and *Copan*. Scientific discussions with S. Mitola and her biochemistry lab @UNIBS are gratefully acknowledged.

Chapter 5

Statistically-based finite strain continuum thermo-mechanics with chemo-transport reaction for biopolymer networks modeling

Matteo Arricca[1,2], Mattia Serpelloni[1,2], Claudia Bonanno[1,3] and Alberto Salvadori[1,2]

[1]The Mechanobiology Research Center, UNIBS, Italy
[2]Department of Mechanical and Industrial Engineering, University of Brescia, Italy
[3]Department of Civil, Environmental, Architectural Engineering and Mathematics, University of Brescia, Italy

5.1 Introduction

In the current notes we aim at extending the theory for cytoskeletal biopolymer structures modeling previously introduced and discussed [2]. Briefly summarizing, the cytoskeleton is an interconnected network of regulatory proteins and filamentous polymers that undergoes massive reorganization during cell deformation, cell rolling and adhesion [89, 115] and in mediating, sensing and transduction of mechanical cues from the micro-environment [116]. As previously specified [2], supported by several publications [19, 20, 21, 73, 95, 96, 97, 98, 99], we assign to the development and reorganization of cytoskeletal structures the main cell structural functions.

Among the main cytoskeletal biopolymer components (actin filaments, intermediate filaments, and microtubules), actin biopolymer structures appear to be the main responsible in cell deformation, adhesion, motility and migration. Diffusion of actin proteins in monomeric form, termed G-actin, polymerization into filamentous proteins (F-actin), branching and bundling, allow the generation of different biopolymer structures that fulfill several functions. For instance, the initial step in cell migration is determined by actin polymerization driven protrusion, which occurs at the leading cell membrane, generated by the lamellipodium - a flat, leaf-like extension filled with branched, dendritic array of short F-actin. To actin polymerization is also assigned the capacity to generate the necessary mechanical forces to change cell shapes. The subsequent generation of focal adhesions allows lamellipodium to exert low traction stresses on the extracellular matrix. Filopodia - F-actin bundles packed tightly together that protrude forward and work as sensors of the local environment - exert significantly less stress than lamellipodial networks [202]. Nascent filaments within the lamellipodium branch from the sides, or tips, of existing filaments in a sterically precise way, and with orientation in the direction of protrusion. Differently from lamellipodia, filopodia assume a fairly ordered parallel conformation. Lamellum filaments either mature into the filopodia or merge with other bundles [5].

Such considerations lead to state that an exhaustive model of the cell mechanical response shall therefore condense polymerization and de-polimerization of actin filaments, the cross-linking process that determine the architecture of cytoskeletal filaments, and the passive mechanical properties of the cytosol [2]. However, distinctions among all biopolymer structures within the cell, in a unified continuum formulation, appears to be a non-achieving task for the progresses made so far. We therefore aim at modeling cytoskeletal structures without any distinction among the aforementioned different type of actin biopolymers.

We base the current manuscript on the statistically-based continuum framework introduced proposed by Vernerey, Long and Brighenti in 2017 [117]. Description of each polymer chain that makes up the whole network is provided by the so-called (equivalent) freely jointed chain model, usually simply termed ideal chain, which represents one of the best and easiest way to model flexible polymers. Despite the recognition that actin polymers are semi-flexible, we do not indulge in attempting a physically-based conversion of F-actin into flexible polymers by means of the Kuhn procedure, for which we make reference to [203], as well as we avoid to provide detailed information about the cytoskeleton, which would be meaningless for the scope of these notes. The framework we aim at formulating is therefore presented in a more general way, with the support of some biologically-based specifications when necessary. The introduction of a statical distribution function at the microscopic scale allows to capture the behavior of interacting chains in the polymer network. Concentration of chains and free energy density of network are derived as a result, as well as a so-called chain distribution tensor is introduced to capture the mechanical behavior of the network at the continuum scale. Such statistically-based continuum quantities aim therefore at providing a continuum description of the polymer network, and are thus coupled with all terms involved in a chemo-transport-thermo-mechanical formulation [10].

Despite the framework we here attempt at using as a basis [117] for modeling cytoskeletal biopolymers has been widely applied in later years, such as in [118, 204, 205, 206, 207], to cite a few, it is right and fair to point out the lack of success of the current formulation with reference to the purpose it has been designed for. Some simplified and non-biologically-based assumptions are highlighted within the manuscript and further discussed. Despite the potential usefulness of the current framework in other application in the field of polymer network modeling, it would be meaningless to provide an exhaustive description of the state of the art and possible applications. As later discussed, further efforts will be required to design an exhaustive formulation for the problem at hand.

The manuscript is organized as follows. Section 5.2 provides some standard definitions in finite strain continuum mechanics and polymer physics. The statistically-based continuum mechanics that aims at describing cytoskeletal biopolymer structures is dealt in Section 5.3. Section 5.4 briefly introduces the mass balance laws and the principles of conservation of linear and angular momentum. The laws of thermodynamics, derivation of the entropy inequality and the resulting thermodynamic prescriptions that arise from the method of Coleman and Noll [8] are described in Section 5.5. Lastly, we discuss assumptions and weaknesses of the framework in Section 5.6.

5.2 Definitions

5.2.1 Motion and deformation gradient

Let $\mathcal{B}_t \in \mathbb{R}^3$ denote the an advecting volume bounded by $\partial\mathcal{B}_t$, image of $\mathcal{B}_R$ whose boundary is $\partial\mathcal{B}_R$, as standard in finite strain mechanics [53, 54]. The transformation of a material point $\boldsymbol{X} \in \mathcal{B}_R$ into a spatial point $\boldsymbol{x} \in \mathcal{B}_t$ is described by means of a smooth one-to-one map $\boldsymbol{\chi}(\boldsymbol{X}, t)$

$$\boldsymbol{x} = \boldsymbol{\chi}(\boldsymbol{X}, t) \ ,$$

which represents the motion of $\boldsymbol{X} \in \mathcal{B}_R$ at time t (see Figure 5.1). We will also assume that $\mathcal{B}_t$ at $t = 0$ coincides with $\mathcal{B}_R$, *i.e.*, for all material points $\boldsymbol{X} = \boldsymbol{\chi}(\boldsymbol{X}, 0)$. We denote with $\dot{\boldsymbol{\chi}}(\boldsymbol{X}, t)$ the material velocity, whereas displacements write as $\boldsymbol{u} = \boldsymbol{\chi} - \boldsymbol{X}$.

At a fixed time t, the deformation gradient is defined by

$$\mathbf{F} = \boldsymbol{\nabla}_{R} \left[\boldsymbol{\chi}(\boldsymbol{X}, t) \right] \ . \tag{5.1}$$

To avoid total material compaction, only motions such that $J = \det\left[\, \mathbf{F} \,\right] > 0$ are admissible.

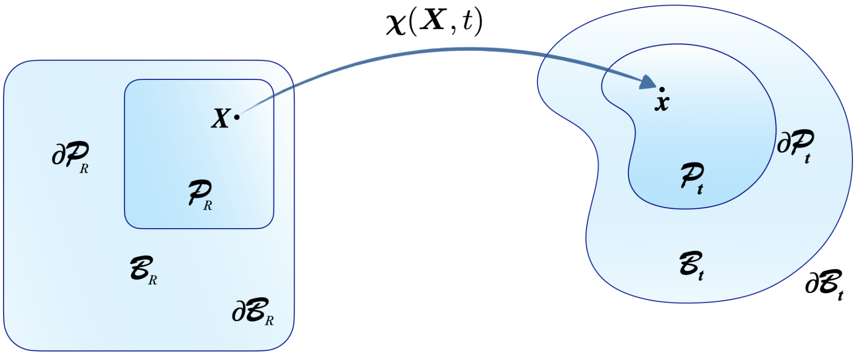

Figure 5.1: Schematic representation of the material and spatial configuration $\mathcal{B}_R$ and $\mathcal{B}_t$, with boundaries $\partial\mathcal{B}_R$ and $\partial\mathcal{B}_t$, and of a generic sub-part $\mathcal{P}_t \subset \partial\mathcal{P}_t$, image of $\mathcal{P}_R \subset \partial\mathcal{P}_R$, with boundaries $\partial\mathcal{P}_t$ and $\partial\mathcal{P}_R$, respectively. A material point $\boldsymbol{X} \in \mathcal{P}_R$ is mapped into a spatial point $\boldsymbol{x} \in \mathcal{P}_t$

5.2.2 The end to end vector and the statistical integral operation

Consider a polymer chain of N non-interacting bond vectors (distance between monomers) $\boldsymbol{r}_i$ of constant length b, according to the ideal chain model [203]. The angle between two consecutive bond vectors is termed bond angle ϑ, whereas the rotation of a bond vector $\boldsymbol{r}_{i+1}$ along the axis defined by $\boldsymbol{r}_i$ at constant ϑ_i defines the torsion angle φ. The sum of the N bond vectors

$$\boldsymbol{r} = \sum_{i=1}^{N} \boldsymbol{r}_i \tag{5.2}$$

is termed end-to-end vector (see Figure 5.2).

Let $\mathcal{C}_s$ define the end-to-end vector configurational space, thus representing the volume space spanned by $\boldsymbol{r}$. The following integral operation is defined

$$\int_{\mathcal{C}_s} \bullet \ \mathrm{d}\boldsymbol{r} = \int_0^{2\pi} \int_0^{\pi} \int_0^{\infty} \bullet \, r^2 \ \mathrm{d}r \sin\vartheta \ \mathrm{d}\vartheta \ \mathrm{d}\varphi \ . \tag{5.3}$$

It is further assumed that the chain space $\mathcal{C}_s$ is a bounded domain embedded in a continuum point $\boldsymbol{x} \in \mathcal{B}_t$.

5.3 Statistically-based continuum mechanics of polymer networks

5.3.1 Statistical mechanics of polymer networks with dynamic bonds

We base the statistical description of the polymer network on [117]. It is stated the existence of a distribution function (see Figure 5.3)

$$\mathcal{F}(\boldsymbol{r}, t) = {}^{a}c_{\mathrm{F}}(t) \, P(\boldsymbol{r}, t) \ . \tag{5.4}$$

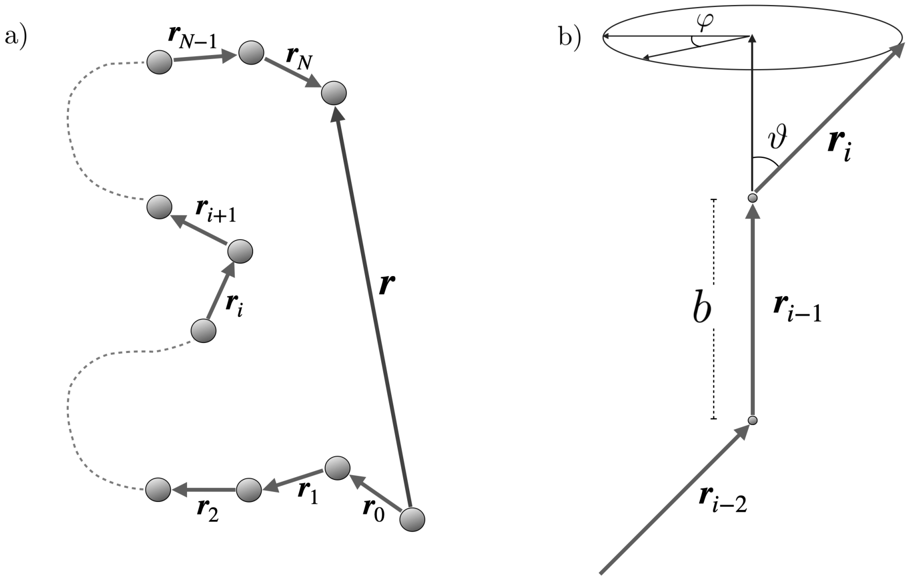

Figure 5.2: Schematic representation of a) the end-to-end $\boldsymbol{r}$ as the sum of N bond vectors $\boldsymbol{r}_i$ and b) the definition of bond angle ϑ and torsion angle φ.

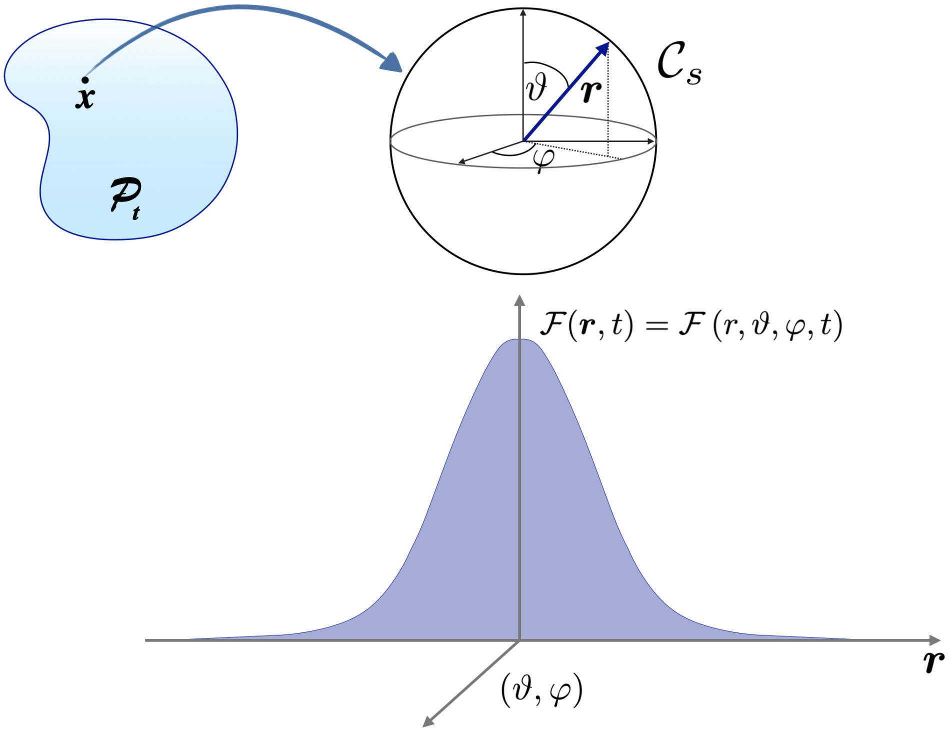

Figure 5.3: Representation of the chain space $\mathcal{C}_s$ embedded in a spatial point $\boldsymbol{x} \in \mathcal{P}_t$, and of the distribution function $\mathcal{F}(\boldsymbol{r}, t)$ whose shape is determined by the Gaussian probability function $P(\boldsymbol{r}, t)$, inspired from [117].

Term ${}^{a}c_{\mathrm{F}}(t)$ represents the concentration of active chains, *i.e.*, chains that are connected to the network at both ends. Function $P(\boldsymbol{r},t)$ is the Gaussian probability function for each chain to have an end-to-end vector $\boldsymbol{r}$, which can be derived by means of the random walk theory, as standard in polymer physics [203]. Integration of the distribution function (5.4) over the chain space, according to definition (5.3), yields

$$\int_{\mathcal{C}_s} \mathcal{F}(\boldsymbol{r},t)\,\mathrm{d}\boldsymbol{r} = {}^{a}c_{\mathrm{F}}(t) \int_{\mathcal{C}_s} P(\boldsymbol{r},t)\,\mathrm{d}\boldsymbol{r} = {}^{a}c_{\mathrm{F}} \;, \tag{5.5}$$

being the integral of the probability function $P(\boldsymbol{r},t)$ over $\mathcal{C}_s$ equals to 1.

It is perhaps worth to point out that the concentration of active chains is a macroscopic quantity, hence ${}^{a}c_{\mathrm{F}}(\boldsymbol{x},t)$. For the sake of clarity, in the current Section 5.3.1 we only show the dependence upon the time when statistical integral operations are performed.

For the assumption of $\mathcal{C}_s$ bounded in $\boldsymbol{x}$, the time derivative of Eq. (5.5) writes

$$\overline{\int_{\mathcal{C}_s} \mathcal{F}(\boldsymbol{r},t)\,\mathrm{d}\boldsymbol{r}}^{\,\cdot} = \int_{\mathcal{C}_s} \frac{\partial \mathcal{F}(\boldsymbol{r},t)}{\partial t}\,\mathrm{d}\boldsymbol{r} = \frac{\partial\, {}^{a}c_{\mathrm{F}}}{\partial t} \;, \tag{5.6}$$

according to Eq. (5.5), and where it has been used the fact that the integral over $\mathcal{C}_s$ of the variation in time of $P(\boldsymbol{r},t)$ vanishes.

The distribution function $\mathcal{F}(\boldsymbol{r},t)$ is supposed to vary in time in two places [117]

$$\frac{\partial \mathcal{F}(\boldsymbol{r},t)}{\partial t} = \left.\frac{\partial \mathcal{F}(\boldsymbol{r},t)}{\partial t}\right|_{\mathbf{F}} + \left.\frac{\partial \mathcal{F}(\boldsymbol{r},t)}{\partial t}\right|_{xl} \;. \tag{5.7}$$

The first right-hand side contribution represents the variation in time of the distribution function due to cross-link dynamics, (*i.e.*, attachment and detachment of chains), and it is evaluated at fixed deformation. A law of mass action-type relation is selected to model $\partial \mathcal{F}(\boldsymbol{r},t)/\partial t|_{\mathbf{F}}$, hence

$$\left.\frac{\partial \mathcal{F}(\boldsymbol{r},t)}{\partial t}\right|_{\mathbf{F}} = k_a\;(c_{\mathrm{F}} - {}^{a}c_{\mathrm{F}})\;P_0(\boldsymbol{r}) - k_d(\boldsymbol{r})\,\mathcal{F}(\boldsymbol{r},t) \;. \tag{5.8}$$

Symbols in Eq. (5.8) have the following meaning. k_a and $k_d(\boldsymbol{r})$ are the kinetic coefficients of attachment and detachment of chains, respectively. The concentration difference $(c_{\mathrm{F}} - {}^{a}c_{\mathrm{F}})$ represents the concentration of detached chains. And $P_0(\boldsymbol{r})$ defines the natural Gaussian probability function, thus the probability function of undeformed chains, whose end-to-end vector is $\boldsymbol{r} = \boldsymbol{r}_0$. Eq. (5.8) assumes that detached chains attach to the network in the stress-free state. Furthermore, for the sake of simplicity we set $k_d(\boldsymbol{r}) = k_d$. We thus assume that the detachment of chains is independent upon the end-to-end vector stretch.

The second contribution to the variation in time of the distribution function $\mathcal{F}(\boldsymbol{r},t)$ is due to the applied (macroscopic) deformation to the network, and evaluated at fixed cross-links xl. This choice implies that the concentration of active chains remains constant, and the variation of $\mathcal{F}(\boldsymbol{r},t)$ is due to the variation of (the mean value of) $\boldsymbol{r}$ in $\mathcal{C}_s$ due to the applied deformation. Furthermore, the assumption of affine deformation is performed [117]. Therefore, the end-to-end vector in the chain space $\mathcal{C}_s$ is subject to an equivalent transformation that applies at the continuum scale to the point it is embedded in, $\mathrm{d}\boldsymbol{x} = \mathbf{F}\mathrm{d}\boldsymbol{X}$. It holds

$$\boldsymbol{r} = \mathbf{F}\,\boldsymbol{r}_0 \;, \tag{5.9}$$

where the deformation gradient, being a macroscopic quantity, is uniform within the chain space, therefore $\mathbf{F} = \mathbf{F}(t)$. Accordingly,

$$\dot{\boldsymbol{r}} = \dot{\mathbf{F}}\,\boldsymbol{r}_0 = \dot{\mathbf{F}}\,\mathbf{F}^{-1}\boldsymbol{r} = \mathbf{L}\,\boldsymbol{r} \;. \tag{5.10}$$

To derive the variation in time due to the applied deformation, we select a volume $\mathcal{V}^* \subset \mathcal{C}_s$. We point out that volume $\mathcal{V}^*$ convects within the bounded space $\mathcal{C}_s$, and any arbitrary volume convecting in $\mathcal{C}_s$ is subjected to the same transformation rules of continuum mechanics. The variation in time of the distribution function $\mathcal{F}(\boldsymbol{r},t)$ under an applied deformation, and for fixed cross-links, has to be interpreted as the spatial time derivative of $\mathcal{F}(\boldsymbol{r},t)$ [117], therefore denoted with $\partial\mathcal{F}(\boldsymbol{r},t)/\partial t|_{xl}$ hereinafter. If cross-links are fixed, the material time derivative of ${}^{a}c_{\mathrm{F}}$ vanishes for any arbitrary convecting volume $\mathcal{V}^* \subset \mathcal{C}_s$. Therefore,

$$\left.\dot{\overline{\int_{\mathcal{V}^*} {}^{a}c_{\mathrm{F}}(t)\, \mathrm{d}\boldsymbol{r}_*}}\right|_{xl} = \int_{\mathcal{V}^*} \left.\frac{\partial\, {}^{a}c_{\mathrm{F}}(t)}{\partial t}\right|_{xl} + {}^{a}c_{\mathrm{F}}(t)\, \mathrm{tr}\,[\,\mathbf{L}\,]\, \mathrm{d}\boldsymbol{r}_* = 0\;, \tag{5.11}$$

after application of the Reynold's transport theorem, whence

$$\left.\frac{\partial\, {}^{a}c_{\mathrm{F}}}{\partial t}\right|_{xl} = -\,{}^{a}c_{\mathrm{F}}\, \mathrm{tr}\,[\,\mathbf{L}\,]\;, \tag{5.12}$$

where $\mathbf{L} = \dot{\mathbf{F}}\,\mathbf{F}^{-1}$ is obtained as $\boldsymbol{\nabla}_{\mathcal{C}_s} \cdot [\,\dot{\boldsymbol{r}}\,]$, with $\boldsymbol{\nabla}_{\mathcal{C}_s} \cdot [\;] = \partial[\,]/\partial\boldsymbol{r}$ and $\mathbf{F} = \partial\boldsymbol{r}/\partial\boldsymbol{r}_0$.

Rather, the distribution function is dependent upon $\boldsymbol{r}$ and t, and thus varies in space and time within $\mathcal{V}^*$. According to Eq.s (5.4), (5.6) and (5.12), for an applied deformation and a fixed set of cross-links,

$$\begin{aligned}\left.\dot{\overline{\int_{\mathcal{V}^*} \mathcal{F}(\boldsymbol{r},t)\, \mathrm{d}\boldsymbol{r}_*}}\right|_{xl} &= \left.\dot{\overline{\int_{\mathcal{V}^*} {}^{a}c_{\mathrm{F}}(t)\, P(\boldsymbol{r},t)\, \mathrm{d}\boldsymbol{r}_*}}\right|_{xl} = \left.\frac{\partial\, {}^{a}c_{\mathrm{F}}(t)}{\partial t}\right|_{xl} \int_{\mathcal{V}^*} P(\boldsymbol{r},t)\, \mathrm{d}\boldsymbol{r}_* \\ &= -\,{}^{a}c_{\mathrm{F}}(t)\, \mathrm{tr}\,[\,\mathbf{L}\,] \int_{\mathcal{V}^*} P(\boldsymbol{r},t)\, \mathrm{d}\boldsymbol{r}_* = -\mathrm{tr}\,[\,\mathbf{L}\,] \int_{\mathcal{V}^*} \mathcal{F}(\boldsymbol{r},t)\, \mathrm{d}\boldsymbol{r}_*\;.\end{aligned} \tag{5.13}$$

In Eq. (5.13) it has been taken advantage from the fact that the variation in time of the integral of $P(\boldsymbol{r},t)$ vanishes, whereas the integral of $P(\boldsymbol{r},t)$ over $\mathcal{V}^* \subset \mathcal{C}_s$ cannot be stated to be equal to 1.

Application of the Reynold's transport theorem to the left-hand side of Eq. (5.13) yields

$$\int_{\mathcal{V}^*} \left.\frac{\partial\mathcal{F}(\boldsymbol{r},t)}{\partial t}\right|_{xl} + \boldsymbol{\nabla}_{\mathcal{C}_s}\,[\,\mathcal{F}(\boldsymbol{r},t)\,] \cdot \dot{\boldsymbol{r}} + \mathcal{F}(\boldsymbol{r},t)\, \mathrm{tr}\,[\,\mathbf{L}\,]\, \mathrm{d}\boldsymbol{r}_* \tag{5.14}$$

Making use of Eq. (5.10) to replace $\dot{\boldsymbol{r}}$, combination of Eq.s (5.13) and (5.14) leads to

$$\int_{\mathcal{V}^*} \left.\frac{\partial\mathcal{F}(\boldsymbol{r},t)}{\partial t}\right|_{xl} + \boldsymbol{\nabla}_{\mathcal{C}_s}\,[\,\mathcal{F}(\boldsymbol{r},t)\,] \cdot \mathbf{L}\,\boldsymbol{r} + \mathcal{F}(\boldsymbol{r},t)\, \mathrm{tr}\,[\,\mathbf{L}\,]\, \mathrm{d}\boldsymbol{r}_* = -\mathrm{tr}\,[\,\mathbf{L}\,] \int_{\mathcal{V}^*} \mathcal{F}(\boldsymbol{r},t)\, \mathrm{d}\boldsymbol{r}_* \tag{5.15}$$

for any $\mathcal{V}^* \subset \mathcal{C}_s$. Therefore, term $\partial\mathcal{F}(\boldsymbol{r},t)/\partial t|_{xl}$ writes

$$\left.\frac{\partial\mathcal{F}(\boldsymbol{r},t)}{\partial t}\right|_{xl} = -\boldsymbol{\nabla}_{\mathcal{C}_s}\,[\,\mathcal{F}(\boldsymbol{r},t)\,] \otimes \boldsymbol{r} : \mathbf{L} - 2\,\mathcal{F}(\boldsymbol{r},t)\, \mathrm{tr}\,[\,\mathbf{L}\,]\;\;, \tag{5.16}$$

where $\boldsymbol{\nabla}_{\mathcal{C}_s}\,[\,\mathcal{F}(\boldsymbol{r},t)\,]$ represents a force in a single chain with end-to-end vector $\boldsymbol{r}$.

After combination of Eq.s (5.8) and (5.16), Eq. (5.7) writes

$$\frac{\partial\mathcal{F}(\boldsymbol{r},t)}{\partial t} = \xi_a\, P_0(\boldsymbol{r}) - k_d\, \mathcal{F}(\boldsymbol{r},t) - \boldsymbol{\nabla}_{\mathcal{C}_s}\,[\,\mathcal{F}(\boldsymbol{r},t)\,] \otimes \boldsymbol{r} : \mathbf{L} - 2\,\mathcal{F}(\boldsymbol{r},t)\, \mathrm{tr}\,[\,\mathbf{L}\,]\;\;, \tag{5.17}$$

where it has been defined $\xi_a = k_a\; (c_{\mathrm{F}} - {}^{a}c_{\mathrm{F}})$.

Integration of Eq. (5.17) over the chain space $\mathcal{C}_s$ yields (derivation in collected in Appendix B.1)

$$\frac{\partial\, {}^{a}c_{\mathrm{F}}}{\partial t} = \xi_a - k_d\, {}^{a}c_{\mathrm{F}} - \,{}^{a}c_{\mathrm{F}}\, \mathrm{tr}\,[\,\mathbf{L}\,]\;\;. \tag{5.18}$$

Furthermore, with the aim to compare the polymer network behavior with its stress-free state, it is defined a natural distribution function [117]. It holds

$$\mathcal{F}_0(\boldsymbol{r},t) = {}^{a}c_{\mathrm{F}}(t)\, P_0(\boldsymbol{r})\;. \tag{5.19}$$

5.3.2 Free energy density of polymer networks

To evaluate the free energy of the polymer network, consider the elastic energy of a single chain defined in accordance with the entropic spring model in the field of entropic elasticity with Gaussian statistics [203],

$$\psi^c(\boldsymbol{r}) = \frac{3}{2}\, k_{\scriptscriptstyle B}\, T\, \frac{|\boldsymbol{r}|^2}{N b^2} = \frac{1}{2}\, k_{\scriptscriptstyle B}\, T\, \tilde{\boldsymbol{r}}^2 \ , \tag{5.20}$$

where $k_{\scriptscriptstyle B}$ is the Boltzmann's constant, and with

$$\tilde{\boldsymbol{r}} = \frac{\boldsymbol{r}}{\sqrt{N b^2/3}} \tag{5.21}$$

normalized end-to-end vector [117].

We point out that Nb represents the maximum length of the polymer chain, Nb^2 the mean square end-to-end vector, $\sqrt{Nb^2/3}$ the mean square of $\boldsymbol{r}$ for each of the three Cartesian axes, and $3\, k_{\scriptscriptstyle B} T / N\, b^2$ is termed entropic spring constant [203]. Additionally, Eq. (5.20) implies a linear-type relation between the force applied to an ideal chain and its $\boldsymbol{r}$, and the model holds for $|\boldsymbol{r}| \ll Nb$.

The free energy of the polymer network is evaluated as [117]

$$\psi^{\mathcal{N}} = \int_{\mathcal{C}_s} \mathcal{F}(\boldsymbol{r}, t)\, \psi^c\,(\boldsymbol{r})\; \mathrm{d}\boldsymbol{r} \ . \tag{5.22}$$

Furthermore, to obtain a vanishing energy function when the polymer network is in a stress-free state, an energy difference of the form [117]

$$\Psi^{\mathcal{N}} = \int_{\mathcal{C}_s} \left(\mathcal{F}(\boldsymbol{r}, t) - \mathcal{F}_0(\boldsymbol{r}, t)\right)\, \psi^c\,(\boldsymbol{r})\; \mathrm{d}\boldsymbol{r} \ , \tag{5.23}$$

is properly selected.

According to Eq. (5.20), and by noting the $\tilde{\boldsymbol{r}}^2$ can be re-written as $\mathrm{tr}[\, \tilde{\boldsymbol{r}} \otimes \tilde{\boldsymbol{r}}\,]$, it holds

$$\Psi^{\mathcal{N}} = \frac{1}{2}\, k_{\scriptscriptstyle B}\, T \int_{\mathcal{C}_s} \left(\mathcal{F}(\boldsymbol{r}, t) - \mathcal{F}_0(\boldsymbol{r}, t)\right)\, \mathrm{tr}[\, \tilde{\boldsymbol{r}} \otimes \tilde{\boldsymbol{r}}\,]\; \mathrm{d}\boldsymbol{r} \ . \tag{5.24}$$

5.3.3 The chain distribution tensor

According to [117], we define the so-called (current) chain distribution tensor

$$\boldsymbol{\Lambda} = \int_{\mathcal{C}_s} P(\boldsymbol{r}, t)\, \tilde{\boldsymbol{r}} \otimes \tilde{\boldsymbol{r}}\; \mathrm{d}\boldsymbol{r} \ , \tag{5.25a}$$

and the natural distribution tensor, corresponding to the polymer network in a stress free state[1],

$$\boldsymbol{\Lambda}_0 = \int_{\mathcal{C}_s} P_0(\boldsymbol{r})\, \tilde{\boldsymbol{r}} \otimes \tilde{\boldsymbol{r}}\; \mathrm{d}\boldsymbol{r} = \boldsymbol{1} \ , \tag{5.25b}$$

We point out that, analogously to the concentration of active chains, the stored elastic energy $\Psi^{\mathcal{N}}$ (5.24), and the distribution tensors $\boldsymbol{\Lambda}$ and $\boldsymbol{\Lambda}_0$, are statistically-based macroscopic quantities. They have therefore to be read as $\Psi^{\mathcal{N}}(\boldsymbol{x}, t)$, $\boldsymbol{\Lambda}(\boldsymbol{x}, t)$ and $\boldsymbol{\Lambda}_0(\boldsymbol{x}, t)$.

The evolution in time of tensor $\boldsymbol{\Lambda}$, whose derivation is collected in Appendix B.3, writes

$$\dot{\boldsymbol{\Lambda}} = \frac{\xi_a}{{}^{a}c_{\mathrm{F}_R}}\, \left(\boldsymbol{\Lambda}_0 - \boldsymbol{\Lambda}\right) + \mathbf{L}\, \boldsymbol{\Lambda} + \left(\mathbf{L}\, \boldsymbol{\Lambda}\right)^{\mathrm{T}} \ . \tag{5.26}$$

---

[1] The tedious demonstration of $\boldsymbol{\Lambda}_0 = \boldsymbol{1}$ is collected in Appendix B.2.

Note also that, according to definitions (5.4) and (5.25), the free energy (5.24) can be re-written in the form

$$\Psi^{\mathcal{N}} = \frac{1}{2}\, k_{_B}\, T\, {}^{a}c_{\mathrm{F}}\, \mathrm{tr}\,[\,\mathbf{\Lambda} - \mathbf{1}\,]\ . \tag{5.27}$$

On the basis of Eq. (5.27), we take $\Psi^{\mathcal{N}}$ as a function of temperature T, concentration of active chains ${}^{a}c_{\mathrm{F}}$, and chain distribution tensor $\mathbf{\Lambda}$. Accordingly,

$$\dot{\Psi}^{\mathcal{N}}(T, {}^{a}c_{\mathrm{F}}, \mathbf{\Lambda}) = \frac{\partial \Psi^{\mathcal{N}}}{\partial T}\,\dot{T} + \frac{\partial \Psi^{\mathcal{N}}}{\partial\, {}^{a}c_{\mathrm{F}}}\,{}^{a}\dot{c}_{\mathrm{F}} + \frac{\partial \Psi^{\mathcal{N}}}{\partial \mathbf{\Lambda}} : \dot{\mathbf{\Lambda}}\ , \tag{5.28}$$

where the first two right-hand side terms easily write

$$\frac{\partial \Psi^{\mathcal{N}}}{\partial T}\,\dot{T} = \frac{1}{2}\, k_{_B}\, {}^{a}c_{\mathrm{F}}\, \mathrm{tr}\,[\,\mathbf{\Lambda} - \mathbf{1}\,]\, \dot{T} \tag{5.29a}$$

and

$$\frac{\partial \Psi^{\mathcal{N}}}{\partial\, {}^{a}c_{\mathrm{F}}}\,{}^{a}\dot{c}_{\mathrm{F}} = \frac{1}{2}\, k_{_B}\, T\, \xi_a\, \mathrm{tr}\,[\,\mathbf{\Lambda} - \mathbf{1}\,] - \frac{1}{2}\, k_{_B}\, T\, k_d\, {}^{a}c_{\mathrm{F}}\, \mathrm{tr}\,[\,\mathbf{\Lambda} - \mathbf{1}\,] - \frac{1}{2}\, k_{_B}\, T\, k_d\, {}^{a}c_{\mathrm{F}}\, \mathrm{tr}\,[\,\mathbf{L}\,]\ \mathrm{tr}\,[\,\mathbf{\Lambda} - \mathbf{1}\,] \tag{5.29b}$$

according to Eq. (5.18)

To evaluate the last right-hand side term of Eq. (5.28) we note that

$$\frac{\partial\, \mathrm{tr}\,[\,\mathbf{\Lambda}\,]}{\partial \mathbf{\Lambda}} = \frac{\partial\, \mathbf{\Lambda} : \mathbf{1}}{\partial \mathbf{\Lambda}} = \mathbf{1}\ ,$$

whence,

$$\frac{\partial \Psi^{\mathcal{N}}}{\partial \mathbf{\Lambda}} : \dot{\mathbf{\Lambda}} = \frac{1}{2}\, k_{_B}\, T\, {}^{a}c_{\mathrm{F}}\, \mathbf{1} : \left[\frac{\xi_a}{{}^{a}c_{\mathrm{F}_R}}\, (\mathbf{\Lambda}_0 - \mathbf{\Lambda}) + \mathbf{L}\,\mathbf{\Lambda} + (\mathbf{L}\,\mathbf{\Lambda})^{\mathrm{T}} \right] \tag{5.29c}$$

according to Eq. (5.26)

Combination of Eq.s (5.28) and (5.29) therefore yields

$$\begin{aligned} \dot{\Psi}^{\mathcal{N}} &= \frac{1}{2}\, k_{_B}\, {}^{a}c_{\mathrm{F}}\, \mathrm{tr}\,[\,\mathbf{\Lambda} - \mathbf{1}\,]\, \dot{T} - \frac{1}{2}\, k_{_B}\, T\, k_d\, {}^{a}c_{\mathrm{F}}\, \mathrm{tr}\,[\,\mathbf{\Lambda} - \mathbf{1}\,] - \frac{1}{2}\, k_{_B}\, T\, {}^{a}c_{\mathrm{F}}\, \mathrm{tr}\,[\,\mathbf{L}\,]\ \mathrm{tr}\,[\,\mathbf{\Lambda} - \mathbf{1}\,] \\ &+ \frac{1}{2}\, k_{_B}\, T\, {}^{a}c_{\mathrm{F}} \left[\mathbf{1} : \mathbf{L}\,\mathbf{\Lambda} + \mathbf{1} : (\mathbf{L}\,\mathbf{\Lambda})^{\mathrm{T}} \right]\ , \end{aligned} \tag{5.30}$$

after recognition that $\mathrm{tr}\,[\,\mathbf{\Lambda} - \mathbf{1}\,] = -\mathrm{tr}\,[\,\mathbf{1} - \mathbf{\Lambda}\,]$, and simple algebra.

Lastly, by noting that the symmetry of the distribution tensor $\mathbf{\Lambda}$ implies

$$\mathbf{1} : \mathbf{L}\,\mathbf{\Lambda} + \mathbf{1} : (\mathbf{L}\,\mathbf{\Lambda})^{\mathrm{T}} = 2\,\mathbf{L} : \mathbf{\Lambda}\ ,$$

the time derivative of the energy function (5.27) writes[2]

$$\begin{aligned} \dot{\Psi}^{\mathcal{N}} &= \frac{1}{2}\, k_{_B}\, {}^{a}c_{\mathrm{F}}\, \mathrm{tr}\,[\,\mathbf{\Lambda} - \mathbf{1}\,]\, \dot{T} - \frac{1}{2}\, k_{_B}\, T\, k_d\, {}^{a}c_{\mathrm{F}}\, \mathrm{tr}\,[\,\mathbf{\Lambda} - \mathbf{1}\,] - \frac{1}{2}\, k_{_B}\, T\, {}^{a}c_{\mathrm{F}}\, \mathrm{tr}\,[\,\mathbf{L}\,]\ \mathrm{tr}\,[\,\mathbf{\Lambda} - \mathbf{1}\,] \\ &+ k_{_B}\, T\, {}^{a}c_{\mathrm{F}}\, \mathbf{\Lambda} : \mathbf{L}\ . \end{aligned} \tag{5.31}$$

Remark. We highlight the fact that derivation of Eq.s (5.26) and (5.31) (see Appendixes B.3 and B.4, respectively) implies an end-to-end vector $\boldsymbol{r}$ no longer dependent upon the time. It is therefore needed, when operation are performed at the macro (continuum) scale, to consider the average end-to-end vector, representing the distribution of $\boldsymbol{r}$ around all possible chain conformations in $\mathcal{C}_s$.

---

[2] It is perhaps worth to point out that Eq. (5.31) differs from what stated in [117]. However, in view of Eq. (5.27), the selected functional dependence of $\Psi^{\mathcal{N}}$ appears to be a reasonable choice. Furthermore, Eq. (5.31) is proven in Appendix B.4 by means of a different procedure, hence directly performing the time derivative of Eq. (5.24) and taking advantage from definitions (5.4), (5.19) and (5.25).

5.3.4 Lagrangian formulation

With the aim to provide a material description of the current framework, and in view of the Coleman-Noll's procedure [8] that will be used in Section 5.5, we need to re-phrase Eq. (5.31) in Lagrangian formulation, as well as to provide the referential counterpart of the distribution tensor $\mathbf{\Lambda}$. We first recall that

$$\overset{\boldsymbol{\cdot}}{\overline{\int_{\mathcal{P}_t} \Psi^{\mathcal{N}}(\boldsymbol{x},t)\,\mathrm{d}v}} = \int_{\mathcal{P}_t} \dot{\Psi}^{\mathcal{N}}(\boldsymbol{x},t)\,\mathrm{d}v = \int_{\mathcal{P}_R} \dot{\Psi}^{\mathcal{N}}_R(\boldsymbol{X},t)\,\mathrm{d}\mathcal{V} \, .$$

for any $\mathcal{P}_t \subset \mathcal{B}_t$ image of $\mathcal{P}_R \subset \mathcal{B}_R$.

For the sake of convenience we directly provide the referential counterpart of Eq. (5.31),

$$\begin{aligned}\dot{\Psi}^{\mathcal{N}}_R &= \frac{1}{2}\,k_B\,{}^a c_{\mathrm{F}_R}\,\mathrm{tr}\,[\,\mathbf{\Lambda}-\mathbf{1}\,]\,\dot{T} - \frac{1}{2}\,k_B\,T\,k_d\,{}^a c_{\mathrm{F}_R}\,\mathrm{tr}\,[\,\mathbf{\Lambda}-\mathbf{1}\,] - \frac{1}{2}\,k_B\,T\,{}^a c_{\mathrm{F}_R}\,\mathrm{tr}\,[\,\mathbf{L}\,]\,\mathrm{tr}\,[\,\mathbf{\Lambda}-\mathbf{1}\,] \\ &\quad + k_B\,T\,{}^a c_{\mathrm{F}_R}\,\mathbf{\Lambda}:\mathbf{L}\;,\end{aligned} \tag{5.32}$$

with

$${}^a c_{\mathrm{F}_R}(\boldsymbol{X},t) = J(\boldsymbol{X},t)\,{}^a c_{\mathrm{F}}(\boldsymbol{x},(\boldsymbol{X},t),t)\;, \tag{5.33}$$

and from which it is possible to define the referential counterpart of $\mathbf{\Lambda}$ as[3]

$$\mathbf{\Lambda}:\mathbf{L} = \mathbf{\Lambda}:\dot{\mathbf{F}}\,\mathbf{F}^{-1} = \mathbf{\Lambda}_R:\dot{\mathbf{F}}\;, \tag{5.34}$$

with

$$\mathbf{\Lambda}_R(\boldsymbol{X},t) = \mathbf{\Lambda}(\boldsymbol{x}(\boldsymbol{X},t),t)\,\mathbf{F}^{-\mathrm{T}}(\boldsymbol{X},t)\;. \tag{5.35}$$

We further take advantage from the fact that $\mathrm{tr}\,[\,\mathbf{L}\,] = \dot{\mathbf{F}} : \mathbf{F}^{-\mathrm{T}}$ to re-write the third right-hand side term of Eq. (5.32) in the form

$$-\frac{1}{2}\,k_B\,T\,{}^a c_{\mathrm{F}_R}\,\mathrm{tr}\,[\,\mathbf{L}\,]\,\mathrm{tr}\,[\,\mathbf{\Lambda}-\mathbf{1}\,] = \frac{1}{2}\,k_B\,T\,{}^a c_{\mathrm{F}_R}\,\mathrm{tr}\left[\,\mathbf{1}-\mathbf{\Lambda}_R\,\mathbf{F}^{\mathrm{T}}\,\right]\,\mathbf{F}^{-\mathrm{T}}:\dot{\mathbf{F}}\;. \tag{5.36}$$

Lastly, combination of Eq.s (5.32), (5.34) and (5.36) yields

$$\begin{aligned}\dot{\Psi}^{\mathcal{N}}_R &= \frac{1}{2}\,k_B\,{}^a c_{\mathrm{F}_R}\,\mathrm{tr}\left[\,\mathbf{\Lambda}_R\,\mathbf{F}^{\mathrm{T}}-\mathbf{1}\,\right]\dot{T} + k_B\,T\,{}^a c_{\mathrm{F}_R}\,\mathbf{\Lambda}_R:\dot{\mathbf{F}} + \frac{1}{2}\,k_B\,T\,{}^a c_{\mathrm{F}_R}\,\mathrm{tr}\left[\,\mathbf{1}-\mathbf{\Lambda}_R\,\mathbf{F}^{\mathrm{T}}\,\right]\,\mathbf{F}^{-\mathrm{T}}:\dot{\mathbf{F}} \\ &\quad - \mathcal{D}_R\;,\end{aligned} \tag{5.37}$$

where it has been defined the mechanical energy dissipation of the network as

$$\mathcal{D}_R = \frac{1}{2}\,k_B\,T\,k_d\,{}^a c_{\mathrm{F}_R}\,\mathrm{tr}\left[\,\mathbf{\Lambda}_R\,\mathbf{F}^{\mathrm{T}}-\mathbf{1}\,\right]\;. \tag{5.38}$$

5.4 Balance laws

5.4.1 Mass balance

We take advantage from what specified in [2] to briefly summarize the mass balance equations for the problem at hand. The transduction of the signal $\mathcal{C}(\boldsymbol{X},t)$ that results in the polymerization of G-actin into F-actin is modeled as a bimolecular reaction [89] of the form

$$\mathrm{G} \underset{k_R^-}{\overset{k_R^+}{\rightleftarrows}} \mathrm{F} \tag{5.39}$$

---

[3] Note that the symmetry of $\mathbf{\Lambda}$ would allow to define Eq. (5.34) in terms of the time derivative of the right Cauchy-Green tensor $\mathbf{C}$, with the same standard procedure in finite strain continuum mechanics that, taking advantage from the the symmetry of the Cauchy stress $\mathbf{T}$, leads at defining $\frac{1}{2}\,\mathbf{S}:\dot{\mathbf{C}}$ from $\mathbf{T}_R:\dot{\mathbf{F}}$, with $\mathbf{T}_R$ and $\mathbf{S}$ first and second Piola-Kirchhoff tensors.

with $k^+_{\scriptscriptstyle R}$ and $k^-_{\scriptscriptstyle R}$ forward and backward kinetic coefficients defining the polymerization and depolymerization processes. The kinetics of reaction (5.39) is modeled via the following law of mass action, properly extended to account for signaling,

$$w^{(5.39)}_{\scriptscriptstyle R}(\boldsymbol{X},t) = \mathcal{C}(\boldsymbol{X},t)\, k^+_{\scriptscriptstyle R}\, \frac{\vartheta_{\mathrm{G}}}{(1-\vartheta_{\mathrm{G}})} - \mathcal{D}(\boldsymbol{X},t)\, k^-_{\scriptscriptstyle R}\, \frac{\vartheta_{\mathrm{F}}}{(1-\vartheta_{\mathrm{F}})}\ , \tag{5.40}$$

with function $\mathcal{D}(\boldsymbol{X},t)$ accounting for the role of the stress in the dissociation of biopolymers [19]. Specifications of $\mathcal{C}(\boldsymbol{X},t)$ and $\mathcal{D}(\boldsymbol{X},t)$ are nonetheless omitted in the current manuscript.

Note that the law of mass action (5.40) is written in accordance with the relations

$$w^{(5.39)}_{\scriptscriptstyle R}(\boldsymbol{X},t) = J(\boldsymbol{X},t)\, w^{(5.39)}_{\scriptscriptstyle R}(\boldsymbol{x}(\boldsymbol{X},t),t)\ , \qquad \vartheta_\beta(\boldsymbol{X},t) = \vartheta_\beta(\boldsymbol{x},t)\ , \tag{5.41}$$

having assumed

$$c^{max}_{\beta_R}(\boldsymbol{X},t) = J(\boldsymbol{X},t)\, c^{max}_{\beta}(\boldsymbol{x}(\boldsymbol{X},t),t)\ , \tag{5.42}$$

as performed in [10]. Therefore, the configuration invariance of ϑ_β implies

$$k^+_{\scriptscriptstyle R}(\boldsymbol{X},t) = J(\boldsymbol{X},t)\, k^+(\boldsymbol{x}(\boldsymbol{X},t),t)\ , \qquad k^-_{\scriptscriptstyle R}(\boldsymbol{X},t) = J(\boldsymbol{X},t)\, k^-(\boldsymbol{x}(\boldsymbol{X},t),t)\ . \tag{5.43}$$

The mass balance of species β has the form

$$\dot{\overline{\int_{\mathcal{P}_R} c_{\beta_R}\, \mathrm{d}\mathcal{V}}} + \int_{\partial\mathcal{P}_R} \boldsymbol{h}_{\beta_R} \cdot \boldsymbol{n}_{\scriptscriptstyle R}\, \mathrm{d}\mathcal{A} \pm \int_{\mathcal{P}_R} w^{(5.39)}_{\scriptscriptstyle R}\, \mathrm{d}\mathcal{V} = \int_{\mathcal{P}_R} s_{\beta_R}\, \mathrm{d}\mathcal{V} \tag{5.44}$$

with

$$c_{\beta_R}(\boldsymbol{X},t) = J(\boldsymbol{X},t)\, c_\beta(\boldsymbol{x}(\boldsymbol{X},t),t)\ , \qquad s_{\beta_R}(\boldsymbol{X},t) = J(\boldsymbol{X},t)\, s_\beta(\boldsymbol{x}(\boldsymbol{X},t),t)\ , \tag{5.45a}$$

reference molarity and mass supply of species β, respectively, and

$$\boldsymbol{h}_{\beta_R}(\boldsymbol{X},t) = J(\boldsymbol{X},t)\, \mathbf{F}^{-1}(\boldsymbol{X},t)\, \boldsymbol{h}_\beta(\boldsymbol{x}(\boldsymbol{X},t),t)\ , \tag{5.45b}$$

reference mass flux vector.

Application of the divergence theorem to Eq. (5.44), and recognition that the resultant integrals must hold for any arbitrary volume, allow to derive the local form of the mass balance equations. For species $\beta = \mathrm{G}, \mathrm{F}$, Eq. (5.44) specializes in

$$\dot{c}_{\mathrm{G_R}} + \boldsymbol{\nabla}_{\scriptscriptstyle R} \cdot [\, \boldsymbol{h}_{\mathrm{G}_R}\,] + w^{(5.39)}_{\scriptscriptstyle R} = s_{\mathrm{G}_R}\ , \tag{5.46a}$$

$$\dot{c}_{\mathrm{F_R}} - w^{(5.39)}_{\scriptscriptstyle R} = s_{\mathrm{G}_R}\ , \tag{5.46b}$$

after assumption that F-actin can be considered motionless due to a much smaller mobility with respect to G-actin, hence $\boldsymbol{h}_{\mathrm{F}_R} = \mathbf{0}$.

Remark. Note that Eq. (5.46b) defines the variation in time of the total amount of F-actin chains in the network. Therefore, let ${}^{d}c_{\mathrm{F}_R} = c_{\mathrm{F}_R} - {}^{a}c_{\mathrm{F}_R}$ denote the referential concentration of detached chains, it obviuosly holds

$${}^{d}c_{\mathrm{F}_R}(\boldsymbol{X},t) = J(\boldsymbol{X},t)\, {}^{d}c_{\mathrm{F}}(\boldsymbol{x}(\boldsymbol{X},t),t)\, .$$

However, the reason why ${}^{d}c_{\mathrm{F}}$ has never been explicitly defined in Section 5.3, but taken as the difference $(c_{\mathrm{F}} - {}^{a}c_{\mathrm{F}})$, lies in the necessity to consider a constant value of total chains. Hence, generation of chains is not allowed in [117]. It is also worth to point out that this limitation has not been overcome within this manuscript, and all statistically-based continuum definitions provided in Section 5.3 have to be evaluate for concentration of chains constant. Furthermore, and for reasons that will be better clear in Section 5.5, we are forced to consider the total concentration c_{F_R} and the concentration of active chains ${}^{a}c_{\mathrm{F}_R}$ as independent variables, despite they cannot be separated unambiguously. At first instance, we therefore assume that c_{F_R} and ${}^{a}c_{\mathrm{F}_R}$ are independent, and their variation in time is regulated by ${}^{d}\dot{c}_{\mathrm{F}_R}$.

5.4.2 Principles of conservation of linear and angular momentum

Let $\boldsymbol{t} = \mathbf{T}\,\boldsymbol{n}$ and $\boldsymbol{t}_R = \mathbf{T}_R\,\boldsymbol{n}_R$ define the current and reference surface tractions, respectively, with $\mathbf{T}$ and $\mathbf{T}_R$ Cauchy and Piola stress tensors. Accordingly

$$\mathbf{T}_R(\boldsymbol{X},t) = J(\boldsymbol{X},t)\;\mathbf{T}(\boldsymbol{x}(\boldsymbol{X},t),t)\;\mathbf{F}^{-\mathrm{T}}(\boldsymbol{X},t)\;. \tag{5.47}$$

Assuming the negligibility of inertial body forces, the local form of the principle of conservation of linear momentum writes

$$\boldsymbol{\nabla}_R \cdot [\,\mathbf{T}_R\,] + \boldsymbol{b}_{0_R} = \mathbf{0}\;, \tag{5.48}$$

where $\boldsymbol{b}_{0_R}$ represents the referential conventional body force, not encompassing the inertial force, and with $\boldsymbol{\nabla}_R \cdot [\,\mathbf{T}_R\,] = \partial \mathrm{T}_{Rij}/\partial X_j$.

The referential local form of the principle of conservation of angular momentum writes

$$\mathbf{T}_R\mathbf{F}^{\mathrm{T}} = \mathbf{F}\,\mathbf{T}_R^{\mathrm{T}}\;. \tag{5.49}$$

5.5 Thermodynamics of polymer networks

As standard in thermodynamics, we write the energy balance and the entropy imbalance in local form, and we derive the Clausius-Duhem inequality, and the restrictions on the constitutive relations that follow from the second law of thermodynamics, via the method of Coleman and Noll [8]. The first and second principle of thermodynamics are briefly summarized hereinafter on the basis of the same procedure followed in [10].

5.5.1 The first and second principle of thermodynamics

The referential form of the energy balance writes

$$\begin{aligned}\int_{\mathcal{P}_R} \dot{u}_R \,\mathrm{d}\mathcal{V} = {} & \int_{\partial\mathcal{P}_R} \dot{\boldsymbol{\chi}} \cdot \boldsymbol{t}_R \,\mathrm{d}\mathcal{A} + \int_{\mathcal{P}_R} \dot{\boldsymbol{\chi}} \cdot \boldsymbol{b}_{0_R} \,\mathrm{d}\mathcal{V} + \int_{\mathcal{P}_R} s_{qR} \,\mathrm{d}\mathcal{V} - \int_{\partial\mathcal{P}_R} \boldsymbol{q}_R \cdot \boldsymbol{n}_R \,\mathrm{d}\mathcal{A} \\ & + \int_{\mathcal{P}_R} {}^u\mu_{\mathrm{G}_R}\, s_{\mathrm{G}_R} + {}^u\mu_{\mathrm{F}_R}\, s_{\mathrm{F}_R} \,\mathrm{d}\mathcal{V} - \int_{\partial\mathcal{P}_R} {}^u\mu_{\mathrm{G}_R}\, \boldsymbol{h}_{\mathrm{G}_R} \cdot \boldsymbol{n}_R \,\mathrm{d}\mathcal{A}\;. \end{aligned} \tag{5.50}$$

Terms in Eq.s (5.50) have the following meaning. The scalar u_R is the specific internal energy (per unit reference volume). Surface traction and body forces, $\boldsymbol{t}_R$ and $\boldsymbol{b}_{0_R}$, have been defined in Section 5.4.2. The terms s_{qR} and $\boldsymbol{q}_R$ represent the heat supplied by external agencies and the heat flux vector, respectively. The scalar ${}^u\mu_\beta$ is the energy provided by a unit supply of moles of species $\beta = \mathrm{F}, \mathrm{G}$, whereas s_{β_R} and $\boldsymbol{h}_{\mathrm{G}_R}$ are the source terms and the G-actin flux vector, respectively, as defined in Section 5.4.1.

According to the definition of $\boldsymbol{t}_R$, making use of Eq.s (5.46) and (5.48) to replace s_{β_R} and $\boldsymbol{b}_{0_R}$, respectively, after application of the divergence theorem and recognition that the resultant integral must hold for any arbitrary volume, Eq. (5.50) localizes as

$$\dot{u}_R = \mathbf{T}_R : \dot{\mathbf{F}} + s_{qR} - \boldsymbol{\nabla}_R \cdot [\,\boldsymbol{q}_R\,] + {}^u\mu_{\mathrm{G}}\, \dot{c}_{\mathrm{G}_\mathrm{R}} - \boldsymbol{h}_{\mathrm{G}_R} \cdot \boldsymbol{\nabla}_R\,[\,{}^u\mu_{\mathrm{G}}\,] + {}^u\mu_{\mathrm{F}}\, \dot{c}_{\mathrm{F}_R} + ({}^u\mu_{\mathrm{G}} - {}^u\mu_{\mathrm{F}})\; w_R^{(5.39)}\;, \tag{5.51}$$

with $\mathbf{T}_R : \dot{\mathbf{F}} = \mathrm{T}_{Rij}\,\dot{\mathrm{F}}_{ij}$.

According to the statement of second law of thermodynamics, which establishes that entropy produced is greater or equals to 0, the entropy imbalance writes

$$\begin{aligned}\int_{\mathcal{P}_R} \dot{\eta}_R \,\mathrm{d}\mathcal{V} - \int_{\mathcal{P}_R} \frac{1}{T}\, s_{qR} \,\mathrm{d}\mathcal{V} + \int_{\partial\mathcal{P}_R} \frac{1}{T}\, \boldsymbol{q}_R \cdot \boldsymbol{n}_R \,\mathrm{d}\mathcal{A} - \int_{\mathcal{P}_R} {}^\eta\mu_{\mathrm{G}}\, s_{\mathrm{G}_R} + {}^\eta\mu_{\mathrm{F}}\, s_{\mathrm{F}_R} \,\mathrm{d}\mathcal{V} & \\ + \int_{\partial\mathcal{P}_R} {}^\eta\mu_{\mathrm{G}}\, \boldsymbol{h}_{\mathrm{G}_R} \cdot \boldsymbol{n}_R \,\mathrm{d}\mathcal{A} \geq 0\;, & \end{aligned} \tag{5.52}$$

with η_R specific net internal entropy (per unit reference volume), and ${}^{\eta}\mu_\beta$ change in specific entropy provided by a unit supply of moles of species $\beta = \mathrm{G}, \mathrm{F}$.

Making use of mass balance equations (5.46) to replace the source terms s_{β_R}, application of the divergence theorem and recognition that the resultant integral must hold for any arbitrary volume yield

$$\begin{aligned} &T\,\dot{\eta}_R - s_{q_R} + \boldsymbol{\nabla}_R \cdot \left[\, \boldsymbol{q}_R \,\right] - \frac{1}{T}\,\boldsymbol{q}_R \cdot \boldsymbol{\nabla}_R\,[\,T\,] - T\,{}^{\eta}\mu_{\mathrm{G}}\,\dot{c}_{\mathrm{G}_R} - T\,{}^{\eta}\mu_{\mathrm{F}}\,\dot{c}_{\mathrm{F}_R} + T\,\boldsymbol{h}_{\mathrm{G}_R} \cdot \boldsymbol{\nabla}_R\,[\,{}^{\eta}\mu_{\mathrm{G}}\,] \\ &\qquad - T\,\left({}^{\eta}\mu_{\mathrm{G}} - {}^{\eta}\mu_{\mathrm{F}}\right)\,w_R^{(5.39)} \geq 0\;. \end{aligned} \tag{5.53}$$

after multiplication by the temperature.

Following [10, 9], we denote with

$$\mu_\beta = {}^{u}\mu_\beta - T\,{}^{\eta}\mu_\beta\;, \qquad A^{(5.39)} = \mu_{\mathrm{F}} - \mu_{\mathrm{G}} \tag{5.54}$$

the chemical potential of species α and the affinity of chemical reaction (5.39)[4], and with

$$\not{\boldsymbol{q}}_R = \boldsymbol{q}_R + T\,{}^{\eta}\mu_{\mathrm{G}}\,\boldsymbol{h}_{\mathrm{G}_R}\;, \tag{5.55}$$

the *new* heat flux vector.

As standard in thermodynamics, the entropy imbalance (5.52) can be re-phrased in terms of internal energy by substituting $-s_{q_R} + \boldsymbol{\nabla}_R \cdot \left[\, \boldsymbol{q}_R \,\right]$ from the energy balance (5.51). Combination of the resultant entropy inequality with Eq.s (5.54) and (5.55) yield (see [10] for details)

$$T\,\dot{\eta}_R - \dot{u}_R + \mathbf{T}_R : \dot{\mathbf{F}} - \frac{1}{T}\,\not{\boldsymbol{q}}_R \cdot \boldsymbol{\nabla}_R\,[\,T\,] + \mu_{\mathrm{G}}\,\dot{c}_{\mathrm{G}_R} + \mu_{\mathrm{F}}\,\dot{c}_{\mathrm{F}_R} - \boldsymbol{h}_{\mathrm{G}_R} \cdot \boldsymbol{\nabla}_R\,[\,\mu_{\mathrm{G}}\,] - A^{(5.39)}\,w_R^{(5.39)} \geq 0\;. \tag{5.56}$$

5.5.2 Clausius-Duhem inequality

We select the Helmholtz free energy density (per unit reference volume)

$$\psi_R = u_R - T\,\eta_R\;, \tag{5.57}$$

as thermodynamic potential.

For the problem at hand, and at first instance, we set $\psi_R = \Psi_R^{\mathcal{N}}$, with $\Psi_R^{\mathcal{N}}$ referential counterpart of Eq. (5.24). We further need to augment the internal variable dependence, with respect to the previously selected for the free energy of the network. Therefore, we select the Helmholtz free energy density as a function of concentrations of G-actin c_{G_R} and total F-actin c_{F_R}, some inelastic tensorial internal variable $\boldsymbol{\Xi}$, temperature T, concentration of active chains ${}^{a}c_{\mathrm{F}_R}$, and chain distribution tensor $\boldsymbol{\Lambda}_R$,

$$\psi_R = \psi_R(c_{\mathrm{G}_R}, c_{\mathrm{F}_R}, \boldsymbol{\Xi}, T, {}^{a}c_{\mathrm{F}_R}, \boldsymbol{\Lambda}_R)\;. \tag{5.58}$$

The selected internal variable dependence in Eq. (5.58) requires some specifications. In first place, the concomitant presence of c_{F_R} and ${}^{a}c_{\mathrm{F}_R}$ may appear ambiguous. However, as specified in Section 5.4.1, we need to enforce this condition and we therefore assume to consider c_{F_R} and ${}^{a}c_{\mathrm{F}_R}$ as independent variables. Furthermore, it is clear that $\boldsymbol{\Lambda}_R = \boldsymbol{\Lambda}_R(\mathbf{F})$. We therefore assume that all deformations are captured by the chain distribution tensor $\boldsymbol{\Lambda}_R$, and point out that the selection of another strain variable would not be allowed in the current formulation.

In view of its selected functional dependence, the time derivative of the ψ_R (5.58) writes

$$\dot{\psi}_R = \frac{\partial \psi_R}{\partial c_{\mathrm{G}_R}}\,\dot{c}_{\mathrm{G}_R} + \frac{\partial \psi_R}{\partial c_{\mathrm{F}_R}}\,\dot{c}_{\mathrm{F}_R} + \frac{\partial \psi_R}{\partial \boldsymbol{\Xi}} : \dot{\boldsymbol{\Xi}} + \frac{\partial \psi_R}{\partial T}\,\dot{T} + \frac{\partial \psi_R}{\partial\, {}^{a}c_{\mathrm{F}_R}}\,{}^{a}\dot{c}_{\mathrm{F}_R} + \frac{\partial \psi_R}{\partial \boldsymbol{\Lambda}_R} : \dot{\boldsymbol{\Lambda}}_R \tag{5.59}$$

---

[4] They actually turn out to be defined chemical potential and affinity after thermodynamic prescriptions

Making use of the time derivative of Eq. (5.57) to replace $T\,\dot{\eta}_R - \dot{u}_R$ in (5.56), the entropy inequality re-writes

$$-\dot{\psi}_R - \dot{T}\,\eta_R + \mathbf{T}_R : \dot{\mathbf{F}} - \frac{1}{T}\,\boldsymbol{q}_R \cdot \boldsymbol{\nabla}_R\,[\,T\,] + \mu_{\mathrm{G}}\,\dot{c}_{\mathrm{G}_R} + \mu_{\mathrm{F}}\,\dot{c}_{\mathrm{F}_R} - \boldsymbol{h}_{\mathrm{G}_R} \cdot \boldsymbol{\nabla}_R\,[\,\mu_{\mathrm{G}}\,] - A^{(5.39)}\,w_R^{(5.39)} \geq 0\;. \quad (5.60)$$

As standard, we make use of Eq. (5.59) to re-write the time derivative of ψ_R in Eq. (5.60). We first recognize that the last three right-hand side terms in Eq. (5.59) corresponds to Eq. (5.37). Furthermore, let

$$\mathbf{X}\!\!\!| = -\frac{\partial \psi_R}{\partial \boldsymbol{\Xi}} \quad (5.61)$$

denote the inelastic stress tensor conjugate to $\boldsymbol{\Xi}$.

Combination of Eq.s (5.37), (5.59) and (5.61) therefore yields

$$\begin{aligned}\dot{\psi}_R = {} & \frac{\partial \psi_R}{\partial c_{\mathrm{G}_R}}\,\dot{c}_{\mathrm{G}_R} + \frac{\partial \psi_R}{\partial c_{\mathrm{F}_R}}\,\dot{c}_{\mathrm{F}_R} - \mathbf{X}\!\!\!| : \dot{\boldsymbol{\Xi}} + \frac{1}{2}\,k_B\,{}^{a}c_{\mathrm{F}_R}\,\mathrm{tr}\left[\,\boldsymbol{\Lambda}_R\,\mathbf{F}^{\mathrm{T}} - \mathbf{1}\,\right]\,\dot{T} - \mathcal{D}_R \\ & + \frac{1}{2}\,k_B\,T\,{}^{a}c_{\mathrm{F}_R}\,\mathrm{tr}\left[\,\mathbf{1} - \boldsymbol{\Lambda}_R\,\mathbf{F}^{\mathrm{T}}\,\right]\,\mathbf{F}^{-\mathrm{T}} : \dot{\mathbf{F}} + k_B\,T\,{}^{a}c_{\mathrm{F}_R}\,\boldsymbol{\Lambda}_R : \dot{\mathbf{F}}\;.\end{aligned} \quad (5.62)$$

Making use of Eq. (5.62) to replace $\dot{\psi}_R$ in Eq. (5.60), the following Clausius-Duhem inequality arises

$$\begin{aligned} & \left(\mathbf{T}_R - \frac{1}{2}\,k_B\,T\,{}^{a}c_{\mathrm{F}_R}\,\mathrm{tr}\left[\,\mathbf{1} - \boldsymbol{\Lambda}_R\,\mathbf{F}^{\mathrm{T}}\,\right]\,\mathbf{F}^{-\mathrm{T}} - k_B\,T\,{}^{a}c_{\mathrm{F}_R}\,\boldsymbol{\Lambda}_R\right) : \dot{\mathbf{F}} \\ & - \left(\eta_R + \frac{1}{2}\,k_B\,\mathrm{tr}\left[\,\boldsymbol{\Lambda}_R\,\mathbf{F}^{\mathrm{T}} - \mathbf{1}\,\right]\right)\dot{T} + \left(\mu_{\mathrm{G}} - \frac{\partial \psi_R}{\partial c_{\mathrm{G}_R}}\right)\dot{c}_{\mathrm{G}_R} + \left(\mu_{\mathrm{F}} - \frac{\partial \psi_R}{\partial c_{\mathrm{F}_R}}\right)\dot{c}_{\mathrm{F}_R} \\ & + \mathbf{X}\!\!\!| : \dot{\boldsymbol{\Xi}} - \frac{1}{T}\,\boldsymbol{q}_R \cdot \boldsymbol{\nabla}_R\,[\,T\,] - \boldsymbol{h}_{\mathrm{G}_R} \cdot \boldsymbol{\nabla}_R\,[\,\mu_{\mathrm{G}}\,] + \mathcal{D}_R - A^{(5.39)}\,w_R^{(5.39)} \geq 0\;.\end{aligned} \quad (5.63)$$

According to the method of Coleman and Noll [8], inequality (5.63) must hold for any value of $\dot{\mathbf{F}}$, $\dot{T}$, $\dot{c}_{\mathrm{G}_R}$ and $\dot{c}_{\mathrm{F}_R}$. The following thermodynamic restrictions thus emanate

$$\mathbf{T}_R = \frac{1}{2}\,k_B\,T\,{}^{a}c_{\mathrm{F}_R}\,\mathrm{tr}\left[\,\mathbf{1} - \boldsymbol{\Lambda}_R\,\mathbf{F}^{\mathrm{T}}\,\right]\,\mathbf{F}^{-\mathrm{T}} - k_B\,T\,{}^{a}c_{\mathrm{F}_R}\,\boldsymbol{\Lambda}_R\;, \quad (5.64a)$$

$$\eta_R = -\frac{1}{2}\,k_B\,\mathrm{tr}\left[\,\boldsymbol{\Lambda}_R\,\mathbf{F}^{\mathrm{T}} - \mathbf{1}\,\right]\;, \quad (5.64b)$$

$$\mu_{\mathrm{G}} = \frac{\partial \psi_R}{\partial c_{\mathrm{G}_R}}\;, \quad (5.64c)$$

$$\mu_{\mathrm{F}} = \frac{\partial \psi_R}{\partial c_{\mathrm{F}_R}}\;. \quad (5.64d)$$

What remains of inequality (5.63) determines restrictions on $\mathbf{X}\!\!\!|$, $\boldsymbol{q}_R$, $\boldsymbol{h}_{\mathrm{G}_R}$, $\mathcal{D}_R$ and $A^{(5.39)}$, namely

$$\mathbf{X}\!\!\!| : \dot{\boldsymbol{\Xi}} - \frac{1}{T}\,\boldsymbol{q}_R \cdot \boldsymbol{\nabla}_R\,[\,T\,] - \boldsymbol{h}_{\mathrm{G}_R} \cdot \boldsymbol{\nabla}_R\,[\,\mu_{\mathrm{G}}\,] + \mathcal{D}_R - A^{(5.39)}\,w_R^{(5.39)} \geq 0\;. \quad (5.65)$$

The Curie's symmetry principles assumption [51] establishes no coupling between fluxes and thermodynamic forces of different tensorial order. The following conditions therefore arise

$$\mathbf{X}\!\!\!| : \dot{\boldsymbol{\Xi}} \geq 0\;, \quad (5.66a)$$

$$\frac{1}{T}\,\boldsymbol{q}_R \cdot \boldsymbol{\nabla}_R\,[\,T\,] + \boldsymbol{h}_{\mathrm{G}_R} \cdot \boldsymbol{\nabla}_R\,[\,\mu_{\mathrm{G}}\,] \leq 0\;, \quad (5.66b)$$

$$\mathcal{D}_R - A^{(5.39)}\,w_R^{(5.39)} \geq 0\;. \quad (5.66c)$$

Constitutive specifications should be now required, *e.g.* for the Helmholtz free energy density, heat and mass flux vectors, and eventual specifications for the stress tensor, after a proper strain decomposition, and chemical kinetics, as performed in [10]. However, it is right and fair to point out a "lack of success" of the current formulation with respect to the aim it has been thought for. The manuscript is therefore interrupted here on purpose on behalf of a discussion on weaknesses encountered within the current model.

5.6 Discussion

Before briefly discuss weaknesses of the current formulation, we highlight some difference with respect to the original framework introduced in [117].

Here, the original work has been slightly extended, *i.e.*, we have here removed the incompressibility assumption, the framework has been re-phrased in Lagrangian setting, and a coupling with a chemo-transport formulation with trapping has been attempted. Furthermore, the evaluation of some statistically-based continuum quantities differs from [117]. It is the case of the variation in time of $\mathcal{F}(\boldsymbol{r},t)$ due to an applied deformation (5.16), the resultant Eq. (5.17) and, especially, the derivation of Eq. (5.31) that provides the variation in time of the free energy of the network. The latter, independently from the Lagrangian formulation, has led to a different thermodynamic prescription for the mechanical stress tensor (5.66a), which has not here an evaluation with respect to the stress-free state.

Rather, the main weaknesses of the framework proposed in the current notes are summarized hereinafter. At first instance, the simplified assumption of $k_d = k_d(\boldsymbol{r})$ performed in Section 5.3.1 implies the far-fetched independence of chain detachments upon the deformation. This assumption is nonetheless admissible for moderate deformations, for which the selection of Gaussian statistics results appropriate. Rather, in the field of finite strain mechanics, the Langevin statistics appears to be a more suitable choice to describe the mechanical behavior of polymer chains. In it, the linear-type relation between force and $\boldsymbol{r}$ stated by Gaussian statistics is replaced by a dependence of the applied force upon the difference between the maximum extension of the end to end vector and its average over the chain space $\mathcal{C}_s$ [203]. However, the "lack of success" of the current formulation does not lie in the selected statistics. Therefore, re-phrasing the framework in terms of Langevin statistics, beyond its complexity, would result meaningless so far.

In Section 5.3.3 it has been specified that all statistically-based continuum quantities need to be evaluated for a time-independent value of the end-to-end vector, from which descends the benefit in introducing the chain distribution tensor $\boldsymbol{\Lambda}$, and for which the requirement of constant chain concentration is necessary. The introduction of $\boldsymbol{\Lambda}$ is of indisputable benefit. Indeed, given that $\boldsymbol{\Lambda}_0 = \mathbf{1}$, the evaluation of the time evolution of $\boldsymbol{\Lambda}$ - which behaves as the distribution function $\mathcal{F}(\boldsymbol{r},t)$ - allows to make comparisons with the stress-free state of the network, and to evaluate how macroscopic quantities are affected by the mechanical (microscopic) behavior of the polymer[5] The chain distribution tensor therefore avoid to perform non-trivial statistical operations and to capture the microscopic behavior of the network at the continuum scale. However, and for the problem at hand, the limitation lies in the condition ${}^{a}\dot{c}_{\mathrm{F}} = 0$, which is required to guarantee a time-independent $\boldsymbol{r}$.

The current formulation results therefore uncoupled. Indeed, mass balance equations (5.46) does not affect the statistically-based description of the network, which is based on active chains, and for which it has been necessary to assume the independence of c_{F_R} from ${}^{a}c_{\mathrm{F}_R}$. In other words, polymerization has here the only aim to "provide" polymer non-active chains, without affecting the microscopic behavior of the network.

Lastly, the selected functional dependence of the Helmholtz free energy density (5.58) stated in Section 5.5.2 is forced by the introduction of the chain distribution tensor, in addition to the assumption of independency between c_{F_R} and ${}^{a}c_{\mathrm{F}_R}$, given that $\boldsymbol{\Lambda}_R = \boldsymbol{\Lambda}_R(\mathbf{F})$. This choice does not represent a limitation, as long as the active chain concentration is constant.

The task to overcome weaknesses in the current formulation is far to be accomplished, and some consideration have to be made.

At first instance, and for the problem at hand, the variation in time of chain distribution function $\mathcal{F}(\boldsymbol{r},t)$ shown in Eq. (5.7) should be augmented in order to account for chain generation, or loss, due to the polymerization and depolymerization processes. Some simplified assumption should be

---

[5] On the basis of [117], the solution of the second order tensorial differential equation (5.26) is provided in Appendix B.5. Currently, the same has not been performed for the $\boldsymbol{\Lambda}_R$, which, however, does not represent one of the limitations of the current formulation.

necessary to convert the bimolecular reaction (5.39) into a time evolution of the distribution function due to the polymerization process. Indeed, whereas chemical reaction (5.39), and the law of mass action (5.40), represent the conversion of monomers into polymers, polymer chains of fixed length should be made instantaneously available in the network for providing a *new* variation in time of $\mathcal{F}(\boldsymbol{r}, t)$.

In view of the aforementioned considerations, the definition of the chain distribution tensor $\mathbf{\Lambda}$ would thus become meaningless for the problem we have aimed at describing. As a consequence, the chain distribution tensor should not be introduced, and all statistically-based evaluations provided in the current framework rather needed to be re-phrased in terms of deformation gradient $\mathbf{F}$. This choice implies an unquestionable additional complexity Lastly, the selection of Langevin statistics may seem a more appropriate choice to formulate a statistically-based finite strain continuum mechanical framework.

The formulation of a statistically-based multi-physics framework for modeling actin cytoskeletal biopolymer structures is far to be accomplished in an exhaustive way and therefore still requires further efforts.

Appendix B

B.1 Proof of Eq. (5.18)

To perform the integral of the ratio of the distribution function $\mathcal{F}(\boldsymbol{r},t)$ (5.17) over the chain space $\mathcal{C}_s$, first recall that the integral over $\mathcal{C}_s$ of the probability functions $P_0(\boldsymbol{r})$ and $P(\boldsymbol{r},t)$ is equal to 1. Furthermore, the independence of the deformation gradient upon $\boldsymbol{r}$ implies that also $\mathbf{L}$ is uniform in $\mathcal{C}_s$. Therefore

$$\int_{\mathcal{C}_s} \frac{\partial \mathcal{F}(\boldsymbol{r},t)}{\partial t}\,\mathrm{d}\boldsymbol{r} = \xi_a - k_d\,{}^a c_{\mathrm{F}} - \mathbf{L} : \int_{\mathcal{C}_s} \boldsymbol{\nabla}_{\mathcal{C}_s}\left[\,\mathcal{F}(\boldsymbol{r},t)\,\right] \otimes \boldsymbol{r}\,\mathrm{d}\boldsymbol{r} - 2\,{}^a c_{\mathrm{F}}\,\mathrm{tr}\left[\,\mathbf{L}\,\right]\ . \tag{B.1}$$

Integration by parts is performed to evaluate the third right-hand side term of Eq. (B.1). It holds

$$-\mathrm{L}_{ij}\int_{\mathcal{C}_s} \frac{\partial \mathcal{F}(\boldsymbol{r},t)}{\partial r_i} r_j\,\mathrm{d}\boldsymbol{r} = -\mathrm{L}_{ij}\,\left[\mathcal{F}(\boldsymbol{r},t)\,r_i\right]_{\mathcal{C}_s} + \mathrm{L}_{ij}\int_{\mathcal{C}_s} \mathcal{F}(\boldsymbol{r},t)\,\frac{\partial r_j}{\partial r_i}\,\mathrm{d}\boldsymbol{r}\ . \tag{B.2}$$

Recognition that $\mathcal{F}(\boldsymbol{r},t)$ is an even function because of the selected Gaussian probability function $P(\boldsymbol{r},t)$ yields

$$-\mathrm{L}_{ij}\int_{\mathcal{C}_s} \frac{\partial \mathcal{F}(\boldsymbol{r},t)}{\partial r_i} r_j\,\mathrm{d}\boldsymbol{r} = \mathrm{L}_{ij}\int_{\mathcal{C}_s} \mathcal{F}(\boldsymbol{r},t)\,\delta_{ji}\,\mathrm{d}\boldsymbol{r} = \mathrm{L}_{ij}\,\delta_{ji}\int_{\mathcal{C}_s} {}^a c_{\mathrm{F}}(t)\,P(\boldsymbol{r},t)\,\mathrm{d}\boldsymbol{r} = {}^a c_{\mathrm{F}}\,\mathrm{tr}\left[\,\mathbf{L}\,\right]\ . \tag{B.3}$$

Combination of Eq. (B.1) and (B.3) implies

$$\int_{\mathcal{C}_s} \frac{\partial \mathcal{F}(\boldsymbol{r},t)}{\partial t}\,\mathrm{d}\boldsymbol{r} = \xi_a - k_d\,{}^a c_{\mathrm{F}} - {}^a c_{\mathrm{F}}\,\mathrm{tr}\left[\,\mathbf{L}\,\right] = \frac{\partial\,{}^a c_{\mathrm{F}}}{\partial t}\ , \tag{B.4}$$

according to Eq. (5.6).

B.2 Proof of Eq. (5.25b)

Recall the integral operation in the chain space (5.3) and the definition of $\boldsymbol{\Lambda}_0$ (5.25b)

$$\begin{aligned}\boldsymbol{\Lambda}_0 &= \int_{\mathcal{C}_s} P_0(\boldsymbol{r})\,\tilde{\boldsymbol{r}}\otimes\tilde{\boldsymbol{r}}\,\mathrm{d}\boldsymbol{r} = \left(\frac{3}{2\pi\,Nb^2}\right)^{\frac{3}{2}}\int_{\mathcal{C}_s} \exp\left(-\frac{\tilde{\boldsymbol{r}}^2}{2}\right)\tilde{\boldsymbol{r}}\otimes\tilde{\boldsymbol{r}}\,\mathrm{d}\boldsymbol{r}\\ &= \left(\frac{3}{2\pi\,Nb^2}\right)^{\frac{3}{2}}\int_0^{2\pi}\int_0^{\pi}\int_0^{\infty} \exp\left(-\frac{\tilde{\boldsymbol{r}}^2}{2}\right)\tilde{\boldsymbol{r}}\otimes\tilde{\boldsymbol{r}}\;r^2\,\mathrm{d}r\sin\vartheta\;\mathrm{d}\vartheta\;\mathrm{d}\varphi\ .\end{aligned} \tag{B.5}$$

By means of Eq. (5.21), and by noting that $\boldsymbol{r}^2 = r^2$ and $\tilde{\boldsymbol{r}}^2 = \tilde{r}^2$,

$$r^2 = \frac{Nb^2}{3}\,\tilde{r}^2\ ,\qquad \mathrm{d}r = \sqrt{\frac{Nb^2}{3}}\,\mathrm{d}\tilde{r}\ , \tag{B.6}$$

hence

$$\int_0^{\infty} \bullet\; r^2\mathrm{d}r = \frac{Nb^2}{3}\sqrt{\frac{Nb^2}{3}}\int_0^{\infty} \bullet\;\tilde{r}\;\mathrm{d}\tilde{r}\ .$$

Accordingly, Eq. (B.5) re-writes

$$\begin{aligned}\boldsymbol{\Lambda}_0 &= \left(\frac{3}{2\pi\,Nb^2}\right)^{\frac{3}{2}} \frac{Nb^2}{3}\sqrt{\frac{Nb^2}{3}} \int_0^{2\pi}\int_0^{\pi}\int_0^{\infty} \exp\left(-\frac{\tilde{r}^2}{2}\right) \tilde{\boldsymbol{r}}\otimes\tilde{\boldsymbol{r}}\;\tilde{r}^2\,\mathrm{d}\tilde{r}\sin\vartheta\;\mathrm{d}\vartheta\;\mathrm{d}\varphi \\ &= \frac{3}{2\pi\,Nb^2}\sqrt{\frac{3}{2\pi\,Nb^2}}\,\frac{Nb^2}{3}\sqrt{\frac{Nb^2}{3}} \int_0^{2\pi}\int_0^{\pi}\int_0^{\infty} \exp\left(-\frac{\tilde{r}^2}{2}\right) \tilde{\boldsymbol{r}}\otimes\tilde{\boldsymbol{r}}\;\tilde{r}^2\,\mathrm{d}\tilde{r}\sin\vartheta\;\mathrm{d}\vartheta\;\mathrm{d}\varphi \\ &= \frac{1}{2\pi\,\sqrt{2\pi}} \int_0^{2\pi}\int_0^{\pi}\int_0^{\infty} \exp\left(-\frac{\tilde{r}^2}{2}\right) \tilde{\boldsymbol{r}}\otimes\tilde{\boldsymbol{r}}\;\tilde{r}^2\,\mathrm{d}\tilde{r}\sin\vartheta\;\mathrm{d}\vartheta\;\mathrm{d}\varphi\;.\end{aligned} \tag{B.7}$$

By re-writing the normalized end-to-end vector in spherical coordinates

$$\tilde{\boldsymbol{r}} = \begin{Bmatrix} \tilde{r}\,\sin\vartheta\,\cos\varphi \\ \tilde{r}\,\sin\vartheta\,\sin\varphi \\ \tilde{r}\,\cos\vartheta \end{Bmatrix}\;, \tag{B.8}$$

then

$$\tilde{\boldsymbol{r}}\otimes\tilde{\boldsymbol{r}} = \begin{bmatrix} \tilde{r}^2\,\sin^2\vartheta\,\cos^2\varphi & \tilde{r}^2\,\sin^2\vartheta\,\cos\varphi\,\cos\vartheta & \tilde{r}^2\,\sin\vartheta\,\cos\varphi\,\cos\vartheta \\ \tilde{r}^2\,\sin^2\vartheta\,\cos\varphi\,\sin\varphi & \tilde{r}^2\,\sin^2\vartheta\,\sin^2\varphi & \tilde{r}^2\,\sin\vartheta\,\sin\varphi\,\cos\vartheta \\ \tilde{r}^2\,\sin\vartheta\,\cos\varphi\,\cos\vartheta & \tilde{r}^2\,\sin\vartheta\,\sin\varphi\,\cos\vartheta & \tilde{r}^2\,\cos^2\vartheta \end{bmatrix}\;. \tag{B.9}$$

For the sake of simplicity of notation, set

$$\tilde{\boldsymbol{r}}\otimes\tilde{\boldsymbol{r}} = \tilde{r}^2\;\left[\Theta\left(\vartheta,\varphi\right)\right]\;, \tag{B.10}$$

so that Eq. (B.7) can be written as

$$\boldsymbol{\Lambda}_0 = \frac{1}{2\pi\,\sqrt{2\pi}} \int_0^{2\pi}\int_0^{\pi}\int_0^{\infty} \exp\left(-\frac{\tilde{R}^2}{2}\right)\,\tilde{r}^4\,\mathrm{d}\tilde{r}\;\left[\Theta\left(\vartheta,\varphi\right)\right]\sin\vartheta\;\mathrm{d}\vartheta\;\mathrm{d}\varphi\;. \tag{B.11}$$

To compute the first integral term it is necessary recall the relation

$$\int_0^{\infty} x^{2n}\,\exp\left(-\frac{x^2}{\alpha^2}\right) = \sqrt{\pi}\,\frac{\alpha^{2n+1}\;(2n-1)!!}{2^{n+1}}\;. \tag{B.12}$$

Set $\tilde{r}^4 = x^{2n}$ and $\alpha^2 = 2$, such that $n = 2$ and $\alpha = \sqrt{2}$, respectively. Therefore

$$\int_0^{\infty} \exp\left(-\frac{\tilde{R}^2}{2}\right)\,\tilde{R}^4\,\mathrm{d}\tilde{R} = \sqrt{\pi}\,\frac{\sqrt{2}^5\;3!!}{2^3} = \sqrt{\pi}\,\frac{3}{\sqrt{2}}\;, \tag{B.13}$$

from which Eq. (B.11) takes the form

$$\boldsymbol{\Lambda}_0 = \frac{3}{4\pi}\int_0^{2\pi}\int_0^{\pi}\left[\Theta\left(\vartheta,\varphi\right)\right]\sin\vartheta\;\mathrm{d}\vartheta\;\mathrm{d}\varphi\;. \tag{B.14}$$

By means of the symmetry of $[\,\Theta\,(\vartheta,\varphi)\,]$, the off-diagonal terms writes

$$
\begin{aligned}
\Theta_{12} = \Theta_{21} &= \frac{3}{4\pi}\int_0^{2\pi}\int_0^{\pi} \sin^2\vartheta\,\cos\varphi\,\sin\varphi\,\sin\vartheta\,\sin\vartheta\;\mathrm{d}\vartheta\;\mathrm{d}\varphi = \frac{3}{4\pi}\int_0^{2\pi}\left(\int_0^{\pi}\sin^3\vartheta\;\mathrm{d}\vartheta\right)\cos\varphi\,\sin\varphi\;\mathrm{d}\varphi \\
&= \frac{3}{4\pi}\left(\int_0^{\pi}\sin^3\vartheta\;\mathrm{d}\vartheta\right)\int_0^{2\pi}\cos\varphi\,\sin\varphi\;\mathrm{d}\varphi = \frac{3}{4\pi}\left(\int_0^{\pi}\sin^3\vartheta\;\mathrm{d}\vartheta\right)\left[-\frac{1}{4}\cos 2\varphi\right]_0^{2\pi} \\
&= \frac{3}{4\pi}\left(\int_0^{\pi}\sin^3\vartheta\;\mathrm{d}\vartheta\right)\left(-\frac{1}{4}\cos 4\varphi + \frac{1}{4}\cos 0\right) = \frac{3}{4\pi}\left(\int_0^{\pi}\sin^3\vartheta\;\mathrm{d}\vartheta\right)\left(-\frac{1}{4}+\frac{1}{4}\right) = 0\;, \\
\Theta_{13} = \Theta_{31} &= \frac{3}{4\pi}\int_0^{2\pi}\int_0^{\pi} \sin\vartheta\,\cos\varphi\,\cos\vartheta\,\sin\vartheta\;\mathrm{d}\vartheta\;\mathrm{d}\varphi = \frac{3}{4\pi}\int_0^{2\pi}\left(\int_0^{\pi}\sin^2\vartheta\,\cos\vartheta\;\mathrm{d}\vartheta\right)\cos\varphi\;\mathrm{d}\varphi \\
&= \frac{3}{4\pi}\left(\int_0^{\pi}\sin^2\vartheta\,\cos\vartheta\;\mathrm{d}\vartheta\right)\int_0^{2\pi}\cos\varphi\;\mathrm{d}\varphi = \frac{3}{4\pi}\left(\int_0^{\pi}\sin^2\vartheta\,\cos\vartheta\;\mathrm{d}\vartheta\right)[\,\sin\varphi\,]_0^{2\pi} \\
&= \frac{3}{4\pi}\left(\int_0^{\pi}\sin^2\vartheta\,\cos\vartheta\;\mathrm{d}\vartheta\right)(\sin 2\pi - \sin 0) = \frac{3}{4\pi}\left(\int_0^{\pi}\sin^2\vartheta\,\cos\vartheta\;\mathrm{d}\vartheta\right)(0-0) = 0\;, \\
\Theta_{23} = \Theta_{23} &= \frac{3}{4\pi}\int_0^{2\pi}\int_0^{\pi} \sin\vartheta\,\sin\varphi\,\cos\vartheta\,\sin\vartheta\;\mathrm{d}\vartheta\;\mathrm{d}\varphi = \frac{3}{4\pi}\int_0^{2\pi}\left(\int_0^{\pi}\sin^2\vartheta\,\cos\vartheta\;\mathrm{d}\vartheta\right)\sin\varphi\;\mathrm{d}\varphi \\
&= \frac{3}{4\pi}\left(\int_0^{\pi}\sin^2\vartheta\,\cos\vartheta\;\mathrm{d}\vartheta\right)\int_0^{2\pi}\sin\varphi\;\mathrm{d}\varphi = \frac{3}{4\pi}\left(\int_0^{\pi}\sin^2\vartheta\,\cos\vartheta\;\mathrm{d}\vartheta\right)[\,-\cos\varphi\,]_0^{2\pi} \\
&= \frac{3}{4\pi}\left(\int_0^{\pi}\sin^2\vartheta\,\cos\vartheta\;\mathrm{d}\vartheta\right)(-\cos 2\pi + \cos 0) = \frac{3}{4\pi}\left(\int_0^{\pi}\sin^2\vartheta\,\cos\vartheta\;\mathrm{d}\vartheta\right)(-0+0) = 0\;,
\end{aligned}
$$

whereas for the diagonal terms of $[\,\Theta\,(\vartheta,\varphi)\,]$ it holds

$$
\begin{aligned}
\Theta_{11} &= \frac{3}{4\pi}\int_0^{2\pi}\int_0^{\pi}\sin^2\vartheta\,\cos^2\varphi\,\sin\vartheta\;\mathrm{d}\vartheta\;\mathrm{d}\varphi = \frac{3}{4\pi}\int_0^{2\pi}\int_0^{\pi}\sin^3\vartheta\;\mathrm{d}\vartheta\;\cos^2\varphi\;\mathrm{d}\varphi \\
&= \frac{3}{4\pi}\int_0^{2\pi}\left[\frac{1}{3}\cos^3\vartheta - \cos\vartheta\right]_0^{\pi}\cos^2\varphi\;\mathrm{d}\varphi = \frac{3}{4\pi}\int_0^{2\pi}\left[\frac{1}{3}\left(\cos^3\pi - \cos^3 0\right) - (\cos\pi - \cos 0)\right]\cos^2\varphi\;\mathrm{d}\varphi \\
&= \frac{3}{4\pi}\int_0^{2\pi}\left(-\frac{2}{3}+2\right)\cos^2\varphi\;\mathrm{d}\varphi = \frac{3}{4\pi}\,\frac{4}{3}\int_0^{2\pi}\cos^2\varphi\;\mathrm{d}\varphi = \frac{1}{\pi}\left[\frac{1}{2}\,(\varphi + \sin\varphi\cos\varphi)\right]_0^{2\pi} = \frac{1}{\pi}\,\frac{1}{2}\,2\pi = 1\;, \\
\Theta_{22} &= \frac{3}{4\pi}\int_0^{2\pi}\int_0^{\pi}\sin^2\vartheta\,\sin^2\varphi\,\sin\vartheta\;\mathrm{d}\vartheta\;\mathrm{d}\varphi = \frac{3}{4\pi}\int_0^{2\pi}\int_0^{\pi}\sin^3\vartheta\;\mathrm{d}\vartheta\;\sin^2\varphi\;\mathrm{d}\varphi \\
&= \frac{3}{4\pi}\,\frac{4}{3}\int_0^{2\pi}\sin^2\varphi\;\mathrm{d}\varphi = \frac{1}{\pi}\left[\frac{1}{2}\,(\varphi - \sin\varphi\cos\varphi)\right]_0^{2\pi} = \frac{1}{\pi}\,\frac{1}{2}\,2\pi = 1\;, \\
\Theta_{33} &= \frac{3}{4\pi}\int_0^{2\pi}\int_0^{\pi}\cos^2\vartheta\,\sin\vartheta\;\mathrm{d}\vartheta\;\mathrm{d}\varphi = \frac{3}{4\pi}\int_0^{2\pi}\int_0^{\pi}\left(1-\sin^2\vartheta\right)\sin\vartheta\;\mathrm{d}\vartheta\;\mathrm{d}\varphi \\
&= \frac{3}{4\pi}\int_0^{2\pi}\int_0^{\pi}\sin\vartheta - \sin^3\vartheta\;\;\mathrm{d}\vartheta\;\mathrm{d}\varphi = \frac{3}{4\pi}\int_0^{2\pi}[-\cos\vartheta]_0^{\pi} - \left[\frac{1}{3}\cos^3\vartheta - \cos\vartheta\right]_0^{\pi}\;\mathrm{d}\varphi \\
&= \frac{3}{4\pi}\left(2-\frac{4}{3}\right)\int_0^{2\pi}\mathrm{d}\varphi = \frac{3}{4\pi}\,\frac{2}{3}\,2\pi = 1\;,
\end{aligned}
$$

whence

$$
\boldsymbol{\Lambda}_0 = \mathbf{1}\;. \tag{B.17}
$$

B.3 Proof of Eq. (5.26)

According to the definition of $\mathcal{F}(\boldsymbol{r},t)$ (5.4), the distribution tensor $\boldsymbol{\Lambda}$ (5.25a) can be re-written in the form

$$
\boldsymbol{\Lambda} = \int_{\mathcal{C}_s}\frac{\mathcal{F}(\boldsymbol{r},t)}{{}^{a}c_{\mathrm{F}}(t)}\,\tilde{\boldsymbol{r}}\otimes\tilde{\boldsymbol{r}}\;\mathrm{d}\boldsymbol{r}\;, \tag{B.18}
$$

whence

$$\dot{\boldsymbol{\Lambda}} = \frac{\partial\, {}^a c_\mathrm{F}{}^{-1}}{\partial t} \int_{\mathcal{C}_s} \mathcal{F}(\boldsymbol{r},t)\, \tilde{\boldsymbol{r}} \otimes \tilde{\boldsymbol{r}}\ \mathrm{d}\boldsymbol{r} + {}^a c_\mathrm{F}{}^{-1} \int_{\mathcal{C}_s} \frac{\partial \mathcal{F}(\boldsymbol{r},t)}{\partial t}\, \tilde{\boldsymbol{r}} \otimes \tilde{\boldsymbol{r}}\ \mathrm{d}\boldsymbol{r}\ . \tag{B.19}$$

Making use of definition (5.4) and Eq. (5.18), the first right-hand side term of Eq. (B.19) writes

$$-\frac{1}{{}^a c_\mathrm{F}{}^2}\ \left(\xi_a - k_d\, {}^a c_\mathrm{F} - {}^a c_\mathrm{F}\, \mathrm{tr}\,[\,\mathbf{L}\,]\right)\, {}^a c_\mathrm{F}(t) \int_{\mathcal{C}_s} P(\boldsymbol{r},t)\, \tilde{\boldsymbol{r}} \otimes \tilde{\boldsymbol{r}}\ \mathrm{d}\boldsymbol{r} = -\frac{\xi_a}{{}^a c_\mathrm{F}}\, \boldsymbol{\Lambda} + k_d\, \boldsymbol{\Lambda} + \boldsymbol{\Lambda}\, \mathrm{tr}\,[\,\mathbf{L}\,]\ , \tag{B.20}$$

according to definition (5.25a).

By means of Eq. (5.17), the second right-hand side term of Eq. (B.19) writes

$${}^a c_\mathrm{F}{}^{-1} \int_{\mathcal{C}_s} \left[\,\xi_a\, P_0(\boldsymbol{r}) - k_d\, \mathcal{F}(\boldsymbol{r},t) - \boldsymbol{\nabla}_{\mathcal{C}_s} [\,\mathcal{F}(\boldsymbol{r},t)\,] \otimes \boldsymbol{r} : \mathbf{L} - 2\, \mathcal{F}(\boldsymbol{r},t)\, \mathrm{tr}\,[\,\mathbf{L}\,]\,\right]\, \tilde{\boldsymbol{r}} \otimes \tilde{\boldsymbol{r}}\ \mathrm{d}\boldsymbol{r}\ , \tag{B.21}$$

whence, according to definitions (5.4), (5.25a) and (5.25b), and recognition that $\mathbf{L}$ is uniform in $\mathcal{C}_s$,

$$\begin{aligned} &\frac{\xi_a}{{}^a c_\mathrm{F}} \int_{\mathcal{C}_s} P_0(\boldsymbol{r})\, \tilde{\boldsymbol{r}} \otimes \tilde{\boldsymbol{r}}\ \mathrm{d}\boldsymbol{r} - k_d \int_{\mathcal{C}_s} P(\boldsymbol{r},t)\, \tilde{\boldsymbol{r}} \otimes \tilde{\boldsymbol{r}}\ \mathrm{d}\boldsymbol{r} - 2\, \mathrm{tr}\,[\,\mathbf{L}\,] \int_{\mathcal{C}_s} P(\boldsymbol{r},t)\, \tilde{\boldsymbol{r}} \otimes \tilde{\boldsymbol{r}}\ \mathrm{d}\boldsymbol{r} \\ &\qquad - {}^a c_\mathrm{F}{}^{-1} \mathbf{L} : \int_{\mathcal{C}_s} \left[\boldsymbol{\nabla}_{\mathcal{C}_s} [\,\mathcal{F}(\boldsymbol{r},t)\,] \otimes \boldsymbol{r}\right]\, \left[\tilde{\boldsymbol{r}} \otimes \tilde{\boldsymbol{r}}\right]\, \mathrm{d}\boldsymbol{r} \\ &\quad = \frac{\xi_a}{{}^a c_\mathrm{F}}\, \boldsymbol{\Lambda}_0 - k_d\, \boldsymbol{\Lambda} - 2\, \boldsymbol{\Lambda}\, \mathrm{tr}\,[\,\mathbf{L}\,] - {}^a c_\mathrm{F}{}^{-1} \mathbf{L} : \int_{\mathcal{C}_s} \left[\,\boldsymbol{\nabla}_{\mathcal{C}_s} [\,\mathcal{F}(\boldsymbol{r},t)\,] \otimes \boldsymbol{r}\,\right]\, \left[\,\tilde{\boldsymbol{r}} \otimes \tilde{\boldsymbol{r}}\,\right]\, \mathrm{d}\boldsymbol{r}\ .\ , \end{aligned} \tag{B.22}$$

Making use of definition (5.21), the last right-hand side integral term of Eq. (B.21) can be cast in the form,

$$\begin{aligned} \int_{\mathcal{C}_s} \frac{\partial \mathcal{F}(\boldsymbol{r},t)}{\partial r_i}\, r_j\, \tilde{r}_k\, \tilde{r}_l\ \mathrm{d}\boldsymbol{r} &= \int_{\mathcal{C}_s} \frac{\partial \mathcal{F}(\boldsymbol{r},t)}{\partial \left(r_i/\sqrt{Nb^2/3}\right)}\, \frac{\partial r_j}{\partial \sqrt{Nb^2/3}}\, \tilde{r}_k\, \tilde{r}_l\ \mathrm{d}\boldsymbol{r} \\ &= \int_{\mathcal{C}_s} \frac{\partial \mathcal{F}(\boldsymbol{r},t)}{\partial \tilde{r}_i}\, \tilde{r}_j\, \tilde{r}_k\, \tilde{r}_l\ \mathrm{d}\boldsymbol{r}\ . \end{aligned} \tag{B.23}$$

Integrating by parts and after recognition that $\mathcal{F}(\boldsymbol{r},t)$ is an even function, the last term of Eq. (B.22) re-writes

$$\begin{aligned} &{}^a c_\mathrm{F}{}^{-1}\, \mathrm{L}_{ij} \int_{\mathcal{C}_s} \mathcal{F}(\boldsymbol{r},t)\, \frac{\partial \tilde{r}_j}{\partial \tilde{r}_i}\, \tilde{r}_k\, \tilde{r}_l + \mathcal{F}(\boldsymbol{r},t)\, \tilde{r}_j\, \frac{\partial \tilde{r}_k}{\partial \tilde{r}_i}\, \tilde{r}_l + \mathcal{F}(\boldsymbol{r},t)\, \tilde{r}_j\, \tilde{r}_k\, \frac{\partial \tilde{r}_l}{\partial \tilde{r}_i}\ \mathrm{d}\boldsymbol{r} \\ &\quad = \mathrm{L}_{ij} \int_{\mathcal{C}_s} P(\boldsymbol{r},t)\, \delta_{ji}\, \tilde{r}_k\, \tilde{r}_l + P(\boldsymbol{r},t)\, \tilde{r}_j\, \delta_{ki} \tilde{r}_l + P(\boldsymbol{r},t)\, \tilde{r}_j\, \tilde{r}_k\, \delta_{il}\ \mathrm{d}\boldsymbol{r} \\ &\quad = \mathrm{L}_{ij}\, \delta_{ji} \int_{\mathcal{C}_s} P(\boldsymbol{r},t)\, \tilde{r}_k\, \tilde{r}_l\ \mathrm{d}\boldsymbol{r} + \mathrm{L}_{ij}\, \delta_{ki} \int_{\mathcal{C}_s} P(\boldsymbol{r},t)\, \tilde{r}_j\, \tilde{r}_l\ \mathrm{d}\boldsymbol{r} + \mathrm{L}_{ij}\, \delta_{li} \int_{\mathcal{C}_s} P(\boldsymbol{r},t)\, \tilde{r}_j\, \tilde{r}_k\ \mathrm{d}\boldsymbol{r} \\ &\quad = \mathrm{L}_{ii}\, \Lambda_{kl} + \mathrm{L}_{kj}\, \Lambda_{jl} + \mathrm{L}_{lj}\, \Lambda_{jk}\ , \end{aligned} \tag{B.24}$$

whence

$$-{}^a c_\mathrm{F}{}^{-1} \mathbf{L} : \int_{\mathcal{C}_s} \left[\,\boldsymbol{\nabla}_{\mathcal{C}_s} [\,\mathcal{F}(\boldsymbol{r},t)\,] \otimes \boldsymbol{r}\,\right]\, \left[\,\tilde{\boldsymbol{r}} \otimes \tilde{\boldsymbol{r}}\,\right]\, \mathrm{d}\boldsymbol{r} = \boldsymbol{\Lambda}\, \mathrm{tr}\,[\,\mathbf{L}\,] + \mathbf{L}\, \boldsymbol{\Lambda} + \left(\mathbf{L}\, \boldsymbol{\Lambda}\right)^\mathrm{T} \tag{B.25}$$

Combination of Eq.s (B.19), (B.21), (B.22) and (B.25) yields

$$\dot{\boldsymbol{\Lambda}} = \frac{\xi_a}{{}^a c_\mathrm{F}}\ \left(\boldsymbol{\Lambda}_0 - \boldsymbol{\Lambda}\right) + \mathbf{L}\, \boldsymbol{\Lambda} + \left(\mathbf{L}\, \boldsymbol{\Lambda}\right)^\mathrm{T}\ \ , \tag{B.26}$$

after simple algebra.

B.4 Proof of Eq. (5.31)

The time derivative of the network free energy $\Psi^{\mathcal{N}}$ (5.24) writes

$$\begin{aligned}\dot{\Psi}^{\mathcal{N}} = &\frac{1}{2}\,k_{_B}\,\dot{T}\int_{\mathcal{C}_s}(\mathcal{F}(\boldsymbol{r},t)-\mathcal{F}_0(\boldsymbol{r},t))\;\mathrm{tr}[\,\tilde{\boldsymbol{r}}\otimes\tilde{\boldsymbol{r}}\,]\;\mathrm{d}\boldsymbol{r}\\ &+\frac{1}{2}\,k_{_B}\,T\int_{\mathcal{C}_s}\left(\frac{\partial\mathcal{F}(\boldsymbol{r},t)}{\partial t}-\frac{\partial\mathcal{F}_0(\boldsymbol{r},t)}{\partial t}\right)\;\mathrm{tr}[\,\tilde{\boldsymbol{r}}\otimes\tilde{\boldsymbol{r}}\,]\;\mathrm{d}\boldsymbol{r}\;,\end{aligned}\tag{B.27}$$

The first right-hand side term of Eq. (B.27) writes

$$\frac{1}{2}\,k_{_B}\,\dot{T}\,{}^a c_{\mathrm{F}}(t)\int_{\mathcal{C}_s}(P(\boldsymbol{r},t)-P_0(\boldsymbol{r}))\;\mathrm{tr}[\,\tilde{\boldsymbol{r}}\otimes\tilde{\boldsymbol{r}}\,]\;\mathrm{d}\boldsymbol{r}=\frac{1}{2}\,k_{_B}\,\dot{T}\,{}^a c_{\mathrm{F}}(t)\,\mathrm{tr}\,[\,\boldsymbol{\Lambda}-\boldsymbol{1}\,]\;,\tag{B.28}$$

according to definitions (5.4), (5.19) and (5.25).

To perform the second right-hand side term of Eq. (B.27), re-writes

$$\int_{\mathcal{C}_s}\frac{\partial\mathcal{F}(\boldsymbol{r},t)}{\partial t}\mathrm{tr}[\,\tilde{\boldsymbol{r}}\otimes\tilde{\boldsymbol{r}}\,]\;\mathrm{d}\boldsymbol{r}-\int_{\mathcal{C}_s}\frac{\partial\mathcal{F}_0(\boldsymbol{r},t)}{\partial t}\;\mathrm{tr}[\,\tilde{\boldsymbol{r}}\otimes\tilde{\boldsymbol{r}}\,]\;\mathrm{d}\boldsymbol{r}\tag{B.29}$$

Taking advantage from Eq. (5.17), the first integral in (B.29) reads

$$\begin{aligned}\int_{\mathcal{C}_s}\frac{\partial\mathcal{F}(\boldsymbol{r},t)}{\partial t}\mathrm{tr}[\,\tilde{\boldsymbol{r}}\otimes\tilde{\boldsymbol{r}}\,]\;\mathrm{d}\boldsymbol{r}=&\;\xi_a\int_{\mathcal{C}_s}P_0(\boldsymbol{r})\,\mathrm{tr}[\,\tilde{\boldsymbol{r}}\otimes\tilde{\boldsymbol{r}}\,]\;\mathrm{d}\boldsymbol{r}-k_d\,{}^a c_{\mathrm{F}}(t)\int_{\mathcal{C}_s}P(\boldsymbol{r},t)\,\mathrm{tr}[\,\tilde{\boldsymbol{r}}\otimes\tilde{\boldsymbol{r}}\,]\;\mathrm{d}\boldsymbol{r}\\ &-\mathbf{L}:\int_{\mathcal{C}_s}\boldsymbol{\nabla}_{\mathcal{C}_s}[\,\mathcal{F}(\boldsymbol{r},t)\,]\otimes\boldsymbol{r}\;\mathrm{tr}[\,\tilde{\boldsymbol{r}}\otimes\tilde{\boldsymbol{r}}\,]\;\mathrm{d}\boldsymbol{r}\\ &-2\,{}^a c_{\mathrm{F}}(t)\,\mathrm{tr}\,[\,\mathbf{L}\,]\int_{\mathcal{C}_s}P(\boldsymbol{r},t)\,\mathrm{tr}[\,\tilde{\boldsymbol{r}}\otimes\tilde{\boldsymbol{r}}\,]\;\mathrm{d}\boldsymbol{r}\\ =&\;\xi_a\,\mathrm{tr}\,[\,\boldsymbol{1}\,]-k_d\,{}^a c_{\mathrm{F}}(t)\,\mathrm{tr}\,[\,\boldsymbol{\Lambda}\,]-\mathbf{L}:\int_{\mathcal{C}_s}\boldsymbol{\nabla}_{\mathcal{C}_s}[\,\mathcal{F}(\boldsymbol{r},t)\,]\otimes\boldsymbol{r}\;\mathrm{tr}[\,\tilde{\boldsymbol{r}}\otimes\tilde{\boldsymbol{r}}\,]\;\mathrm{d}\boldsymbol{r}\\ &-2\,{}^a c_{\mathrm{F}}(t)\,\mathrm{tr}\,[\,\mathbf{L}\,]\;\mathrm{tr}\,[\,\boldsymbol{\Lambda}\,]\;,\end{aligned}$$

according to Eq.s (5.4) and (5.25). Similarly to what performed in Appendix B.3, by noting that

$$\begin{aligned}-\mathbf{L}:\int_{\mathcal{C}_s}\boldsymbol{\nabla}_{\mathcal{C}_s}[\,\mathcal{F}(\boldsymbol{r},t)\,]\otimes\boldsymbol{r}\;\mathrm{tr}[\,\tilde{\boldsymbol{r}}\otimes\tilde{\boldsymbol{r}}\,]\;\mathrm{d}\boldsymbol{r}=&\;\mathbf{L}:\int_{\mathcal{C}_s}\frac{\partial\mathcal{F}(\boldsymbol{r},t)}{\partial\boldsymbol{r}}\otimes\boldsymbol{r}\;\mathrm{tr}[\,\tilde{\boldsymbol{r}}\otimes\tilde{\boldsymbol{r}}\,]\;\mathrm{d}\boldsymbol{r}\\ =&-\mathbf{L}:\int_{\mathcal{C}_s}\frac{\partial\mathcal{F}(\boldsymbol{r},t)}{\partial\tilde{\boldsymbol{r}}}\otimes\tilde{\boldsymbol{r}}\;\mathrm{tr}[\,\tilde{\boldsymbol{r}}\otimes\tilde{\boldsymbol{r}}\,]\;\mathrm{d}\boldsymbol{r}\end{aligned}$$

integration by parts and recognition that $\mathcal{F}(\boldsymbol{r},t)$ is an even function yields

$$\begin{aligned}\mathrm{L}_{ij}\int_{\mathcal{C}_s}\mathcal{F}(\boldsymbol{r},t)\,\frac{\partial}{\partial\tilde{r}_i}\,\tilde{r}_j\,\tilde{r}_k\,\tilde{r}_k\;\mathrm{d}\boldsymbol{r}=&\,{}^a c_{\mathrm{F}}(t)\,\mathrm{L}_{ij}\int_{\mathcal{C}_s}P(\boldsymbol{r},t)\,(\delta_{ij}\,\tilde{r}_k\,\tilde{r}_k+\tilde{r}_j\,\delta_{ki}\,\tilde{r}_k+\tilde{r}_j\,\tilde{r}_k\,\delta_{ki})\;\mathrm{d}\boldsymbol{r}=\\ =&\,{}^a c_{\mathrm{F}}\,\mathrm{L}_{ij}\delta_{ij}\int_{\mathcal{C}_s}P(\boldsymbol{r},t)\,\tilde{r}_k\,\tilde{r}_k\;\mathrm{d}\boldsymbol{r}+{}^a c_{\mathrm{F}}\,\mathrm{L}_{ij}\int_{\mathcal{C}_s}P(\boldsymbol{r},t)\,\tilde{r}_j\,\tilde{r}_i\;\mathrm{d}\boldsymbol{r}\\ &+{}^a c_{\mathrm{F}}\,\mathrm{L}_{ij}\int_{\mathcal{C}_s}\tilde{r}_j\,\tilde{r}_i\;\mathrm{d}\boldsymbol{r}\\ =&\,{}^a c_{\mathrm{F}}\,\mathrm{L}_{ii}\,\Lambda_{kk}\;+{}^a c_{\mathrm{F}}\,\mathrm{L}_{ij}\,\Lambda_{ji}\;+{}^a c_{\mathrm{F}}\,\mathrm{L}_{ij}\,\Lambda_{ji}\;.\end{aligned}$$

If follows that the first integral in (B.29) writes

$$\int_{\mathcal{C}_s}\frac{\partial\mathcal{F}(\boldsymbol{r},t)}{\partial t}\mathrm{tr}[\,\tilde{\boldsymbol{r}}\otimes\tilde{\boldsymbol{r}}\,]\;\mathrm{d}\boldsymbol{r}=\xi_a\,\mathrm{tr}\,[\,\boldsymbol{1}\,]-k_d\,{}^a c_{\mathrm{F}}(t)\,\mathrm{tr}\,[\,\boldsymbol{\Lambda}\,]-{}^a c_{\mathrm{F}}(t)\,\mathrm{tr}\,[\,\mathbf{L}\,]\;\mathrm{tr}\,[\,\boldsymbol{\Lambda}\,]+2\,{}^a c_{\mathrm{F}}\,\boldsymbol{\Lambda}:\mathbf{L}\;,\tag{B.30}$$

where it has been taken advantage from the symmetry of the distribution teensor to write $\mathrm{L}_{ij}\,\Lambda_{ji} = \mathbf{L} : \boldsymbol{\Lambda}$.

To perform the second integral of (B.29), note that we do not have the evolution law $\partial\mathcal{F}_0(\boldsymbol{r},t)/\partial t$. However, taking advantage from the definition of $\mathcal{F}_0(\boldsymbol{r},t)$ (5.19), it is possible to write

$$\begin{aligned}\int_{\mathcal{C}_s} \frac{\partial \mathcal{F}_0(\boldsymbol{r},t)}{\partial t}\,\mathrm{tr}[\,\tilde{\boldsymbol{r}}\otimes\tilde{\boldsymbol{r}}\,]\,\mathrm{d}\boldsymbol{r} &= \frac{\partial{}^{a}c_{\mathrm{F}}(t)}{\partial t}\int_{\mathcal{C}_s} P_0(\boldsymbol{r})\,\mathrm{tr}[\,\tilde{\boldsymbol{r}}\otimes\tilde{\boldsymbol{r}}\,]\,\mathrm{d}\boldsymbol{r} = \frac{\partial{}^{a}c_{\mathrm{F}}(t)}{\partial t}\,\mathrm{tr}\,[\,\mathbf{1}\,] \\ &= \xi_a\,\mathrm{tr}\,[\,\mathbf{1}\,] - k_d\,{}^{a}c_{\mathrm{F}}(t)\,\mathrm{tr}\,[\,\mathbf{1}\,] - {}^{a}c_{\mathrm{F}}(t)\,\mathrm{tr}\,[\,\mathbf{L}\,]\;\mathrm{tr}\,[\,\mathbf{1}\,]\end{aligned} \tag{B.31}$$

according to Eq. (5.18). Combination of Eq.s (B.29), (B.30) and (B.31) yields

$$\begin{aligned}\int_{\mathcal{C}_s}\left(\frac{\partial\mathcal{F}(\boldsymbol{r},t)}{\partial t} - \frac{\partial\mathcal{F}_0(\boldsymbol{r},t)}{\partial t}\right)\mathrm{tr}[\,\tilde{\boldsymbol{r}}\otimes\tilde{\boldsymbol{r}}\,]\,\mathrm{d}\boldsymbol{r} &= k_d\,{}^{a}c_{\mathrm{F}}(t)\,\mathrm{tr}\,[\,\mathbf{1}-\boldsymbol{\Lambda}\,] + {}^{a}c_{\mathrm{F}}(t)\,\mathrm{tr}\,[\,\mathbf{L}\,]\;\mathrm{tr}\,[\,\mathbf{1}-\boldsymbol{\Lambda}\,] \\ &\quad + 2\,{}^{a}c_{\mathrm{F}}(t)\,\boldsymbol{\Lambda}:\mathbf{L}\,.\end{aligned} \tag{B.32}$$

Therefore, entering Eq.s (B.28) and (B.32) into Eq. (B.27), the time derivative of the network free energy $\Psi^{\mathcal{N}}$ (5.24) finally writes

$$\begin{aligned}\dot{\Psi}^{\mathcal{N}} &= \frac{1}{2}\,k_{B}\,\dot{T}\,{}^{a}c_{\mathrm{F}}\,\mathrm{tr}\,[\,\boldsymbol{\Lambda}-\mathbf{1}\,] + \frac{1}{2}\,k_{B}\,T\,k_d\,{}^{a}c_{\mathrm{F}}\,\mathrm{tr}\,[\,\mathbf{1}-\boldsymbol{\Lambda}\,] + \frac{1}{2}\,k_{B}\,T\,{}^{a}c_{\mathrm{F}}\,\mathrm{tr}\,[\,\mathbf{L}\,]\;\mathrm{tr}\,[\,\mathbf{1}-\boldsymbol{\Lambda}\,] \\ &\quad + k_{B}\,T\,{}^{a}c_{\mathrm{F}}\,\boldsymbol{\Lambda}:\mathbf{L}\,.\end{aligned} \tag{B.33}$$

B.5 Solution of $\dot{\boldsymbol{\Lambda}}$

Let $\mathbf{A}$ denote the following second order tensor $\mathbf{A} = \mathbf{F}^{-1}\boldsymbol{\Lambda}\,\mathbf{F}^{-\mathrm{T}}$. The first order tensorial differential equation

$$\dot{\mathbf{A}} + \frac{\xi_a}{{}^{a}c_{\mathrm{F}}}\,\mathbf{A} = \frac{\xi_a}{{}^{a}c_{\mathrm{F}}}\,\mathbf{F}^{-1}\mathbf{F}^{-\mathrm{T}} \tag{B.34}$$

is therefore an equivalent form of the evolution law for the distribution tensor (5.26). Indeed

$$\dot{\mathbf{A}} = \dot{\mathbf{F}}^{-1}\boldsymbol{\Lambda}\,\mathbf{F}^{-\mathrm{T}} + \mathbf{F}^{-1}\dot{\boldsymbol{\Lambda}}\,\mathbf{F}^{-\mathrm{T}} + \mathbf{F}^{-1}\boldsymbol{\Lambda}\,\dot{\mathbf{F}}^{-\mathrm{T}}\,, \tag{B.35}$$

which allows to re-write Eq. (B.34) as

$$\dot{\mathbf{F}}^{-1}\boldsymbol{\Lambda}\,\mathbf{F}^{-\mathrm{T}} + \mathbf{F}^{-1}\dot{\boldsymbol{\Lambda}}\,\mathbf{F}^{-\mathrm{T}} + \mathbf{F}^{-1}\boldsymbol{\Lambda}\,\dot{\mathbf{F}}^{-\mathrm{T}} + \frac{\xi_a}{{}^{a}c_{\mathrm{F}}}\,\mathbf{F}^{-1}\boldsymbol{\Lambda}\,\mathbf{F}^{-\mathrm{T}} = \frac{\xi_a}{{}^{a}c_{\mathrm{F}}}\,\mathbf{F}^{-1}\mathbf{F}^{-\mathrm{T}}\,. \tag{B.36}$$

Left and right multiplication of Eq. (B.36) by $\mathbf{F}$ and $\mathbf{F}^{\mathrm{T}}$, respectively, yields

$$\begin{aligned}&\mathbf{F}\,\dot{\mathbf{F}}^{-1}\boldsymbol{\Lambda}\,\mathbf{F}^{-\mathrm{T}}\,\mathbf{F}^{\mathrm{T}} + \mathbf{F}\,\mathbf{F}^{-1}\dot{\boldsymbol{\Lambda}}\,\mathbf{F}^{-\mathrm{T}}\,\mathbf{F}^{\mathrm{T}} + \mathbf{F}\,\mathbf{F}^{-1}\boldsymbol{\Lambda}\,\dot{\mathbf{F}}^{-\mathrm{T}}\,\mathbf{F}^{\mathrm{T}} + \frac{\xi_a}{{}^{a}c_{\mathrm{F}}}\,\mathbf{F}\,\mathbf{F}^{-1}\boldsymbol{\Lambda}\,\mathbf{F}^{-\mathrm{T}}\,\mathbf{F}^{\mathrm{T}} \\ &\qquad = \frac{\xi_a}{{}^{a}c_{\mathrm{F}}}\,\mathbf{F}\,\mathbf{F}^{-1}\mathbf{F}^{-\mathrm{T}}\,\mathbf{F}^{\mathrm{T}}\,,\end{aligned} \tag{B.37}$$

whence

$$\mathbf{F}\,\dot{\mathbf{F}}^{-1}\boldsymbol{\Lambda} + \dot{\boldsymbol{\Lambda}} + \boldsymbol{\Lambda}\,\dot{\mathbf{F}}^{-\mathrm{T}}\,\mathbf{F}^{\mathrm{T}} + \frac{\xi_a}{{}^{a}c_{\mathrm{F}}}\,\boldsymbol{\Lambda} = \frac{\xi_a}{{}^{a}c_{\mathrm{F}}}\,\mathbf{1}\,. \tag{B.38}$$

By noting that

$$\begin{aligned}\mathbf{F}\,\dot{\mathbf{F}}^{-1} &= -\dot{\mathbf{F}}\,\mathbf{F}^{-1} = -\mathbf{L}\,, \\ \dot{\mathbf{F}}^{-\mathrm{T}}\mathbf{F}^{\mathrm{T}} &= -\mathbf{F}^{-\mathrm{T}}\dot{\mathbf{F}}^{\mathrm{T}} = -\mathbf{L}^{\mathrm{T}},\end{aligned}$$

Eq. (B.38) can be easily cast in the form

$$\dot{\boldsymbol{\Lambda}} - \mathbf{L}\,\boldsymbol{\Lambda} - (\mathbf{L}\,\boldsymbol{\Lambda})^{\mathrm{T}} + \frac{\xi_a}{{}^{a}c_{\mathrm{F}}}\,\boldsymbol{\Lambda} = \frac{\xi_a}{{}^{a}c_{\mathrm{F}}}\,\mathbf{1}\,, \tag{B.40}$$

whence

$$\dot{\mathbf{\Lambda}} = \frac{\xi_a}{{}^{a}c_{\mathrm{F}}} \left(\mathbf{1} - \mathbf{\Lambda}\right) + \mathbf{L}\,\mathbf{\Lambda} + \left(\mathbf{L}\,\mathbf{\Lambda}\right)^{\mathrm{T}} \;, \tag{B.41}$$

which is equivalent form of the evolution law for the distribution tensor shown in Eq. (5.26).

For $t = 0$, $\mathbf{\Lambda}(t = 0) = \mathbf{\Lambda}_0 = \mathbf{1}$ and $\mathbf{F}(t = 0) = \mathbf{1}$. Accordingly, the general solution of the tensorial differential equation (B.34) writes[1]

$$\mathbf{A} = \exp\left(-\int_0^t \frac{\xi_a}{{}^{a}c_{\mathrm{F}}}\,\mathrm{d}\tau\right)\mathbf{1} + \int_0^t \frac{\xi_a}{{}^{a}c_{\mathrm{F}}}\,\mathbf{F}^{-1}(\tau)\,\mathbf{F}^{-\mathrm{T}}(\tau)\,\exp\left(-\int_0^t \frac{\xi_a}{{}^{a}c_{\mathrm{F}}}(t-\tau)\,\mathrm{d}\tau\right)\mathrm{d}\tau\;, \tag{B.42}$$

whence, the general solution of the distribution tensor, $\mathbf{\Lambda}$, is obtained by performing $\mathbf{F}(t)\,\mathbf{A}\,\mathbf{F}^{\mathrm{T}}(t)$, hence it takes the form

$$\begin{aligned} \mathbf{\Lambda}(t) = {} & \exp\left(-\int_0^t \frac{\xi_a}{{}^{a}c_{\mathrm{F}}}\,\mathrm{d}\tau\right)\mathbf{F}(t)\,\mathbf{F}^{\mathrm{T}}(t) \\ & + \int_0^t \frac{\xi_a}{{}^{a}c_{\mathrm{F}}}\,\mathbf{F}(t)\,\mathbf{F}^{-1}(\tau)\,\mathbf{F}^{-\mathrm{T}}(\tau)\,\mathbf{F}^{\mathrm{T}}(t)\,\exp\left(-\int_0^t \frac{\xi_a}{{}^{a}c_{\mathrm{F}}}(t-\tau)\,\mathrm{d}\tau\right)\mathrm{d}\tau\;. \end{aligned} \tag{B.43}$$

Furthermore, for permanent cross-links ($k_a = k_d = 0$), Eq. (B.43) becomes [117]

$$\mathbf{\Lambda} = \mathbf{F}\,\mathbf{F}^{\mathrm{T}} = \mathbf{B}\;, \tag{B.44}$$

with $\mathbf{B}$ left Cauchy-Green tensor, therefore the framework degenerates to a neo-Hookean model. For density of active chains achieved at the steady state, that is, for ${}^{a}\dot{c}_{\mathrm{F}} = 0$, $\xi_a = k_d\,{}^{a}c_{\mathrm{F}}$, the model degenerates to standard viscoelasticity, and the solution of the chain distribution tensor, $\mathbf{\Lambda}$, writes [117]

$$\mathbf{\Lambda}(t) = \exp\left(-k_d\,t\right)\mathbf{F}(t)\,\mathbf{F}^{\mathrm{T}}(t) + k_d\int_0^t \mathbf{F}(t)\,\mathbf{F}^{-1}(\tau)\,\mathbf{F}^{-\mathrm{T}}(\tau)\,\mathbf{F}^{\mathrm{T}}(t)\,\exp\left(-k_d\left(t-\tau\right)\right)\mathrm{d}\tau\;. \tag{B.45}$$

---

[1] Let $\dot{\mathbf{Y}}(t) + a_0(t)\,\mathbf{Y}(t) = \mathbf{G}(t)$ be a first order tensorial differential equation. Its solution writes

$$\mathbf{Y}(t) = \exp\left(-A(t)\right)\left[\mathbf{Y}_0 + \int_{t_0}^t \mathbf{G}(s)\,\exp\left(A(s)\right)\mathrm{d}s\right]$$

with $A(t) := \int_{t_0}^t a_0(s)\,\mathrm{d}s$.

Chapter 6

A finite strain continuum thermo-mechanical formulation coupled with Cahn-Hilliard theory-based species diffusion and trapping

Matteo Arricca[1,2], Mattia Serpelloni[1,2] and Alberto Salvadori[1,2]

[1]The Mechanobiology Research Center, UNIBS, Italy
[2]Department of Mechanical and Industrial Engineering, University of Brescia, Italy

Abstract. We present a coupled finite strain chemo-thermo-mechanical formulation with trapping and Cahn-Hilliard-type species diffusion for phase segregation. The requirement of an interfacial free energy term to account for the transition zone between the freely diffusive and the segregated phase of species is discussed early on, as well as a straight-forward procedure is shown to design a thermodynamically consistent framework. The trapping processes is modeled by means of a chemical reaction that portrays the conversion of mobile to immobilized species, and vice-versa. Therefore, trapped species are not directly affected by the Cahn-Hilliard theory, as well as the laws of mechanics. Conversely, the Cahn-Hilliard-type species diffusion enters into the mass balance equation for diffusive species by means of a *new* chemical potential that describes the mass flux, properly obtained by augmenting the first law of thermodynamics with a *new* flow of energy that sustains the transition zone. Thermodynamic prescriptions are identified on the basis of the functional dependence of the Helmholtz free energy density, which requires to be a-priori specified. Governing equations, with associated boundary conditions, are derived after constitutive prescriptions for chemical potentials, heat and mass fluxes, chemical kinetics and the generalized heat equation.

6.1 Introduction to the Cahn-Hilliard theory

The classical Cahn-Hilliard (CH) theory [208] is central to material science since it characterizes important qualitative features of two-phase systems, and governs the evolution of an order parameter, such as the density or the concentration of species [208, 209]. It has been therefore widely studied over the years. Applications can be found, for instance, on the early stage of phase-transition (spinodal decomposition) [209, 210], in crystals change of phase and composition [211], and in phase-separating Lithium ion electrode materials [55, 65]. Efforts on such theory have been performed in designing phase-field models for multi-phase mixtures with a mathematically rigorous method, and with investigations on the thermodynamic consistency of the framework, as well as for constraints [212, 213, 214, 215, 216, 217, 55, 218], to cite a few.

As objected by Gurtin in [214], the derivation of the Cahn-Hilliard equations requires an a-priori constitutive specification. Take a volume with composition determined by the concentration c_{L_R} of freely diffusive species L. For an isotropic system of non-uniform composition, the Helmholtz free energy density is required to be described by

$$\psi_R = \psi_R(c_{L_R}, \boldsymbol{\nabla}_R\,[\,c_{L_R}\,]) = \psi_R(c_{L_R}) + \psi_R(\boldsymbol{\nabla}_R\,[\,c_{L_R}\,]) = \psi_R(c_{L_R}) + \varkappa\,|\boldsymbol{\nabla}_R\,[\,c_{L_R}\,]\,|^2\,. \tag{6.1}$$

The term $\psi_R(c_{L_R})$ in Eq. (6.1) represents the free energy of a non equilibrium homogeneous material of composition between two phases [208]; namely, the coarse-grain energy of mixing, a non-convex double-well potential whose wells define the phases [55, 214]. Rather, $\psi_R(\boldsymbol{\nabla}_R\,[\,c_{L_R}\,])$ represents the increase in free energy due to the introduction of a composition gradient, giving rise to surface tension [209]. It is defined as a gradient energy, or interfacial energy, and it aims at characterizing the energy of a flat interface between two co-existing isotropic phases, with different composition, of the species L. The coefficient $\varkappa > 0$ usually depends on temperature T and concentration c_{L_R}, but it is constant for a regular solution [208]. The introduction of $\psi_R(\boldsymbol{\nabla}_R\,[\,c_{L_R}\,])$ may appear controversial from a continuum scale point of view, because of the dimension of the interface, which is related to the width of the interface (probably of the order of few atomic distances). Usefulness of introducing the interfacial energy in a phase-field theory is to avoid *sharp* interfaces with a *jump* in the concentration, therefore allowing to deal with a *smooth* diffusive interface [55, 219].

For theories in which ψ_R has a dependence upon the concentration gradient, the chemical potential μ_L is incompatible with its standard definition. Instead, the chemical potential in the CH theory is defined by the following variational derivative [214, 55]

$$\mu_L = \frac{\delta\psi_R(c_{L_R}, \boldsymbol{\nabla}_R\,[\,c_{L_R}\,])}{\delta c_{L_R}} = \frac{\partial\psi_R(c_{L_R})}{\partial c_{L_R}} - \boldsymbol{\nabla}_R \cdot \left[\, \frac{\partial\psi_R(\boldsymbol{\nabla}\,[\,c_{L_R}\,])}{\partial\boldsymbol{\nabla}_R\,[\,c_{L_R}\,]} \,\right] \,. \tag{6.2}$$

Entering Eq. (6.2) into the *standard* mass balance equation,

$$\dot{c}_{L_R} = -\boldsymbol{\nabla}_R \cdot [\,\boldsymbol{h}_{L_R}\,]\ , \tag{6.3}$$

with the mass flux $\boldsymbol{h}_{L_R}$ constitutively defined via Fick's law by means of a positive definite mobility tensor $\mathbf{M}_L$,

$$\boldsymbol{h}_{L_R} = -\mathbf{M}_L \boldsymbol{\nabla}_R\,[\,\mu_L\,]\ , \tag{6.4}$$

the Cahn-Hilliard equation writes [214]

$$\dot{c}_{L_R} = \mathbf{M}_L\,\boldsymbol{\Delta}_R\,\left[\frac{\delta\psi_R}{\delta c_{L_R}}\right]\ , \tag{6.5}$$

with $\boldsymbol{\Delta}_R$ Laplacian.

The definition of the chemical potential as variational derivative (6.2) represents the standard derivation of the chemical potential provided by the CH theory. Gurtin [213] developed a non-equilibrium thermodynamic formulation for phase transition, and other phenomena involving large concentration gradient. Still Gurtin [214] proposed a straight-forward thermodynamically consistent derivation based on a micro-force balance. Following a virtual power approach [220, 221], Anand [55] introduced macro-force and micro-force balances for the forces associated with the rate-like kinematical descriptors, supplemented with thermodynamically consistent constitutive equations.

We here simply show the introduction of a *new* flow of energy due to species that freely diffuse over and above a transition zone between phases, as presented in [213] for the first time. It has the form

$$\int_{\partial\mathcal{P}_R} \zeta_L(\boldsymbol{n}_R)\,\dot{c}_{L_R}\,\mathrm{d}\mathcal{A} = \int_{\partial\mathcal{P}_R} (\boldsymbol{\zeta}_L\cdot\boldsymbol{n}_R)\,\dot{c}_{L_R}\,\mathrm{d}\mathcal{A}\,, \tag{6.6}$$

where $\zeta_L(\boldsymbol{n}_R)$ represents an external scalar micro-traction that expends power on $\dot{c}_{L_R}$, with $\boldsymbol{\zeta}_L$ internal micro-stress that expends power on $\boldsymbol{\nabla}\,[\,\dot{c}_{L_R}\,]$ [55, 214]. Application of the divergence theorem leads to

$$\int_{\mathcal{P}_R} \boldsymbol{\nabla}_R \cdot [\,\boldsymbol{\zeta}_L\,] + \boldsymbol{\zeta} \cdot \boldsymbol{\nabla}\,[\,\dot{c}_{L_R}\,]\;\mathrm{d}\mathcal{V}\;. \tag{6.7}$$

The introduction of the *new* flow of energy allows to consider the energy necessary to sustain the phase interface surface, thought as a thin transition zone [213], even in the absence of mass transfer. Roughly speaking, the energy necessary to sustain the transition zone should be independent upon the mass transfer, therefore it is not strictly related to the *standard* mass term

$$-\int_{\partial\mathcal{P}_R} \mu_L\,\boldsymbol{h}_{L_R} \cdot \boldsymbol{n}_R\;\mathrm{d}\mathcal{A}\;, \tag{6.8}$$

representing the flow of energy across $\partial\mathcal{P}_R$ due to a mass flux $\boldsymbol{h}_{L_R}$ of species L.

Coupling of Eq. (6.6) with Eq. (6.8) in a thermodynamic framework allows the derivation of the chemical potential (6.2) and the Cahn-Hilliard equation (6.5) in a thermodynamic consistent way.

Boundary conditions associated with a Cahn-Hilliard-type diffusion problem have usually the form [213]

$$\boldsymbol{\zeta}_L \cdot \boldsymbol{n}_R = 0\;, \qquad \boldsymbol{h}_{L_R} \cdot \boldsymbol{n}_R = 0\;, \qquad \text{on}\quad \partial\mathcal{P}_R \tag{6.9}$$

for isolated boundary, and

$$\mu_L = \overline{\mu}_L\;, \qquad c_{L_R} = \overline{c}_{L_R}\;, \qquad \text{on}\quad \partial\mathcal{P}_R \tag{6.10}$$

with $\overline{\mu}_L$ and $\overline{c}_{L_R}$ constant values, for uniform boundary.

The problem of the boundary conditions associated with the models derived from the constitutive equations proposed by Gurtin was analyzed in [215]. The CH equation is associated with either periodic or Neumann boundary conditions. Periodic boundary conditions are consistent and the models are still conservation laws [222, 223], whereas it is no longer the general case when considering Neumann boundary conditions [224] especially if the effects of deformations are taken into account [215].

After having introduced the basics of the CH theory and of a straight-forward procedure to design a thermodynamic consistent framework that accounts for CH-type diffusion, the rest of the manuscript is organized as follows. Section 7.2 provides some standard definitions to facilitate the exposition of the Lagnangian formulation of the framework. Mass balance equations and the laws of continuum mechanics are introduced in Section 6.3. Section 6.4 presents the two principles of thermodynamics, accounting for the *new* flow of energy introduced in Eq. (6.6), and deriving thermodynamic prescriptions according to the method of Coleman and Noll [8], and under the assumption of Curie's symmetry principles. The constitutive theory, based on an additive decomposition of the Helmholtz free energy density, is shown and discussed in Section 6.5, and provides consistent phenomenological specifications for mechanical stress tensor, chemical potentials, heat and mass fluxes. Chemical kinetics in Section 6.6 and governing equations in Section 6.7 complete the manuscript.

6.2 Definitions

6.2.1 Motion and deformation gradient

Denote with $\mathcal{B}_t \in \mathbb{R}^3$ the spatial description of an advecting body volume and with $\partial\mathcal{B}_t$ its surface. Let $\mathcal{B}_R$ and $\partial\mathcal{B}_R$ be their referential (material) counterparts, as standard in the finite strain theory in continuum mechanics [53, 54]. The transformation of a material point $\boldsymbol{X} \in \mathcal{B}_R$ into a spatial point $\boldsymbol{x} \in \mathcal{B}_t$ is described by means of a smooth function $\boldsymbol{\chi}(\boldsymbol{X}, t)$

$$\boldsymbol{x} = \boldsymbol{\chi}(\boldsymbol{X}, t)\;,$$

with $\boldsymbol{\chi}(\boldsymbol{X},t)$ one-to-one map representing the motion of $\boldsymbol{X} \in \mathcal{B}_{_R}$ at time t. We assume that $\mathcal{B}_t$ at $t=0$ coincides with $\mathcal{B}_{_R}$, *i.e.*, for all material points $\boldsymbol{X} = \boldsymbol{\chi}(\boldsymbol{X},0)$. The material velocity is given by $\dot{\boldsymbol{\chi}}(\boldsymbol{X},t)$, whereas displacements write as $\boldsymbol{u} = \boldsymbol{\chi} - \boldsymbol{X}$.

At a fixed time t, we name

$$\mathbf{F} = \boldsymbol{\nabla}_{_R} \left[\boldsymbol{\chi}(\boldsymbol{X},t) \right] \, , \tag{6.11}$$

the deformation gradient, *i.e.*, $\mathrm{F}_{ij} = \partial x_i / \partial X_j$. Only motions such that $J = \det[\,\mathbf{F}\,] > 0$ are admissible, in order to avoid total material compaction.

6.2.2 Transformation rules

Denote with $\mathcal{P}_t \subset \mathcal{B}_t$ an arbitrary volume region, with surface $\partial\mathcal{P}_t \subset \partial\mathcal{B}_t$, and let $\mathcal{P}_{_R} \subset \mathcal{B}_{_R}$ and $\partial\mathcal{P}_{_R} \subset \partial\mathcal{B}_{_R}$ define their respective material descriptions. Take a generic tensorial function of any order $f^{\mathcal{V}}(\boldsymbol{x},t) \in \mathcal{P}_t$, and its material description $f^{\mathcal{V}}_{_R}(\boldsymbol{X},t) \in \mathcal{P}_{_R}$. According to the Nanson's formula for volume changes, $\mathrm{d}v = J(\boldsymbol{X},t)\,\mathrm{d}V$, the following transformation rule applies

$$f^{\mathcal{V}}_{_R}(\boldsymbol{X},t) = J(\boldsymbol{X},t)\, f^{\mathcal{V}}(\boldsymbol{x}(\boldsymbol{X},t),t) \, . \tag{6.12}$$

Let $\boldsymbol{f}^{\mathcal{S}}(\boldsymbol{x},t)$ be a spatial vector, with $\boldsymbol{x} \in \partial\mathcal{P}_t$ and $\partial\mathcal{P}_t$ oriented surface defined by the direction of the outward normal vector $\boldsymbol{n}$. Denote with $\boldsymbol{f}^{\mathcal{S}}_{_R}(\boldsymbol{X},t)$ its referential counterpart, with $\boldsymbol{X} \in \partial\mathcal{P}_{_R}$ and $\boldsymbol{n}_{_R}$ outward normal vector to the oriented surface $\partial\mathcal{P}_{_R}$. According to the Nanson's formula for area changes, $\boldsymbol{n}\,\mathrm{d}a = J\,\mathbf{F}^{-\mathrm{T}}\,\boldsymbol{n}_{_R}\mathrm{d}\mathcal{A}$, the material vector $\boldsymbol{f}_{_R}$ transforms according to

$$\boldsymbol{f}^{\mathcal{S}}_{_R}(\boldsymbol{X},t) = J(\boldsymbol{X},t)\,\mathbf{F}^{-1}(\boldsymbol{X},t)\,\boldsymbol{f}^{\mathcal{S}}(\boldsymbol{x}(\boldsymbol{X},t),t) \, . \tag{6.13}$$

6.3 Balance laws

The phase change of species is modeled as a trapping process by means of a one-component two-phases chemical reaction. The mass transport of species have only an interstitial lattice contribution [50, 56], meaning that freely diffusive species L, in an ideal lattice hosting network H, once trapped in isolated trap sites, are converted in trapped species T and stay immobilized. This assumption [9, 10] arises form the consideration of *non-continuous* path for diffusive species. Only saturable and reversible isolated trap sites are therefore considered.

With reference to the terminology introduced in Section 6.1, it is perhaps worth to clarify that we model the *change* of *phase* from free L to trapped T, and vice-versa, by means of the aforementioned chemical reaction. Rather, the two *co-existing phases* provided by the CH theory to account for *phase-segregation* are merely referred to the freely diffusive species L. No chemical reaction therefore occurs within the phase-segregation process. Furthermore, being the hosting material modeled as a regular lattice network, phase-segregation is meaningless for trapped species T.

6.3.1 Mass balance

Consider a generic species α at a point $\boldsymbol{X} \in \mathcal{P}_{_R}$, with $\alpha = L, T$. Within the hosting material H, the change of phase from freely mobile to trapped species, and vice-versa, is described via the following chemical reaction

$$\mathrm{H}_L \underset{k^-_{_R}}{\overset{k^+_{_R}}{\rightleftarrows}} \mathrm{H}_T \, , \tag{6.14}$$

where $k^+_{_R}$ represent the referential positive rate factors for the forward reaction, yielding trapped species, and $k^-_{_R}$ stands for the backward reaction, yielding free species.

Let $w^{(6.14)}_{_R}$ denotes the reaction rate of Eq. (6.14), and $s_{\alpha R}$ a source term representing mass production or consumption (moles per unit reference volume per unit time). The referential form of the mass balance equation, written in terms of concentration of species c_{α_R}, has the form

$$\overset{\cdot}{\overline{\int_{\mathcal{P}_R} c_{\alpha_R}(\boldsymbol{X},t)\,\mathrm{d}\mathcal{V}}} + \int_{\partial\mathcal{P}_R} \boldsymbol{h}_{\alpha_R}(\boldsymbol{X},t)\cdot\boldsymbol{n}_R\,\mathrm{d}\mathcal{A} \pm \int_{\mathcal{P}_R} w_R^{(6.14)}(\boldsymbol{X},t)\,\mathrm{d}\mathcal{V} = \int_{\mathcal{P}_R} s_{\alpha_R}\,\mathrm{d}\mathcal{V}\,. \tag{6.15}$$

After application of the divergence theorem, and recognition that the resultant integrals must hold for any arbitrary region $\mathcal{P}_R \subset \mathcal{B}_R$, Eq. (6.15) specifies for species L and T as

$$\dot{c}_{L_R} + \boldsymbol{\nabla}_R\cdot[\,\boldsymbol{h}_{L_R}\,] + w_R^{(6.14)} = s_{L_R}\,, \tag{6.16a}$$

$$\dot{c}_{T_R} - w_R^{(6.14)} = s_{T_R}\,, \tag{6.16b}$$

where $\boldsymbol{h}_{T_R} = \boldsymbol{0}$ for the assumption of immobilized trapped species.

The terms c_{α_R}, $w_R^{(6.14)}$, and s_{α_R}, being defined over a volume, transform according to Eq. (7.3), namely

$$c_{\alpha_R}(\boldsymbol{X},t) = J\,c_\alpha\,, \qquad w_R^{(6.14)}(\boldsymbol{X},t) = J\,w^{(6.14)} \qquad s_{\alpha_R}(\boldsymbol{X},t) = J\,s_\alpha\,, \tag{6.17}$$

whereas the mass flux $\boldsymbol{h}_{L_R}$ follows the rule stated by Eq. (7.6),

$$\boldsymbol{h}_{L_R}(\boldsymbol{X},t) = J\,\mathbf{F}^{-1}\,\boldsymbol{h}_L\,. \tag{6.18}$$

6.3.2 Balance of linear and angular momentum

We define the current surface traction $\boldsymbol{t}$ and the referential surface traction $\boldsymbol{t}_R$ as

$$\boldsymbol{t}(\boldsymbol{x},t) = \mathbf{T}\,\boldsymbol{n}\,, \qquad \boldsymbol{t}_R(\boldsymbol{X},t) = \mathbf{T}_R\,\boldsymbol{n}_R\,, \tag{6.19}$$

respectively, with $\mathbf{T}$ Cauchy stress tensor and $\mathbf{T}_R$ nominal (first Piola-Kirchhoff) stress tensor. It holds

$$\int_{\partial\mathcal{P}_t} \boldsymbol{t}(\boldsymbol{x},t)\,\mathrm{d}a = \int_{\partial\mathcal{P}_R} \boldsymbol{t}_R(\boldsymbol{X},t)\,\mathrm{d}\mathcal{A}\,, \tag{6.20}$$

whence, by means the Nanson's formula for the transformation of areas, the following definition of the nominal stress yields

$$\mathbf{T}_R = J\,\mathbf{T}\,\mathbf{F}^{-\mathrm{T}}\,. \tag{6.21}$$

The assumption of negligible inertia body forces implies that the balance of linear momentum takes the form

$$\int_{\partial\mathcal{P}_R} \boldsymbol{t}_R\,\mathrm{d}\mathcal{A} + \int_{\mathcal{P}_R} \boldsymbol{b}_{0_R}\,\mathrm{d}\mathcal{V} = \boldsymbol{0}\,. \tag{6.22}$$

with $\boldsymbol{b}_{0_R}$ referential conventional body force, not encompassing the inertial force. According to Eq. $(6.19)_2$, the local balance of linear momentum has the standard form

$$\boldsymbol{\nabla}_R\cdot[\,\mathbf{T}_R\,] + \boldsymbol{b}_{0_R} = \boldsymbol{0}\,, \tag{6.23}$$

with $\boldsymbol{\nabla}_R\cdot[\,\mathbf{T}_R\,] = \partial\,\mathrm{T}_{R\,ij}/\partial X_j$.

The referential form of the balance of angular momentum writes as

$$\int_{\partial\mathcal{P}_R} \boldsymbol{\chi}\times\boldsymbol{t}_R\,\mathrm{d}\mathcal{A} + \int_{\mathcal{P}_R} \boldsymbol{\chi}\times\boldsymbol{b}_{0_R}\,\mathrm{d}\mathcal{V} = \boldsymbol{0}\,, \tag{6.24}$$

whence

$$\mathbf{T}_R\mathbf{F}^{\mathrm{T}} = \mathbf{F}\,\mathbf{T}_R^{\mathrm{T}}\,. \tag{6.25}$$

6.4 Thermodynamics

6.4.1 Energy balance

For the problem at hand, the first law of thermodynamics provides the variation of the internal energy of $\mathcal{P}_R$ as the sum of the power expended by external micro- and macro- forces on $\mathcal{P}_R$, the heat transferred in $\mathcal{P}_R$, and the power due to mass exchanged on $\mathcal{P}_R$. Furthermore, the assumption of negligible inertial force implies no kinetic energy in the energy balance. It holds

$$\begin{aligned}\int_{\mathcal{P}_R} \dot{u}_R \, \mathrm{d}\mathcal{V} = &\int_{\partial\mathcal{P}_R} \boldsymbol{t}_R \cdot \dot{\boldsymbol{\chi}} \, \mathrm{d}\mathcal{A} + \int_{\mathcal{P}_R} \boldsymbol{b}_{0R} \cdot \dot{\boldsymbol{\chi}} \, \mathrm{d}\mathcal{V} + \int_{\partial\mathcal{P}_R} \zeta_L(\boldsymbol{n}_R) \, \dot{c}_{LR} \, \mathrm{d}\mathcal{A} + \int_{\mathcal{P}_R} s_{qR} \, \mathrm{d}\mathcal{V} \\ &- \int_{\partial\mathcal{P}_R} \boldsymbol{q}_R \cdot \boldsymbol{n}_R \, \mathrm{d}\mathcal{A} + \int_{\mathcal{P}_R} {}^{u}\mu_L \, s_{LR} + {}^{u}\mu_T \, s_{TR} \, \mathrm{d}\mathcal{V} - \int_{\partial\mathcal{P}_R} {}^{u}\mu_L \, \boldsymbol{h}_{LR} \cdot \boldsymbol{n}_R \, \mathrm{d}\mathcal{A} \, .\end{aligned} \tag{6.26}$$

Terms in Eq. (6.26) have the following meaning. The left hand-side integral represents the variation of the net internal energy, with u_R specific internal energy. The mechanical external power is described by the macro-forces $\boldsymbol{t}_R$ and $\boldsymbol{b}_{0R}$, defined in Section 6.3.2, which expend power on $\dot{\boldsymbol{\chi}}$, and by the external scalar micro-traction $\zeta_L(\boldsymbol{n}_R)$ that expends power on $\dot{c}_{LR}$, as explained in Section 6.1. The power due to heat transferred in $\mathcal{P}_R$ is described by the heat supplied by external agencies s_{qR} and the heat flux vector $\boldsymbol{q}_R$ across $\partial\mathcal{P}_R$. The last two integrals account for the power due to mass transferred, with ${}^{u}\mu_L$ and ${}^{u}\mu_T$ energy provided by a unit supply of moles of species L and T, and with s_{LR}, s_{TR}, $\boldsymbol{h}_{LR}$ as defined in Section 6.3.1.

Making use of the definition of referential surface traction $(6.19)_2$, the balance of linear momentum (6.23), and the mass balance equations (6.16), taking advantage from Eq.s (6.6) and (6.7), and after application of the divergence theorem, simple algebra leads to the following localized form of the referential energy balance (details can be found in [10])

$$\begin{aligned}\dot{u}_R = &\, \mathbf{T}_R : \dot{\mathbf{F}} + s_{qR} - \boldsymbol{\nabla}_R \cdot \left[\boldsymbol{q}_R \right] + ({}^{u}\mu_L + \boldsymbol{\nabla}_R \cdot [\, \boldsymbol{\zeta}_L \,]) \, \dot{c}_{LR} + {}^{u}\mu_T \, \dot{c}_{TR} - \boldsymbol{\nabla}_R \, [\, {}^{u}\mu_L \,] \cdot \boldsymbol{h}_{LR} \\ &+ \boldsymbol{\nabla}_R \, [\, \dot{c}_{LR} \,] \cdot \boldsymbol{\zeta}_L - ({}^{u}\mu_L - {}^{u}\mu_T) \, w_R^{(6.14)} \, ,\end{aligned} \tag{6.27}$$

with $\mathbf{T}_R$ defined by Eq. (6.21), $\dot{\mathbf{F}} = \boldsymbol{\nabla}_R \, [\, \dot{\boldsymbol{\chi}} \,] = \dot{\mathrm{F}}_{ij}$, and $\mathbf{T}_R : \dot{\mathbf{F}} = \mathrm{T}_{R\,ij} \, \dot{\mathrm{F}}_{ij}$.

6.4.2 Entropy imbalance

By assuming that the mechanics does not contribute directly to the total entropy flow [54, 51], the second law of thermodynamics for the problem at hand is defined by the contributions of the internal entropy of $\mathcal{P}_R$ and the entropy transferred in $\mathcal{P}_R$ due to the heat transferred in $\mathcal{P}_R$ and the mass exchanged on $\mathcal{P}_R$. According to the statement of the second law of thermodynamics by which the entropy produced inside $\mathcal{P}_R$ is greater or equal to zero, the entropy imbalance writes as

$$\begin{aligned}\int_{\mathcal{P}_R} \dot{\eta}_R \, \mathrm{d}\mathcal{V} - \int_{\mathcal{P}_R} \frac{1}{T} \, s_{qR} \, \mathrm{d}\mathcal{V} + \int_{\partial\mathcal{P}_R} \frac{1}{T} \, \boldsymbol{q}_R \cdot \boldsymbol{n}_R \, \mathrm{d}\mathcal{A} - \int_{\mathcal{P}_R} {}^{\eta}\mu_L \, s_{LR} + {}^{\eta}\mu_T \, s_{TR} \, \mathrm{d}\mathcal{V} \\ + \int_{\partial\mathcal{P}_R} {}^{\eta}\mu_L \, \boldsymbol{h}_{LR} \cdot \boldsymbol{n}_R \, \mathrm{d}\mathcal{A} \geq 0 \, .\end{aligned} \tag{6.28}$$

The first term of Eq. (6.28) represents the ratio of the the net internal entropy of $\mathcal{P}_R$, with η_R specific net internal entropy (per unit reference volume). The entropy per unit time due to the heat transfer is defined by the heat source s_{qR} and the heat flux $\boldsymbol{q}_R$, divided by the temperature T. The entropy per unit time due to mass transfer has the same form of the power due to mass transferred in the energy balance (6.26), where ${}^{\eta}\mu_\alpha$ is the change in specific entropy provided by a unit supply of moles of free and trapped species.

After application of the divergence theorem, multiplication by the temperature T, and taking advantage from mass balance equations (6.16), the referential entropy imbalance (6.28) can be localized in the form (see [10] for details)

$$\begin{aligned} & T\,\dot{\eta}_{R} - s_{q_R} + \boldsymbol{\nabla}_{R} \cdot \left[\, \boldsymbol{q}_{R} \,\right] - \frac{1}{T}\, \boldsymbol{q}_{R} \cdot \boldsymbol{\nabla}_{R}\, [\, T\,] - T\, {}^{\eta}\!\mu_L\, \dot{c}_{L_R} - T\, {}^{\eta}\!\mu_T\, \dot{c}_{T_R} + T\, \boldsymbol{\nabla}_{R}\, [\, {}^{\eta}\!\mu_L\,] \cdot \boldsymbol{h}_{L_R} \\ & \qquad - T\, \left({}^{\eta}\!\mu_L - {}^{\eta}\!\mu_T \right) w_{R}^{(6.14)} \geq 0\ . \end{aligned} \tag{6.29}$$

As standards, the entropy imbalance (6.29) can be re-phrased in terms of internal energy by substituting the term $-s_{q_R} + \boldsymbol{\nabla}_{R} \cdot \left[\, \boldsymbol{q}_{R} \,\right]$ by means of the energy balance (6.27). Denoting with [9, 10]

$$\mu_\alpha = {}^{u}\!\mu_\alpha - T\, {}^{\eta}\!\mu_\alpha\ , \qquad A^{(6.14)} = \mu_T - \mu_L\ , \tag{6.30}$$

the Clausius-Duhem inequality arises in the following form

$$\begin{aligned} & T\,\dot{\eta}_{R} - \dot{u}_{R} + \mathbf{T}_{R} : \dot{\mathbf{F}} - \frac{1}{T}\, \boldsymbol{q}_{R} \cdot \boldsymbol{\nabla}_{R}\, [\, T\,] + \left(\mu_L + \boldsymbol{\nabla}_{R} \cdot [\, \boldsymbol{\zeta}_L\,]\right) \dot{c}_{L_R} + \mu_T\, \dot{c}_{T_R} + \boldsymbol{\zeta}_L \cdot \boldsymbol{\nabla}_{R}\, [\, \dot{c}_{L_R}\,] \\ & \qquad - \boldsymbol{h}_{L_R} \cdot \left(\boldsymbol{\nabla}_{R}\, [\, \mu_L\,] + {}^{\eta}\!\mu_L\, \boldsymbol{\nabla}_{R}\, [\, T\,] \right) - A^{(6.14)}\, w_{R}^{(6.14)} \geq 0\ . \end{aligned} \tag{6.31}$$

As usually performed in finite strain continuum mechanics, the mechanical contribution $\mathbf{T}_{R} : \dot{\mathbf{F}}$ can be re-written in terms of the second Piola-Kirchhoff stress tensor $\mathbf{S}$ and the right Cauchy-Green strain tensor $\mathbf{C}$. According to the relations

$$\mathbf{T}_{R} = \mathbf{F}\, \mathbf{S}\, , \qquad \mathbf{C} = \mathbf{F}^{\mathrm{T}}\, \mathbf{F}\ , \tag{6.32}$$

and taking advantage from the symmetry of the Cauchy stress $\mathbf{T}$, which implies the symmetry of $\mathbf{S}$, it holds

$$\mathbf{T}_{R} : \dot{\mathbf{F}} = \frac{1}{2}\, \mathbf{S} : \dot{\mathbf{C}}\ . \tag{6.33}$$

6.4.3 Clausius-Duhem inequality

We select the Helmholtz free energy density (per unit referential volume),

$$\psi_{R} = u_{R} - T\, \eta_{R}\ , \tag{6.34}$$

as thermodynamic potential.

Taking advantage from the time derivative of ψ_{R} to re-write the first two terms of Eq. (6.31), and in accordance with Eq. (6.33), the localized referential second law of thermodynamics (6.31) can be cast in the form

$$\begin{aligned} & -\dot{\psi}_{R} - \dot{T}\, \eta_{R} - \frac{1}{T}\, \boldsymbol{q}_{R} \cdot \boldsymbol{\nabla}_{R}\, [\, T\,] + \frac{1}{2}\, \mathbf{S} : \dot{\mathbf{C}} + \left(\mu_L + \boldsymbol{\nabla}_{R} \cdot [\, \boldsymbol{\zeta}\,]\right) \dot{c}_{L_R} + \mu_T\, \dot{c}_{T_R} + \boldsymbol{\zeta}_L \cdot \boldsymbol{\nabla}_{R}\, [\, \dot{c}_{L_R}\,] \\ & \qquad - \boldsymbol{h}_{L_R} \cdot \left(\boldsymbol{\nabla}_{R}\, [\, \mu_L\,] + {}^{\eta}\!\mu_L\, \boldsymbol{\nabla}_{R}\, [\, T\,] \right) - A^{(6.14)}\, w_{R}^{(6.14)} \geq 0\ . \end{aligned} \tag{6.35}$$

We take the Helmholtz free energy density as a function of temperature T, concentrations of species c_{L_R} and c_{T_R}, concentration gradient $\boldsymbol{\nabla}_{R}\, [\, c_{L_R}\,]$ according to the Cahn-Hilliard theory [208], right Cauchy-Green strain tensor $\mathbf{C}$, and of some kinematic tensorial internal strain variable $\boldsymbol{\Xi}$ that compare with the usual meaning in inelastic constitutive laws [53, 54, 58, 59, 60, 61]. Therefore

$$\psi_{R} = \psi_{R}\left(T, c_{L_R}, c_{T_R}, \boldsymbol{\nabla}_{R}\, [\, c_{L_R}\,], \mathbf{C}, \boldsymbol{\Xi}\right)\ . \tag{6.36}$$

In view of its selected functional dependence, the time derivative of ψ_{R} writes as

$$\dot{\psi}_{R} = \frac{\partial \psi_{R}}{\partial T}\, \dot{T} + \frac{\partial \psi_{R}}{\partial c_{L_R}}\, \dot{c}_{L_R} + \frac{\partial \psi_{R}}{\partial c_{T_R}}\, \dot{c}_{T_R} + \frac{\partial \psi_{R}}{\partial \boldsymbol{\nabla}_{R}\, [\, c_{L_R}\,]} \cdot \boldsymbol{\nabla}_{R}\, [\, \dot{c}_{L_R}\,] + \frac{\partial \psi_{R}}{\partial \mathbf{C}} : \dot{\mathbf{C}} + \frac{\partial \psi_{R}}{\partial \boldsymbol{\Xi}} : \dot{\boldsymbol{\Xi}}\ . \tag{6.37}$$

By denoting the plastic internal stress tensor conjugate to $\boldsymbol{\Xi}$ with

$$\mathbf{X}\!\!\!| = -\frac{\partial \psi_{_R}}{\partial \boldsymbol{\Xi}} \ , \tag{6.38}$$

combination of Eq.s (6.35), (6.37) and (6.38) leads to write the Clausius-Duhem inequality in the from

$$\begin{aligned} &\left(\frac{1}{2}\, \mathbf{S} - \frac{\partial \psi_{_R}}{\partial \mathbf{C}} \right) : \dot{\mathbf{C}} - \left(\eta_{_R} + \frac{\partial \psi_{_R}}{\partial T} \right) \dot{T} + \left(\mu_L + \boldsymbol{\nabla}_{_R} \cdot [\, \boldsymbol{\zeta}_L \,] - \frac{\partial \psi_{_R}}{\partial c_{L_R}} \right) \dot{c}_{L_R} + \left(\mu_T - \frac{\partial \psi_{_R}}{\partial c_{T_R}} \right) \dot{c}_{L_R} \\ &+ \left(\boldsymbol{\zeta}_L - \frac{\partial \psi_{_R}}{\partial \boldsymbol{\nabla}_{_R} [\, c_{L_R} \,]} \right) \cdot \boldsymbol{\nabla}_{_R} [\, \dot{c}_{L_R} \,] + \mathbf{X}\!\!\!| : \dot{\boldsymbol{\Xi}} - \frac{1}{T}\, \boldsymbol{q}_{_R} \cdot \boldsymbol{\nabla}_{_R} [\, T \,] - \boldsymbol{h}_{L_R} \cdot (\, \boldsymbol{\nabla}_{_R} [\, \mu_L \,] + {}^{\eta}\mu_L \, \boldsymbol{\nabla}_{_R} [\, T \,] \,) \\ &- A^{(6.14)} \, w_{_R}^{(6.14)} \geq 0 \ . \end{aligned} \tag{6.39}$$

According to the method of Coleman and Noll [8], inequality (6.39) must hold for any value of the time derivative of $\mathbf{C}$, c_{L_R} and c_{T_R}, $\boldsymbol{\nabla}_{_R} [\, c_{L_R} \,]$, and T. The following thermodynamic restrictions thus hold

$$\mathbf{S} = 2\, \frac{\partial \psi_{_R}}{\partial \mathbf{C}} \ , \tag{6.40a}$$

$$\eta_{_R} = \frac{\partial \psi_{_R}}{\partial T} \ , \tag{6.40b}$$

$$\mu_L + \boldsymbol{\nabla}_{_R} \cdot [\, \boldsymbol{\zeta}_L \,] = \frac{\partial \psi_{_R}}{\partial c_{L_R}} \ , \tag{6.40c}$$

$$\mu_T = \frac{\partial \psi_{_R}}{\partial c_{T_R}} \ , \tag{6.40d}$$

$$\boldsymbol{\zeta}_L = \frac{\partial \psi_{_R}}{\partial \boldsymbol{\nabla}_{_R} [\, c_{L_R} \,]} \ . \tag{6.40e}$$

What remains of inequality (6.39),

$$\mathbf{X}\!\!\!| : \dot{\boldsymbol{\Xi}} - \boldsymbol{h}_{L_R} \cdot (\, \boldsymbol{\nabla}_{_R} [\, \mu_L \,] + {}^{\eta}\mu_L \, \boldsymbol{\nabla}_{_R} [\, T \,] \,) - \frac{1}{T}\, \boldsymbol{q}_{_R} \cdot \boldsymbol{\nabla}_{_R} [\, T \,] - A^{(6.14)} \, w_{_R}^{(6.14)} \geq 0 \ , \tag{6.41}$$

determines restrictions on the values that $\mathbf{X}\!\!\!|$, $\boldsymbol{h}_{L_R}$, $\boldsymbol{q}_{_R}$ and $A^{(6.14)}$ can assume.

No coupling between fluxes and thermodynamic forces of different tensorial order is sated by means of the assumption of Curie's symmetry principles [51], therefore the following three conditions arise

$$\mathbf{X}\!\!\!| : \dot{\boldsymbol{\Xi}} \geq 0 \ , \tag{6.42a}$$

$$\boldsymbol{h}_{L_R} \cdot (\, \boldsymbol{\nabla}_{_R} [\, \mu_L \,] + {}^{\eta}\mu_L \, \boldsymbol{\nabla}_{_R} [\, T \,] \,) + \frac{1}{T}\, \boldsymbol{q}_{_R} \cdot \boldsymbol{\nabla}_{_R} [\, T \,] \leq 0 \ , \tag{6.42b}$$

$$A^{(6.14)} \, w_{_R}^{(6.14)} \leq 0 \ . \tag{6.42c}$$

Inequalities (6.42a), (6.42b) and (6.42c) represent the inelastic, the thermo-diffusive, and the chemical contribution to the internal entropy production (6.41), respectively.

Remark. In view of thermodynamic restrictions (6.40c), (6.40e), the following definition of *new* chemical potential for free diffusive species arises

$$\mu_L = \frac{\partial \psi_{_R}}{\partial c_{L_R}} - \boldsymbol{\nabla}_{_R} \cdot \left[\frac{\partial \psi_{_R}}{\partial \boldsymbol{\nabla}_{_R} [\, c_{L_R} \,]} \right] \ ,$$

in accordance with definition (6.2), whereas for trapped species T the chemical potential has the *standard* definition, as Eq. (6.40d) shows. Lastly, prescription (6.42c) defines $A^{(6.14)}$ as the affinity of the chemical reaction (6.14).

6.4.4 Specifications for ${}^{u}\mu_{\alpha}$ and ${}^{\eta}\mu_{\alpha}$

The internal micro-stress $\boldsymbol{\zeta}_L$ writes as

$$\boldsymbol{\zeta}_L = \frac{\partial \psi_R}{\partial \boldsymbol{\nabla}_R \left[c_{L_R} \right]} = \frac{\partial u_R}{\partial \boldsymbol{\nabla}_R \left[c_{L_R} \right]} + \frac{\partial u_R}{\partial \eta_R} \frac{\partial \eta_R}{\partial \boldsymbol{\nabla}_R \left[c_{L_R} \right]} - T \frac{\partial \eta_R}{\boldsymbol{\nabla}_R \left[c_{L_R} \right]} = \frac{\partial u_R}{\partial \boldsymbol{\nabla}_R \left[c_{L_R} \right]} \,, \tag{6.43}$$

according to Eq. (6.34), whence

$$\mu_L = \frac{\partial \psi_R}{\partial c_{L_R}} - \boldsymbol{\nabla}_R \cdot \left[\frac{\partial \psi_R}{\partial \boldsymbol{\nabla}_R \left[c_{L_R} \right]} \right] = \frac{\partial u_R}{\partial c_{L_R}} - \boldsymbol{\nabla}_R \cdot \left[\frac{\partial \psi_R}{\partial \boldsymbol{\nabla}_R \left[c_{L_R} \right]} \right] \,, \tag{6.44}$$

where it has been used the fact that $\partial u_R / \partial \eta_R = T$.

The term ${}^{\eta}\mu_L$ is computed as [9, 10]

$${}^{\eta}\mu_L = \frac{\partial \eta_R}{\partial c_{L_R}} = -\frac{\partial}{\partial c_{L_R}} \frac{\partial \psi_R}{\partial T} = -\frac{\partial \mu_L}{\partial T} \,, \tag{6.45}$$

consistent with definition $(6.30)_1$, whence

$$\begin{aligned} {}^{u}\mu_L &= \frac{\partial u_R}{\partial c_{L_R}} + \frac{\partial u_R}{\partial \eta_R} \frac{\partial \eta_R}{\partial c_{L_R}} - T \frac{\partial \eta_R}{\partial c_{L_R}} - \boldsymbol{\nabla}_R \cdot \left[\frac{\partial u_R}{\partial \boldsymbol{\nabla}_R \left[c_{L_R} \right]} \right] + T \frac{\partial \eta_R}{\partial c_{L_R}} \\ &= \frac{\mathrm{d} u_R}{\mathrm{d} c_{L_R}} - \boldsymbol{\nabla}_R \cdot \left[\frac{\partial u_R}{\partial \boldsymbol{\nabla}_R \left[c_{L_R} \right]} \right] \,. \end{aligned} \tag{6.46}$$

The following specifications for ${}^{\eta}\mu_L$ and ${}^{u}\mu_L$ therefore arise

$${}^{\eta}\mu_L = -\frac{\partial^2 \psi_R}{\partial T \, \partial c_{L_R}} \,, \tag{6.47a}$$

$${}^{u}\mu_L = \frac{\partial \psi_R}{\partial c_{L_R}} - T \frac{\partial^2 \psi_R}{\partial T \, \partial c_{L_R}} - \boldsymbol{\nabla}_R \cdot \left[\frac{\partial \psi_R}{\partial \boldsymbol{\nabla}_R \left[c_{L_R} \right]} \right] \,. \tag{6.47b}$$

Being the chemical potential of trapped species μ_T defined as the partial derivative of ψ_R with respect to c_{T_R}, as standard, specifications for ${}^{\eta}\mu_T$ and ${}^{u}\mu_T$ have the following form [9, 10]

$${}^{\eta}\mu_T = -\frac{\partial^2 \psi_R}{\partial T \, \partial c_{T_R}} \,, \tag{6.48a}$$

$${}^{u}\mu_T = \frac{\partial \psi_R}{\partial c_{T_R}} - T \frac{\partial^2 \psi_R}{\partial T \, \partial c_{T_R}} \,. \tag{6.48b}$$

Remark. The specifications for the energetic and entropic contributions of μ_L allow to establish the independence of the vector $\boldsymbol{\nabla}_R \left[\mu_L \right] + {}^{\eta}\mu_L \, \boldsymbol{\nabla}_R \left[T \right]$, appearing in Eq. (6.42b), upon the temperature gradient $\boldsymbol{\nabla}_R \left[T \right]$. Indeed

$$\begin{aligned} \boldsymbol{\nabla}_R \left[\mu_L \right] &= \boldsymbol{\nabla}_R \left[\frac{\partial \psi_R}{\partial c_{L_R}} - \boldsymbol{\nabla}_R \cdot \left[\frac{\partial \psi_R}{\partial \boldsymbol{\nabla}_R \left[c_{L_R} \right]} \right] \right] = \boldsymbol{\nabla}_R \left[\frac{\partial \psi_R}{\partial c_{L_R}} \right] - \boldsymbol{\nabla}_R \left[\boldsymbol{\nabla}_R \cdot \left[\frac{\partial \psi_R}{\partial \boldsymbol{\nabla}_R \left[c_{L_R} \right]} \right] \right] \\ &= \frac{\partial^2 \psi_R}{\partial c_{L_R} \partial T} \boldsymbol{\nabla}_R \left[T \right] + \frac{\partial^2 \psi_R}{\partial c_{L_R}^2} \boldsymbol{\nabla}_R \left[c_{L_R} \right] + \frac{\partial^2 \psi_R}{\partial c_{L_R} \partial \boldsymbol{\nabla}_R \left[c_{L_R} \right]} \cdot \boldsymbol{\nabla}_R \left[\boldsymbol{\nabla}_R \left[c_{L_R} \right] \right] \\ &+ \frac{\partial^2 \psi_R}{\partial c_{L_R} \partial \mathbf{C}} : \boldsymbol{\nabla}_R \left[\mathbf{C} \right] + \frac{\partial^2 \psi_R}{\partial c_{L_R} \partial \boldsymbol{\Xi}} : \boldsymbol{\nabla}_R \left[\boldsymbol{\Xi} \right] - \boldsymbol{\nabla}_R \left[\boldsymbol{\nabla}_R \cdot \left[\frac{\partial \psi_R}{\partial \boldsymbol{\nabla}_R \left[c_{L_R} \right]} \right] \right] \,, \end{aligned} \tag{6.49}$$

whereas the vector ${}^{\eta}\mu_L \, \boldsymbol{\nabla}_R \left[T \right]$, according to the definition (6.47a), simply writes as

$${}^{\eta}\mu_L \, \boldsymbol{\nabla}_R \left[T \right] = -\frac{\partial^2 \psi_R}{\partial c_{L_R} \partial T} \boldsymbol{\nabla}_R \left[T \right] \,. \tag{6.50}$$

Combination of Eq.s (6.49) and (6.50) therefore yields

$$\begin{aligned}\nabla_R\left[\,\mu_L\,\right] + {}^{\eta}\mu_L\,\nabla_R\left[\,T\,\right] = \frac{\partial^2\psi_R}{\partial c_{L_R}^2}\,\nabla_R\left[\,c_{L_R}\,\right] + \frac{\partial^2\psi_R}{\partial c_{L_R}\partial\mathbf{C}} : \nabla_R\left[\,\mathbf{C}\,\right] + \frac{\partial^2\psi_R}{\partial c_{L_R}\partial\boldsymbol{\Xi}} : \nabla_R\left[\,\boldsymbol{\Xi}\,\right] \\ - \nabla_R\left[\nabla_R\cdot\left[\frac{\partial\psi_R}{\partial\nabla_R\left[\,c_{L_R}\,\right]}\right]\right] ,\end{aligned} \tag{6.51}$$

where it has been taken advantage from

$$\frac{\partial^2\psi_R}{\partial c_{L_R}\partial\nabla_R\left[\,c_{L_R}\,\right]} = \frac{\partial}{\partial c_{L_R}}\,\frac{\partial\psi_R(\nabla_R\left[\,c_{L_R}\,\right])}{\partial\nabla_R\left[\,c_{L_R}\,\right]} = 0 \; , \tag{6.52}$$

according to the a-priori selected functional dependence of the Helmholtz free energy (6.1), and the consideration of c_{L_R} and $\nabla_R\left[\,c_{L_R}\,\right]$ as independent variables.

Eq. (6.51) will be used in Section 6.5.4 to constitutively define the mass flux vector $\boldsymbol{h}_{L_R}$.

6.5 Constitutive theory

6.5.1 Helmholtz free energy

Following the same path of reasoning of [9, 10], and according to what shown in Eq. (6.1), the referential Helmholtz free energy density is here subjected to the following additive decomposition

$$\begin{aligned}\psi_R(T, c_{L_R}, c_{T_R}, \nabla_R\left[\,c_{L_R}\,\right], \mathbf{C}, \boldsymbol{\Xi}) = {} & \psi_R^{th}(T, c_{L_R}, c_{T_R}) + \psi_R^{diff}(T, c_{L_R}, c_{T_R}, \mathbf{C}, \boldsymbol{\Xi}) \\ & + \psi_R^{el}(T, c_{L_R}, c_{T_R}, \mathbf{C}) + \psi_R^{in}(T, c_{L_R}, c_{T_R}, \boldsymbol{\Xi}) \\ & + \psi_R^{\varkappa}(T, \nabla_R\left[\,c_{L_R}\,\right]) \; ,\end{aligned} \tag{6.53}$$

with ψ_R^{th}, ψ_R^{diff}, ψ_R^{el} and ψ_R^{in} representing the thermal, diffusive, elastic and inelastic contributions, respectively, whereas $\psi_R^{\varkappa}$ defines the gradient energy, as specified in Eq. (6.1) and in accordance with to the CH theory.

For the sake of brevity, we here show only the two essential contributions to describe the CH theory, ψ_R^{diff} and $\psi_R^{\varkappa}$. Other contributions have been shown in [9, 10], and a detailed analysis can be found in [63], For the problem at hand, and in its continuum approximation of mixing, the diffusive term is described by a regular solution model [55, 52] as

$$\psi_R^{diff}(T, c_{L_R}, c_{T_R}, \mathbf{C}, \boldsymbol{\Xi}) = \mu_L^0\, c_{L_R} - T\,\eta_{L_R}^{diff} + \mu_T^0\, c_{T_R} - T\,\eta_{T_R}^{diff} - T\,\eta_{L_R}^{\chi} \; . \tag{6.54}$$

Eq. (6.54) therefore accounts for the entropy of mixing and the energetic interactions, whereas the terms μ_L^0 and μ_T^0 represent reference values of chemical potentials that specify the free energy in the absence of interaction and entropic contributions.

The entropy of mixing $\eta_{\alpha_R}^{diff}$ is provided by the Boltzmann's equation, and in terms of the density of states $\mathfrak{N}_\alpha$ for a two-state system [64]. It holds

$$\eta_{\alpha_R}^{diff} = -R\,c_{\alpha_R}^{max}\,\left(\vartheta_{\alpha_R}\ln\left[\,\vartheta_{\alpha_R}\,\right] + (1-\vartheta_{\alpha_R})\ln\left[\,1-\vartheta_{\alpha_R}\,\right]\right) \; , \tag{6.55}$$

with R universal gas constant, $c_{\alpha_R}^{max}$ referential saturation limit of the species involved in chemical reaction (6.14), and $\vartheta_{\alpha_R} = c_{\alpha_R}\,{c_{\alpha_R}^{max}}^{-1}$. Conversely to [10], we here assume the invariance of the maximum number of moles per unit volume,

$$c_{\alpha_R}^{max}(\boldsymbol{X}, t) = c_{\alpha}^{max}\,(\boldsymbol{x}, t) \; , \tag{6.56}$$

which implies that ϑ_{α_R} transforms according to Eq. (7.3), namely

$$\vartheta_{\alpha_R}(\boldsymbol{X}, t) = J(\boldsymbol{X}, t)\,\vartheta_\alpha(\boldsymbol{x}(\boldsymbol{X}, t), t) \; . \tag{6.57}$$

The term $\eta^{\chi}_{L_R}$, which multiplied by $-T$ represents the excess Gibbs energy, writes as

$$\eta^{\chi}_{L_R} = -R\, c_L^{max}\, \chi\, \vartheta_{L_R}\, (1 - \vartheta_{L_R}) \ , \tag{6.58}$$

where the Flory interaction parameter has to be $\chi > 2$, in order to endow the free energy density with a non convex behavior with respect to c_{L_R}, according to the non-convex double-well potential provided by the CH theory.

Combining Eq.s (6.55), (6.58), the referential diffusive contribution to the Helmholtz free energy writes as

$$\begin{aligned} \psi_R^{diff}(T, c_{L_R}, c_{T_R}, \mathbf{C}, \boldsymbol{\Xi}) &= R\,T\, c_L^{max}\, \chi\, \vartheta_{L_R}\, (1 - \vartheta_{L_R}) + \sum_{\alpha=L,T} \mu^0_{\alpha}\, c_{\alpha R} \\ &+ \sum_{\alpha=L,T} R\,T\, c_{\alpha}^{max}\, (\vartheta_{\alpha R} \ln[\,\vartheta_{\alpha R}\,] + (1-\vartheta_{\alpha R}) \ln[\,1 - \vartheta_{\alpha R}\,]) \ . \end{aligned} \tag{6.59}$$

The interfacial free energy density $\psi_R^{\varkappa}$ can be re-written in terms of ϑ_{L_R} as

$$\psi_R^{\varkappa}(T, \boldsymbol{\nabla}_R\,[\,c_{L_R}\,]) = c_L^{max}\, \varkappa\, |\, \boldsymbol{\nabla}_R\,[\,\vartheta_{L_R}\,]\,|^2 \ , \tag{6.60}$$

where $\varkappa = \frac{1}{2}\,\kappa$, with κ gradient energy coefficient [55].

According to Eq.s (6.53), (6.60), and thermodynamic prescription (6.40e), the internal micro-stress $\boldsymbol{\zeta}_L$ writes as

$$\boldsymbol{\zeta}_L = \frac{\partial \psi_R}{\partial \boldsymbol{\nabla}_R\,[\,c_{L_R}\,]} = \frac{\partial \psi_R^{\varkappa}}{\partial \boldsymbol{\nabla}_R\,[\,c_{L_R}\,]} = \kappa\, \boldsymbol{\nabla}_R\,[\,\vartheta_{L_R}\,] \ . \tag{6.61}$$

6.5.2 Contributions to the second Piola-Kirchhoff stress tensor

The additive decomposition of ψ_R performed in Eq. (6.53), according to the stated functional dependence of each contribution and to thermodynamic restriction (6.40a), leads to establish the dependence of the second Piola-Kirchhoff stress tensor $\mathbf{S}$ upon two contributions, namely

$$\mathbf{S} = 2\,\frac{\partial}{\partial \mathbf{C}}\, \psi_R(T, c_{L_R}, c_{T_R} \boldsymbol{\nabla}_R\,[\,c_{L_R}\,], \mathbf{C}, \boldsymbol{\Xi}) = 2\,\frac{\partial \psi_R^{diff}}{\partial \mathbf{C}} + 2\,\frac{\partial \psi_R^{el}}{\partial \mathbf{C}} \ . \tag{6.62}$$

Specification of $\mathbf{S}$ is performed in an analogous way to [10], and therefore briefly summarized hereinafter. The first right-hand side term of Eq. (6.62) depends upon $\mathbf{C}$ by means of J, according to

$$2\,\frac{\partial \psi_R^{diff}}{\partial \mathbf{C}} + 2\,\frac{\partial \psi_R^{diff}}{\partial J}\,\frac{\partial J}{\partial \mathbf{C}} = \frac{\partial \psi_R^{diff}}{\partial J}\, J\, \mathbf{C}^{-1} \ .$$

Recalling Eq. (6.59), we find that

$$\frac{\partial \psi_R^{diff}}{\partial J}\, J = R\,T\, c_L^{max}\, \chi\, \vartheta_{L_R}\, (1 - 2\,\vartheta_{L_R}) + \sum_{\alpha=L,T} R\,T\, c_{\alpha}^{max}\, \vartheta_{\alpha R} \ln\left[\frac{\vartheta_{\alpha R}}{1 - \vartheta_{\alpha R}}\right] \ , \tag{6.63}$$

whence,

$$\mathbf{S} = R\,T\left(c_L^{max}\, \chi\, \vartheta_{L_R}\, (1 - 2\,\vartheta_{L_R}) + \sum_{\alpha=L,T} c_{\alpha}^{max}\, \vartheta_{\alpha R} \ln\left[\frac{\vartheta_{\alpha R}}{1 - \vartheta_{\alpha R}}\right]\right) \mathbf{C}^{-1} + 2\,\frac{\partial \psi_R^{el}}{\partial \mathbf{C}} \ . \tag{6.64}$$

6.5.3 Chemical potentials

Recall the additive decomposition of the Helmholtz free energy density (6.53), and the expression of the diffusive contribution ψ_R^{diff} shown in Eq. (6.59). The chemical potential of species L has the form

$$\mu_L = \mu_L^0 + R\,T\,\chi\,(1-2\,\vartheta_{L_R}) + R\,T\ln\left[\frac{\vartheta_{L_R}}{1-\vartheta_{L_R}}\right] - \varkappa\,\nabla_R\cdot[\,\nabla_R\,[\,\vartheta_{L_R}\,]\,] + \frac{\partial\psi_R^{th}}{\partial c_{L_R}} + \frac{\partial\psi_R^{el}}{\partial c_{L_R}} + \frac{\partial\psi_R^{in}}{\partial c_{L_R}}\;, \tag{6.65a}$$

according to Eq.s (6.40c), (6.40e), and (6.61), whereas the chemical potential of trapped species simply writes as

$$\mu_T = \mu_T^0 + R\,T\ln\left[\frac{\vartheta_{T_R}}{1-\vartheta_{T_R}}\right] + \frac{\partial\psi_R^{th}}{\partial c_{T_R}} + \frac{\partial\psi_R^{el}}{\partial c_{T_R}} + \frac{\partial\psi_R^{in}}{\partial c_{T_R}}\;. \tag{6.65b}$$

6.5.4 Heat and mass fluxes

To satisfy thermodynamic prescription (6.42b), we model the heat flux $\boldsymbol{q}_R$ via Fourier's law by means of a positive definite heat conductivity tensor $\mathbb{K}$

$$\boldsymbol{q}_R = -\mathbb{K}\,\nabla_R\,[\,T\,]\;, \tag{6.66}$$

whereas the mass flux $\boldsymbol{h}_{L_R}$ is related to the vector term $\nabla_R\,[\,\mu_L\,] + {}^{\eta}\mu_L\,\nabla_R\,[\,T\,]$ [9, 10], which has been shown in Eq. (6.51) to be independent upon the temperature gradient, and modeled via Fick's law by means of a positive definite mobility tensor $\mathbf{M}_L$,

$$\boldsymbol{h}_{L_R} = -\mathbf{M}_L(c_{L_R})\;(\nabla_R\,[\,\mu_L\,] + {}^{\eta}\mu_L\,\nabla_R\,[\,T\,])\;. \tag{6.67}$$

To account for saturation and to satisfy the physical requirement that both the pure and the saturated phases, $c_{L_R}=0$ and $c_L = c_L^{max}$, have vanishing mobility, the mobility tensor $\mathbf{M}_L(c_{L_R})$ is chosen of the following isotropic non linear form [55]

$$\mathbf{M}_L(c_{L_R}) = \mathbb{u}_L\,c_L^{max}\;\vartheta_{L_R}\;(1-\vartheta_{L_R})\,\mathbf{1}\;, \tag{6.68}$$

with $\mathbb{u}_L > 0$ mobility of interstitial chemical species.

Recalling Eq. (6.51), Fick's law (6.67) re-writes as

$$\begin{aligned}\boldsymbol{h}_{L_R} = &-\mathbf{M}_L\left(\frac{\partial^2\psi_R}{\partial c_{L_R}^2}\,\nabla_R\,[\,c_{L_R}\,] + \frac{\partial^2\psi_R}{\partial c_{L_R}\partial\mathbf{C}} : \nabla_R\,[\,\mathbf{C}\,] + \frac{\partial^2\psi_R}{\partial c_{L_R}\partial\boldsymbol{\Xi}} : \nabla_R\,[\,\boldsymbol{\Xi}\,]\right)\\ &-\mathbf{M}_L\,\nabla_R\left[\nabla_R\cdot\left[\frac{\partial\psi_R}{\partial\nabla_R\,[\,c_{L_R}\,]}\right]\right]\;,\end{aligned} \tag{6.69}$$

where the last term modifies the *standard* Fick's law in accordance with the phenomena the CH theory aims to describe.

Being the tensors $\mathbf{M}_L$ and $\mathbb{K}$ positive definite, according to Eq.s (6.66) and (6.67), thermodynamic prescription (6.42b) re-writes as

$$-\mathbf{M}_{L_R}(c_{L_R})\;(\nabla_R\,[\,\mu_L\,] + {}^{\eta}\mu_L\,\nabla_R\,[\,T\,])\cdot(\nabla_R\,[\,\mu_L\,] + {}^{\eta}\mu_L\,\nabla_R\,[\,T\,]) - \frac{1}{T}\,\mathbb{K}\,\nabla_R\,[\,T\,]\cdot\nabla_R\,[\,T\,] \le 0\;,$$

and it is immediately satisfied.

6.6 Chemical kinetics

For an ideal system, in which the solvent does not take part in reactions, the kinetics of reaction (6.14) is well modeled via the following law of mass action [51]

$$w_{R}^{(6.14)}(\boldsymbol{X},t) = k_{R}^{+}\, \frac{\vartheta_{L_R}}{1-\vartheta_{L_R}} - k_{R}^{-}\, \frac{\vartheta_{T_R}}{1-\vartheta_{T_R}} \; . \tag{6.70}$$

In agreement with the transformation rule $(6.17)_2$ and assumption (6.56), the rate factors for both the forward and reverse reaction, k_{R}^{+} and k_{R}^{-}, are configuration invariant, namely

$$k_{R}^{+}(\boldsymbol{X},t) = k^{+}(\boldsymbol{x},t) \; , \qquad k_{R}^{-}(\boldsymbol{X},t) = k^{-}(\boldsymbol{x},t) \; , \tag{6.71}$$

and have the form

$$k^{+} = \tilde{k}^{+} \, \exp\left(\frac{1}{RT} \frac{\partial \psi_{R}^{th}}{\partial c_{T_R}} \right) \exp\left(\frac{1}{RT} \frac{\partial \psi_{R}^{el}}{\partial c_{T_R}} \right) \exp\left(\frac{1}{RT} \frac{\partial \psi_{R}^{in}}{\partial c_{T_R}} \right) \; , \tag{6.72a}$$

$$k^{-} = \tilde{k}^{-} \, \exp\left(\chi\,(1-2\,\vartheta_{L_R})\right) \exp\left(\frac{1}{RT} \frac{\partial \psi_{R}^{th}}{\partial c_{L_R}} \right) \exp\left(\frac{1}{RT} \frac{\partial \psi_{R}^{el}}{\partial c_{L_R}} \right) \exp\left(\frac{1}{RT} \frac{\partial \psi_{R}^{in}}{\partial c_{L_R}} \right) \; , \tag{6.72b}$$

with $\tilde{k}^{+}$ and $\tilde{k}^{-}$ constant values.

At equilibrium $w_{R}^{(6.14)} = 0$, and taking advantage from Eq.s (6.70), (6.72), the equilibrium constant $K_{eq}^{(6.14)}$ of chemical reaction (6.14) writes as

$$\begin{aligned} K_{eq}^{(6.14)} = \frac{\tilde{k}^{+}}{\tilde{k}^{-}} = \frac{\vartheta_{T_R}^{eq}}{1-\vartheta_{T_R}^{eq}} \, \frac{1-\vartheta_{L_R}^{eq}}{\vartheta_{L_R}^{eq}} \, \exp\left[-\chi\,(1-2\,\vartheta_{L_R})\right] \exp\left[\frac{1}{RT} \left(\frac{\partial \psi_{R}^{th}}{\partial c_{T_R}} - \frac{\partial \psi_{R}^{th}}{\partial c_{L_R}} \right) \right] \\ \exp\left[\frac{1}{RT} \left(\frac{\partial \psi_{R}^{el}}{\partial c_{T_R}} - \frac{\partial \psi_{R}^{el}}{\partial c_{L_R}} \right) \right] \exp\left[\frac{1}{RT} \left(\frac{\partial \psi_{R}^{in}}{\partial c_{T_R}} - \frac{\partial \psi_{R}^{in}}{\partial c_{L_R}} \right) \right] \; . \end{aligned} \tag{6.73}$$

6.7 Governing equations

The derivation of the governing equations can be obtained by incorporating the constitutive definition of the second Piola-Kirchhoff stress tensor $\mathbf{S}$ (6.64), and the constitutive definitions of the referential mass flux $\boldsymbol{h}_{L_R}$ (6.69) and the heat flux $\boldsymbol{q}_{R}$ (6.66) into the balance of linear momentum (6.23), the mass balance equation (6.16), and into the generalized heat equation shown hereinafter (6.76). Governing equations are written in terms of concentrations c_{L_R} and c_{T_R}, displacements $\boldsymbol{u}$, and temperature T.

The mass balance equations write as

$$\dot{c}_{L_R} + \boldsymbol{\nabla}_{R} \cdot \left[\boldsymbol{h}_{L_R}(T, c_{L_R}, \boldsymbol{\nabla}_{R} \left[c_{L_R} \right], c_{T_R}, \mathbf{C}, \boldsymbol{\Xi}) \right] + w_{R}^{(6.14)}(T, c_{L_R}, c_{T_R}, \mathbf{C}, \boldsymbol{\Xi}) = s_{L_R} \tag{6.74a}$$

$$\dot{c}_{T_R} - w_{R}^{(6.14)}(T, c_{L_R}, c_{T_R}, \mathbf{C}, \boldsymbol{\Xi}) = s_{T_R} \tag{6.74b}$$

By means of Eq. (6.64), the governing balance of linear momentum writes as

$$\boldsymbol{\nabla}_{R} \cdot \left[\mathbf{T}_{R} \left(\mathbf{S}, \mathbf{C}, c_{L_R}, c_{T_R}, T \right) \right] + \boldsymbol{b}_{0_R} = \mathbf{0} \; . \tag{6.75}$$

Lastly, the generalized heat equation, whose derivation is collected in Appendix C.1, writes as

$$
\begin{aligned}
-T \, \frac{\partial^2 \psi_R}{\partial T^2} \dot{T} - \boldsymbol{\nabla}_R \cdot [\, \mathbf{K} \;\; \boldsymbol{\nabla}_R \, [\, T \,] \,] = & \\
= s_{q_R} + T \, \frac{\partial^2 \psi_R}{\partial T \partial \mathbf{C}} : \dot{\mathbf{C}} + \left(\mathbf{X} + \frac{\partial^2 \psi_R}{\partial T \partial \boldsymbol{\Xi}} \right) : \dot{\boldsymbol{\Xi}} + \frac{\partial^2 \psi_R}{\partial T \partial \boldsymbol{\nabla}_R \, [\, c_{L_R} \,]} \cdot \boldsymbol{\nabla}_R \, [\, \dot{c}_{L_R} \,] & \\
+ \, \mathbf{M}_{L_R} \left(\frac{\partial^2 \psi_R}{\partial c_{L_R}^2} \, \boldsymbol{\nabla}_R \, [\, c_{L_R} \,] + \frac{\partial^2 \psi_R}{\partial c_{L_R} \partial \mathbf{C}} : \boldsymbol{\nabla}_R \, [\, \mathbf{C} \,] + \frac{\partial^2 \psi_R}{\partial c_{L_R} \partial \boldsymbol{\Xi}} : \boldsymbol{\nabla}_R \, [\, \boldsymbol{\Xi} \,] \right. & \\
\left. + \, \boldsymbol{\nabla}_R \left[\boldsymbol{\nabla}_R \cdot \left[\frac{\partial \psi_R}{\partial \boldsymbol{\nabla}_R \, [\, c_{L_R} \,]} \right] \right] \right) \cdot \boldsymbol{\nabla}_R \left[\frac{\partial \psi_R}{\partial c_{L_R}} - T \, \frac{\partial^2 \psi_R}{\partial T \, \partial c_{L_R}} - \boldsymbol{\nabla}_R \cdot \left[\frac{\partial \psi_R}{\partial \boldsymbol{\nabla}_R \, [\, c_{L_R} \,]} \right] \right] & \\
+ \left[\frac{\partial \psi_R}{\partial c_{L_R}} - \frac{\partial \psi_R}{\partial c_{T_R}} - T \left(\frac{\partial^2 \psi_R}{\partial T \, \partial c_{L_R}} - \frac{\partial^2 \psi_R}{\partial T \, \partial c_{T_R}} \right) - \boldsymbol{\nabla}_R \cdot \left[\frac{\partial \psi_R}{\partial \boldsymbol{\nabla}_R \, [\, c_{L_R} \,]} \right] \right] w_R^{(6.14)} \; . &
\end{aligned}
\tag{6.76}
$$

Boundary conditions

$$\boldsymbol{h}_{L_R} \cdot \boldsymbol{n}_R = \overline{h}_{L_R} \; , \tag{6.77a}$$

$$\boldsymbol{q}_R \cdot \boldsymbol{n}_R = \overline{q}_R \; , \tag{6.77b}$$

$$\boldsymbol{t}_R = \overline{\boldsymbol{t}}_R \; , \tag{6.77c}$$

$$\boldsymbol{\zeta}_L \cdot \boldsymbol{n}_R = \overline{\zeta}_L \; , \tag{6.77d}$$

are imposed along Neumann boundaries $\partial^N \Omega_R$. To ensure solvability of the problem, Dirichlet boundary conditions have to be enforced along $\partial^D \Omega_R$, hence

$$T = \overline{T} \; , \tag{6.78a}$$

$$\boldsymbol{u} = \overline{\boldsymbol{u}} \; . \tag{6.78b}$$

Initial conditions are usually imposed for the concentrations $c_{L_R}(\boldsymbol{X}, t = 0)$ and $c_{T_R}(\boldsymbol{X}, t = 0)$, for the concentration gradient $\boldsymbol{\nabla}_R \, [\, c_{L_R} \,] \, (\boldsymbol{X}, t = 0)$, and for temperature, $T(\boldsymbol{X}, t = 0)$. Balance of momentum, together with boundary conditions, provide the necessary and sufficient equations to solve for $\boldsymbol{u}$ at $t = 0$.

6.8 Concluding remarks

A theoretical formulation to couple Chan-Hilliard-type mass transport, chemical reactions with trapping, and finite strain thermo-mechanics has been presented, following the rigorous setting developed in [9, 10]. The CH theory is discussed early on, and related to the interstitial motion of free diffusive species in a hosting material. It accounts for the interfacial free energy due to inhomogeneity in composition and phase segregation. Trapped species are considered to stay immobile, therefore the do not contribute to the mass flux of specie and are unaffected by the CH theory. Mass balance equations are augmented with the reaction rate of the chemical reaction, which portrays the conversion of mobile guest species to trapped species, and vice-versa, and a source term to describe mass production or consumption. With reference to diffusive species, despite the mass balance equation maintains its *standard* structure, it is affected by the CH theory via the definition of a *new* chemical potential that enters into the mass flux vector. The energetic and the entropic contributions of the mass flux lead to define the chemical potential as the sum of energetic and entropic contribution (multiplied by the temperature) [9, 10]. Furthermore, a purely energetic contribution related to the CH theory modifies the chemical potential of diffusive species. The standard method of Coleman and Noll, and the assumption of Curie's symmetry principles, determine all thermodynamic prescriptions and the resulting thermodynamic consistency of the CH theory within the presented framework. The referential Helmholtz free energy density is constitutively subjected to an additive decomposition to account for all processes involved in the problem at hand, including the dependence upon the concentration gradient that needs to be a-priori specified. The additive splitting of $\psi_{_R}$, and the functional dependence of each contribution, drive the constitutive specifications for chemical potentials, heat and mass fluxes, and chemical kinetics. Governing equations, with associated constrains, are derived to finalize the coupled finite strain chemo-thermo-mechanics with CH-type species transport formulation.

Appendix C

C.1 The generalized heat equation

To derive the generalized heat equation, recall the referential localized energy balance (6.27) and replace the mechanical contribution $\mathbf{T}_R : \dot{\mathbf{F}}$ taking advantage from Eq. (6.33). Then

$$\begin{aligned} \dot{u}_R = {} & \frac{1}{2}\,\mathbf{S} : \dot{\mathbf{C}} + s_{qR} - \boldsymbol{\nabla}_R \cdot \left[\, \boldsymbol{q}_R \,\right] + \left({}^u\mu_L + \boldsymbol{\nabla}_R \cdot \left[\, \boldsymbol{\zeta}_L \,\right]\right) \dot{c}_{L_R} + {}^u\mu_T\, \dot{c}_{T_R} - \boldsymbol{\nabla}_R \left[\, {}^u\mu_L \,\right] \cdot \boldsymbol{h}_{L_R} \\ & + \boldsymbol{\nabla}_R \left[\, \dot{c}_{L_R} \,\right] \cdot \boldsymbol{\zeta}_L + \left({}^u\mu_L - {}^u\mu_T\right) w_R^{(6.14)} \, . \end{aligned} \tag{C.1}$$

By means of the time derivatives of the Helmholtz free energy (6.34) and (6.37), it follows that

$$\begin{aligned} T\,\dot{\eta}_R - \dot{u}_R = -\dot{\psi}_R - \dot{T}\,\eta_R = {} & -\frac{\partial \psi_R}{\partial T}\,\dot{T} - \frac{\partial \psi_R}{\partial c_{L_R}}\,\dot{c}_{L_R} - \frac{\partial \psi_R}{\partial c_{T_R}}\,\dot{c}_{T_R} - \frac{\partial \psi_R}{\partial \boldsymbol{\nabla}_R \left[\, c_{L_R} \,\right]} \cdot \boldsymbol{\nabla}_R \left[\, \dot{c}_{L_R} \,\right] \\ & - \frac{\partial \psi_R}{\partial \mathbf{C}} : \dot{\mathbf{C}} - \frac{\partial \psi_R}{\partial \boldsymbol{\Xi}} : \dot{\boldsymbol{\Xi}} - \dot{T}\,\eta_R \, . \end{aligned} \tag{C.2}$$

Taking advantage from the definition of the plastic internal stress tensor $\mathbf{X}\mkern-10mu|$ (6.38), and from the thermodynamic prescriptions for $\mathbf{S}$ (6.40a), η_R (6.40b), μ_L (6.40c), μ_T (6.40d), and for $\boldsymbol{\zeta}_L$ (6.40e), to substitute the partial derivatives of ψ_R in Eq. (C.2), it holds

$$\begin{aligned} T\,\dot{\eta}_R - \dot{u}_R = -\dot{\psi}_R - \dot{T}\,\eta_R = {} & -\frac{1}{2}\,\mathbf{S} : \dot{\mathbf{C}} - \left(\mu_L + \boldsymbol{\nabla}_R \cdot \left[\, \boldsymbol{\zeta}_L \,\right]\right) \dot{c}_{L_R} + \mu_T\, \dot{c}_{T_R} - \boldsymbol{\zeta}_L \cdot \boldsymbol{\nabla}_R \left[\, \dot{c}_{L_R} \,\right] \\ & + \mathbf{X}\mkern-10mu| : \dot{\boldsymbol{\Xi}} \, , \end{aligned} \tag{C.3}$$

whence

$$T\,\dot{\eta}_R = -T\,\frac{\partial \dot{\psi}_R}{\partial T} = \dot{u}_R - \frac{1}{2}\,\mathbf{S} : \dot{\mathbf{C}} - \left(\mu_L + \boldsymbol{\nabla}_R \cdot \left[\, \boldsymbol{\zeta}_L \,\right]\right) \dot{c}_{L_R} + \mu_T\, \dot{c}_{T_R} - \boldsymbol{\zeta}_L \cdot \boldsymbol{\nabla}_R \left[\, \dot{c}_{L_R} \,\right] + \mathbf{X}\mkern-10mu| : \dot{\boldsymbol{\Xi}} \, . \tag{C.4}$$

making use of Eq. (C.1) to replace $\dot{u}_R$ in Eq. (C.4), it follows that

$$\begin{aligned} -T\,\frac{\partial \dot{\psi}_R}{\partial T} = {} & s_{qR} - \boldsymbol{\nabla}_R \cdot \left[\, \boldsymbol{q}_R \,\right] + \left({}^u\mu_L - \mu_L\right) \dot{c}_{L_R} + \left({}^u\mu_T - \mu_T\right) \dot{c}_{T_R} - \boldsymbol{\nabla}_R \left[\, {}^u\mu_L \,\right] \cdot \boldsymbol{h}_{L_R} \\ & + \left({}^u\mu_L - {}^u\mu_T\right) w_R^{(6.14)} + \mathbf{X}\mkern-10mu| : \dot{\boldsymbol{\Xi}} \, , \end{aligned} \tag{C.5}$$

According to (6.37),

$$\begin{aligned} -T\,\frac{\partial \dot{\psi}_R}{\partial T} = -T\, \Bigg(& \frac{\partial^2 \psi_R}{\partial T^2}\,\dot{T} + \frac{\partial^2 \psi_R}{\partial T \partial c_{L_R}}\,\dot{c}_{L_R} + \frac{\partial^2 \psi_R}{\partial T \partial c_{T_R}}\,\dot{c}_{T_R} + \frac{\partial^2 \psi_R}{\partial T \partial \boldsymbol{\nabla}_R \left[\, c_{L_R} \,\right]} \cdot \boldsymbol{\nabla}_R \left[\, \dot{c}_{L_R} \,\right] \\ & + \frac{\partial^2 \psi_R}{\partial T \partial \mathbf{C}} : \dot{\mathbf{C}} + \frac{\partial^2 \psi_R}{\partial T \partial \boldsymbol{\Xi}} : \dot{\boldsymbol{\Xi}} \Bigg) \, , \end{aligned} \tag{C.6}$$

whence, equating Eq.s (C.5) and (C.6) to re-write the terms

$$-T\,\frac{\partial^2 \psi_R}{\partial T^2}\,\dot{T} + \boldsymbol{\nabla}_R \cdot \left[\, \boldsymbol{q}_R \,\right] \, ,$$

it follows that

$$\begin{aligned} -T\,\frac{\partial^2\psi_R}{\partial T^2}\,\dot{T} + \boldsymbol{\nabla}_R\cdot\left[\,\boldsymbol{q}_R\,\right] = s_{qR} &+ \left({}^{u}\mu_L - \mu_L + T\,\frac{\partial^2\psi_R}{\partial T\partial c_{L_R}}\right) + \left({}^{u}\mu_T - \mu_T + T\,\frac{\partial^2\psi_R}{\partial T\partial c_{T_R}}\right) \\ &- \boldsymbol{\nabla}_R\left[{}^{u}\mu_L\right]\cdot\boldsymbol{h}_{L_R} + \left({}^{u}\mu_L - {}^{u}\mu_T\right)\,w_R^{(6.14)} + \left(\mathbf{X} + \frac{\partial^2\psi_R}{\partial T\partial\boldsymbol{\Xi}}\right) : \dot{\boldsymbol{\Xi}} \\ &+ \frac{\partial^2\psi_R}{\partial T\partial\boldsymbol{\nabla}_R\left[\,c_{L_R}\right]}\cdot\boldsymbol{\nabla}_R\left[\,\dot{c}_{L_R}\right] + T\,\frac{\partial^2\psi_R}{\partial T\partial\mathbf{C}} : \dot{\mathbf{C}}\;. \end{aligned} \tag{C.7}$$

In respect of the definition of μ_α stated in Eq. $(6.30)_1$, and according to the specifications for ${}^{\eta}\mu_\alpha$ (6.47a) and (6.48a),

$${}^{u}\mu_\alpha - \mu_L + T\,\frac{\partial^2\psi_R}{\partial T\partial c_{\alpha_R}} = 0\;,$$

for $\alpha = L, T$, therefore

$$\begin{aligned} -T\,\frac{\partial^2\psi_R}{\partial T^2}\,\dot{T} + \boldsymbol{\nabla}_R\cdot\left[\,\boldsymbol{q}_R\,\right] = s_{qR} &- \boldsymbol{h}_{L_R}\cdot\boldsymbol{\nabla}_R\left[{}^{u}\mu_L\right] + \left({}^{u}\mu_L - {}^{u}\mu_T\right)\,w_R^{(6.14)} + \left(\mathbf{X} + \frac{\partial^2\psi_R}{\partial T\partial\boldsymbol{\Xi}}\right) : \dot{\boldsymbol{\Xi}} \\ &+ \frac{\partial^2\psi_R}{\partial T\partial\boldsymbol{\nabla}_R\left[\,c_{L_R}\right]}\cdot\boldsymbol{\nabla}_R\left[\,\dot{c}_{L_R}\right] + T\,\frac{\partial^2\psi_R}{\partial T\partial\mathbf{C}} : \dot{\mathbf{C}}\;. \end{aligned} \tag{C.8}$$

Lastly, by means of the constitutive prescriptions for the Fick's law (6.69) and the Fourier's law (6.66), and taking advantage from Eq.s (6.47b) and (6.48b) to substitute the terms ${}^{u}\mu_L$ and ${}^{u}\mu_T$, the following generalized heat equation arises

$$\begin{aligned} -T\,\frac{\partial^2\psi_R}{\partial T^2}\dot{T} &- \boldsymbol{\nabla}_R\cdot\left[\mathbf{K}\;\;\boldsymbol{\nabla}_R\left[T\right]\right] = \\ &= s_{qR} + T\,\frac{\partial^2\psi_R}{\partial T\partial\mathbf{C}} : \dot{\mathbf{C}} + \left(\mathbf{X} + \frac{\partial^2\psi_R}{\partial T\partial\boldsymbol{\Xi}}\right) : \dot{\boldsymbol{\Xi}} + \frac{\partial^2\psi_R}{\partial T\partial\boldsymbol{\nabla}_R\left[\,c_{L_R}\right]}\cdot\boldsymbol{\nabla}_R\left[\,\dot{c}_{L_R}\right] \\ &+ \mathbf{M}_{L_R}\left(\frac{\partial^2\psi_R}{\partial c_{L_R}^2}\,\boldsymbol{\nabla}_R\left[\,c_{L_R}\right] + \frac{\partial^2\psi_R}{\partial c_{L_R}\partial\mathbf{C}} : \boldsymbol{\nabla}_R\left[\,\mathbf{C}\,\right] + \frac{\partial^2\psi_R}{\partial c_{L_R}\partial\boldsymbol{\Xi}} : \boldsymbol{\nabla}_R\left[\,\boldsymbol{\Xi}\,\right]\right. \\ &\left. + \boldsymbol{\nabla}_R\left[\boldsymbol{\nabla}_R\cdot\left[\frac{\partial\psi_R}{\partial\boldsymbol{\nabla}_R\left[\,c_{L_R}\right]}\right]\right]\right)\cdot\boldsymbol{\nabla}_R\left[\frac{\partial\psi_R}{\partial c_{L_R}} - T\,\frac{\partial^2\psi_R}{\partial T\,\partial c_{L_R}} - \boldsymbol{\nabla}_R\cdot\left[\frac{\partial\psi_R}{\partial\boldsymbol{\nabla}_R\left[\,c_{L_R}\right]}\right]\right] \\ &+ \left[\frac{\partial\psi_R}{\partial c_{L_R}} - \frac{\partial\psi_R}{\partial c_{T_R}} - T\left(\frac{\partial^2\psi_R}{\partial T\,\partial c_{L_R}} - \frac{\partial^2\psi_R}{\partial T\,\partial c_{T_R}}\right) - \boldsymbol{\nabla}_R\cdot\left[\frac{\partial\psi_R}{\partial\boldsymbol{\nabla}_R\left[\,c_{L_R}\right]}\right]\right]\,w_R^{(6.14)}\;. \end{aligned} \tag{C.9}$$

Chapter 7

A non-relativistic theoretical coupled framework of Galilean electromagnetism with finite strain continuum thermo-mechanics

Matteo Arricca[1,2], Alberto Salvadori[1,2] and Robert M. McMeeking[1,3,4,5]

[1]The Mechanobiology Research Center, UNIBS, Italy
[2]Department of Mechanical and Industrial Engineering, University of Brescia, Italy
[3]Materials and Mechanical Engineering Departments, University of California, Santa Barbara, USA
[4]School of Engineering, University of Aberdeen, King's College, Scotland, United Kingdom
[5]INM-Leibniz Institute for New Materials, Saarbruecken 66123, Germany

Abstract. We propose a general non-relativistic theory to couple Galilean electromagnetism with thermodynamics and finite strain continuum mechanics. The two pairs of Maxwell's equations, and the aether relations in the form due to Lorentz, are provided in Lagrangian formulation and in terms of Galilean invariants for a moving and deformable body. No restrictions on the electromagnetic theory are assumed early on, yielding an exhaustive treatment of all phenomena involved in considering a charge-carrying convecting body. The Euler's laws of mechanics are coupled with the electromagnetic theory in two places. We introduce a *new* velocity vector field, which encompasses the material velocity plus some electromagnetic terms, and whose specifications is stated by thermodynamic prescriptions. Furthermore, the component of the electromagnetic surface traction and body force are considered, in addition to the mechanical forces. Rather, the coupling between electromagnetism and thermodynamics is ensured by the introduction of an electromagnetic energy flux vector that had a set of expenditure of power in the body due to electric and the magnetic fields. A fully coupled finite strain electro-magneto-thermo-mechanical formulation results therefore provided. The electromagnetic Helmholtz free energy density is properly selected to account for electric and magnetic effects, and to further yield all the necessary thermodynamic prescriptions. Constitutive specifications of the conduction current density and the heat flux are provided before emanating the governing equations.

7.1 Introduction

We follow the thoroughness of the method used by Kovetz [225] to couple the Galilean electromagnetic theory for a moving and deformable body, with finite strain continuum mechanics and thermodynamics. The a-priori specification of some common transformation rules for configuration changes allows us to directly provide the Lagrangian formulation of the first and second pair of Maxwell's equations in integral form, before proper localization. The aether relations in the form due to Lorentz are analogously formulated in Lagrangian description and allows to couple the first and the second pairs of Maxwell's equations, and to provide a (first) connection between electromagnetism and mechanics. The necessity to write the framework in terms of electromagnetic Galilean invariants results from the consideration of a charge-carrying moving and deformable body (see [225]).

The seminal article by Le Bellac and Lévy-Leblond [226] has paved the way towards the Galilean electromagnetic theory, identifying two Galilean limits (electric and magnetic), and providing a more general Galilean invariant theory. An incomplete list of publications concerning Galilean electromagnetism comprises the works of Santos *et al.* [227], where a non-relativistic Galilean covariant Lagrangian model was proposed; Rousseaux [228], who identified how the Lorenz gauge condition applies in the electric limit of [226], whereas the Coulomb gauge condition is the magnetic limit of the Lorenz gauge condition; de Montigny and Rousseaux [229], where some applications of Galilean electrodynamics of moving bodies were discussed; Heras [230], who introduced a third instantaneous limit for speed light at the limit at infinity, in addition to the two Galilean limits of Maxwell's equation identified in [226]; and lastly, still Rousseaux [231], who presented a review on Galilean electromagnetism entitled *Forty years of Galilean Electromagnetism (1973–2013).*

An exhaustive treatment of Galilean electromagnetism falls beyond the scope of this paper. Therefore, we use the general Galilean electromagnetic theory presented in [225], and we keep the focus on the coupling betwee Galilean electromagnetism and finite strain thermo-mechanics, where the electromagnetic theory not subjected to any restriction.

In the current paper, we re-phrase the *classical* Euler's laws of mechanics in terms of electro-magneto-mechanical laws in two places. Following [225], we introduce a *new* velocity vector field, which differs from the material velocity for the presence of electromagnetic effects and whose specifications arises after thermodynamic prescriptions. Furthermore, making reference to the work of McMeeking and Landis [232], we consider *total* surface traction and body forces, given by the sum of mechanical and electromagnetic contributions. Consequently, the resultant stress tensor appearing in the local form of the Euler's laws is not constrained to a purely mechanical stress. Rather, we define the total *true* stress in the material, which encompasses the sum of the Piola and Maxwell stresses, and where the latter reads as the Maxwell stress in regions of space without material [232, 233].

Inspiration is taken from the just mentioned works [232, 233], where a coupled framework of mechanics with electrostatics has been formulated. Electrical traction and body forces have been introduced in addition to mechanical forces. It has been established that the mechanical and the electrical tractions must be balanced by the mechanical (Cauchy) stress difference across a surface, whereas the sum of Cauchy and Maxwell stresses has been termed total *true* stress in the material. The consideration of the total *true* stress has been motivated by the lack of experiments that allow to separate the effects of mechanical and electrical stresses unambiguously [232, 234, 235, 236]. Similar procedures on the forces splitting have been performed in [40], within a finite strain multi-physics mechanical formulation for ion transport, which also encompasses the additional contribution of chemical traction and body forces. For an exhaustive treatment on the electromagnetic forces in deformable bodies we refer to the works of Pao [237], Maugin [238] and Tiersten [239], to cite a few.

It is also worth to mention some works of Dorfmann and Ogden, in the field of non-linear magnetoelasticity [240], magnetoelasticity for elastomers [241, 242], and electroelasticity [243]. Additionally, such frameworks are rephrased in Lagrangian description. In the more general formulation previously proposed by the same authors [242], Galilean invariance in thermodynamic equations is also accounted for, prior to reduce the system of equations for magneto-elastic elastomers. Electromagnetic body force [242], magnetic body force [240, 241], and electric body force [243] have been considered. A total stress given by the sum of the Cauchy and (electric or magnetic) Maxwell stresses has been conveniently used.

Comprehensive analysis and discussion on the Maxwell stress, and the identification of the body force arising from two-particle force interactions as its divergence are detailed in [244], in contrast to [245] where the Maxwell stress was interpreted as a surface traction to justify two-particle force interactions.

The coupling between electromagnetism and thermodynamics occurs by means of the energy balance. The introduction of an electromagnetic energy flux vector, and the presence of the *new* velocity in the (electro-magneto-)mechanical external power arising from Euler's laws, establish the coupling between the Galilean electromagnetic theory with finite strain thermo-mechanics. The non trivial manipulation of the electromagnetic energy flux vector leads to the introduction of an electromagnetic nominal stress tensor, in which the Maxwell stress in the aether appears explicitly as a result of the proper manipulation of the electromagnetic vector identity. Such electromagnetic stress tensor encompasses the total *true* stress in the material and the Maxwell stress in the aether, leading to a similar stresses coupling introduced in [232, 233], plus an additional electromagnetic term arising from the the consideration of Galilean invariants.

The Clausius-Duhem inequality and resulting thermodynamic prescriptions are derived by means of the method of Coleman and Noll [8], as standard in thermodynamics. For the theory at hand, in addition to select properly the electromagnetic Helmholtz free energy internal variables dependence, constitutive specifications are required for the heat flux vector and the conduction current density vector.

The manuscript is organized as follows. Section 7.2 provides some standard definition in finite strain continuum mechanics, and the necessary transformation rules to derive all equations in Lagrangian formulation. The charge conservation law is introduced in Section 7.3. The Lagrangian formulation of Maxwell's equations and aether relations, in terms of Galilean invariants for a convecting body, is presented in Section 7.4. Section 7.5 defines the electro-magneto-mechanical balance laws. Thermodynamics is dealt in Section 7.6. Constitutive specifications for the heat flux and conduction current vectors in Section 7.7 and governing equations in Section 7.8 complete the paper.

7.2 Definitions

7.2.1 Motion and deformation gradient.

Denote with $\mathcal{B}_t \in \mathbb{R}^3$ the spatial description of an advecting body volume and with $\partial\mathcal{B}_t$ its surface. Let $\mathcal{B}_{_R}$ and $\partial\mathcal{B}_{_R}$ be their referential (material) counterparts, as standard in the finite strain theory in continuum mechanics [53, 54]. The transformation of a material point $\boldsymbol{X} \in \mathcal{B}_{_R}$ into a spatial point $\boldsymbol{x} \in \mathcal{B}_t$ is described by means of a smooth function $\boldsymbol{\chi}(\boldsymbol{X}, t)$

$$\boldsymbol{x} = \boldsymbol{\chi}(\boldsymbol{X}, t) \ ,$$

with $\boldsymbol{\chi}(\boldsymbol{X}, t)$ one-to-one map representing the motion of $\boldsymbol{X} \in \mathcal{B}_{_R}$ at time t. We assume that $\mathcal{B}_t$ at $t = 0$ coincides with $\mathcal{B}_{_R}$, *i.e.*, for all material points $\boldsymbol{X} = \boldsymbol{\chi}(\boldsymbol{X}, 0)$. The material velocity is given by $\dot{\boldsymbol{\chi}}(\boldsymbol{X}, t)$, whereas displacements write as $\boldsymbol{u} = \boldsymbol{\chi} - \boldsymbol{X}$.

At a fixed time t, we name

$$\mathbf{F} = \boldsymbol{\nabla}_{_R} \left[\boldsymbol{\chi}(\boldsymbol{X}, t) \right] \tag{7.1}$$

the deformation gradient, with $\mathrm{F}_{ij} = \partial\chi_i / \partial X_j$.

Only motions such that

$$J = \det\left[\mathbf{F} \right] > 0$$

are admissible, in order to avoid total material compaction.

7.2.2 Transformation rules.

Denote with $\mathcal{P}_t \subset \mathcal{B}_t$ an arbitrary volume region, with surface $\partial\mathcal{P}_t \subset \partial\mathcal{B}_t$, and let $\mathcal{P}_{_R} \subset \mathcal{B}_{_R}$ and $\partial\mathcal{P}_{_R} \subset \partial\mathcal{B}_{_R}$ define their respective material descriptions (see Figure 7.1). Take two generic tensorial

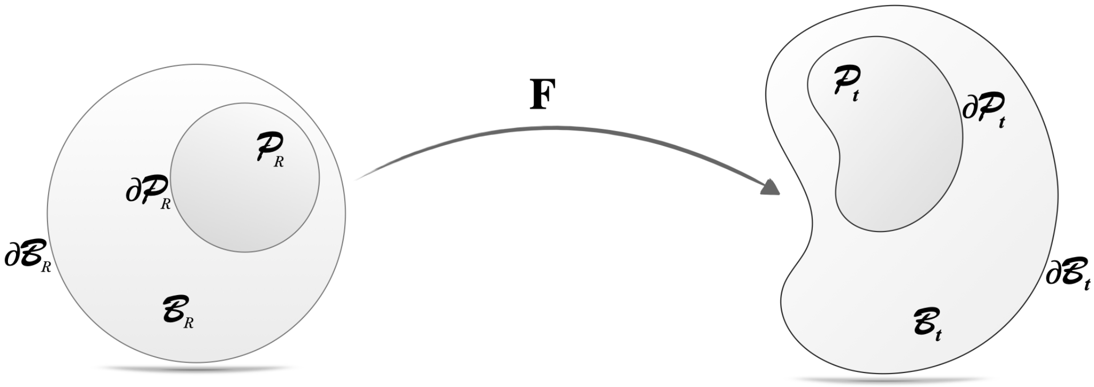

Figure 7.1: Schematic representation of the material and spatial configuration $\mathcal{B}_R$ and $\mathcal{B}_t$, with boundaries $\partial\mathcal{B}_R$ and $\partial\mathcal{B}_t$, and of a generic sub-part $\mathcal{P}_t \subset \partial\mathcal{P}_t$, image of $\mathcal{P}_R \subset \partial\mathcal{P}_R$, with boundaries $\partial\mathcal{P}_t$ and $\partial\mathcal{P}_R$, respectively.

functions of any order $f^{\mathcal{V}}(\boldsymbol{x},t) \in \mathcal{P}_t$ and $f^{\mathcal{V}}_R(\boldsymbol{X},t) \in \mathcal{P}_R$. If

$$\int_{\mathcal{P}_t} f^{\mathcal{V}}(\boldsymbol{x},t)\,\mathrm{d}v = \int_{\mathcal{P}_R} f^{\mathcal{V}}_R(\boldsymbol{X},t)\,\mathrm{d}\mathcal{V}\,, \tag{7.2}$$

then, according to the Nanson's formula for volume changes, $\mathrm{d}v = J(\boldsymbol{X},t)\,\mathrm{d}\mathcal{V}$, the following transformation rule applies

$$f^{\mathcal{V}}_R(\boldsymbol{X},t) = J(\boldsymbol{X},t)\,f^{\mathcal{V}}(\boldsymbol{x}(\boldsymbol{X},t),t)\,. \tag{7.3}$$

Let $\boldsymbol{f}^{\mathcal{S}}(\boldsymbol{x},t)$ be a spatial vector, with $\boldsymbol{x} \in \partial\mathcal{P}_t$ and $\partial\mathcal{P}_t$ oriented surface defined by the direction of the outward normal vector $\boldsymbol{n}$. Denote with $\boldsymbol{f}^{\mathcal{S}}_R(\boldsymbol{X},t)$ its referential counterpart, with $\boldsymbol{X} \in \partial\mathcal{P}_R$ and $\boldsymbol{n}_R$ outward normal vector to the oriented surface $\partial\mathcal{P}_R$. It holds

$$\int_{\partial\mathcal{P}_t} \boldsymbol{f}^{\mathcal{S}}(\boldsymbol{x},t)\cdot\boldsymbol{n}\,\mathrm{d}a = \int_{\partial\mathcal{P}_R} \boldsymbol{f}^{\mathcal{S}}_R(\boldsymbol{X},t)\cdot\boldsymbol{n}_R\,\mathrm{d}\mathcal{A}\,. \tag{7.4}$$

By means of the Nanson's formula for area changes,

$$\boldsymbol{n}\,\mathrm{d}a = J\,\mathbf{F}^{-\mathrm{T}}\,\boldsymbol{n}_R\,\mathrm{d}\mathcal{A}\,, \tag{7.5}$$

the material vector $\boldsymbol{f}^{\mathcal{S}}_R$ transforms according to

$$\boldsymbol{f}^{\mathcal{S}}_R(\boldsymbol{X},t) = J(\boldsymbol{X},t)\,\mathbf{F}^{-1}(\boldsymbol{X},t)\,\boldsymbol{f}^{\mathcal{S}}(\boldsymbol{x}(\boldsymbol{X},t),t)\,. \tag{7.6}$$

Let $\mathcal{C}_t$ be the boundary of an oriented surface $\partial\mathcal{P}_t \subset \partial\mathcal{B}_t$, and $\mathcal{C}_R$ its referential description. Denote with $\boldsymbol{l}(\boldsymbol{x},t)$ and $\boldsymbol{l}_R(\boldsymbol{X},t)$ the tangent vectors at $\boldsymbol{x} \in \mathcal{C}_t$ and $\boldsymbol{X} \in \mathcal{C}_R$, respectively (see Figure 7.2), and recall the covariant transformation rule for tangent vectors,

$$\boldsymbol{l} = \mathbf{F}\,\boldsymbol{l}_R\,. \tag{7.7}$$

Let $\boldsymbol{f}^{\mathcal{L}}(\boldsymbol{x},t)$ denote a vector field and $\boldsymbol{f}^{\mathcal{L}}_R(\boldsymbol{X},t)$ its referential counterpart. By means of the Stokes' theorem,

$$\int_{\partial\mathcal{P}_t} \boldsymbol{\nabla}\times[\,\boldsymbol{f}^{\mathcal{L}}\,]\cdot\boldsymbol{n}\,\mathrm{d}a = \int_{\mathcal{C}_t} \boldsymbol{f}^{\mathcal{L}}\cdot\boldsymbol{l}\,\mathrm{d}\ell\,, \tag{7.8}$$

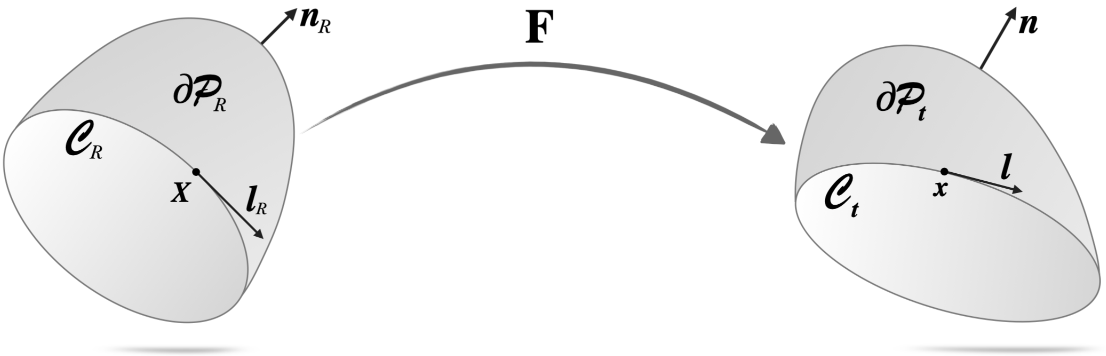

Figure 7.2: Schematic representation of a generic open material and spatial surface $\partial\mathcal{P}_R$ and $\partial\mathcal{P}_t$, bounded by $\mathcal{C}_R$ and $\mathcal{C}_t$, and oriented according to the direction of $\boldsymbol{n}_R$ and $\boldsymbol{n}$, respectively.

and taking advantage from the right-hand side term of Eq. (7.8), it holds

$$\int_{\mathcal{C}_t} \boldsymbol{f}^{\mathcal{L}}(\boldsymbol{x},t)\cdot\boldsymbol{l}\,\mathrm{d}\ell = \int_{\mathcal{C}_R} \boldsymbol{f}^{\mathcal{L}}_R(\boldsymbol{X},t)\cdot\boldsymbol{l}_R\,\mathrm{d}\mathcal{L}\;. \tag{7.9}$$

Making use of Eq. (7.7) to re-write the tangent vector $\boldsymbol{l}$,

$$\int_{\mathcal{C}_t} \boldsymbol{f}^{\mathcal{L}}(\boldsymbol{x},t)\cdot\boldsymbol{l}\,\mathrm{d}\ell = \int_{\mathcal{C}_R} \boldsymbol{f}^{\mathcal{L}}(\boldsymbol{x}(\boldsymbol{X},t),t)\cdot\mathbf{F}(\boldsymbol{X},t)\,\boldsymbol{l}_R\,\mathrm{d}\mathcal{L} = \int_{\mathcal{C}_R} \boldsymbol{f}^{\mathcal{L}}_R(\boldsymbol{x},t)\cdot\boldsymbol{l}_R\,\mathrm{d}\mathcal{L}\;, \tag{7.10}$$

the transformation rule for the vector field $\boldsymbol{f}^{\mathcal{L}}(\boldsymbol{x},t)$ is stated as

$$\boldsymbol{f}^{\mathcal{L}}_R(\boldsymbol{X},t) = \mathbf{F}^{\mathrm{T}}(\boldsymbol{X},t)\,\boldsymbol{f}^{\mathcal{L}}(\boldsymbol{x}(\boldsymbol{X},t),t)\;. \tag{7.11}$$

It further holds

$$\int_{\partial\mathcal{P}_t} \boldsymbol{\nabla}\times[\,\boldsymbol{f}^{\mathcal{L}}(\boldsymbol{x},t)\,]\cdot\boldsymbol{n}\,\mathrm{d}a = \int_{\partial\mathcal{P}_R} \boldsymbol{\nabla}_R\times\left[\,\boldsymbol{f}^{\mathcal{L}}_R(\boldsymbol{X},t)\,\right]\cdot\boldsymbol{n}_R\,\mathrm{d}\mathcal{A}\;. \tag{7.12}$$

7.3 Charge conservation

The electric charge is a property of the material and has to be interpreted as uniformly distributed over the volume of the body. It is therefore possible to define a charge density ζ_R as

$$\mathrm{Z}_R = \int_{\mathcal{P}_R} \zeta_R\,\mathrm{d}\mathcal{V}\;. \tag{7.13}$$

It is assumed that ζ_R is a conservative quantity which therefore obeys to the conservation law

$$\overline{\int_{\mathcal{P}_R} \zeta_R\,\mathrm{d}\mathcal{V}}^{\,\cdot} + \int_{\partial\mathcal{P}_R} \boldsymbol{j}_R\cdot\boldsymbol{n}_R\,\mathrm{d}\mathcal{A} = 0\;, \tag{7.14}$$

with $\boldsymbol{j}_R$ referential current density.

Application of the divergence theorem yields

$$\dot{\zeta}_R + \boldsymbol{\nabla}_R\cdot\left[\,\boldsymbol{j}_R\,\right] = 0\;, \tag{7.15}$$

for any arbitrary $\mathcal{P}_R \subset \mathcal{B}_R$.

7.4 The referential laws of electromagnetism

The first two principles of electromagnetism are represented by the first and second pair of Maxwell's equations, respectively. The first pair of Maxwell's equations deals with the conservation law for the charge density ζ_R, whereas the second pair can be seen as a conservation law for the magnetic flux [225]. The aether relations represent the third principle of electromagnetism. In addition to provide a link between Maxwell's equations, they establish a connection between electromagnetism and mechanics by assuming the existence of an inertial frame in which the aether relations hold [225].

7.4.1 Maxwell's equations for a convecting body.

The first pair of Maxwell's equations *i*) relates ζ_R with the flux of the electric displacement $\boldsymbol{D}_R$ through $\partial\mathcal{P}_R$, and *ii*) establishes the link among the ratio of the flux of $\boldsymbol{D}_R$, the flux of the conduction current density $\boldsymbol{\mathcal{J}}_R$ through $\partial\mathcal{P}_R$, and the circulation of the magnetomotive intensity $\boldsymbol{\mathcal{H}}_R$ along the contour $\mathcal{C}_R$. In integral form,

$$\int_{\mathcal{P}_R} \zeta_R \,\mathrm{d}\mathcal{V} = \int_{\partial\mathcal{P}_R} \boldsymbol{D}_R \cdot \boldsymbol{n}_R \,\mathrm{d}\mathcal{A} \,, \tag{7.16a}$$

$$\int_{\partial\mathcal{P}_R} \boldsymbol{\mathcal{J}}_R \cdot \boldsymbol{n}_R \,\mathrm{d}\mathcal{A} = \int_{\mathcal{C}_R} \boldsymbol{\mathcal{H}}_R \cdot \boldsymbol{l}_R \,\mathrm{d}\mathcal{L} - \dot{\overline{\int_{\partial\mathcal{P}_R} \boldsymbol{D}_R \cdot \boldsymbol{n}_R \,\mathrm{d}\mathcal{A}}} \,, \tag{7.16b}$$

for any arbitrary $\mathcal{P}_R \subset \mathcal{B}_R$ with surface $\partial\mathcal{P}_R \subset \partial\mathcal{B}_R$ bounded by $\mathcal{C}_R$.

Terms in Eq.s (7.16) transform as follow. The referential current density ζ_R transforms according to Eq. (7.3), $\boldsymbol{D}_R$ and $\boldsymbol{\mathcal{J}}_R$ as Eq. (7.6), whereas $\boldsymbol{\mathcal{H}}_R$ follows the transformation rule (7.11), namely,

$$\zeta_R = J\,\zeta \,, \qquad \boldsymbol{D}_R = J\,\mathbf{F}^{-1}\,\boldsymbol{D} \,, \qquad \boldsymbol{\mathcal{J}}_R = J\,\mathbf{F}^{-1}\,\boldsymbol{\mathcal{J}} \,, \qquad \boldsymbol{\mathcal{H}}_R = \mathbf{F}^{\mathrm{T}}\,\boldsymbol{\mathcal{H}} \,. \tag{7.17}$$

The conduction current density $\boldsymbol{\mathcal{J}}_R$ and the magnetomotive intensity $\boldsymbol{\mathcal{H}}_R$ represent Galilean invariants for the current density $\boldsymbol{j}_R$ and the current potential $\boldsymbol{H}_R$, respectively. It holds

$$\boldsymbol{\mathcal{J}}_R = \boldsymbol{j}_R - \zeta_R\,\mathbf{F}^{-1}\,\dot{\boldsymbol{\chi}} \,, \qquad \boldsymbol{\mathcal{H}}_R = \boldsymbol{H}_R - \mathbf{F}^{\mathrm{T}}\left(\dot{\boldsymbol{\chi}} \times J^{-1}\mathbf{F}\,\boldsymbol{D}_R\right) \,, \tag{7.18}$$

where $\boldsymbol{H}_R$ transforms according to Eq. (7.11), as $\boldsymbol{\mathcal{H}}_R$.

Application of the divergence and Stokes' theorem to Eq.s (7.16) yields

$$\int_{\mathcal{P}_R} \zeta_R \,\mathrm{d}\mathcal{V} = \int_{\mathcal{P}_R} \boldsymbol{\nabla}_R \cdot [\,\boldsymbol{D}_R\,] \,\mathrm{d}\mathcal{V} \,, \tag{7.19a}$$

$$\int_{\partial\mathcal{P}_R} \boldsymbol{\mathcal{J}}_R \cdot \boldsymbol{n}_R \,\mathrm{d}\mathcal{A} = \int_{\partial\mathcal{P}_R} \boldsymbol{\nabla}_R \times [\,\boldsymbol{\mathcal{H}}_R\,] \cdot \boldsymbol{n}_R \,\mathrm{d}\mathcal{A} - \int_{\partial\mathcal{P}_R} \dot{\boldsymbol{D}}_R \cdot \boldsymbol{n}_R \,\mathrm{d}\mathcal{A} \,, \tag{7.19b}$$

for any arbitrary $\mathcal{P}_R \subset \mathcal{B}_R$ and $\partial\mathcal{P}_R \subset \partial\mathcal{B}_R$.

The second pair of Maxwell's equations *i*) states that the magnetic field $\boldsymbol{B}_R$ is divergence free, and *ii*) links the ratio of $\boldsymbol{B}_R$ to the circulation of the electromotive intensity $\boldsymbol{\mathcal{E}}_R$ along the boundary $\mathcal{C}_R$. In integral form,

$$\int_{\partial\mathcal{P}_R} \boldsymbol{B}_R \cdot \boldsymbol{n}_R \,\mathrm{d}\mathcal{A} = 0 \,, \tag{7.20a}$$

$$\dot{\overline{\int_{\partial\mathcal{P}_R} \boldsymbol{B}_R \cdot \boldsymbol{n}_R \,\mathrm{d}\mathcal{A}}} = -\int_{\mathcal{C}_R} \boldsymbol{\mathcal{E}}_R \cdot \boldsymbol{l}_R \,\mathrm{d}\mathcal{L} \,, \tag{7.20b}$$

for all $\partial\mathcal{P}_R \subset \partial\mathcal{B}_R$ bounded by $\mathcal{C}_R$.

The magnetic field $\boldsymbol{B}_R$ and the electromotive intensity $\boldsymbol{\mathcal{E}}_R$ transform according to Eq.s (7.6) and (7.11), respectively, therefore

$$\boldsymbol{B}_R = J\,\mathbf{F}^{-1}\,\boldsymbol{B} \,, \qquad \boldsymbol{\mathcal{E}}_R = \mathbf{F}^{\mathrm{T}}\,\boldsymbol{\mathcal{E}} \,. \tag{7.21}$$

The electromotive intensity $\boldsymbol{\mathcal{E}}_R$ represents the Galilean invariant for the electric field $\boldsymbol{E}_R$,

$$\boldsymbol{\mathcal{E}}_R = \boldsymbol{E}_R + \mathbf{F}^{\mathrm{T}} \left(\dot{\boldsymbol{\chi}} \times J^{-1} \, \mathbf{F} \, \boldsymbol{B}_R \right) \ , \tag{7.22}$$

with $\boldsymbol{E}_R$ transforming according to Eq. (7.11), as $\boldsymbol{\mathcal{E}}_R$.

Application of the divergence and Stokes' theorem to Eq.s (7.20) yields

$$\int_{\mathcal{P}_R} \boldsymbol{\nabla}_R \cdot [\, \boldsymbol{B}_R \,] \, \mathrm{d}\mathcal{V} = 0 \ , \tag{7.23a}$$

$$\int_{\partial\mathcal{P}_R} \dot{\boldsymbol{B}}_R \cdot \boldsymbol{n}_R \, \mathrm{d}\mathcal{A} = - \int_{\partial\mathcal{P}_R} \boldsymbol{\nabla}_R \times [\, \boldsymbol{\mathcal{E}}_R \,] \cdot \boldsymbol{n}_R \, \mathrm{d}\mathcal{A} \ , \tag{7.23b}$$

for any arbitrary sub-part $\mathcal{P}_R \subset \mathcal{B}_R$ and $\partial\mathcal{P}_R \subset \partial\mathcal{B}_R$.

7.4.2 The Lorentz's aether relations.

Let $\boldsymbol{P}_R$ and $\boldsymbol{\mathcal{M}}_R$ define the polarization and the Lorentz magnetization, respectively. The latter represents the Galilean invariant for the magnetization $\boldsymbol{M}_R$. We write the Lagrangian formulation of the third principle of electromagnetism, in the form due to Lorentz, as

$$\boldsymbol{D}_R = \kappa_0 \, J \, \mathbf{C}^{-1} \boldsymbol{E}_R + \boldsymbol{P}_R \ , \tag{7.24a}$$

$$\boldsymbol{\mathcal{H}}_R = \mu_0^{-1} J^{-1} \mathbf{C} \, \boldsymbol{B}_R - \mathbf{F}^{\mathrm{T}} \left(\dot{\boldsymbol{\chi}} \times \kappa_0 \, \mathbf{F}^{-\mathrm{T}} \boldsymbol{E}_R \right) - \boldsymbol{\mathcal{M}}_R \ . \tag{7.24b}$$

Eq.s (7.24) states the existence of an inertial frame and hold everywhere and at all times, both within the body and in the empty space. Universal constants κ_0 and μ_0 are positive defined, whereas $\mathbf{C} = \mathbf{F}^{\mathrm{T}}\mathbf{F}$ represents the right Cauchy-Green strain tensor.

Note that aether relations (7.24) provide a connection between (charge and current) potentials and (electric and magnetic) fields, and therefore deal with terms that respond to different laws of transformation.

As made clear in [243], transformation rule for the polarization vector $\boldsymbol{P}_R$ is not uniquely defined, and the same applies to the Lorentz magnetization $\boldsymbol{\mathcal{M}}_R$. Following [243], Eq. (7.24a) implies that $\boldsymbol{P}_R$ transforms as $\boldsymbol{D}_R$, according to Eq. (7.6), hence

$$\boldsymbol{P}_R = J \, \mathbf{F}^{-1} \, \boldsymbol{P} \ , \tag{7.25}$$

whereas $\boldsymbol{\mathcal{M}}_R$ in Eq. (7.24b), which is given by the relation

$$\boldsymbol{\mathcal{M}}_R = \boldsymbol{M}_R + \mathbf{F}^{\mathrm{T}} \left(\dot{\boldsymbol{\chi}} \times J^{-1} \, \mathbf{F} \, \boldsymbol{P}_R \right) \ , \tag{7.26}$$

following [241], transforms as $\boldsymbol{\mathcal{H}}_R$, according to Eq. (7.11), and the same choice has been performed on $\boldsymbol{M}_R$. Therefore,

$$\boldsymbol{\mathcal{M}}_R = \mathbf{F}^{\mathrm{T}} \, \boldsymbol{\mathcal{M}} \ , \qquad \boldsymbol{M}_R = \mathbf{F}^{\mathrm{T}} \, \boldsymbol{M} \ . \tag{7.27}$$

7.4.3 Local form of the three principles of Galilean electromagnetism.

The coupling between the two pairs of Maxwell's equations (7.19) and (7.23) and the aether relations (7.24) establishes the referential form of the three principles of Galilean electromagnetism. Since they must hold for any arbitrary sub-part $\mathcal{P}_R \subset \mathcal{B}_R$, and $\partial\mathcal{P}_R \subset \partial\mathcal{B}_R$, they can be localized as

$$\boldsymbol{\nabla}_R \cdot [\, \boldsymbol{D}_R \,] = \zeta_R \ , \tag{7.28a}$$

$$\boldsymbol{\nabla}_R \times [\, \boldsymbol{\mathcal{H}}_R \,] = \boldsymbol{\mathcal{J}}_R + \dot{\boldsymbol{D}}_R \ , \tag{7.28b}$$

$$\boldsymbol{\nabla}_R \cdot [\, \boldsymbol{B}_R \,] = 0 \ , \tag{7.28c}$$

$$\boldsymbol{\nabla}_R \times [\, \boldsymbol{\mathcal{E}}_R \,] = -\dot{\boldsymbol{B}}_R \ , \tag{7.28d}$$

$$\boldsymbol{D}_R = \kappa_0 \, J \, \mathbf{C}^{-1} \boldsymbol{E}_R + \boldsymbol{P}_R \ , \tag{7.28e}$$

$$\boldsymbol{\mathcal{H}}_R = \mu_0^{-1} J^{-1} \mathbf{C} \, \boldsymbol{B}_R - \mathbf{F}^{\mathrm{T}} \left(\dot{\boldsymbol{\chi}} \times \kappa_0 \, \mathbf{F}^{-\mathrm{T}} \boldsymbol{E}_R \right) - \boldsymbol{\mathcal{M}}_R \ . \tag{7.28f}$$

7.5 The Euler's laws of electro-magneto-mechanics

Assuming the existence of an inertial frame in which, for a fixed point $\boldsymbol{O}$, the Euler's laws of mechanics hold, the presence of an electromagnetic field implies some modifications to the *classical* mechanical laws.

Following [225], we assume the existence of a *new* velocity vector field $\boldsymbol{\gamma}$, which must reduce to $\dot{\boldsymbol{\chi}}$ in absence of any electric and magnetic effect. Furthermore, we follow the same path of reasoning of [232] to introduce the components of the electromagnetic surface traction $\boldsymbol{t}_R^{\mathcal{E}}$ and the body force $\boldsymbol{b}_R^{\mathcal{E}}$, in addition to the mechanical forces. Also, the assumption of electromagnetic effects that induce first order moments must be allowed, *e.g.*, due to electric and magnetic fields acting on dipoles in the material [232].

Accordingly, the principles of conservation of linear and angular momentum are stated as

$$\overset{\cdot}{\overline{\int_{\mathcal{P}_R} \rho_R\, \boldsymbol{\gamma}\, \mathrm{d}\mathcal{V}}} = \int_{\partial\mathcal{P}_R} \boldsymbol{t}_R + \boldsymbol{t}_R^{\mathcal{E}}\, \mathrm{d}\mathcal{A} + \int_{\mathcal{P}_R} \boldsymbol{b}_{0_R} + \boldsymbol{b}_R^{\mathcal{E}}\, \mathrm{d}\mathcal{V} \,, \tag{7.29a}$$

and

$$\overset{\cdot}{\overline{\int_{\mathcal{P}_R} \boldsymbol{\chi} \times \rho_R\, \boldsymbol{\gamma}\, \mathrm{d}\mathcal{V}}} = \int_{\partial\mathcal{P}_R} \boldsymbol{\chi} \times (\boldsymbol{t}_R + \boldsymbol{t}_R^{\mathcal{E}})\, \mathrm{d}\mathcal{A} + \int_{\mathcal{P}_R} \boldsymbol{\chi} \times (\boldsymbol{b}_{0_R} + \boldsymbol{b}_R^{\mathcal{E}})\, \mathrm{d}\mathcal{V} + \int_{\mathcal{P}_R} \boldsymbol{O}^{\mathcal{E}}\, \mathrm{d}\mathcal{V} \,. \tag{7.29b}$$

Terms in Eq.s (7.29) have the following meaning. The scalar ρ_R is the referential mass density. Vectors $\boldsymbol{t}_R$ and $\boldsymbol{b}_{0_R}$ are the mechanical surface traction and the conventional body force that not encompass the inertial body force. Inertial effects are accounted for within the left-hand side term of Eq.s (7.29). The sums of mechanical and electromagnetic forces are termed *total* surface traction and *total* body force. Vector $\boldsymbol{O}^{\mathcal{E}}$ stands for the assumption of an angular momentum due to the combined effects of electric and magnetic dipoles [232, 40].

We further assume the same relations-type stated in [232] in the field of electroelasticity. Therefore, the electromagnetic body force is derived from the Maxwell stress in regions of space without material $\mathbf{T}_R^{\mathrm{M}}$, according to

$$\boldsymbol{b}_R^{\mathcal{E}} = \boldsymbol{\nabla}_R \cdot [\, \mathbf{T}_R^{\mathrm{M}} \,] \,, \tag{7.30}$$

with $\boldsymbol{\nabla}_R \cdot [\, \mathbf{T}_R^{\mathrm{M}} \,] = \partial \mathrm{T}^{\mathrm{M}}_{R\,ij} / \partial X_j$. The traction relation for the Maxwell stress writes as

$$\boldsymbol{t}_R^{\mathcal{E}} = \| \mathbf{T}_R^{\mathrm{M}} \| \, \boldsymbol{n}_R \,, \tag{7.31}$$

with $\| \mathbf{T}_R^{\mathrm{M}} \|$ Maxwell stress difference across a surface.

To satisfy the balance of linear momentum (7.29a) the Piola stress $\mathbf{T}_R$ must balance the *total* surface traction, hence

$$\int_{\partial\mathcal{P}_R} \boldsymbol{t}_R + \boldsymbol{t}_R^{\mathcal{E}}\, \mathrm{d}\mathcal{A} = -\int_{\partial\mathcal{P}_R} \| \mathbf{T}_R \| \, \boldsymbol{n}_R\, \mathrm{d}\mathcal{A} = \int_{\mathcal{P}_R} \boldsymbol{\nabla}_R \cdot [\, \mathbf{T}_R \,]\, \mathrm{d}\mathcal{V} \,, \tag{7.32}$$

with $\| \mathbf{T}_R \|$ mechanical stress difference across a surface, and $\boldsymbol{\nabla}_R \cdot [\, \mathbf{T}_R \,] = \partial \mathrm{T}_{R\,ij} / \partial X_j$. The second right-hand side term of Eq. (7.32) establishes the following relation for the mechanical traction

$$\boldsymbol{t}_R = -\| \mathbf{T}_R + \mathbf{T}_R^{\mathrm{M}} \| \, \boldsymbol{n}_R \,. \tag{7.33}$$

Since any mechanical traction $\boldsymbol{t}_R$ is related to the sum of the Piola and Maxwell stresses, Eq. (7.33) clarifies why it is more effective to consider the sum of the mechanical and electromagnetic stresses instead of trying to identify them separately [232, 233]. Nevertheless, following the *standard* procedures in finite strain continuum mechanics, according to the Nanson's formula for area changes (7.5), we state

$$\mathbf{T}_R = J\, \mathbf{T}\, \mathbf{F}^{-\mathrm{T}} \,, \qquad \mathbf{T}_R^{\mathrm{M}} = J\, \mathbf{T}^{\mathrm{M}}\, \mathbf{F}^{-\mathrm{T}} \,, \tag{7.34}$$

with $\mathbf{T}$ and $\mathbf{T}^{\rm M}$ spatial mechanical (Cauchy) and Maxwell stresses.

Application of the divergence theorem to Eq.s (7.29), combinations with Eq.s (7.30), (7.32) and (7.33), and recognition that the resultant integrals must hold for any arbitrary $\mathcal{P}_R \subset \mathcal{B}_R$ lead to the following local forms of the balance of linear momentum

$$\rho_R \, \dot{\boldsymbol{\gamma}} = \boldsymbol{\nabla}_R \cdot [\, \mathbf{T}_R \,] + \boldsymbol{\nabla}_R \cdot [\, \mathbf{T}^{\rm M}_R \,] + \boldsymbol{b}_{0R} \ , \tag{7.35a}$$

and the angular momentum

$$[\mathbf{T}_R + \mathbf{T}^{\rm M}_R] \ \mathbf{F}^{\rm T} + \dot{\boldsymbol{\chi}} \otimes \rho_R \, \boldsymbol{\gamma} = \mathbf{F} \ [\mathbf{T}_R + \mathbf{T}^{\rm M}_R]^{\rm T} + \rho_R \, \boldsymbol{\gamma} \otimes \dot{\boldsymbol{\chi}} \ , \tag{7.35b}$$

with $\mathbf{T}_R + \mathbf{T}^{\rm M}_R$ total *true* stress in the material. Derivation of Eq. (7.35b) is collected in Appendix D.1.

Note that the standard definition of the conservation of angular momentum in finite strain continuum mechanics, $\mathbf{T}_R \, \mathbf{F}^{\rm T} = \mathbf{F} \, \mathbf{T}^{\rm T}_R$, is restored if and only if $\boldsymbol{\gamma} = \dot{\boldsymbol{\chi}}$, therefore in the absence of any electromagnetic field, as stated introducing the *new* velocity. However as long as $\boldsymbol{\gamma} \neq \dot{\boldsymbol{\chi}}$, for Eq. (7.35b) to be satisfied the symmetry of the tensor $[\mathbf{T}_R + \mathbf{T}^{\rm M}_R] \ \mathbf{F}^{\rm T}$ is not sufficient, as well as there is no requirement that $\mathbf{T}_R \, \mathbf{F}^{\rm T}$ and $\mathbf{T}^{\rm M}_R \, \mathbf{F}^{\rm T}$ are symmetric tensors.

7.6 The laws of thermodynamics.

The first law of thermodynamics for the problem at hand is defined by the interplay among the internal energy of $\mathcal{P}_R$, the mechanical power expended on $\mathcal{P}_R$, the heat transferred in $\mathcal{P}_R$, and the power due to electric and the magnetic fields in $\mathcal{P}_R$. The latter contribution had a set of an energy flux vector across $\partial\mathcal{P}_R$ given by the cross product between the electromotive and the magnetomotive intensities.

Let $\mathcal{U}$ denote the net internal energy, $\mathcal{K}$ the kinetic energy, $\mathcal{W}_u$ the mechanical external power, $\mathcal{Q}_u$ the power due to heat transferred, and $\mathcal{E}_u$ the power due to the electromagnetic flux vector. It holds

$$\dot{\mathcal{U}}(\mathcal{P}_R) + \dot{\mathcal{K}}(\mathcal{P}_R) = \mathcal{W}_u(\mathcal{P}_R) + \mathcal{Q}_u(\mathcal{P}_R) + \mathcal{E}_u(\mathcal{P}_R) \ . \tag{7.36}$$

Denote with u_R and $\frac{1}{2} \, \rho_R \, \dot{\boldsymbol{\chi}}^2$ the net internal energy and the kinetic energy (per unit reference volume), respectively. The individual contributions of Eq. (7.36) write as

$$\dot{\mathcal{U}}(\mathcal{P}_R) = \int_{\mathcal{P}_R} \dot{u}_R \ {\rm d}\mathcal{V} \ , \tag{7.37a}$$

$$\dot{\mathcal{K}}(\mathcal{P}_R) = \int_{\mathcal{P}_R} \rho_R \, \ddot{\boldsymbol{\chi}} \cdot \dot{\boldsymbol{\chi}} \ {\rm d}\mathcal{V} \ , \tag{7.37b}$$

$$\mathcal{W}_u(\mathcal{P}_R) = \int_{\partial\mathcal{P}_R} \dot{\boldsymbol{\chi}} \cdot \boldsymbol{t}_R \ {\rm d}\mathcal{A} + \int_{\mathcal{P}_R} \dot{\boldsymbol{\chi}} \cdot \boldsymbol{b}_{0R} \ {\rm d}\mathcal{V} \ , \tag{7.37c}$$

$$\mathcal{Q}_u(\mathcal{P}_R) = \int_{\mathcal{P}_R} s_{qR} \ {\rm d}\mathcal{V} - \int_{\partial\mathcal{P}_R} \boldsymbol{q}_R \cdot \boldsymbol{n}_R \ {\rm d}\mathcal{A} \ , \tag{7.37d}$$

$$\mathcal{E}_u(\mathcal{P}_R) = -\int_{\partial\mathcal{P}_R} \boldsymbol{\mathcal{E}}_R \times \boldsymbol{\mathcal{H}}_R \cdot \boldsymbol{n}_R \ {\rm d}\mathcal{A} \ . \tag{7.37e}$$

Symbols in Eq.s (7.37) have the following meaning. The term $\rho_R \, \ddot{\boldsymbol{\chi}}$ represents the inverse of the inertial body force, generally called d'Alembert body force [53]. The term s_{qR} stands for the heat supplied by external agencies, or radiant heating, whereas $\boldsymbol{q}_R$ denotes the heat flux vector. Traction e body forces $\boldsymbol{t}_R$ and $\boldsymbol{b}_{0R}$, and electromotive and magnetomotive intensities $\boldsymbol{\mathcal{E}}_R$ and $\boldsymbol{\mathcal{H}}_R$, have been defined in Section 7.5 and 7.4.1, respectively.

Making use of the balance of linear momentum (7.35a) to replace $\boldsymbol{b}_{0R}$ in Eq. (7.37c), and after application of the divergence theorem, we find that

$$\mathcal{W}(\mathcal{P}_R) = \int_{\mathcal{P}_R} [\mathbf{T}_R + \mathbf{T}_R^{\mathrm{M}}] : \dot{\mathbf{F}} + \rho_R\, \dot{\boldsymbol{\gamma}} \cdot \dot{\boldsymbol{\chi}} \, \mathrm{d}\mathcal{V} \, . \tag{7.38}$$

Application of the divergence theorem to Eq.s (7.37d) and (7.37e), combination of the resultant integrals with Eq.s (7.37a), (7.37b) and (7.38), and recognition that the result must hold for any $\mathcal{P}_R \subset \mathcal{B}_R$ lead to the following local energy balance

$$\dot{u}_R + \rho_R\, \ddot{\boldsymbol{\chi}} \cdot \dot{\boldsymbol{\chi}} = [\mathbf{T}_R + \mathbf{T}_R^{\mathrm{M}}] : \dot{\mathbf{F}} + \rho_R\, \dot{\boldsymbol{\gamma}} \cdot \dot{\boldsymbol{\chi}} - \boldsymbol{\nabla}_R \cdot \left[\, \boldsymbol{q}_R \,\right] + s_{qR} - \boldsymbol{\nabla}_R \cdot [\, \boldsymbol{\mathcal{E}}_R \times \boldsymbol{\mathcal{H}}_R \,] \, . \tag{7.39}$$

Mechanics is assumed to not contribute directly to the total entropy flow [54, 51]. Similarly, electromagnetic fields are expected to do not have any entropic contribution [225]. The second law of thermodynamics is therefore defined as the balance of the interplay among the internal entropy of $\mathcal{P}_R$ and the entropy produced in $\mathcal{P}_R$ due to heat transfer.

Denote with $\mathcal{S}$ the net internal entropy of $\mathcal{P}_R$, with $\mathcal{S}_i$ the entropy produced inside $\mathcal{P}_R$, and with $\mathcal{Q}_\eta$ the entropy per unit time produced inside $\mathcal{P}_R$ due to heat transfer. According to the statement of second law of thermodynamics, $\dot{\mathcal{S}}_i(\mathcal{P}_R) \geq 0$, the following entropy imbalance holds

$$\dot{\mathcal{S}}(\mathcal{P}_R) - \mathcal{Q}_\eta(\mathcal{P}_R) \geq 0 \, , \tag{7.40}$$

where

$$\dot{\mathcal{S}}(\mathcal{P}_R) = \int_{\mathcal{P}_R} \dot{\eta}_R \, \mathrm{d}\mathcal{V} \, , \tag{7.41a}$$

$$\mathcal{Q}_\eta(\mathcal{P}_R) = \int_{\mathcal{P}_R} \frac{1}{T}\, s_{qR} \, \mathrm{d}\mathcal{V} - \int_{\partial\mathcal{P}_R} \frac{1}{T}\, \boldsymbol{q}_R \cdot \boldsymbol{n}_R \, \mathrm{d}\mathcal{A} \, , \tag{7.41b}$$

with η_R specific net internal entropy (per unit reference volume).

Combination of Eq.s (7.41), application of the divergence theorem, and recognition that the resultant integral must hold for any arbitrary sub-region region $\mathcal{P}_R \subset \mathcal{B}_R$ yield

$$\dot{\eta}_R - \frac{1}{T}\, s_{qR} + \frac{1}{T}\, \boldsymbol{\nabla}_R \cdot \left[\, \boldsymbol{q}_R \,\right] - \frac{1}{T^2}\, \boldsymbol{q}_R \cdot \boldsymbol{\nabla}_R \, [\, T \,] \geq 0 \, . \tag{7.42}$$

7.6.1 The electromagnetic Clausius-Duhem inequality.

The method of Coleman and Noll [8] is used to derive the Clausius-Duhem inequality and to determine the restrictions on the constitutive relations that follow from the second law of thermodynamics. The entropy imbalance (7.42) can be rephrased in terms of internal energy by replacing the term s_{qR} from the energy balance (7.39). After multiplication by the temperature T,

$$T\, \dot{\eta}_R - \dot{u}_R - \rho_R\, \ddot{\boldsymbol{\chi}} \cdot \dot{\boldsymbol{\chi}} + \rho_R\, \dot{\boldsymbol{\gamma}} \cdot \dot{\boldsymbol{\chi}} + [\mathbf{T}_R + \mathbf{T}_R^{\mathrm{M}}] : \dot{\mathbf{F}} - \boldsymbol{\nabla}_R \cdot [\, \boldsymbol{\mathcal{E}}_R \times \boldsymbol{\mathcal{H}}_R \,] - \frac{1}{T}\, \boldsymbol{q}_R \cdot \boldsymbol{\nabla}_R \, [\, T \,] \geq 0 \, . \tag{7.43}$$

A non-trivial calculation collected in Appendix D.2 allows to cast the vector identity $-\boldsymbol{\nabla}_R \cdot [\, \boldsymbol{\mathcal{E}}_R \times \boldsymbol{\mathcal{H}}_R \,]$ of inequality (7.43) in the form

$$\begin{aligned} -\boldsymbol{\nabla}_R \cdot [\, \boldsymbol{\mathcal{E}}_R \times \boldsymbol{\mathcal{H}}_R \,] = {} & \boldsymbol{\mathcal{J}}_R \cdot \boldsymbol{\mathcal{E}}_R - \boldsymbol{\mathcal{M}}_R \cdot \dot{\boldsymbol{B}}_R - \boldsymbol{P}_R \cdot \dot{\boldsymbol{\mathcal{E}}}_R + \kappa_0\, \mathbf{F}^{-\mathrm{T}}\, \boldsymbol{E}_R \times \mathbf{F}\, \boldsymbol{B}_R \cdot \ddot{\boldsymbol{\chi}} \\ & + \Big[\tfrac{1}{2}\, \kappa_0\, J\, \left(\mathbf{F}^{-\mathrm{T}}\, \boldsymbol{E}_R \right)^2 + \tfrac{1}{2}\, \mu_0^{-1} J^{-1} \left(\mathbf{F}\, \boldsymbol{B}_R \right)^2 - \kappa_0\, J\, \mathbf{F}^{-\mathrm{T}}\, \boldsymbol{E}_R \otimes \mathbf{F}^{-\mathrm{T}}\, \boldsymbol{E}_R \\ & \quad - \mu_0^{-1} J^{-1} \mathbf{F}\, \boldsymbol{B}_R \otimes \mathbf{F}\, \boldsymbol{B}_R - \kappa_0\, \mathbf{F}^{-\mathrm{T}}\, \boldsymbol{E}_R \times \mathbf{F}\, \boldsymbol{B}_R \otimes \dot{\boldsymbol{\chi}} \Big]\, \mathbf{F}^{-\mathrm{T}} : \dot{\mathbf{F}} \\ & + \dot{\overline{\tfrac{1}{2}\, \kappa_0\, J\, \left(\mathbf{F}^{-\mathrm{T}}\, \boldsymbol{E}_R \right)^2 + \tfrac{1}{2}\, \mu_0^{-1} J^{-1} \left(\mathbf{F}\, \boldsymbol{B}_R \right)^2 + \boldsymbol{\mathcal{E}}_R \cdot \boldsymbol{P}_R}} \\ & \dot{\overline{-\kappa_0\, \mathbf{F}^{-\mathrm{T}}\, \boldsymbol{E}_R \times \mathbf{F}\, \boldsymbol{B}_R \cdot \dot{\boldsymbol{\chi}}}} \, . \end{aligned} \tag{7.44}$$

Combination of Eq.s (7.43) and (7.44) yields

$$\begin{aligned} & T\,\dot{\eta}_R - \dot{u}_R - \rho_R\,\ddot{\boldsymbol{\chi}}\cdot\dot{\boldsymbol{\chi}} + \rho_R\,\dot{\boldsymbol{\gamma}}\cdot\dot{\boldsymbol{\chi}} + \boldsymbol{\mathcal{J}}_R\cdot\boldsymbol{\mathcal{E}}_R - \boldsymbol{\mathcal{M}}_R\cdot\dot{\boldsymbol{B}}_R - \boldsymbol{P}_R\cdot\dot{\boldsymbol{\mathcal{E}}}_R + \kappa_0\,\mathbf{F}^{-\mathrm{T}}\,\boldsymbol{E}_R\times\mathbf{F}\,\boldsymbol{B}_R\cdot\ddot{\boldsymbol{\chi}} \\ & \quad + \mathbf{T}^{\mathcal{E}}_R : \dot{\mathbf{F}} - \frac{1}{T}\,\boldsymbol{q}_R\cdot\boldsymbol{\nabla}_R\,[\,T\,] \\ & \quad + \dot{\overline{\tfrac{1}{2}\,\kappa_0\,J\,\left(\mathbf{F}^{-\mathrm{T}}\,\boldsymbol{E}_R\right)^2 + \tfrac{1}{2}\,{\mu_0}^{-1}J^{-1}\,(\mathbf{F}\,\boldsymbol{B}_R)^2 + \boldsymbol{\mathcal{E}}_R\cdot\boldsymbol{P}_R - \kappa_0\,\mathbf{F}^{-\mathrm{T}}\,\boldsymbol{E}_R\times\mathbf{F}\,\boldsymbol{B}_R\cdot\dot{\boldsymbol{\chi}}}} \geq 0\,, \end{aligned} \tag{7.45}$$

where it has been defined the electromagnetic nominal stress $\mathbf{T}^{\mathcal{E}}_R$ as

$$\mathbf{T}^{\mathcal{E}}_R = \mathbf{T}_R + \mathbf{T}^{\mathrm{M}}_R - \hat{\mathbf{T}}^{\mathrm{M}}_R - \left[\kappa_0\,\mathbf{F}^{-\mathrm{T}}\,\boldsymbol{E}_R\times\mathbf{F}\,\boldsymbol{B}_R\otimes\dot{\boldsymbol{\chi}}\right]\,\mathbf{F}^{-\mathrm{T}}\,. \tag{7.46}$$

with

$$\begin{aligned} \hat{\mathbf{T}}^{\mathrm{M}}_R = & \Big[\kappa_0\,J\left(\mathbf{F}^{-\mathrm{T}}\boldsymbol{E}_R\otimes\mathbf{F}^{-\mathrm{T}}\boldsymbol{E}_R - \tfrac{1}{2}\left(\mathbf{F}^{-\mathrm{T}}\boldsymbol{E}_R\right)^2\right) \\ & + {\mu_0}^{-1}J^{-1}\left(\mathbf{F}\,\boldsymbol{B}_R\otimes\mathbf{F}\,\boldsymbol{B}_R - \tfrac{1}{2}\,(\mathbf{F}\,\boldsymbol{B}_R)^2\right)\Big]\,\mathbf{F}^{-\mathrm{T}}\,, \end{aligned} \tag{7.47}$$

Maxwell stress in the aether [232, 233] arising from vector identity (7.44).

The definition of the electromagnetic referential Helmholtz free energy ψ_R can be provided either per unit reference mass or per unit reference volume[1]. It holds

$$\begin{aligned} \psi_R = & \, u_R - T\,\eta_R - \rho_R\,\boldsymbol{\gamma}\cdot\dot{\boldsymbol{\chi}} + \rho_R\,\dot{\boldsymbol{\chi}}^2 \\ & - \left[\tfrac{1}{2}\,\kappa_0\,J\,\left(\mathbf{F}^{-\mathrm{T}}\,\boldsymbol{E}_R\right)^2 + \tfrac{1}{2}\,{\mu_0}^{-1}J^{-1}\,(\mathbf{F}\,\boldsymbol{B}_R)^2 + \boldsymbol{\mathcal{E}}_R\cdot\boldsymbol{P}_R - \kappa_0\,\mathbf{F}^{-\mathrm{T}}\,\boldsymbol{E}_R\times\mathbf{F}\,\boldsymbol{B}_R\cdot\dot{\boldsymbol{\chi}}\right]\,, \end{aligned} \tag{7.48}$$

whence

$$\begin{aligned} \dot{\psi}_R = & \, \dot{u}_R - \dot{T}\,\eta_R - T\,\dot{\eta}_R - \rho_R\,\dot{\boldsymbol{\gamma}}\cdot\dot{\boldsymbol{\chi}} - \rho_R\,\boldsymbol{\gamma}\cdot\ddot{\boldsymbol{\chi}} + 2\,\rho_R\,\dot{\boldsymbol{\chi}}\cdot\ddot{\boldsymbol{\chi}} \\ & - \dot{\overline{\left[\tfrac{1}{2}\,\kappa_0\,J\,\left(\mathbf{F}^{-\mathrm{T}}\,\boldsymbol{E}_R\right)^2 + \tfrac{1}{2}\,{\mu_0}^{-1}J^{-1}\,(\mathbf{F}\,\boldsymbol{B}_R)^2 + \boldsymbol{\mathcal{E}}_R\cdot\boldsymbol{P}_R - \kappa_0\,\mathbf{F}^{-\mathrm{T}}\,\boldsymbol{E}_R\times\mathbf{F}\,\boldsymbol{B}_R\cdot\dot{\boldsymbol{\chi}}\right]}}\,. \end{aligned} \tag{7.49}$$

Taking advantage from Eq. (7.49), the electromagnetic entropy inequality (7.45) re-writes as

$$\begin{aligned} & -\dot{\psi}_R - \dot{T}\,\eta_R - \left(\rho_R\,\boldsymbol{\gamma} - \rho_R\,\dot{\boldsymbol{\chi}} - \kappa_0\,\mathbf{F}^{-\mathrm{T}}\,\boldsymbol{E}_R\times\mathbf{F}\,\boldsymbol{B}_R\right)\cdot\ddot{\boldsymbol{\chi}} + \boldsymbol{\mathcal{J}}_R\cdot\boldsymbol{\mathcal{E}}_R - \boldsymbol{\mathcal{M}}_R\cdot\dot{\boldsymbol{B}}_R - \boldsymbol{P}_R\cdot\dot{\boldsymbol{\mathcal{E}}}_R \\ & \quad + \mathbf{T}^{\mathcal{E}}_R : \dot{\mathbf{F}} - \frac{1}{T}\,\boldsymbol{q}_R\cdot\boldsymbol{\nabla}_R\,[\,T\,] \geq 0\,. \end{aligned} \tag{7.50}$$

We take ψ_R as a function of temperature T, deformation gradient $\mathbf{F}$, electromotive intensity $\boldsymbol{\mathcal{E}}_R$, and magnetic field $\boldsymbol{B}_R$, hence

$$\psi_R = \psi_R\left(T, \mathbf{F}, \boldsymbol{\mathcal{E}}_R, \boldsymbol{B}_R\right)\,. \tag{7.51}$$

In view of the selected functional dependence of ψ_R, its time derivative writes as

$$\dot{\psi}_R = \frac{\partial\psi_R}{\partial T}\,\dot{T} + \frac{\partial\psi_R}{\partial\mathbf{F}} : \dot{\mathbf{F}} + \frac{\partial\psi_R}{\partial\boldsymbol{\mathcal{E}}_R}\cdot\dot{\boldsymbol{\mathcal{E}}}_R + \frac{\partial\psi_R}{\partial\boldsymbol{B}_R}\cdot\dot{\boldsymbol{B}}_R\,, \tag{7.52}$$

whence, combination of Eq.s (7.50) and (7.52) yields

$$\begin{aligned} & -\left(\eta_R + \frac{\partial\psi_R}{\partial T}\right)\dot{T} + \left(\mathbf{T}^{\mathcal{E}}_R - \frac{\partial\psi_R}{\partial\mathbf{F}}\right) : \dot{\mathbf{F}} - \left(\boldsymbol{\mathcal{M}}_R + \frac{\partial\psi_R}{\partial\boldsymbol{B}_R}\right)\cdot\dot{\boldsymbol{B}}_R - \left(\boldsymbol{P}_R + \frac{\partial\psi_R}{\partial\boldsymbol{\mathcal{E}}_R}\right)\cdot\dot{\boldsymbol{\mathcal{E}}}_R \\ & \quad - \left(\rho_R\,\boldsymbol{\gamma} - \rho_R\,\dot{\boldsymbol{\chi}} - \kappa_0\,\mathbf{F}^{-\mathrm{T}}\,\boldsymbol{E}_R\times\mathbf{F}\,\boldsymbol{B}_R\right)\cdot\ddot{\boldsymbol{\chi}} + \boldsymbol{\mathcal{J}}_R\cdot\boldsymbol{\mathcal{E}}_R - \frac{1}{T}\,\boldsymbol{q}_R\cdot\boldsymbol{\nabla}_R\,[\,T\,] \geq 0\,. \end{aligned} \tag{7.53}$$

According to the Coleman and Noll's method [8], the Clausius-Duhem inequality (7.53) must hold for any admissible process. For spatially homogeneous and time-dependent temperature, and

---

[1] It is perhaps worth to point out that this does not apply in spatial description, where the necessity to provide the definition of the electromagnetic Helmholtz free energy per unit mass appears to be the unique possible procedure to further properly derive $\dot{\psi}\,(\boldsymbol{x}, t)$.

orthogonality between electromotive intensity and conduction current density, the last two left-hand side terms of (7.53) vanish. Take four of the five terms $\dot{T}$, $\dot{\mathbf{F}}$, $\dot{\boldsymbol{B}}_R$, $\dot{\boldsymbol{\mathcal{E}}}_R$, and $\ddot{\boldsymbol{\chi}}$ null, and one of them arbitrarily chosen in turns. Accordingly, the following thermodynamic restrictions emanate

$$\eta_R = - \left.\frac{\partial \psi_R}{\partial T}\right|_{\mathbf{F}, \boldsymbol{\mathcal{E}}_R, \boldsymbol{B}_R} , \tag{7.54a}$$

$$\mathbf{T}_R^{\mathcal{E}} = \left.\frac{\partial \psi_R}{\partial \mathbf{F}}\right|_{T, \boldsymbol{\mathcal{E}}_R, \boldsymbol{B}_R} , \tag{7.54b}$$

$$\boldsymbol{\mathcal{M}}_R = - \left.\frac{\partial \psi_R}{\partial \boldsymbol{B}_R}\right|_{T, \mathbf{F}, \boldsymbol{\mathcal{E}}_R} , \tag{7.54c}$$

$$\boldsymbol{P}_R = - \left.\frac{\partial \psi_R}{\partial \boldsymbol{\mathcal{E}}_R}\right|_{T, \mathbf{F}, \boldsymbol{B}_R} , \tag{7.54d}$$

$$\boldsymbol{\gamma} = \dot{\boldsymbol{\chi}} + \rho_R^{-1} \kappa_0 \, \mathbf{F}^{-\mathrm{T}} \, \boldsymbol{E}_R \times \mathbf{F} \, \boldsymbol{B}_R \; . \tag{7.54e}$$

Thermodynamic prescription (7.54e) determines the *new* velocity $\boldsymbol{\gamma}$, which reduces to $\dot{\boldsymbol{\chi}}$ in absence of any electromagnetic field, as required. Furthermore, it is clear that the consideration of $\boldsymbol{\gamma}$ is restricted to the Galilean electromagnetic theory.

Consider time-independent distributions of deformation gradient, magnetic field, electromotive intensity and acceleration, and spatially inhomogeneous but time-independent distribution of T. Since inequality (7.53) must hold for any value of and $\boldsymbol{\mathcal{E}}_R$ and $\boldsymbol{\nabla}_R\,[\,T\,]$, restrictions on the conduction current density $\boldsymbol{\mathcal{J}}_R$ and the heat flux $\boldsymbol{q}_R$ are determined. What remains of inequality (7.53) therefore writes as

$$\boldsymbol{\mathcal{J}}_R \cdot \boldsymbol{\mathcal{E}}_R - \frac{1}{T} \, \boldsymbol{q}_R \cdot \boldsymbol{\nabla}_R\,[\,T\,] \geq 0 \; . \tag{7.55}$$

An important property of $\boldsymbol{\mathcal{J}}_R$ and $\boldsymbol{q}_R$ is that they must both vanish whenever $\boldsymbol{\mathcal{E}}_R$ and $\boldsymbol{\nabla}_R\,[\,T\,]$ both vanish [225], which is a necessary but not sufficient condition to satisfy inequality (7.55). Constitutive specifications of $\boldsymbol{\mathcal{J}}_R$ and $\boldsymbol{q}_R$ are thus necessary.

Remark. The electromagnetic stress tensor $\mathbf{T}_R^{\mathcal{E}}$ has been introduced in Eq. (7.46). Defining a spatial electromagnetic stress as

$$\tilde{\mathbf{T}}^{\mathcal{E}} = \mathbf{T} + \left[\tfrac{1}{2}\,\kappa_0\,\boldsymbol{E}^2 + \tfrac{1}{2}\,\mu_0^{-1}\boldsymbol{B}^2\right] \mathbf{1} - \kappa_0\,\boldsymbol{E}\otimes\boldsymbol{E} - \mu_0^{-1}\boldsymbol{B}\otimes\boldsymbol{B} - \kappa_0\,\boldsymbol{E}\times\boldsymbol{B}\otimes\dot{\boldsymbol{x}} \; , \tag{7.56}$$

according to transformation rules (7.6) and (7.11) for $\boldsymbol{E}$ and $\boldsymbol{B}$, respectively, we find that $\mathbf{T}_R^{\mathcal{E}}$ can be expressed as

$$\mathbf{T}_R^{\mathcal{E}} = J \, \tilde{\mathbf{T}}^{\mathcal{E}} \, \mathbf{F}^{-\mathrm{T}} \; , \tag{7.57}$$

coherently with Eq.s (7.34).

However, Eq. (7.56) does not represent the *real* spatial description of $\mathbf{T}_R^{\mathcal{E}}$ insofar the contribution of Lorentz magnetization, electromotive intensity and polarization, in the form $(\boldsymbol{\mathcal{M}}\cdot\boldsymbol{B})\;\mathbf{1}$, $\boldsymbol{\mathcal{M}}\otimes\boldsymbol{B}$, and $\boldsymbol{\mathcal{E}}\otimes\boldsymbol{P}$, are missing (see [225]).

7.7 Constitutive definition of the conduction current and the heat flux.

The conduction current $\boldsymbol{\mathcal{J}}_R$ and the heat flux $\boldsymbol{q}_R$ must be modeled in such a way to satisfy thermodynamic prescription (7.55). A general strategy may be represented by [225][2]

$$\boldsymbol{q}_R = \Pi \, \boldsymbol{\mathcal{J}}_R - \kappa \, \boldsymbol{\nabla}_R\,[\,T\,] \; , \qquad \boldsymbol{\mathcal{J}}_R = \sigma \, \boldsymbol{\mathcal{E}}_R - \sigma \, \alpha \, \boldsymbol{\nabla}_R\,[\,T\,] \; , \tag{7.58}$$

---

[2] This choice does not represent the most general case. Generally, for *linearly conducting perfect fluids*, a linear dependence of $\boldsymbol{\mathcal{J}}_R$ and $\boldsymbol{q}_R$ upon $\boldsymbol{\mathcal{E}}_R$ and $\boldsymbol{\nabla}_R\,[\,T\,]$ is commonly assumed. For highly isotropic materials, a more general constitutive definition of the conduction current and the heat flux encompasses *Hall*, *Nernst*, *Ettingshausen* and *Leduc-Righi* effects. If such effects are negligible, Eq.s (7.58) are recovered [225].

where the thermal conductivity κ and the electric conductivity σ are positive definite coefficients, related to the Peltier Π and Thomson α coefficients by means of the restriction [225]

$$T\,\frac{\kappa}{\sigma} \geq (\Pi - T\,\alpha)^2 \ . \tag{7.59}$$

If the Thomson and the Peltier coefficients vanish, Eq.s (7.58) reduce to the well-known Fourier's and Ohm's laws,

$$\boldsymbol{q}_R = -\kappa\,\boldsymbol{\nabla}_R\,[\,T\,] \ , \qquad \boldsymbol{\mathcal{J}}_R = \sigma\,\boldsymbol{\mathcal{E}}_R \ . \tag{7.60}$$

7.8 Governing equations

The governing equations emanate by properly incorporating thermodynamic prescriptions (7.54) and constitutive specifications (7.58) (or (7.60)) into the balance equations and the generalized heat equation, whose derivation is collected in Appendix D.3.

Governing equations are written in term of the state variables T, $\boldsymbol{\mathcal{E}}_R$, $\boldsymbol{B}_R$, and $\boldsymbol{u}$. The law of charge conservation writes as

$$\dot{\zeta}_R + \boldsymbol{\nabla}_R \cdot [\,\boldsymbol{j}_R\,] = 0 \ . \tag{7.61a}$$

with $\boldsymbol{j}_R = \boldsymbol{j}_R\,(\boldsymbol{\mathcal{J}}_R)$, and $\boldsymbol{\mathcal{J}}_R$ constitutively defined by Eq. $(7.58)_2$ (eventually Eq. $(7.60)_2$).

The first pair of Maxwell's equations writes as

$$\boldsymbol{\nabla}_R \cdot [\,\boldsymbol{D}_R\,] = \zeta_R \ , \tag{7.61b}$$

with $\boldsymbol{D}_R$ defined by aether relation (7.28e), encompassing $\boldsymbol{P}_R$ prescribed by (7.54d), and

$$\boldsymbol{\nabla}_R \times [\,\boldsymbol{\mathcal{H}}_R\,] = \boldsymbol{\mathcal{J}}_R + \dot{\boldsymbol{D}}_R \ , \tag{7.61c}$$

with $\boldsymbol{\mathcal{J}}_R$ constitutively defined by Eq. $(7.58)_2$ (or Eq. $(7.60)_2$), $\boldsymbol{D}_R$ and $\boldsymbol{\mathcal{H}}_R$ by aether relations (7.28e) and (7.28f), where $\boldsymbol{P}_R$ and $\boldsymbol{\mathcal{M}}_R$ are provided by thermodynamic restrictions (7.54c) and (7.54d).

The second pair of Maxwell's equations reads

$$\boldsymbol{\nabla}_R \cdot [\,\boldsymbol{B}_R\,] = 0 \tag{7.61d}$$

$$\boldsymbol{\nabla}_R \times [\,\boldsymbol{\mathcal{E}}_R\,] + \dot{\boldsymbol{B}}_R = 0 \tag{7.61e}$$

The balance of linear momentum writes as

$$\boldsymbol{\nabla}_R \cdot [\,\mathbf{T}_R + \mathbf{T}_R^{\mathrm{M}}\,] + \boldsymbol{b}_{0R} = \rho_R\,\dot{\boldsymbol{\gamma}} \ , \tag{7.61f}$$

with $[\mathbf{T}_R + \mathbf{T}_R^{\mathrm{M}}]$ function of $\mathbf{T}_R^{\mathcal{E}}$ whose thermodynamic prescriptions is stated by Eq. (7.54b), and according to the thermodynamic restriction (7.54e) for $\boldsymbol{\gamma}$.

Lastly, the generalized heat equation has the form

$$T\,\frac{\partial \eta_R}{\partial T}\,\dot{T} + \boldsymbol{\nabla}_R \cdot [\,\boldsymbol{q}_R\,] = s_{qR} + \boldsymbol{\mathcal{J}}_R \cdot \boldsymbol{\mathcal{E}}_R + T\,\frac{\partial \mathbf{T}_R^{\mathcal{E}}}{\partial T} : \dot{\mathbf{F}} - T\,\frac{\partial \boldsymbol{P}_R}{\partial T} \cdot \dot{\boldsymbol{\mathcal{E}}}_R - T\,\frac{\partial \boldsymbol{\mathcal{M}}_R}{\partial T} \cdot \dot{\boldsymbol{B}}_R \ , \tag{7.61g}$$

with η_R, $\mathbf{T}_R^{\mathcal{E}}$, $\boldsymbol{\mathcal{M}}_R$ and $\boldsymbol{P}_R$ defined by thermodynamic restrictions (7.54a), (7.54b), (7.54c) and (7.54d), respectively, and with $\boldsymbol{q}_R$ and $\boldsymbol{\mathcal{J}}_R$ constitutively specified via of Eq.s (7.58) (or Eq.s (7.60)).

The boundary conditions

$$\boldsymbol{q}_R \cdot \boldsymbol{n}_R = \overline{q}_R \qquad \boldsymbol{X} \in \partial^N \mathcal{V} \ , \tag{7.62a}$$

$$\boldsymbol{\mathcal{E}}_R \times \boldsymbol{\mathcal{H}}_R \cdot \boldsymbol{n}_R = \overline{\mathcal{E}_{\mathcal{R}} \times \mathcal{H}_{\mathcal{R}}} \qquad \boldsymbol{X} \in \partial^N \mathcal{V} \ , \tag{7.62b}$$

$$\mathbf{T}_R\,\boldsymbol{n}_R = \bar{\boldsymbol{t}}_R \qquad \boldsymbol{X} \in \partial^N \mathcal{V} \ , \tag{7.62c}$$

are imposed along Neumann boundaries $\partial^N \mathcal{V}$. To ensure solvability of the problem, Dirichlet boundary conditions have to be enforced along the complementary boundary $\partial^D \mathcal{V}$, hence

$$T = \overline{T} \qquad \boldsymbol{X} \in \partial^D \mathcal{V} \; , \tag{7.63a}$$

$$\boldsymbol{u} = \overline{\boldsymbol{u}} \qquad \boldsymbol{X} \in \partial^D \mathcal{V} \; . \tag{7.63b}$$

Initial conditions are usually imposed for velocity $\dot{\boldsymbol{\chi}}(\boldsymbol{X}, t = 0)$, electromotive intensity $\boldsymbol{\mathcal{E}}_R(\boldsymbol{X}, t = 0)$, magnetic field $\boldsymbol{B}_R(\boldsymbol{X}, t = 0)$ and temperature $T(\boldsymbol{X}, t = 0)$.

7.9 Concluding remarks

We briefly conclude the manuscript highlighting the key features of the proposed framework. A general Galilean electromagnetic theory has been provided in Lagrangian formulation and coupled with thermodynamics and finite-strain continuum mechanics. The principles of conservation of linear and angular momentum establish the coupling between electromagnetism and mechanics in two places. Firstly, via the introduction of the *new* velocity vector field, which is recognized to encompass the material velocity and the cross product between the electric and magnetic fields by thermodynamic prescriptions. Additionally, Euler's laws are written in terms of *total* forces, accounting for electromagnetic and mechanical surface traction and body forces. Relations between electromagnetic forces and the Maxwell stress are stated, and the forces coupling leads to the introduction of the total *true* stress, given by the sum of the mechanical Piola and electromagnetic Maxwell stresses. The principles of conservation of linear and angular momentum are therefore termed Euler's laws of electro-magneto-mechanics. Thermodynamics is augmented via the introduction of an electromagnetic energy flux, therefore providing a fully coupled framework of Galilean electromagnetism with finite strain continuum thermo-mechanics is therefore provided. Manipulation of the electromagnetic vector identity gives rise to the definition of the electromagnetic nominal stress, in addition to provide information on the selection of the electromagnetic referential Helmholtz free energy, and to generate all electromagnetic terms that contribute to the entropy inequality. Thermodynamic restrictions are established for entropy, electromagnetic nominal stress, Lorentz magnetization, invariant current density and the *new* velocity vector field. The dissipation inequality provides restrictions on the conduction current density and the heat flux vector, which require to be constitutively specified. A general formulation of the required constitutive definitions is therefore provided, before emanating the governing equations with associated Neumann and Dirichlet boundary conditions.

Appendix D

D.1 The referential balance of angular momentum

Recall the balance of angular momentum (7.29b). The assumption of electromagnetic effects inducing first order moments [232] implies the existence of an angular momentum O^{ε}_i that we set [40]

$$\int_{\mathcal{P}_R} O^{\varepsilon}_i \;\mathrm{d}\mathcal{V} = \int_{\mathcal{P}_t} o^{\varepsilon}_i \;\mathrm{d}v = \int_{\mathcal{P}_t} \epsilon_{ijk}\, \mathrm{T}^{\mathrm{M}}{}_{kj} \;\mathrm{d}v \;. \tag{D.1}$$

Then, conservation of angular momentum (7.29b) re-writes

$$\dot{\overline{\int_{\mathcal{P}_R} \epsilon_{ijk}\, \chi_j\, \rho_R\, \gamma_k \;\mathrm{d}\mathcal{V}}} = \int_{\partial\mathcal{P}_R} \epsilon_{ijk}\, \chi_j \left(t_{R\,k} + t^{\varepsilon}_{R\,k}\right) \mathrm{d}\mathcal{A} + \int_{\mathcal{P}_R} \epsilon_{ijk}\, \chi_j \left(b_{0R\,k} + b^{\varepsilon}_{R\,k}\right) \mathrm{d}\mathcal{V} + \int_{\mathcal{P}_t} \epsilon_{ijk}\, \mathrm{T}^{\mathrm{M}}{}_{kj} \;\mathrm{d}v \;. \tag{D.2}$$

Integral terms of Eq. (D.2) write

$$\dot{\overline{\int_{\mathcal{P}_R} \epsilon_{ijk}\, \chi_j\, \rho_R\, \gamma_k \;\mathrm{d}\mathcal{V}}} = \int_{\mathcal{P}_R} \epsilon_{ijk}\, \dot{\chi}_j\, \rho_R\, \gamma_k + \epsilon_{ijk}\, \chi_j\, \rho_R\, \dot{\gamma}_k \;\mathrm{d}\mathcal{V} \;, \tag{D.3a}$$

according to the law of mass conservation, $\dot{\rho}_R = 0$,

$$\begin{aligned}\int_{\partial\mathcal{P}_R} \epsilon_{ijk}\, \chi_j \left(t_{R\,k} + t^{\varepsilon}_{R\,k}\right) \mathrm{d}\mathcal{A} = -\int_{\partial\mathcal{P}_R} \epsilon_{ijk}\, \chi_j\, \|\mathrm{T}_{R\,kl}\|\, n_l \;\mathrm{d}\mathcal{A} &= \int_{\mathcal{P}_R} \epsilon_{ijk}\, \mathrm{F}_{jl}\, \mathrm{T}_{R\,kl} + \epsilon_{ijk}\, \chi_j\, \frac{\partial \mathrm{T}_{R\,kl}}{\partial X_l} \;\mathrm{d}\mathcal{V} \\ &= \int_{\mathcal{P}_R} -\epsilon_{ijk}\, \mathrm{T}_{R\,jl}\, \mathrm{F}^{\mathrm{T}}_{lk} + \epsilon_{ijk}\, \chi_j\, \frac{\partial \mathrm{T}_{R\,kl}}{\partial X_l} \;\mathrm{d}\mathcal{V} \;.\end{aligned} \tag{D.3b}$$

according to Eq. (7.33) and with $\partial \chi_j / \partial X_l = \mathrm{F}_{jl}$,

$$\int_{\mathcal{P}_R} \epsilon_{ijk}\, \chi_j \left(b_{0R\,k} + b^{\varepsilon}_{R\,k}\right) \mathrm{d}\mathcal{V} = \int_{\mathcal{P}_R} \epsilon_{ijk}\, \chi_j\, b_{0R\,k} + \epsilon_{ijk}\, \chi_j\, \frac{\partial \mathrm{T}^{\mathrm{M}}_{R\,kl}}{\partial X_l} \;\mathrm{d}\mathcal{V} \tag{D.3c}$$

according to Eq. (7.30), and

$$\int_{\mathcal{P}_t} \epsilon_{ijk}\, \mathrm{T}^{\mathrm{M}}{}_{kj} \;\mathrm{d}v = \int_{\mathcal{P}_R} \epsilon_{ijk}\, \mathrm{T}^{\mathrm{M}}_{R\,kl}\, \mathrm{F}^{\mathrm{T}}_{lj} \;\mathrm{d}\mathcal{V} = \int_{\mathcal{P}_R} -\epsilon_{ijk}\, \mathrm{T}^{\mathrm{M}}_{R\,jl}\, \mathrm{F}^{\mathrm{T}}_{lk} \;\mathrm{d}\mathcal{V} \;, \tag{D.3d}$$

according to Eq. $(7.34)_2$.

Combination of Eq.s (D.3) and recognition that all integrals must be valid for any arbitrary volume yield

$$\epsilon_{ijk} \left(\dot{\chi}_j\, \rho_R\, \gamma_k + \chi_j\, \rho_R\, \dot{\gamma}_k\right) = \epsilon_{ijk} \left(-\mathrm{T}_{R\,jl}\, \mathrm{F}^{\mathrm{T}}_{lk} + \chi_j\, \frac{\partial \mathrm{T}_{R\,kl}}{\partial X_l} + \chi_j\, b_{0R\,k} + \chi_j\, \frac{\partial \mathrm{T}^{\mathrm{M}}_{R\,kl}}{\partial X_l} - \mathrm{T}^{\mathrm{M}}_{R\,jl}\, \mathrm{F}^{\mathrm{T}}_{lk}\right) \;, \tag{D.4}$$

which can be re-arranged as

$$\epsilon_{ijk}\,\chi_j\left(\rho_R\,\dot{\gamma}_k - \frac{\partial \mathrm{T}_{Rkl}}{\partial X_l} - \frac{\partial \mathrm{T}^{\mathrm{M}}_{Rkl}}{\partial X_l} - b_{0Rk}\right) = -\epsilon_{ijk}\left(\mathrm{T}_{Rjl}\,\mathrm{F}^{\mathrm{T}}_{lk} + \mathrm{T}^{\mathrm{M}}_{Rjl}\,\mathrm{F}^{\mathrm{T}}_{lk} + \dot{\chi}_j\,\rho_R\,\gamma_k\right) . \tag{D.5}$$

According to the balance of linear momentum (7.35a), the left-hand side term of Eq. (D.5) vanishes, therefore

$$\epsilon_{ijk}\left(\mathrm{T}_{Rjl}\,\mathrm{F}^{\mathrm{T}}_{lk} + \mathrm{T}^{\mathrm{M}}_{Rjl}\,\mathrm{F}^{\mathrm{T}}_{lk} + \dot{\chi}_j\,\rho_R\,\gamma_k\right) = 0 \; , \tag{D.6}$$

whence

$$[\,\mathrm{T}_{Rjl} + \mathrm{T}^{\mathrm{M}}_{Rjl}\,]\,\mathrm{F}^{\mathrm{T}}_{lk} + \dot{\chi}_j\,\rho_R\,\gamma_k = \mathrm{F}_{jl}\,\left[\,\mathrm{T}_{Rlk} + \mathrm{T}^{\mathrm{M}}_{Rlk}\,\right]^{\mathrm{T}} + \rho_R\,\gamma_j\,\dot{\chi}_k \; . \tag{D.7}$$

D.2 Evaluation of the vector identity $-\boldsymbol{\nabla}_R \cdot [\,\boldsymbol{\mathcal{E}}_R \times \boldsymbol{\mathcal{H}}_R\,]$

The divergence term $-\boldsymbol{\nabla}_R \cdot [\,\boldsymbol{\mathcal{E}}_R \times \boldsymbol{\mathcal{H}}_R\,]$ of Eq. (7.43), by means of the cross product rule (for the divergence of a cross product), can be re-written in the form

$$-\boldsymbol{\nabla}_R \cdot [\,\boldsymbol{\mathcal{E}}_R \times \boldsymbol{\mathcal{H}}_R\,] = \boldsymbol{\mathcal{E}}_R \cdot \boldsymbol{\nabla}_R \times [\,\boldsymbol{\mathcal{H}}_R\,] - \boldsymbol{\mathcal{H}}_R \cdot \boldsymbol{\nabla}_R \times [\,\boldsymbol{\mathcal{E}}_R\,] \; , \tag{D.8}$$

whence, according to Maxwell's equations (7.28b) and (7.28d),

$$-\boldsymbol{\nabla}_R \cdot [\,\boldsymbol{\mathcal{E}}_R \times \boldsymbol{\mathcal{H}}_R\,] = \boldsymbol{\mathcal{H}}_R \cdot \dot{\boldsymbol{B}}_R + \boldsymbol{\mathcal{J}}_R \cdot \boldsymbol{\mathcal{E}}_R + \boldsymbol{\mathcal{E}}_R \cdot \dot{\boldsymbol{D}}_R \; . \tag{D.9}$$

Taking advantage from aether relation (7.28f) and definition (7.22) to replace the magnetomotive intensity $\boldsymbol{\mathcal{H}}_R$ and the electromotive intensity $\boldsymbol{\mathcal{E}}_R$, respectively, it holds

$$\begin{aligned} -\boldsymbol{\nabla}_R \cdot [\,\boldsymbol{\mathcal{E}}_R \times \boldsymbol{\mathcal{H}}_R\,] = {} & \boldsymbol{\mathcal{J}}_R \cdot \boldsymbol{\mathcal{E}}_R - \boldsymbol{\mathcal{M}}_R \cdot \dot{\boldsymbol{B}}_R + \boldsymbol{E}_R \cdot \dot{\boldsymbol{D}}_R + \dot{\boldsymbol{\chi}} \times J^{-1}\,\mathbf{F}\,\boldsymbol{B}_R \cdot \mathbf{F}\,\dot{\boldsymbol{D}}_R \\ & + \mu_0^{-1}\,J^{-1}\mathbf{F}\,\boldsymbol{B}_R \cdot \mathbf{F}\,\dot{\boldsymbol{B}}_R - \dot{\boldsymbol{\chi}} \times \kappa_0\,\mathbf{F}^{-\mathrm{T}}\boldsymbol{E}_R \cdot \mathbf{F}\,\dot{\boldsymbol{B}}_R \; . \end{aligned} \tag{D.10}$$

Making use of aether relation (7.28e) to perform the time derivative of $\boldsymbol{D}_R$, and recalling that $\dot{J} = J\,\mathrm{tr}[\,\dot{\mathbf{F}}\,\mathbf{F}^{-1}\,] = \mathrm{J}\,\mathrm{tr}\,[\,\mathbf{L}\,]$, Eq. (D.10) can be re-organized as follows

$$\begin{aligned} -\boldsymbol{\nabla}_R \cdot [\,\boldsymbol{\mathcal{E}}_R \times \boldsymbol{\mathcal{H}}_R\,] = {} & \boldsymbol{\mathcal{J}}_R \cdot \boldsymbol{\mathcal{E}}_R - \boldsymbol{\mathcal{M}}_R \cdot \dot{\boldsymbol{B}}_R + \boldsymbol{\mathcal{E}}_R \cdot \dot{\boldsymbol{P}}_R \\ & + \kappa_0\,J\,\mathbf{F}^{-\mathrm{T}}\boldsymbol{E}_R \cdot \mathbf{F}^{-\mathrm{T}}\boldsymbol{E}_R\,\mathrm{tr}\,[\,\mathbf{L}\,] + \kappa_0\,J\,\boldsymbol{E}_R \cdot \dot{\mathbf{F}}^{-1}\,\mathbf{F}^{-\mathrm{T}}\boldsymbol{E}_R \\ & + \kappa_0\,J\,\mathbf{F}^{-\mathrm{T}}\boldsymbol{E}_R \cdot \dot{\mathbf{F}}^{-\mathrm{T}}\boldsymbol{E}_R + \kappa_0\,J\,\mathbf{F}^{-\mathrm{T}}\boldsymbol{E}_R \cdot \mathbf{F}^{-\mathrm{T}}\dot{\boldsymbol{E}}_R \\ & + \dot{\boldsymbol{\chi}} \times \mathbf{F}\,\boldsymbol{B}_R \cdot \kappa_0\,\mathbf{F}^{-\mathrm{T}}\boldsymbol{E}_R\,\mathrm{tr}\,[\,\mathbf{L}\,] + \dot{\boldsymbol{\chi}} \times \mathbf{F}\,\boldsymbol{B}_R \cdot \kappa_0\,\mathbf{F}\,\dot{\mathbf{F}}^{-1}\,\mathbf{F}^{-\mathrm{T}}\boldsymbol{E}_R \\ & + \dot{\boldsymbol{\chi}} \times \mathbf{F}\,\boldsymbol{B}_R \cdot \kappa_0\,\dot{\mathbf{F}}^{-\mathrm{T}}\boldsymbol{E}_R + \dot{\boldsymbol{\chi}} \times \mathbf{F}\,\boldsymbol{B}_R \cdot \kappa_0\,\mathbf{F}^{-\mathrm{T}}\dot{\boldsymbol{E}}_R \\ & + \mu_0^{-1}\,J^{-1}\mathbf{F}\,\boldsymbol{B}_R \cdot \mathbf{F}\,\dot{\boldsymbol{B}}_R - \dot{\boldsymbol{\chi}} \times \kappa_0\,\mathbf{F}^{-\mathrm{T}}\boldsymbol{E}_R \cdot \mathbf{F}\,\dot{\boldsymbol{B}}_R \; . \end{aligned} \tag{D.11}$$

By re-writing the terms

$$\boldsymbol{\mathcal{E}}_R \cdot \dot{\boldsymbol{P}}_R = \dot{\overline{\boldsymbol{\mathcal{E}}_R \cdot \boldsymbol{P}_R}} - \dot{\boldsymbol{\mathcal{E}}}_R \cdot \boldsymbol{P}_R \; , \tag{D.12a}$$

$$\begin{aligned} \kappa_0\,J\,\mathbf{F}^{-\mathrm{T}}\boldsymbol{E}_R \cdot \left(\mathbf{F}^{-\mathrm{T}}\boldsymbol{E}_R\mathrm{tr}\,[\,\mathbf{L}\,] + \dot{\mathbf{F}}^{-\mathrm{T}}\boldsymbol{E}_R + \mathbf{F}^{-\mathrm{T}}\dot{\boldsymbol{E}}_R\right) = {} & \dot{\overline{\tfrac{1}{2}\,\kappa_0\,J\,(\mathbf{F}^{-\mathrm{T}}\boldsymbol{E}_R)^2}} \\ & + \tfrac{1}{2}\,\kappa_0\,J\left(\mathbf{F}^{-\mathrm{T}}\boldsymbol{E}_R\right)^2\;\mathrm{tr}\,[\,\mathbf{L}\,] \; , \end{aligned} \tag{D.12b}$$

$$\begin{aligned} \mu_0^{-1}\,J^{-1}\mathbf{F}\,\boldsymbol{B}_R \cdot \mathbf{F}\,\dot{\boldsymbol{B}}_R = {} & \dot{\overline{\tfrac{1}{2}\,\mu_0^{-1}\,J^{-1}\,(\mathbf{F}\,\boldsymbol{B}_R)^2}} + \tfrac{1}{2}\,\mu_0^{-1}\,J^{-1}\,(\mathbf{F}\,\boldsymbol{B}_R)^2\,\mathrm{tr}\,[\,\mathbf{L}\,] \\ & - \mu_0^{-1}\,J^{-1}\mathbf{F}\,\boldsymbol{B}_R \cdot \dot{\mathbf{F}}\,\boldsymbol{B}_R \; , \end{aligned} \tag{D.12c}$$

combination of Eq.s (D.11) and (D.12) yields

$$
\begin{aligned}
-\boldsymbol{\nabla}_R\cdot[\,\boldsymbol{\mathcal{E}}_R\times\boldsymbol{\mathcal{H}}_R\,] &= \boldsymbol{\mathcal{J}}_R\cdot\boldsymbol{\mathcal{E}}_R-\boldsymbol{\mathcal{M}}_R\cdot\dot{\boldsymbol{B}}_R-\dot{\boldsymbol{\mathcal{E}}}_R\cdot\boldsymbol{P}_R\\
&\quad+\tfrac12\,\kappa_0\,J\left(\mathbf{F}^{-\mathrm{T}}\boldsymbol{E}_R\right)^2\,\mathrm{tr}\,[\,\mathbf{L}\,]+\kappa_0\,J\,\boldsymbol{E}_R\cdot\dot{\mathbf{F}}^{-1}\,\mathbf{F}^{-\mathrm{T}}\boldsymbol{E}_R\\
&\quad+\dot{\boldsymbol{\chi}}\times\mathbf{F}\,\boldsymbol{B}_R\cdot\kappa_0\,\mathbf{F}^{-\mathrm{T}}\boldsymbol{E}_R\,\mathrm{tr}\,[\,\mathbf{L}\,]+\dot{\boldsymbol{\chi}}\times\mathbf{F}\,\boldsymbol{B}_R\cdot\kappa_0\,\mathbf{F}\,\dot{\mathbf{F}}^{-1}\,\mathbf{F}^{-\mathrm{T}}\boldsymbol{E}_R\\
&\quad+\dot{\boldsymbol{\chi}}\times\mathbf{F}\,\boldsymbol{B}_R\cdot\kappa_0\,\dot{\mathbf{F}}^{-\mathrm{T}}\boldsymbol{E}_R+\dot{\boldsymbol{\chi}}\times\mathbf{F}\,\boldsymbol{B}_R\cdot\kappa_0\,\mathbf{F}^{-\mathrm{T}}\dot{\boldsymbol{E}}_R\\
&\quad+\tfrac12\,\mu_0^{-1}\,J^{-1}\,(\mathbf{F}\,\boldsymbol{B}_R)^2\,\mathrm{tr}\,[\,\mathbf{L}\,]-\mu_0^{-1}\,J^{-1}\mathbf{F}\,\boldsymbol{B}_R\cdot\dot{\mathbf{F}}\,\boldsymbol{B}_R\\
&\quad-\dot{\boldsymbol{\chi}}\times\kappa_0\,\mathbf{F}^{-\mathrm{T}}\boldsymbol{E}_R\cdot\mathbf{F}\,\dot{\boldsymbol{B}}_R\\
&\quad+\overset{\boldsymbol{\cdot}}{\overline{\tfrac12\,\kappa_0\,J\,(\mathbf{F}^{-\mathrm{T}}\boldsymbol{E}_R)^2+\tfrac12\,\mu_0^{-1}\,J^{-1}\,(\mathbf{F}\,\boldsymbol{B}_R)^2+\boldsymbol{\mathcal{E}}_R\cdot\boldsymbol{P}_R}}\;.
\end{aligned}
\tag{D.13}
$$

By means of the relation $\dot{\mathbf{F}}^{-1}=-\mathbf{F}^{-1}\dot{\mathbf{F}}\,\mathbf{F}^{-1}$,

$$
\kappa_0\,J\,\boldsymbol{E}_R\cdot\dot{\mathbf{F}}^{-1}\,\mathbf{F}^{-\mathrm{T}}\boldsymbol{E}_R=-\kappa_0\,J\,\mathbf{F}^{-\mathrm{T}}\boldsymbol{E}_R\cdot\dot{\mathbf{F}}\,\mathbf{F}^{-1}\,\mathbf{F}^{-\mathrm{T}}\boldsymbol{E}_R\;,
\tag{D.14a}
$$

and

$$
\dot{\boldsymbol{\chi}}\times\mathbf{F}\,\boldsymbol{B}_R\cdot\kappa_0\,\mathbf{F}\,\dot{\mathbf{F}}^{-1}\,\mathbf{F}^{-\mathrm{T}}\boldsymbol{E}_R=-\dot{\boldsymbol{\chi}}\times\mathbf{F}\,\boldsymbol{B}_R\cdot\kappa_0\,\dot{\mathbf{F}}\,\mathbf{F}^{-1}\,\mathbf{F}^{-\mathrm{T}}\boldsymbol{E}_R\;.
\tag{D.14b}
$$

Furthermore, Eq. (D.14a) can be re-written in the form

$$
\begin{aligned}
-\kappa_0\,J\,\mathbf{F}^{-\mathrm{T}}\boldsymbol{E}_R\cdot\dot{\mathbf{F}}\,\mathbf{F}^{-1}\,\mathbf{F}^{-\mathrm{T}}\boldsymbol{E}_R &= -\kappa_0\,J\,\mathrm{F}^{-\mathrm{T}}_{ij}\,\mathrm{E}_{Rj}\,\dot{\mathrm{F}}_{ik}\,\mathrm{F}^{-1}_{kl}\,\mathrm{F}^{-\mathrm{T}}_{lm}\,\mathrm{E}_{Rm}\\
&= -\kappa_0\,J\,\mathrm{F}^{-\mathrm{T}}_{ij}\,\mathrm{E}_{Rj}\,\mathrm{F}^{-\mathrm{T}}_{lm}\,\mathrm{E}_{Rm}\,\mathrm{F}^{-\mathrm{T}}_{lk}\,\dot{\mathrm{F}}_{ik}\\
&= -\kappa_0\,J\,\left(\mathbf{F}^{-\mathrm{T}}\boldsymbol{E}_R\otimes\mathbf{F}^{-\mathrm{T}}\boldsymbol{E}_R\right)\mathbf{F}^{-\mathrm{T}}:\dot{\mathbf{F}}\;.
\end{aligned}
\tag{D.15}
$$

Making use of vector identities, Eq. (D.14b) re-writes

$$
-\dot{\boldsymbol{\chi}}\times\mathbf{F}\,\boldsymbol{B}_R\cdot\kappa_0\,\dot{\mathbf{F}}\,\mathbf{F}^{-1}\,\mathbf{F}^{-\mathrm{T}}\boldsymbol{E}_R=\kappa_0\,\dot{\mathbf{F}}\,\mathbf{F}^{-1}\,\mathbf{F}^{-\mathrm{T}}\boldsymbol{E}_R\times\mathbf{F}\,\boldsymbol{B}_R\cdot\dot{\boldsymbol{\chi}}\;.
\tag{D.16}
$$

whereas

$$
\dot{\boldsymbol{\chi}}\times\mathbf{F}\,\boldsymbol{B}_R\cdot\kappa_0\,\mathbf{F}^{-\mathrm{T}}\boldsymbol{E}_R\,\mathrm{tr}\,[\,\mathbf{L}\,]=-\kappa_0\,\mathbf{F}^{-\mathrm{T}}\boldsymbol{E}_R\times\mathbf{F}\,\boldsymbol{B}_R\cdot\dot{\boldsymbol{\chi}}\,\mathrm{tr}\,[\,\mathbf{L}\,]\;\;.
\tag{D.17}
$$

With similar steps performed in Eq. (D.15),

$$
\begin{aligned}
-\mu_0^{-1}\,J^{-1}\,\mathbf{F}\,\boldsymbol{B}_R\cdot\dot{\mathbf{F}}\,\boldsymbol{B}_R &= -\mu_0^{-1}\,J^{-1}\,\mathrm{F}_{ij}\,\mathrm{B}_{Rj}\,\dot{\mathrm{F}}_{ik}\,\mathrm{B}_{Rk}=-\mu_0^{-1}\,J^{-1}\,\mathrm{F}_{ij}\,\mathrm{B}_{Rj}\,\dot{\mathrm{F}}_{il}\,\mathrm{F}^{-1}_{lm}\,\mathrm{F}_{mk}\,\mathrm{B}_{Rk}\\
&= -\mu_0^{-1}\,J^{-1}\,\mathrm{F}_{ij}\,\mathrm{B}_{Rj}\,\mathrm{F}_{mk}\,\mathrm{B}_{Rk}\,\mathrm{F}^{-\mathrm{T}}_{ml}\,\dot{\mathrm{F}}_{il}\\
&= -\mu_0^{-1}\,J^{-1}\,(\mathbf{F}\,\boldsymbol{B}_R\otimes\mathbf{F}\,\boldsymbol{B}_R)\,\mathbf{F}^{-\mathrm{T}}:\dot{\mathbf{F}}\;.
\end{aligned}
\tag{D.18}
$$

By entering Eq.s (D.15), (D.16), (D.17) and (D.18) into Eq. (D.13),

$$
\begin{aligned}
-\boldsymbol{\nabla}_R\cdot[\,\boldsymbol{\mathcal{E}}_R\times\boldsymbol{\mathcal{H}}_R\,] &= \boldsymbol{\mathcal{J}}_R\cdot\boldsymbol{\mathcal{E}}_R-\boldsymbol{\mathcal{M}}_R\cdot\dot{\boldsymbol{B}}_R-\boldsymbol{P}_R\cdot\dot{\boldsymbol{\mathcal{E}}}_R\\
&\quad+\Big[\tfrac12\,\kappa_0\,J\left(\mathbf{F}^{-\mathrm{T}}\boldsymbol{E}_R\right)^2+\tfrac12\,\mu_0^{-1}\,J^{-1}\,(\mathbf{F}\,\boldsymbol{B}_R)^2\\
&\quad-\,\kappa_0\,\mathbf{F}^{-\mathrm{T}}\boldsymbol{E}_R\times\mathbf{F}\,\boldsymbol{B}_R\cdot\dot{\boldsymbol{\chi}}\Big]\,\mathrm{tr}\,[\,\mathbf{L}\,]\\
&\quad-\,\Big[\kappa_0\,J\,\mathbf{F}^{-\mathrm{T}}\boldsymbol{E}_R\otimes\mathbf{F}^{-\mathrm{T}}\boldsymbol{E}_R+\mu_0^{-1}\,J^{-1}\mathbf{F}\,\boldsymbol{B}_R\otimes\mathbf{F}\,\boldsymbol{B}_R\Big]\;\mathbf{F}^{-\mathrm{T}}:\dot{\mathbf{F}}\\
&\quad+\,\kappa_0\,\dot{\mathbf{F}}\,\mathbf{F}^{-1}\,\mathbf{F}^{-\mathrm{T}}\boldsymbol{E}_R\times\mathbf{F}\,\boldsymbol{B}_R\cdot\dot{\boldsymbol{\chi}}\\
&\quad+\dot{\boldsymbol{\chi}}\times\mathbf{F}\,\boldsymbol{B}_R\cdot\kappa_0\,\dot{\mathbf{F}}^{-\mathrm{T}}\boldsymbol{E}_R+\dot{\boldsymbol{\chi}}\times\mathbf{F}\,\boldsymbol{B}_R\cdot\kappa_0\,\mathbf{F}^{-\mathrm{T}}\dot{\boldsymbol{E}}_R-\dot{\boldsymbol{\chi}}\times\kappa_0\,\mathbf{F}^{-\mathrm{T}}\boldsymbol{E}_R\cdot\mathbf{F}\,\dot{\boldsymbol{B}}_R\\
&\quad+\overset{\boldsymbol{\cdot}}{\overline{\tfrac12\,\kappa_0\,J\,(\mathbf{F}^{-\mathrm{T}}\boldsymbol{E}_R)^2+\tfrac12\,\mu_0^{-1}\,J^{-1}\,(\mathbf{F}\,\boldsymbol{B}_R)^2+\boldsymbol{\mathcal{E}}_R\cdot\boldsymbol{P}_R}}\;.
\end{aligned}
\tag{D.19}
$$

Note that the terms

$$
\begin{aligned}
\dot{\boldsymbol{\chi}}\times\mathbf{F}\,\boldsymbol{B}_R\cdot\kappa_0\,\dot{\mathbf{F}}^{-\mathrm{T}}\boldsymbol{E}_R+\dot{\boldsymbol{\chi}}\times\mathbf{F}\,\boldsymbol{B}_R\cdot\kappa_0\,\mathbf{F}^{-\mathrm{T}}\dot{\boldsymbol{E}}_R-\dot{\boldsymbol{\chi}}\times\kappa_0\,\mathbf{F}^{-\mathrm{T}}\boldsymbol{E}_R\cdot\mathbf{F}\,\dot{\boldsymbol{B}}_R&\\
=-\,\kappa_0\,\dot{\mathbf{F}}^{-\mathrm{T}}\boldsymbol{E}_R\times\mathbf{F}\,\boldsymbol{B}_R\cdot\dot{\boldsymbol{\chi}}-\mathbf{F}\,\boldsymbol{B}_R\times\kappa_0\,\mathbf{F}^{-\mathrm{T}}\dot{\boldsymbol{E}}_R\cdot\dot{\boldsymbol{\chi}}&\\
-\,\kappa_0\,\mathbf{F}^{-\mathrm{T}}\boldsymbol{E}_R\times\mathbf{F}\,\dot{\boldsymbol{B}}_R\cdot\dot{\boldsymbol{\chi}}&
\end{aligned}
$$

can be re-phrased in the form

$$= -\overset{\cdot}{\overline{\kappa_0\,\mathbf{F}^{-\mathrm{T}}\boldsymbol{E}_R \times \mathbf{F}\,\boldsymbol{B}_R \cdot \boldsymbol{\chi}}} + \kappa_0\,\mathbf{F}^{-\mathrm{T}}\boldsymbol{E}_R \times \dot{\mathbf{F}}\,\boldsymbol{B}_R \cdot \dot{\boldsymbol{\chi}} + \kappa_0\,\mathbf{F}^{-\mathrm{T}}\boldsymbol{E}_R \times \mathbf{F}\,\boldsymbol{B}_R \cdot \ddot{\boldsymbol{\chi}}\,. \tag{D.20}$$

Combination of Eq.s (D.19) and (D.20) yields

$$\begin{aligned}
-\boldsymbol{\nabla}_R \cdot [\,\boldsymbol{\mathcal{E}}_R \times \boldsymbol{\mathcal{H}}_R\,] &= \boldsymbol{\mathcal{J}}_R \cdot \boldsymbol{\mathcal{E}}_R - \boldsymbol{\mathcal{M}}_R \cdot \dot{\boldsymbol{B}}_R - \boldsymbol{P}_R \cdot \dot{\boldsymbol{\mathcal{E}}}_R + \kappa_0\,\mathbf{F}^{-\mathrm{T}}\boldsymbol{E}_R \times \mathbf{F}\,\boldsymbol{B}_R \cdot \ddot{\boldsymbol{\chi}} \\
&+ \Big[\tfrac{1}{2}\,\kappa_0\,J\,\big(\mathbf{F}^{-\mathrm{T}}\boldsymbol{E}_R\big)^2 + \tfrac{1}{2}\,\mu_0^{-1}\,J^{-1}\,(\mathbf{F}\,\boldsymbol{B}_R)^2 \\
&\quad -\kappa_0\,\mathbf{F}^{-\mathrm{T}}\boldsymbol{E}_R \times \mathbf{F}\,\boldsymbol{B}_R \cdot \dot{\boldsymbol{\chi}}\Big]\,\mathrm{tr}\,[\,\mathbf{L}\,] \\
&- \big[\kappa_0\,J\,\mathbf{F}^{-\mathrm{T}}\boldsymbol{E}_R \otimes \mathbf{F}^{-\mathrm{T}}\boldsymbol{E}_R - \mu_0^{-1}\,J^{-1}\mathbf{F}\,\boldsymbol{B}_R \otimes \mathbf{F}\,\boldsymbol{B}_R\big]\;\mathbf{F}^{-\mathrm{T}} : \dot{\mathbf{F}} \\
&+ \kappa_0\,\dot{\mathbf{F}}\,\mathbf{F}^{-1}\,\mathbf{F}^{-\mathrm{T}}\boldsymbol{E}_R \times \mathbf{F}\,\boldsymbol{B}_R \cdot \dot{\boldsymbol{\chi}} + \kappa_0\,\mathbf{F}^{-\mathrm{T}}\boldsymbol{E}_R \times \dot{\mathbf{F}}\,\boldsymbol{B}_R \cdot \dot{\boldsymbol{\chi}} \\
&+ \overset{\cdot}{\overline{\tfrac{1}{2}\,\kappa_0\,J\,(\mathbf{F}^{-\mathrm{T}}\boldsymbol{E}_R)^2 + \tfrac{1}{2}\,\mu_0^{-1}\,J^{-1}\,(\mathbf{F}\,\boldsymbol{B}_R)^2 + \boldsymbol{\mathcal{E}}_R \cdot \boldsymbol{P}_R}} \\
&\quad \overset{\cdot}{\overline{-\kappa_0\,\mathbf{F}^{-\mathrm{T}}\boldsymbol{E}_R \times \mathbf{F}\,\boldsymbol{B}_R \cdot \dot{\boldsymbol{\chi}}}}\,.
\end{aligned} \tag{D.21}$$

Consider the terms

$$-\kappa_0\,\mathbf{F}^{-\mathrm{T}}\boldsymbol{E}_R \times \mathbf{F}\,\boldsymbol{B}_R \cdot \dot{\boldsymbol{\chi}}\;\mathrm{tr}\,[\,\mathbf{L}\,] + \kappa_0\,\dot{\mathbf{F}}\,\mathbf{F}^{-1}\,\mathbf{F}^{-\mathrm{T}}\boldsymbol{E}_R \times \mathbf{F}\,\boldsymbol{B}_R \cdot \dot{\boldsymbol{\chi}} + \kappa_0\,\mathbf{F}^{-\mathrm{T}}\boldsymbol{E}_R \times \dot{\mathbf{F}}\,\boldsymbol{B}_R \cdot \dot{\boldsymbol{\chi}}\,. \tag{D.22}$$

whence, taking into account that $\mathrm{tr}\,[\,\mathbf{L}\,] = \mathbf{1} : \mathbf{L}$ and $\dot{\mathbf{F}}\,\mathbf{F}^{-1} = \mathbf{L}$,

$$\big(-\kappa_0\,\mathbf{F}^{-\mathrm{T}}\boldsymbol{E}_R \times \mathbf{F}\,\boldsymbol{B}_R \cdot \dot{\boldsymbol{\chi}}\big)\,\mathbf{1} : \mathbf{L} + \kappa_0\,\mathbf{L}\,\mathbf{F}^{-\mathrm{T}}\boldsymbol{E}_R \times \mathbf{F}\,\boldsymbol{B}_R \cdot \dot{\boldsymbol{\chi}} + \kappa_0\,\mathbf{F}^{-\mathrm{T}}\boldsymbol{E}_R \times \mathbf{L}\,\mathbf{F}\,\boldsymbol{B}_R \cdot \dot{\boldsymbol{\chi}}\,. \tag{D.23}$$

The first term of Eq. (D.23) can be re-written, according to the identity

$$(\boldsymbol{U} \times \boldsymbol{V} \cdot \boldsymbol{Z})\,\mathbf{1} = \boldsymbol{U} \times \boldsymbol{V} \otimes \boldsymbol{Z} + \boldsymbol{V} \times \boldsymbol{Z} \otimes \boldsymbol{U} + \boldsymbol{Z} \times \boldsymbol{U} \otimes \boldsymbol{V}\;, \tag{D.24}$$

for three generic vectors $\boldsymbol{U}$, $\boldsymbol{V}$ and $\boldsymbol{Z}$, as

$$\begin{aligned}
\big(-\kappa_0\,\mathbf{F}^{-\mathrm{T}}\boldsymbol{E}_R \times \mathbf{F}\,\boldsymbol{B}_R \cdot \dot{\boldsymbol{\chi}}\big)\,\mathbf{1} : \mathbf{L} = &- \kappa_0\,\mathbf{F}^{-\mathrm{T}}\boldsymbol{E}_R \times \mathbf{F}\,\boldsymbol{B}_R \otimes \dot{\boldsymbol{\chi}} : \mathbf{L} \\
&- \mathbf{F}\,\boldsymbol{B}_R \times \dot{\boldsymbol{\chi}} \otimes \kappa_0\,\mathbf{F}^{-\mathrm{T}}\boldsymbol{E}_R : \mathbf{L} \\
&- \dot{\boldsymbol{\chi}} \times \kappa_0\,\mathbf{F}^{-\mathrm{T}}\boldsymbol{E}_R \otimes \mathbf{F}\,\boldsymbol{B}_R : \mathbf{L}
\end{aligned} \tag{D.25}$$

The last two right-hand side terms of Eq. (D.25) can be cast in the form

$$\begin{aligned}
-\mathbf{F}\,\boldsymbol{B}_R \times \dot{\boldsymbol{\chi}} \otimes \kappa_0\,\mathbf{F}^{-\mathrm{T}}\boldsymbol{E}_R : \mathbf{L} &= -\epsilon_{ijk}\,\mathrm{F}_{jl}\,B_{Rl}\,\dot{\chi}_k\;\kappa_0\,\mathrm{F}^{-\mathrm{T}}_{mn}\,E_{Rn}\,\mathrm{L}_{im} \\
&= -\epsilon_{ijk}\,\mathrm{F}_{jl}\,B_{Rl}\,\dot{\chi}_k\;\kappa_0\,\mathrm{L}_{im}\,\mathrm{F}^{-\mathrm{T}}_{mn}\,E_{Rn} \\
&= -\mathbf{F}\,\boldsymbol{B}_R \times \dot{\boldsymbol{\chi}} \cdot \kappa_0\,\mathbf{L}\,\mathbf{F}^{-\mathrm{T}}\boldsymbol{E}_R = -\kappa_0\,\mathbf{L}\,\mathbf{F}^{-\mathrm{T}}\boldsymbol{E}_R \times \mathbf{F}\,\boldsymbol{B}_R \cdot \dot{\boldsymbol{\chi}}
\end{aligned} \tag{D.26a}$$

and

$$\begin{aligned}
-\dot{\boldsymbol{\chi}} \times \kappa_0\mathbf{F}^{-\mathrm{T}}\boldsymbol{E}_R \otimes \mathbf{F}\,\boldsymbol{B}_R : \mathbf{L} &= -\epsilon_{ijk}\,\dot{\chi}_j\,\kappa_0\,\mathrm{F}^{-\mathrm{T}}_{kl}E_{Rl}\,\mathrm{F}_{mn}\,B_{Rn}\,\mathrm{L}_{im} \\
&= -\epsilon_{ijk}\,\dot{\chi}_j\,\kappa_0\,\mathrm{F}^{-\mathrm{T}}_{kl}E_{Rl}\,\mathrm{L}_{im}\,\mathrm{F}_{mn}\,B_{Rn} \\
&= -\dot{\boldsymbol{\chi}} \times \kappa_0\,\mathbf{F}^{-\mathrm{T}}\boldsymbol{E}_R \cdot \mathbf{L}\,\mathbf{F}\,\boldsymbol{B}_R = -\kappa_0\,\mathbf{F}^{-\mathrm{T}}\boldsymbol{E}_R \times \mathbf{L}\,\mathbf{F}\,\boldsymbol{B}_R \cdot \dot{\boldsymbol{\chi}}\,.
\end{aligned} \tag{D.26b}$$

Combination of Eq.s (D.23), (D.25) and (D.26) reduces Eq. (D.22) to

$$-\kappa_0\,\mathbf{F}^{-\mathrm{T}}\boldsymbol{E}_R \times \mathbf{F}\,\boldsymbol{B}_R \otimes \dot{\boldsymbol{\chi}} : \mathbf{L} = -\,\big[\kappa_0\,\mathbf{F}^{-\mathrm{T}}\boldsymbol{E}_R \times \mathbf{F}\,\boldsymbol{B}_R \otimes \dot{\boldsymbol{\chi}}\big]\,\mathbf{F}^{-\mathrm{T}} : \dot{\mathbf{F}}\,. \tag{D.27}$$

whence, according to $\mathrm{tr}\,[\,\mathbf{L}\,] = \dot{\mathbf{F}} : \mathbf{F}^{-\mathrm{T}}$, allows to writes Eq. (D.21) in the final form

$$\begin{aligned}
-\boldsymbol{\nabla}_R \cdot [\,\boldsymbol{\mathcal{E}}_R \times \boldsymbol{\mathcal{H}}_R\,] &= \boldsymbol{\mathcal{J}}_R \cdot \boldsymbol{\mathcal{E}}_R - \boldsymbol{\mathcal{M}}_R \cdot \dot{\boldsymbol{B}}_R - \boldsymbol{P}_R \cdot \dot{\boldsymbol{\mathcal{E}}}_R + \kappa_0\,\mathbf{F}^{-\mathrm{T}}\boldsymbol{E}_R \times \mathbf{F}\,\boldsymbol{B}_R \cdot \ddot{\boldsymbol{\chi}} \\
&+ \Big[\tfrac{1}{2}\,\kappa_0\,J\,\big(\mathbf{F}^{-\mathrm{T}}\boldsymbol{E}_R\big)^2 + \tfrac{1}{2}\,\mu_0^{-1}\,J^{-1}\,(\mathbf{F}\,\boldsymbol{B}_R)^2 - \kappa_0\,\mathbf{F}^{-\mathrm{T}}\boldsymbol{E}_R \times \mathbf{F}\,\boldsymbol{B}_R \otimes \dot{\boldsymbol{\chi}} \\
&\quad -\,\kappa_0\,J\,\mathbf{F}^{-\mathrm{T}}\boldsymbol{E}_R \otimes \mathbf{F}^{-\mathrm{T}}\boldsymbol{E}_R - \mu_0^{-1}\,J^{-1}\mathbf{F}\,\boldsymbol{B}_R \otimes \mathbf{F}\,\boldsymbol{B}_R\Big]\;\mathbf{F}^{-\mathrm{T}} : \dot{\mathbf{F}} \\
&+ \overset{\cdot}{\overline{\tfrac{1}{2}\,\kappa_0\,J\,(\mathbf{F}^{-\mathrm{T}}\boldsymbol{E}_R)^2 + \tfrac{1}{2}\,\mu_0^{-1}\,J^{-1}\,(\mathbf{F}\,\boldsymbol{B}_R)^2 + \boldsymbol{\mathcal{E}}_R \cdot \boldsymbol{P}_R}} \\
&\quad \overset{\cdot}{\overline{-\kappa_0\,\mathbf{F}^{-\mathrm{T}}\boldsymbol{E}_R \times \mathbf{F}\,\boldsymbol{B}_R \cdot \dot{\boldsymbol{\chi}}}}\,.
\end{aligned} \tag{D.28}$$

D.3 The generalized heat equation

To derive the generalized heat equation for the problem at hand, recall the localized energy balance (7.39), the expressions of the vector identity $-\boldsymbol{\nabla}_R \cdot [\, \boldsymbol{\mathcal{E}}_R \times \boldsymbol{\mathcal{H}}_R \,]$ (7.44), the electromagnetic nominal stress $\mathbf{T}_R^{\mathcal{E}}$ (7.46), and the time derivatives of the Helmholtz free energy density (7.49) and (7.52). It holds

$$\begin{aligned} T\,\dot{\eta}_R = &-\frac{\partial \psi_R}{\partial T}\,\dot{T} - \frac{\partial \psi_R}{\partial \mathbf{F}} : \dot{\mathbf{F}} - \frac{\partial \psi_R}{\partial \boldsymbol{\mathcal{E}}_R} \cdot \dot{\boldsymbol{\mathcal{E}}}_R - \frac{\partial \psi_R}{\partial \boldsymbol{B}_R} \cdot \dot{\boldsymbol{B}}_R + \mathbf{T}_R^{\mathcal{E}} : \dot{\mathbf{F}} - \boldsymbol{\nabla}_R \cdot \big[\, \boldsymbol{q}_R \,\big] + s_{qR} + \boldsymbol{\mathcal{J}}_R \cdot \boldsymbol{\mathcal{E}}_R \\ &- \boldsymbol{\mathcal{M}}_R \cdot \dot{\boldsymbol{B}}_R - \boldsymbol{P}_R \cdot \dot{\boldsymbol{\mathcal{E}}}_R - \dot{T}\,\eta_R - \big(\rho_R\,\boldsymbol{\gamma} - \rho_R\,\dot{\boldsymbol{\chi}} - \kappa_0\,\mathbf{F}^{-\mathrm{T}}\boldsymbol{E}_R \times \mathbf{F}\,\boldsymbol{B}_R\big) \cdot \ddot{\boldsymbol{\chi}} \,. \end{aligned} \tag{D.29}$$

By means of thermodynamic restrictions (7.54), Eq. (D.29) simplifies as

$$T\,\dot{\eta}_R = -\boldsymbol{\nabla}_R \cdot \big[\, \boldsymbol{q}_R \,\big] + s_{qR} + \boldsymbol{\mathcal{J}}_R \cdot \boldsymbol{\mathcal{E}}_R \,. \tag{D.30}$$

Taking advantage from the thermodynamic prescription for the entropy (7.54a) to re-write the left-hand side term, and making use of the time derivative of the Helmholtz free energy density in view of its functional dependence (7.52), Eq. (D.30) re-writes

$$-T\,\frac{\partial^2 \psi_R}{\partial T^2}\,\dot{T} - T\,\frac{\partial^2 \psi_R}{\partial T \partial \mathbf{F}} : \dot{\mathbf{F}} - T\,\frac{\partial^2 \psi_R}{\partial T \partial \boldsymbol{\mathcal{E}}_R} \cdot \dot{\boldsymbol{\mathcal{E}}}_R - T\,\frac{\partial^2 \psi_R}{\partial T \partial \boldsymbol{B}_R} \cdot \dot{\boldsymbol{B}}_R = -\boldsymbol{\nabla}_R \cdot \big[\, \boldsymbol{q}_R \,\big] + s_{qR} + \boldsymbol{\mathcal{J}}_R \cdot \boldsymbol{\mathcal{E}}_R \,, \tag{D.31}$$

whence, the following generalized heat equations arises

$$-T\,\frac{\partial^2 \psi_R}{\partial T^2}\,\dot{T} + \boldsymbol{\nabla}_R \cdot \big[\, \boldsymbol{q}_R \,\big] = s_{qR} + \boldsymbol{\mathcal{J}}_R \cdot \boldsymbol{\mathcal{E}}_R + T\,\frac{\partial^2 \psi_R}{\partial T \partial \mathbf{F}} : \dot{\mathbf{F}} + T\,\frac{\partial^2 \psi_R}{\partial T \partial \boldsymbol{\mathcal{E}}_R} \cdot \dot{\boldsymbol{\mathcal{E}}}_R + T\,\frac{\partial^2 \psi_R}{\partial T \partial \boldsymbol{B}_R} \cdot \dot{\boldsymbol{B}}_R \,, \tag{D.32}$$

with $\boldsymbol{q}_R$ and $\boldsymbol{\mathcal{J}}_R$ constitutively specified by means of Eq.s (7.58) (eventually Eq.s (7.60)).

Chapter 8

Conclusions and outlook

Accompanied by well-defined biological motivations as backdrop, theoretical multi-physics frameworks with application in mechanobiolgy, and other research areas, have been introduced in this thesis. Conclusions for each multi-physics model are summarized hereinafter, as well as a discussion and further developments arising from the proposed thesis.

Concluding remarks. A coupled model of finite-strain continuum thermo-mechanics with mass transport and chemical reactions with trapping [10] has been proposed in Chapter 2. Interstitial motion of free diffusive species in a hosting material, and chemical reactions with trapping, have been properly coupled with finite-strain continuum mechanics and thermodynamics. An exhaustive treatment in terms of kinematics, balance equations, thermodynamics and constitutive theory has been provided. The framework extends a previous work set in the field of small strain mechanics [9] and may find application in several research areas, as discussed in Section 2.1. For the sake of generality, no particular restrictions have been applied to the model, aiming at providing a comprehensive and general multi-physics formulation. It is the case of kinematical specifications, where the deformation gradient encompasses several contributions that are not always accounted for (as for the thermal contribution), as well as the commonly performed assumption of plastic flow incompressible and irrotational that has been removed. Constitutive theory is further introduced to embrace all physics accounted for within the model.
Following [9], chemical potentials have been assumed to have both energetic and entropic contributions, leading to provide proper specifications, to define a *new* heat flux vector that encompasses a mass transport contribution, and to identify the independence of the mass flux vector upon the temperature gradient, in view of constitutive specifications. It is perhaps worth to point out that neither the energetic nor the entropic contribution to the chemical potentials are partial molar quantities.
Differently from the small strain theory, finite strain mechanics provides some modification that may require attention. Proper assumptions have to be performed with reference to the concentration saturation limit, and two paradigmatic cases have been highlighted. The resulting reaction rate of the chemical reaction that models the trapping process is affected by the assumption performed. Additionally, the stress tensor has been stated to have not only a mechanical dependence, being affected by diffusion of species by means of the configurational dependence of the saturation concentration, properly captured by the diffusive contribution to the Helmholtz free energy. The model [10] introduced in Chapter 2 has been then used, in a simplified setting, to derive some of the other formulations proposed in the thesis.

A straightforward application of [10] in the realm of mechanobiology has been presented for modeling receptor dynamics along cell membrane, cell adhesion, spreading and motility, also accounting for the formation of biopolymer structures within the cell [2]. Despite the well-defined application in mechanogiology and the aim at describing several phenomena involved at the early stages of tumor angiogenesis, the model is presented in a more general setting. Some of the equations introduced in

[10] have been properly re-phrased to model relocation and reaction of receptors along the advecting two-dimensional manifold membrane. Chemical reaction and mass action law for receptor–ligand interactions have been extended to account for the presence of an additional species, represented by ligands, which interacting with receptors generate complexes.
On the basis of well-justified biological considerations, a different assumption for the concentration saturation limit on the membrane has been performed, differently from [10]. Furthermore, the mass balance equation for ligands has been properly re-phrased on the cell membrane, with respect to its first definition on the substrate. The consideration of thermodynamic equilibrium at all times has led to fully define the problem by means of *only* the two concentrations of receptors and ligands. Relocation and reaction of actin proteins to form biopolymer structures within the bulk of the cell have been accounted for, with a similar setting to [10]. The assignment of the structural response to the bulk of the cell has led to simplified thermodynamic prescriptions and constitutive specifications for the phenomena involved on the membrane. Rather, thermo-chemo-mechanics of cells has called for more attention in terms of thermodynamic restrictions, stress-strain decompositions and constitutive specification, which have been derived following [10].
Despite some limitation highlighted within the chapter, the formulation [2] might represents a cornerstone to account for further processes that affect cell behavior in response to extracellular stimuli, encompassing the main phenomena that drive protein dynamics and cell mechanics, and providing an exhaustive discussion of the complex scenario investigated.

An insight on multi-physics computational models in mechanobiology for receptor relocation and recruitment along advecting lipid membranes has followed in Chapter 4, reproduced from [11]. Theoretical and computational approaches developed since late 1970s have been summarized. The definition of suitable diffusion laws for receptor transport on cell membrane, the theoretical evaluation of the protein diffusion coefficient, and a comprehensive analysis of the receptor–ligand kinetics have been discussed. The overview aims at providing a collection of some of the most emblematic methodologies developed to characterize receptor dynamics along cell membranes, as well as an introduction to a scientific topic that is object of great interest nowadays. Indeed, the need to identify limiting factors with significant accuracy, and to predict protein dynamics and the cell behavior, in biological processes is called as a support for biological and medical research.

Cytoskeletal biopolymers structures have been modeled by means of a statistically-based finite strain continuum mechanical formulation introduced in Chapter 5. Following [117], the microscopic behavior of polymer networks with dynamic bonds has been well-captured by defining a statistical distribution function. Continuum-scale quantities are derived as a result. It is the case of the concentration of active chains, the free energy of the polymer network, and the so-called chain distribution tensor that captures polymer deformations and re-defines the mechanical stress, the mechanical energy dissipation, and the entropy.
The model has been partially coupled with [2] to account for actin diffusion and polymerization within the cell to generate biopolymer structures. The original framework [117] has been extended to *generic* materials, therefore removing the incompressibility assumption, and re-phrased in Lagrangian formulation. Some discrepancy with respect to [117] has been highlighted and properly motivated. Despite the statistically-based continuum model may find applications in other research areas, as well as the original publication [117] is widely and successfully applied, weaknesses of the framework introduced in this thesis with respect to the aim it has been designed for have not been hidden. The necessity to overcome some limitations undoubtedly requires in-depth investigations and efforts. Among others, modifications are particularly needed in the evaluation of the variation in time of the distribution function, and in the introduction of the chain distribution tensor, as discussed in Section 5.6.

The Chan-Hilliard theory for species diffusion and phase segregation has been introduced in Chapter 6 and coupled to finite strain continuum thermo-mechanics and chemical reactions with trapping,

in a general multi-physics model. The requirement of a-priori constitutive specifications for Cahn-Hilliard equations, the *new* definition of chemical potential as variational derivative, as well as the necessity to introduce a *new* flow of energy to derive a consistent thermodynamic framework, have been widely discussed on the basis of previous publications ([55, 213], among others).
The framework introduced follows the same setting presented in [10], and provides slight extensions with respect to previous works based on the Chan-Hilliard-type theory for species diffusion, as for the consideration of chemical reaction with trapping and specification for energetic and entropic contributions to the chemical potential. The treatment has been nevertheless presented in a simplified setting, keeping the focus on the modifications that the Cahn-Hilliard theory provides to thermodynamic prescriptions and constitutive specifications. Differently from [10], no stress-strain decompositions have been performed. Beyond the aim to provide a simplified treatment, it also worth to point out that the concomitant presence of diffusive species that may be subjected to phase segregation, and immobile trapped species, may lead to ambiguities in properly attribute the swelling contribution to the deformation gradient.

Following [225], the Galilean electromagnetic theory has been re-phrased in Lagrangian formulation and fully coupled with thermodynamics and finite-strain continuum mechanics. Due to the non-trivial task of coupling among theories, no other phenomena have been accounted for, and the focus has been kept on an exhaustive treatment of Galilean electromagnetism and its coupling with finite strain thermo-mechanics.
With particular inspiration from [232], the principle of conservation of linear and angular momentum have been augmented to account for the concomitant effects of mechanical and electromagnetic surface traction and body forces. Traction relations for the Maxwell and Piola stresses have been stated as a consequence, and the definition of the total *true* stress in the material has been introduced. Additionally, by assuming the existence of a *new* velocity vector field, which differs from the material velocity due to the presence of electromagnetic effects, proper derivations of *non-standard* electro-magneto-mechanical laws have been performed. Thermodynamics has been augmented via the introduction of an electromagnetic energy flux vector, and the non-trivial derivation of the Clausius-Duhem inequality has led to define the Maxwell stress in the aether.
The framework introduced in Chapter 7 therefore represents a rigorous and comprehensive coupling between the Galilean electromagnetic theory and finite strain continuum thermo-mechanics.

Further developments. The multi-physics formulations presented in this thesis undoubtedly open new perspectives for further developments. Beyond the overview on receptor dynamics along advecting membranes presented in Chapter 4, which may nevertheless be subjected to improvements and updating in the coming years, forthcoming developments are expected for each of the proposed frameworks. Despite some of the multi-physics models introduced may appear somehow unrelated to each other, strict relations between improvements in one of them and the resulting development of another formulation can be easily identified.

Some limitations of the framework [2] introduced in Chapter 3 have been highlighted. In particular, the uncoupling between receptor dynamics along the cell membrane with the cytoskeletal activity, which in turn drives the formation of focal adhesion sites, stress fibers generation and cell contractility. The characterization of the multiscale scenario of cell viscoelasticity, and the requirement of specialization of the constitutive equation for the cytoskeletal contractile machinery, certainly call for overcoming the weaknesses of the statistically-based continuum mechanical model introduced in Chapter 5. Modifications required have been highlighted and discussed in Section 5.6, as for the necessity to couple actin diffusion and polymerization with the statistically-based description of the active polymer network, to overcome the restriction of constant concentration of active chains, and to select the more appropriate Langevin statistics for the coupling with finite strain continuum mechanics.

Despite the big picture of the necessary developments to perform appears clear, great efforts are required to carry out all modifications proposed, aiming at obtaining a comprehensive characterization of the formation and reorganization of actin biopolymer structures within the cell. This part of the thesis still remains a wide open research field. Successful developments of such framework certainly represent improvements to add to the general framework for receptor dynamics, cell adhesion, spreading and motility [2], for providing a wider characterization of cell behavior in angiogenesis-dependent diseases or, more generally, of cell response to extracellular stimuli. However, beyond the weaknesses in modeling actin biopolymer structures, a statistically-based continuum formulation has been nonetheless provided, even if not entirely concluded. With proper specifications, it might find applications in other fields, *e.g.* in permeation of a solvent in a cross-linked polymer, polyelectrolyte gels and electro-active polymers, also in view of a coupling with a *simplified* electromagnetic theory that can be easily derived from Chapter 7.

No particular extensions are expected for Chapter 6. Despite the consideration of the trapping process represents a slight novelty with respect to what introduced by other authors, the Cahn-Hilliard theory has been widely studied over the years and well coupled with thermo-mechanical formulations. However, and as previously anticipated, in view of a multiplicative decomposition of the deformation gradient to capture body deformations arising from different contributions, some ambiguities may arise and further investigations are required. Indeed, the swelling contribution of the deformation gradient is commonly associated to the trapping process, as in [9, 10], or to the segregated *phase* of species (see [55], for instance). The concomitant consideration of both trapped and segregated *phases* calls for investigations on the proper multiplicative decomposition of the deformations gradient to perform, and resulting specifications. However, it is perhaps worth to recognize that kinematical specifications are not always strictly required.

Lastly, straightforwards developments are certainly ready to be performed for the formulations introduced in Chapters 2 and 7. Despite the coupled model of transport-reaction-mechanics with trapping [10] represents a general and rather comprehensive multi-physics model, broadening of the framework by means of the electromagnetic contributions represents a forthcoming development, as specified in the introductory Section 2.1. It appears therefore evident a forthcoming coupling between the models introduced in Chapters 2 and 7. On this purpose, and in view of applications not explicitly provided but discussed in Section 2.1, the best candidate to extend [10] is represented by the electro quasi-static approximation of the electromagnetic theory. The electro quasi-static approximation can be easily derived from the theoretical coupled framework of Galilean electromagnetism with finite strain continuum thermo-mechanics introduced in Chapter 7, as well as other simplified electromagnetic theories commonly adopted, *e.g.* electrostatics and magnetostatics.
Analogously, taking advantage from [10], the framework proposed in Chapter 7 may be in turn coupled with mass transport and chemical reactions with trapping. In it, no particular difficulties are expected. The model in Chapter 7 has been introduced without the consideration of other phenomena for a better analysis of the non-trivial coupling between Galilean electromagnetism and finite strain thermo-mechanics. However, the consideration of additional phenomena appears to be straightforward, and a forthcoming framework will be devoted to provide a broader multi-physics formulation.

Bibliography

[1] M. Serpelloni, M. Arricca, V. Damioli, C. Ravelli, E. Grillo, S. Mitola, and A. Salvadori. A model of integrin and vegf receptors recruitment on endothelial cells. In B. E. Abali and I. Giorgio, editors, Developments and Novel Approaches in Biomechanics and Metamaterials, pages 163–198. Springer International Publishing, Cham, 2020.

[2] M. Serpelloni, M. Arricca, C. Bonanno, and A. Salvadori. Modeling cells spreading, motility, and receptors dynamics: a general framework. ACTA MECH SIN, 37(6):1013–1030, 2021.

[3] R. Soldi, S. Mitola, M. Strasly, P. Defilippi, G. Tarone, and F. Bussolino. Role of $\alpha_v\beta_3$ integrin in the activation of vascular endothelial growth factor receptor-2. The EMBO journal, 18(4):882–892, February 1999.

[4] C. Ravelli, S. Mitola, M. Corsini, and M. Presta. Involvement of $\alpha_v\beta_3$ integrin in gremlin-induced angiogenesis. ANGIOGENESIS, 16(1):235–43, 2013.

[5] A. Mogilner and B. Rubinstein. The physics of filopodial protrusion. BIOPHYS J, 89:782—795, 2005.

[6] V. Damioli, A. Salvadori, G. P. Beretta, C. Ravelli, and S. Mitola. Multi-physics interactions drive VEGFR2 relocation on endothelial cells. SCI REP-UK, 7(1):16700, 2017.

[7] Mattia Serpelloni. Response of endothelial cells to angiogenic stimuli: experiments, modeling and simulations. PhD thesis, University of Brescia, 2020.

[8] B. D. Coleman and W. Noll. The thermodynamics of elastic materials with heat conduction and viscosity. ARCH RATION MECH ANAL, 13(1):167–178, 1963.

[9] A. Salvadori, R. M. McMeeking, D. Grazioli, and M. Magri. A coupled model of transport-reaction-mechanics with trapping. Part I - small strain analysis. J MECH PHYS SOLIDS, 114:1–30, 2018.

[10] M. Arricca, M. Serpelloni, C. Bonanno, R. M. McMeeking, and A. Salvadori. A coupled model of transport-reaction-mechanics with trapping. Part II - Large strain analysis. 2022.

[11] M. Arricca, A. Salvadori, C. Bonanno, and M. Serpelloni. Modeling receptor motility along advecting lipid membranes. MEMBRANES, 12(7):652, 2022.

[12] G. I. Bell. Models for the specific adhesion of cells to cells. SCIENCE, 200(4342):618–627, 1978.

[13] A. Boulbitch, Z. Guttenberg, and E. Sackmann. Kinetics of membrane adhesion mediated by ligand-receptor interaction studied with a biomimetic system. BIOPHYS J, 81(5):2743–2751, 2001.

[14] L. B. Freund and Y. Lin. The role of binder mobility in spontaneous adhesive contact and implication for cell adhesion. J MECH PHYS SOLIDS, 52:2455–2472, 2004.

[15] V. B. Shenoy and L. B. Freund. Growth and shape stability of a biological membrane adhesion complex in the diffusion-mediated regime. PNAS, 102(9):3213–3218, 2005.

[16] P. Liu, Y. W. Zhang, Q. H. Cheng, and C. Lu. Simulation of the spreading of a vesicle on a substrate surface mediated by receptor-ligand binding. J MECH PHYS SOLIDS, 55(6):1166–1181, 2007.

[17] A. F. Golestaneh and B. Nadler. Modeling of cell adhesion and deformation mediated by receptor-ligand interactions. BIOMECH MODEL MECHANOBIOL, 15:371–387, 2016.

[18] M. Serpelloni, M. Arricca, C. Bonanno, and A. Salvadori. Chemo-transport-mechanics in advecting membranes. INT J ENG SCI, 181(1):103746, 2022. submitted to INT J ENG SCI.

[19] V. S. Deshpande, R. M. McMeeking, and A. G. Evans. A model for the contractility of the cytoskeleton including the effects of stress-fiber formation and dissociation. P R SOC A, 463:787–815, 2007.

[20] V. S. Deshpande, M. Mrksich, R. M. McMeeking, and A. G. Evans. A bio-mechanical model for coupling cell contractility with focal adhesion formation. J MECH PHYS SOLIDS, 56:1484–1510, 2008.

[21] R. M. McMeeking and V. S. Deshpande. A bio-chemo-mechanical model for cell contractility, adhesion, signaling, and stress-fiber remodeling. In G.A. Holzapfel and R.W. Ogden, editors, Biomechanics: Trends in Modeling and Simulation., volume 20 of Studies in Mechanobiology, Tissue Engineering and Biomaterials, pages 53–81. Springer, 2017.

[22] F. J. Vernerey and M. Farsad. A mathematical model of the coupled mechanisms of cell adhesion, contraction and spreading. J MATH BIOL, 68:989–1022, 2014.

[23] Q. H. Cheng, P. Liu, H. J. Gao, and Y. W. Zhang. A computational modeling for micropipette-manipulated cell detachment from a substrate mediated by receptor-ligand binding. J MECH PHYS SOLIDS, 57:205–220, 2009.

[24] A. Salvadori, V. Damioli, C. Ravelli, and S. Mitola. Modeling and simulation of VEGF receptors recruitment in angiogenesis. MATH PROBL ENG, 2018.

[25] A. McNabb and P.K. Foster. A new analysis of the diffusion of hydrogen in iron and ferritic steels. T METALL SOC AIME, 227:618–627, 1963.

[26] R.A. Oriani. The diffusion and trapping of hydrogen in steel. ACTA METALL MATER, 18(1):147–157, 1970.

[27] J.P. Hirth. Effects of hydrogen on the properties of iron and steel. METALL TRANS A, 11A:861–876, 1980.

[28] P. Sofronis and R.M. McMeeking. Numerical analysis of hydrogen transport near a blunting crack tip. J MECH PHYS SOLIDS, 37(317-350), 1989.

[29] A.J. Kumnick and H.H Johnson. Deep trapping states for hydrogen in deformed iron. ACTA METALL MATER, 28:33–39, 1980.

[30] A.H.M. Krom, R.W.J Koers, and A. Bakker. Hydrogen transport near a blunting crack tip. J MECH PHYS SOLIDS, 47:971–992, 1999.

[31] A.H.M. Krom and A. Bakker. Hydrogen trapping models in steel. METALL MATER TRANS B, 31B:1475–1482, 2000.

[32] J. Toribio and V. Kharin. A generalised model of hydrogen diffusion in metals with multiple trap types. PHILOS MAG, 95(31):3429–3451, 2015.

[33] Q. Zhang and R.E. White. Moving boundary model for the discharge of a $LiCoO_2$ electrode. J ELECTROCHEM SOC, 154(6):A587–A596, 2007.

[34] X.H. Liu, J.W. Wang, S. Huang, F. Fan, X. Huang, Y. Liu, S. Krylyuk, J. Yoo, S.A. Dayeh, A.V. Davydov, S.X. Mao, S.T. Picraux, S. Zhang, J. Li, T. Zhu, and J.Y. Huang. In situ atomic-scale imaging of electrochemical lithiation in silicon. NAT NANOTECHNOL, 7:749–756, 2012.

[35] M. Pharr, K. Zhao, X. Wang, Z. Suo, and J.J. Vlassak. Kinetics of initial lithiation of crystalline silicon electrodes of lithium-ion batteries. NANO LETT, 12:5039–5047, 2012.

[36] K. Zhao, M. Pharr, Q. Wan, W.L. Wang, E. Kaxiras, J.J. Vlassak, and Z. Suo. Concurrent reaction and plasticity during initial lithiation of crystalline silicon in Lithium-ion batteries. J ELECTROCHEM SOC, 159:A238–A243, 2012.

[37] M.T. McDowell, S.W. Lee, J.T. Harris, B.A. Korgel, C. Wang, W.D. Nix, and Y. Cui. In situ TEM of two-phase lithiation of amorphous silicon nanospheres. NANO LETT, 13(2):758–764, 2013.

[38] J. W. Wang, Y. He, F. Fan, X.H. Liu, S. Xia, Y. Liu, C.T. Harris, H. Li, J.Y. Huang, S.X. Mao, and T. Zhu. Two-phase electrochemical lithiation in amorphous silicon. NANO LETT, 13(2):709–715, 2013.

[39] A.D. Drozdov. Viscoplastic response of electrode particles in Li-ion batteries driven by insertion of Lithium. INT J SOLIDS STRUCT, 51:690–705, 2014.

[40] M. Ganser, F. E. Hildenbrand, M. Kamlah, and R. M. McMeeking. A finite strain electro-chemo-mechanical theory for ion transport with application to binary solid electrolytes. J MECH PHYS SOLIDS, 125:681–713, 2019.

[41] L. Cabras, D. Danilov, W. Subber, V. Oancea, and A. Salvadori. A two-mechanism and multiscale compatible approach for solid state electrolytes of (Li-ion) batteries. J ENERGY STORAGE, 48:103842, 2022.

[42] L. Cabras, M. Serpelloni, and A. Salvadori. Electro-chemo-mechanics of solid state batteries with lithium plating and stripping. FRONT MATER, page 1052617, 2022.

[43] M. Magri, B. Boz, L. Cabras, and A. Salvadori. Quantitative investigation of the influence of electrode morphology in the electro-chemo-mechanical response of li-ion batteries. ELECTROCHIM ACTA, 405:139778, 2022.

[44] A. Lucantonio, L. Teresi, and A. DeSimone. Continuum theory of swelling material surfaces with applications to thermo-responsive gel membranes and surface mass transport. J MECH PHYS SOLIDS, 89:96–109, 2016.

[45] M. Bacca and R. M. McMeeking. A viscoelastic constitutive law for hydrogels. MECCANICA, 52:3345–3355, 2017.

[46] M. Bacca, O. A. Saleh, and R. M. McMeeking. Contraction of polymer gels created by the activity of molecular motors. SOFT MATTER, 15:4467–4475, 2019.

[47] Z. Zhong, B. Qin, and J. Chen. A coupled theory for soft materials at finite strain with heat conduction, diffusion and chemical reactions. COMP MATER SCI, 188, 2021.

[48] A. Hajikhani, P. Wriggers, and M. Marino. Chemo-mechanical modelling of swelling and crosslinking reaction kinetics in alginate hydrogels: A novel theory and its numerical implementation. J MECH PHYS SOLIDS, 153, 2021.

[49] S. Narayan and L. Anand. A coupled electro-chemo-mechanical theory for polyelectrolyte gels with application to modeling their chemical stimuli-driven swelling response. J MECH PHYS SOLIDS, 159, 2022.

[50] F. Larche and J.W. Cahn. A linear theory of thermochemical equilibrium under stress. ACTA METALL MATER, 21:1051–1063, 1973.

[51] S. R. De Groot and P. Mazur. Non-Equilibrium Thermodynamics. Dover, 1984.

[52] R. DeHoff. Thermodynamic in material science. CRC Press - Taylor and Francis, 2006.

[53] M. E. Gurtin, E. Fried, and L. Anand. The Mechanics and Thermodynamics of Continua. Cambridge University Press, 2010.

[54] E. B. Tadmor, R. E. Miller, and R. S. Elliott. Continuum Mechanics and Thermodynamics: From Fundamental Concepts to Governing Equations. Cambridge University Press, 2011.

[55] L. Anand. A Cahn-Hilliard-type theory for species diffusion coupled with large elastic-plastic deformations. J MECH PHYS SOLIDS, 60(12):1983–2002, 2012.

[56] F. Larche and J.W. Cahn. Non linear theory of thermochemical equilibrium under stress. ACTA METALL MATER, 26:53–60, 1978.

[57] P. Steinmann, M. Scherer, and R. Denzer. Secret and joy of configurational mechanics: From foundations in continuum mechanics to applications in computational mechanics. Z ANGEW MATH MECH, 89(8), 2009.

[58] S. Paolucci. Continuum Mechanics and Thermodynamics of Matter. Cambridge University Press, 2016.

[59] G. Holzapfel. Nonlinear Solid Mechanics: A Continuum Approach for Engineering. John Wiley & Sons, Ltd., 2001.

[60] J.C. Simo. A framework for finite strain elastoplasticity based on maximum plastic dissipation and the multiplicative decomposition: Part I. Continuum formulation. COMPUT METHOD APPL M, 66(2):199 – 219, 1988.

[61] J.C. Simo. A framework for finite strain elastoplasticity based on maximum plastic dissipation and the multiplicative decomposition. Part II: Computational aspects. COMPUT METHOD APPL M, 68(1):1 – 31, 1988.

[62] I. Prigogine. Nobel lecture: Time, structure and fluctuations, 1977.

[63] P. Rosakis, A.J. Rosakis, G. Ravichandran, and J. Hodowany. A thermodynamic internal variable model for the partition of plastic work into heat and stored energy in metals. J MECH PHYS SOLIDS, 48:581–607, 2000.

[64] S. Shell. Thermodynamics and statistical mechanics: an integrated approach. Cambridge University Press, 2015.

[65] C. Di Leo, E. Rejovitzky, and L. Anand. A Cahn-Hilliard-type phase-field theory for species diffusion coupled with large elastic deformations: Application to phase-separating Li-ion electrode materials. J MECH PHYS SOLIDS, 70:1–29, 2014.

[66] E. Bohn, T. Eckl, M. Kamlah, and R. M. McMeeking. A model for Lithium diffusion and stress generation in an intercalation storage particle with phase change. J ELECTROCHEM SOC, 160(10):A1638–A1652, 2013.

[67] S. Doll and K. Schweizerhof. On the development of volumetric strain energy functions. ASME J APPL MECH, 67:17–21, 2000.

[68] K Bentley and S. Chakravartula. The temporal basis of angiogenesis. PHIL TRANS R SOC B, 372: 20150522, 2017.

[69] Brunhilde Felding-Habermann. Integrin adhesion receptors in tumor metastasis. CLIN EXP METASTASIS, 20(3):203–213, 2003.

[70] W. Stillwell. An Introduction to Biological Membranes: Composition, Structure and Function, chapter Chapter 17 - Moving Components Through the Cell: Membrane Trafficking, pages 369–379. Elsevier B.V., 2016.

[71] G. Huang, F. Xu, G. Genin, and T. Lu. Mechanical microenvironments of living cells: a critical frontier in mechanobiology. ACTA MECH SIN, 35(2), 2019.

[72] Z. You, L. Zhong, W. Li, C. Huang, and Y. Du. Mechanical microenvironment as a key cellular regulator in the liver. ACTA MECH SIN, 35(2):289–298, 2019.

[73] V. S. Deshpande, R. M. McMeeking, and A. G. Evans. A bio-chemo-mechanical model for cell contractility. PNAS, 103(45):17064–17065, 2006.

[74] H. Gao. Probing mechanical principles of cell–nanomaterial interactions. J MECH PHYS SOLIDS, 62:312–339, 2014.

[75] H. Gao, W. Shi, and L. B. Freund. Mechanics of receptor-mediated endocytosis. PROC NATL ACAD SCI USA, 102(27):9469–9474, 2005.

[76] T. Wiegold, S. Klinge, R. P. Gilbert, and G. A. Holzapfel. Computational modeling of adhesive contact between a virus and a cell during receptor driven endocytosis. PAMM · PROC APPL MATH MECH, 19(e201900161), 2019.

[77] A. R. Carotenuto, L. Lunghi, V. Piccolo, M. Babaei, K. Dayal, N. Pugno, M. Zingales, L. Deseri, and M. Fraldi. Mechanobiology predicts raft formations triggered by ligand-receptor activity across the cell membrane. J MECH PHYS SOLIDS, 141, 2020.

[78] F. Bubba, T. Lorenzi, and F. R. Macfarlane. From a discrete model of chemotaxis with volume-filling to a generalized patlak–keller–segel model. PROC R SOC A, 476(20190871), 2020.

[79] A. Liberman, M. Mussel, G. Kario, D. Sprinzak, and U. Nevo. Modelling cell surface dynamics and cell–cell interactions using cell studio: a three-dimensional visualization tool based on gaming technology. J R SOC INTERFACE, 16(20190264), 2019.

[80] D. Ambrosi, M. Ben Amar, C. Cyron, A. DeSimone, A. Goriely, J. Humphrey, and E. Kuhl. Growth and remodeling of living tissues: perspectives, challenges and opportunities. J R SOC INTERFACE, 16, 2019.

[81] Cynthia A. Reinhart-King, Micah Dembo, and Daniel A. Hammer. The dynamics and mechanics of endothelial cell spreading. BIOPHYS J, 89(1):676–689, jul 2005.

[82] C.E. Weatherburn. On differential invariants in geometry of surfaces, with some applications to mathematical physics. Q J PURE APPL MATH, L(3):230–296, 1925.

[83] E. Evans. New membrane concept applied to the analysis of fluid shear and micro-pipette deformed red blood cells. BIOPHYS J, 13(9):941–954, 1973.

[84] P Sens and MS Turner. Budded membrane microdomains as tension regulators. PHYS REV E, 73:031918, Mar 2006.

[85] M. Ubbink. The courtship of proteins: Understanding the encounter complex. FEBS Letters, 583:1060–1066, 2009.

[86] T. Selzer and G. Schreiber. New insights into the mechanism of protein-protein association. Proteins: Struct., Funct., Genet., 45:190–198, 2001.

[87] P. Bongrand. Ligand-receptor interactions. REP PROG PHYS, 62(921), 1999.

[88] Bruce Alberts. Molecular biology of the cell. New York : Garland Science, c2002., 4th ed. edition, 2002.

[89] C.R. Jacobs, H. Huang, and R.Y. Kwon. Introduction to Cell Mechanics and Mechanobiology. Garland Science, Taylor and Francis Group, 2013.

[90] J. F. Joanny, K. Kruse, J. Prost, and S. Ramaswamy. The actin cortex as an active wetting layer. EUR PHYS J E, 36(5), 2013.

[91] K. Kruse, J. F. Joanny, F. Jülicher, J. Prost, and K. Sekimoto. Generic theory of active polar gels: A paradigm for cytoskeletal dynamics. European Physical Journal E, 16(1):5–16, 2005.

[92] Ernest Latorre, Sohan Kale, Laura Casares, Manuel Gómez-González, Marina Uroz, Léo Valon, Roshna V. Nair, Elena Garreta, Nuria Montserrat, Aránzazu del Campo, Benoit Ladoux, Marino Arroyo, and Xavier Trepat. Active superelasticity in three-dimensional epithelia of controlled shape. Nature, 563(7730):203–208, 2018.

[93] J. Prost, F. Jülicher, and J. F. Joanny. Active gel physics. Nature Physics, 11(2):111–117, 2015.

[94] M. Rahimi and M. Arroyo. Shape dynamics, lipid hydrodynamics, and the complex viscoelasticity of bilayer membranes. PHYS REV E, 86:011932, Jul 2012.

[95] E. McEvoy, V. S. Deshpande, and P. McGarry. Free energy analysis of cell spreading. J MECH BEHAV BIOMED, 74:283–295, 2017.

[96] A. Pathak, R. M. McMeeking, A. G. Evans, and V. S. Deshpande. An analysis of the cooperative mechano-sensitive feedback between intracellular signaling, focal adhesion development, and stress fiber contractility. J APPL MECH, 78, 2011.

[97] W. Ronan, V. S. Deshpande, R. M. McMeeking, and J. P. McGarry. Numerical investigation of the active role of the actin cytoskeleton in the compression resistance of cells. J MECH BEHAV BIOMED, 14:143–157, 2012.

[98] W. Ronan, V. S. Deshpande, R. M. McMeeking, and J. P. McGarry. Cellular contractility and substrate elasticity: a numerical investigation of the actin cytoskeleton and cell adhesion. BIOMECH MODEL MECHANOBIOL, 13(417-435), 2014.

[99] A. Vigliotti, W. Ronan, F. P. T. Baaijens, and V. S. Deshpande. A thermodynamically motivated model for stress-fiber reorganization. BIOMECH MODEL MECHAN, 15:761–789, 2016.

[100] B. Gong, J. Lin, and J. Qian. Growing actin networks regulated by obstacle size and shape. ACTA MECH SIN, 33(2):222—233, 2017.

[101] G. I. Bell, M. Dembo, and P. Bongrand. Cell adhesion. competition between nonspecific repulsion and specific bonding. BIOPHYS J, 45(6):1051–1064, 1984.

[102] R Allena. Cell migration with multiple pseudopodia: Temporal and spatial sensing models. B MATH BIOL, 75(2):288–316, 2013.

[103] J.N. Israelachvili. Intermolecular and Surface Forces. Academic Press, 2011.

[104] R. Milo and R. Phillips. Cell Biology By The Numbers. Garland Science, Taylor and Francis Group, 2016.

[105] E. Schrödinger. What is Life – the Physical Aspect of the Living Cell. . Cambridge University Press, 1944.

[106] S. S. Shishvan, A. Vigliotti, and V. S. Deshpande. The homeostatic ensemble for cells. BIOMECH MODEL MECHAN, 17:1631–1662, 2018.

[107] A. Buskermolen, H. Suresh, S. Shishvan, A. Vigliotti, A. DeSimone, N. Kurniawan, C. Bouten, and V. S. Deshpande. Entropic forces drive cellular contact guidance. BIOPHYS J, 116(10):1994–2008, 2019.

[108] Y. Xia, C. Pfeifer, and D. Discher. Nuclear mechanics during constricted migration. ACTA MECH SIN, 35, 2019.

[109] S. He, X. Li, and B. Ji. Mechanical force drives the polarization and orientation of cells. ACTA MECH SIN, 35, 2019.

[110] J. Wei, X. Chen, and B. Chen. Harnessing structural instability for cell durotaxis. ACTA MECH SIN, 35, 2019.

[111] Y. Wang and J. Qian. Buckling of filamentous actin bundles in filopodial protrusion. ACTA MECH SIN, 35, 2019.

[112] S. Hervas-Raluy, J. M. Garcia-Aznar, and M. J. Gomez-Benito. Modelling actin polymerization: the effect on confined cell migration. BIOMECH MODEL MECHANOBIOL, 18(4):1177–1187, 2019.

[113] J. Chen and N. Wang. Tissue cell differentiation and multicellular evolution via cytoskeletal stiffening in mechanically stressed microenvironments. ACTA MECH SIN, 35, 2019.

[114] X. Liu, H. Yang, Y. Liu, X. Gong, and H Huang. Numerical study of clathrin-mediated endocytosis of nanoparticles by cells under tension. ACTA MECH SIN, 35, 2019.

[115] Q. Wen and P. A. Janmey. Polymer physics of the cytoskeleton. CURR OPIN SOLID ST M, 15(5):177 – 182, 2011.

[116] Elias H. Barriga and Roberto Mayor. Adjustable viscoelasticity allows for efficient collective cell migration. SEMIN CELL DEV BIOL, 93:55 – 68, 2019. SI: Viscoelasticity.

[117] F. J. Vernerey, R. Long, and R. Brighenti. A statistically-based continuum theory for polymers with transient networks. J MECH PHYS SOLIDS, 107:1–20, 2017.

[118] F. J. Vernerey. Transient response of nonlinear polymer networks: A kinetic theory. J MECH PHYS SOLIDS, 115:230 – 247, 2018.

[119] F.J. Vernerey and M. Farsad. A constrained mixture approach to mechano-sensing and force generation in contractile cells. J MECH BEHAV BIOMED, 4(8):1683–1699, 2011.

[120] O. Lieleg, K. M. Schmoller, M. M. A. E. Claessens, and A. R. Bausch. Cytoskeletal polymer networks: Viscoelastic properties are determined by the microscopic interaction potential of cross-links. BIOPHYS J, 96(11):4725–4732, 2009.

[121] E. J. Campbell and P. Bagchi. A computational model of amoeboid cell swimming. PHYS FLUIDS, 29(10):101902, 2017.

[122] E. J. Campbell and P. Bagchi. A computational study of amoeboid motility in 3d: the role of extracellular matrix geometry, cell deformability, and cell–matrix adhesion. BIOMECH MODEL MECHANOBIOL, 2020.

[123] R. M. Cooper, N. S. Wingreen, and E. C. Cox. An excitable cortex and memory model successfully predicts new pseudopod dynamics. PLoS ONE, 7(3):e33528, 2012.

[124] Z. Eidi. Discrete modeling of amoeboid locomotion and chemotaxis in dictyostelium discoideum by tracking pseudopodium growth direction. SCI REP, 7(1), 2017.

[125] C. Bächer and S. Gekle. Computational modeling of active deformable membranes embedded in three-dimensional flows. PHYS REV E, 99:062418, Jun 2019.

[126] A Moure and H. Gomez. Three-dimensional simulation of obstacle-mediated chemotaxis. BIOMECH MODEL MECHANOBIOL, 17(5):1243–1268, 2018.

[127] A Moure and H Gomez. Phase-field modeling of individual and collective cell migration. ARCH COMPUT METHOD E, 2019.

[128] C Giverso and L Preziosi. Mechanical perspective on chemotaxis. PHYS REV E, 98:062402, 2018.

[129] J. Fouchard, D. Mitrossilis, and A. Asnacios. Acto-myosin based response to stiffness and rigidity sensing. CELL ADHES MIGR, 5(1):16–19, 2011.

[130] A. Diz-Muñoz, D. A. Fletcher, and O. D. Weiner. Use the force: membrane tension as an organizer of cell shape and motility. TRENDS CELL BIOL, 23(2):47 – 53, 2013.

[131] A.V. Hill. The heat of shortening and the dynamic constants of muscle. PROC R SOC B, 126(136-195), 1938.

[132] S. De, S. Kuwahara, and A. Saito. The endocytic receptor megalin and its associated proteins in proximal tubule epithelial cells. MEMBRANES, 4:333–355, 2014.

[133] S. C. Haering, D. Tapken, S. Pahl, and M. Hollmann. Auxiliary subunits: Shepherding ampa receptors to the plasma membrane. MEMBRANES, 4:469–490, 2014.

[134] C. Bucci, P. Alifano, and L. Cogli. The role of rab proteins in neuronal cells and in the trafficking of neurotrophin receptors. MEMBRANES, 4:642–677, 2014.

[135] S. C. Klinger, P. Siupka, and M. S. Nielsen. Retromer-mediated trafficking of transmembrane receptors and transporters. MEMBRANES, 5:288–306, 2015.

[136] R. Kawaguchi, M. Zhong, M. Kassai, M. Ter-Stepanian, and H. Sun. Vitamin a transport mechanism of the multitransmembrane cell-surface receptor stra6. MEMBRANES, 5(3)(425–453), 2015.

[137] T. Azad, R. Singaravelu, M. J. F. Crupi, T. Jamieson, J. Dave, E. E. F. Brown, R. Rezaei, Z. Taha, S. Boulton, N. T. Martin, A. Surendran, J. Poutou, M. Ghahremani, K. Nouri, J. T. Whelan, J. Doung, S. Tucker, J-S Diallo, J. C. Bell, and C. S. Ilkow. Implications for sars-cov-2 vaccine design: Fusion of spike glycoprotein transmembrane domain to receptor-binding domain induces trimerization. MEMBRANES, 10(215), 2020.

[138] M. C. Klaiss-Luna and M. Manrique-Moreno. Infrared spectroscopic study of multi-component lipid systems: A closer approximation to biological membrane fluidity. MEMBRANES, 12(534), 2022.

[139] A. Aragón-Muriel, Y. Lisciano, D. Morales-Morales, D. Polo-Cerón, and J. Oñate-Garzón. A study of the interaction of a new benzimidazole schiff base with synthetic and simulated membrane models of bacterial and mammalian membranes. MEMBRANES, 11(449), 2021.

[140] E. Brémaud, C. Favard, and D. Mariaux. Deciphering the assembly of enveloped viruses using model lipid membranes. MEMBRANES, 12(441), 2022.

[141] A. Fletcher. The cell membrane and receptors. ANAESTH INTENS CARE MED, 18(6):316–320, 2017.

[142] J. Martí and C. Calero. Modeling and simulation of lipid membranes. MEMBRANES, 12(549), 2022.

[143] N. Zec, G. Mangiapia, A. C. Hendry, R. Barker, A. Koutsioubas, H. Frielinghaus, M. Campana, J. L. Ortega-Roldan, and S. Bush. Mutually beneficial combination of molecular dynamics computer simulations and scattering experiments. MEMBRANES, 11(507), 2021.

[144] N. Radhakrishnan, S. C. Kaul, R. Wadhwa, D. Sundar, and A. Hernández-Machado. Phosphatidylserine exposed lipid bilayer models for understanding cancer cell selectivity of natural compounds: A molecular dynamics simulation study. MEMBRANES, 12(64), 2022.

[145] C. Trejo-Soto, Làzaro G. R., I. Pagonabarraga, and A. Hernández-Machado. Microfluidics approach to the mechanical properties of red blood cell membrane and their effect on blood rheology. MEMBRANES, 12(217), 2022.

[146] L. Sessa, S. Concilio, P. Walde, T. Robinson, P. S. Dittrich, A. Porta, B. Panunzi, U. Caruso, and S. Piotto. Study of the interaction of a novel semi-synthetic peptide with model lipid membranes. MEMBRANES, 10(294), 2020.

[147] B. Goldstein, C. Wofsy, and G. I. Bell. Interactions of low density lipoprotein receptors with coated pits on human fibroblasts: Estimate of the forward rate constant and comparison with the diffusion limit. Proc Natl Acad Sci USA, 78(9):5695–5698, 1981.

[148] B. Goldstein, R. Griego, and C. Wofsy. Diffusion-limited forward rate constants in two dimensions. application to the trapping of cell surface receptors by coated pits. BIOPHYS J, 46(5):573–586, 1984.

[149] T. Sohail, T. Tang, and B. Nadler. Adhesive contact of a fluid-filled membrane driven by electrostatic forces. INT J SOLIDS STRUCT, 50:2678–2690, 2013.

[150] A. Vigliotti, R. M. McMeeking, and V. S. Deshpande. Simulation of the cytoskeletal response of cells on grooved or patterned substrates. J R SOC INTERFACE, 12(20141320), 2015.

[151] R. M. McMeeking and V. S. Deshpande. A bio-chemo-mechanical model for cell contractility, adhesion, signaling, and stress-fiber remodeling. In G.A. Holzapfel and R.W. Ogden, editors, Biomechanics: Trends in Modeling and Simulation, volume 20 of Studies in Mechanobiology, Tissue Engineering and Biomaterials. Springer International Pu, 2017.

[152] M. Mikucki and Y. C. Zhou. Curvature-driven molecular flow on membrane surface. SIAM J APPL MATH, 77(5):1587–1605, 2017.

[153] S. Mitola, C. Ravelli, E. Moroni, V. Salvi, D. Leali, K. Ballmer-Hofer, L. Zammataro, and M. Presta. Gremlin is a novel agonist of the major proangiogenic receptor VEGFR2. BLOOD, 116(18):3677–3680, 2010.

[154] E. Grillo, C. Ravelli, M. Corsini, K. Ballmer-Hofer, P. Oreste, G. Zoppetti, C. Tobia, R. Ronca, M. Presta, and S. Mitola. Monomeric gremlin is a novel vascular endothelial growth factor receptor-2 antagonist. ONCOTARGET, 7(23):35353 – 35368, 2016.

[155] C. Ravelli, E. Grillo, M. Corsini, D. Coltrini, M. Presta, and S. Mitola. β_3 Integrin Promotes Long-Lasting Activation and Polarization of Vascular Endothelial Growth Factor Receptor 2 by Immobilized Ligand. ARTERIOSCL THROM VAS, 35(10):2161–2171, 2015.

[156] A. Salvadori, D. Grazioli, M.G.D. Geers, D. Danilov, and P.H.L Notten. A multiscale-compatible approach in modeling ionic transport in the electrolyte of (Lithium ion) batteries. J POWER SOURCES, 293:892–911, 2015.

[157] A. Salvadori, D. Grazioli, M. Magri, M.G.D. Geers, D. Danilov, and P.H.L. Notten. On the role of saturation in modeling ionic transport in the electrolyte of (Li-ion) batteries. J POWER SOURCES, 294:696–710, 2015.

[158] C. Ravelli, S. Mitola, M. Corsini, and M. Presta. Involvement of $\alpha_v\beta_3$ integrin in gremlin-induced angiogenesis. ANGIOGENESIS, 16(1):235–243, 2013.

[159] P. Decuzzi and M. Ferrari. The receptor-mediated endocytosis of nonspherical particles. BIOPHYS J, 94(10):3790–3797, 2008.

[160] T. Wiegold, S. Klinge, R. P. Gilbert, and G. A. Holzapfel. Numerical simulation of the viral entry into a cell driven by the receptor diffusion. bioRxiv, 2019.

[161] R. C. Lee, T. R. Gowrishankar, R. M. Basch, K. K. Patel, and D. E. Golan. Cell shape-dependent rectification of surface receptor transport in a sinusoidal electric field. BIOPHYS J, 64:44–57, 1993.

[162] F. Mac Gabhann and A. S. Popel. Model of competitive binding of vascular endothelial growth factor and placental growth factor to VEGF receptors on endothelial cells. AM J PHYSIOL HEART CIRC PHYSIOL, 286:H153–H164, 2004.

[163] R. J. Filion and A. S. Popel. A reaction-diffusion model of basic fibroblast growth factor interactions with cell surface receptors. ANN BIOMED ENG, 32(5):645–663, 2004.

[164] C. Rattanakul, Y. Lenbury, J. Bell, V. Chatsudthipong, W. Triampo, and P. S. Crooke. Spatial turing-type pattern formation in a model of signal transduction involving membrane-based receptors coupled by g proteins. CANCER INFORM, 2:329–343, 2006.

[165] B. A. Earnshaw and P. C. Bressloff. Biophysical model of ampa receptor trafficking and its regulation during long-term potentiation/long-term depression. J NEUROSCI, 26(47):12362–12373, 2006.

[166] B. A. Earnshaw and P. C. Bressloff. Modeling the role of lateral membrane diffusion in ampa receptor trafficking along spiny dendrite. J COMPUT NEUROSCI, 25:366–389, 2008.

[167] D. R. Daniels. Receptor-ligand diffusion-limited reaction rates on curved membranes. CHEM PHYS LETT, 795, 2022.

[168] A. Kusumi, Y. Sako, and M. Yamamoto. Confined lateral diffusion of membrane receptors as studied by single particle tracking (nanovid microscopy). effects of calcium-induced differentiation in cultured epithelial cells. BIOPHYS J, 65:2021–2040, 1993.

[169] K. Ritchie, X-Y. Shan, J. Kondo, K. Iwasawa, T. Fujiwara, and A. Kusumi. Detection of non-brownian diffusion in the cell membrane in single molecule tracking. BIOPHYS J, 88:2266–2277, 2005.

[170] E. Atilgan and X. C. Sun. Shape transitions in lipid membranes and protein mediated vesicle fusion and fission. J CHEM PHYS, 16(095102), 2007.

[171] S. J. Briddon, J. Gandía, O. B. Amaral, S. Ferré, C. Lluís, R. Franco, S. J. Hill, and F. Ciruela. Plasma membrane diffusion of g protein-coupled receptor oligomers. BIOCHIM BIOPHYS ACTA, 1783:2262–2268, 2008.

[172] M. J. Paszek, D. Boettiger, V. M. Weaver, and D. A. Hammer. Integrin clustering is driven by mechanical resistance from the glycocalyx and the substrate. PLOS COMPUT BIO, 5(12), 2009.

[173] T. Duke and I. Graham. Equilibrium mechanisms of receptor clustering. PROG BIOPHYS MOL BIO, 100:18–24, 2009.

[174] J. F. Allard, O. Dushek, K. Coombs, and P. A. van der Merwe. Mechanical modulation of receptor-ligand interactions at cell-cell interface. BIOPHYS J, 102:1265–1273, 2012.

[175] D. Iron and J. Rumsey. A model of surface receptor aggregation. J MATH BIOL, 75:705–731, 2017.

[176] L. Martini, S. Brameyer, E. Hoyer, K. Jung, and U. Gerland. Dynamics of chromosomal target search by a membrane-integrated one-component receptor. PLOS COMPUT BIO, 17(2), 2021.

[177] B. J. Dubin-Thaler, G. Giannone, H-G. Döbereiner, and M. P. Sheetz. Nanometer analysis of cell spreading on matrix-coated surfaces reveals two distinct cell states and steps. BIOPHYS J, 86:1794–1806, 2004.

[178] C. A. Reinhart-King, M. Dembo, and D. A. Hammer. The dynamics and mechanics of endothelial cell spreading. BIOPHYS J, 89:676–689, 2005.

[179] P. G. Saffman and M. Delbrück. Brownian motion in biological membranes. PNAS, 72(8):3111–3113, 1975.

[180] E. Reister and U. Seifert. Lateral diffusion of a protein on a fluctuating membrane. EPL, 71(5):859–865, sep 2005.

[181] S.M. Leitenberger, E. Reister-Gottfried, and U. Seifert. Curvature coupling dependence of membrane protein diffusion coefficients. LANGMUIR, 24(4):1254–1261, 2008.

[182] E. Reister-Gottfried, S. M. Leitenberger, and U. Seifert. Diffusing proteins on a fluctuating membrane: Analytical theory and simulations. PHYS REV E, 81:031903, Mar 2010.

[183] Y. Gambin, R. Lopez-Esparza, M. Reffay, E. Sierecki, N. S. Gov, M. Genest, R. S. Hodges, and W. Urbach. Lateral mobility of proteins in liquid membranes revisited. PNAS, 103(7):2098–2102, 2006.

[184] Y. Gambin, M. Reffay, E. Sierecki, F. Homblé, R. S. Hodges, N. S. Gov, N. Taulier, and W. Urbach. Variation of the lateral mobility of transmembrane peptides with hydrophobic mismatch. J PHYS CHEM B, 144(10):3559–3566, 2010.

[185] P. G. Saffman. Brownian motion in thin sheets of viscous fluid. J FLUID MECH, 73:593–602, 1975.

[186] N. Oppenheimer and H. Diamant. Correlated diffusion of membrane proteins and their effect on membrane viscosity. BIOPHYS J, 96:3041–3049, 2009.

[187] N. Oppenheimer and H. Diamant. In-plane dynamics of membranes with immobile inclusions. PHYS REV LETT, 107, 2011.

[188] B. A. Camley and F. L. H. Brown. Contributions to membrane-embedded-protein diffusion beyond hydrodynamic theories. PHYS REV E, 85, 2012.

[189] B. A. Camley and F. L. H. Brown. Diffusion of complex objects embedded in free and supported lipid bilayer membranes: role of shape anisotropy and leaflet structure. SOFT MATTER, 9:4767–4779, 2013.

[190] B. A. Camley, M. G. Lerner, R. W. Pastor, and F. L. H. Brown. Strong influence of periodic boundary conditions on lateral diffusion in lipid bilayer membranes. J CHEM PHYS, 143, 2015.

[191] R. M. Venable, H. I. Ingólfsson, M. G. Lerner, B. S. Perrin Jr., B. A. Camley, S. J. Marrink, F. L. H. Brown, and R. W. Pastor. Lipid and peptide diffusion in bilayers: the saffman-delbrück model and periodic boundary conditions. J PHYS CHEM B, 121(15):3443–3457, 2017.

[192] S. Ramadurai, A. Holt, V. Krasnikov, G. van den Bogaart, J. A. Killian, and B. Poolman. Lateral diffusion of membrane proteins. J AM CHEM SOC, 131(35):12650–12656, 2009.

[193] S. Ramadurai, A. Holt, L. V. Schäfer, V. V. Krasnikov, D. T. S. Rijkers, S. J. Marrink, J. A. Killian, and B. Poolman. Influence of hydrophobic mismatch and amino acid composition on the lateral diffusion of transmembrane peptides. BIOPHYS J, 99:1447–1454, 2010.

[194] M. W. Lee, N. W. Schmidt, and G. C. L. Wong. Mechanisms of membrane curvature generation by peptides and proteins: A unified perspective on antimicrobial peptides. In Safinya C. R. and J. O. Rädler, editors, Handbook of Lipid Membranes, volume 1. CRC Press, 2021.

[195] M. W. Lee, M. Han, G. V. Bossa, C. Snell, Z. Song, H. Tang, L. Yin, J. Cheng, S. May, E. Luijten, and G. C. L. Wong. Interactions between membranes and "metaphilic" polypeptide architectures with diverse side-chain populations. ACS NANO, 11:2858–2871, 2017.

[196] A. Callan-Jones, M. Durand, and J-B. Fournier. Hydrodynamics of bilayer membranes with diffusing transmembrane proteins. SOFT MATTER, 12:1791–1800, 2016.

[197] R. Worch, Z. Petrášek, P. Schwille, and T. Weidemann. Diffusion of single-pass transmembrane receptors: From the plasma membrane into giant liposomes. J MEMBRANE BIOL, 250:393–406, 2017.

[198] J. R. Houser, D. J. Busch, D. Bell, B. Li, P. Ren, and J. C. Stachowlak. The impact of physiological crowding on the diffusivity of membrane bound proteins. SOFT MATTER, 12(7):2127–2134, 2016.

[199] A. Naji, A. J. Levine, and P. A. Pincus. Corrections to the saffman-delbrück mobility for membrane bound proteins. BIOPHYS J, 2007.

[200] E. Evans. Detailed mechanic of membrane-membrane adhesion and separation. I. Continuum of molecular cross-bridges. BIOPHYS J, 48:175–183, 1985.

[201] M. Dembo, D. Torney, K. Saxman, and D. A. Hammer. The reaction-limited kinetics of membrane-to-surface adhesion and detachment. PROC R SOC LONDON B, 234(55–83), 1988.

[202] J. Stricker, T. Falzone, and M Gardel. Mechanics of the F-actin Cytoskeleton. J Biomech., 43(1):1–12, 2010.

[203] M. Rubinstein and R. H. Colby. Polymer Physics. Oxford University Press, 2003.

[204] R. Brighenti, A. Menzel, and F. J. Vernerey. A physics-based micromechanical model for electroactive viscoelastic polymers. J INTELL MATER SYST STRUCT, 29(14):2902—2918, 2018.

[205] T. Shen, R. Long, and F. J. Vernerey. Computational modeling of the large deformation and flow of viscoelastic polymers. COMPUT MECH, 63:725—745, 2019.

[206] T. Shen and F. J. Vernerey. Rate-dependent fracture of transient networks. J MECH PHYS SOLIDS, 143, 2020.

[207] S. L. Sridhar and F. J. Vernerey. Mechanics of transiently cross-linked nematic networks. J MECH PHYS SOLIDS, 141, 2020.

[208] J. W. Cahn and J. E. Hilliard. Free energy of a nonuniform system. I. interfacial free energy. J CHEM PHYS, 28:258–267, 1958.

[209] J. W. Cahn. On spinoidal decomposition. ACTA METALLURGICA, 9:798–801, 1961.

[210] V. P. Skripov and A. V. Skripov. Spinodal decomposition (phase transitions via unstable states). SOV PHYS USP, 22(389), 1979.

[211] F. C. Larché and J. W. Cahn. The interactions of composition and stress in crystalline solids. J RES NAT BUR STAND, 89(6):467–500, 1984.

[212] Blowey J. F. and Elliot C. M. The Cahn-Hilliard gradient theory for phase separation with non-smooth free energy Part I: Mathematical analysis. EUR J APPL MATH, 2:233–279, 1991.

[213] M. E. Gurtin. On a nonequilibrium thermodynamics of capillarity and phase. QUART APPL MATH, XLVII(1):129–145, 1989.

[214] M. E. Gurtin. Generalized Ginzburg-Landau and Cahn-Hilliard equations based on a microforce balance. PHYSICA D, 92:178–192, 1996.

[215] A. Miranville. Consistent models of Cahn-Hilliard-Gurtin equations with Neumann boundary conditions. PHYSICA D, 158:233–257, 2001.

[216] P. Podio-Guidugli. Models of phase segregation and diffusion of atomic species on a lattice. RICERCHE MAT, 55:105–118, 2006.

[217] A. Morro. Phase-field model for fluid mixtures. MATH COMPUT MODEL, 45(1042–1052), 2007.

[218] F. P. Duda, A. F. Sarmiento, and E. Fried. Coupled diffusion and phase transition: Phase fields, constraints, and the Cahn–Hilliard equation. MECCANICA, 56:1707—1725, 2021.

[219] L. Q. Chen. Phase-field models for microstructure evolution. ANNU REV MATER RES, 32:113–140, 2002.

[220] P. Germain. The method of virtual power in continuum mechanics. Part 2: microstructure. SIAM J APPL MATH, 25:556–575, 1973.

[221] M. E. Gurtin. A gradient theory of single-crystal viscoplasticity that accounts for geometrically necessary dislocations. J MECH PHYS SOLIDS, 50:5–32, 2002.

[222] A. Miranville. Some generalizations of the Cahn-Hilliard equation. ASYMPTOTIC ANALYSIS, 22:235–259, 2000.

[223] A. Bonfoh and A. Miranville. On Cahn-Hilliard-Gurtin equations. NONLINEAR ANALYSIS, 47, 2001.

[224] A. Miranville. Long time behavior of models of Cahn-Hilliard equations in deformable continua. NONLINEAR ANALYSIS SER B, 2(3):273–304, 2001.

[225] A. Kovetz. Electromagnetic Theory. Oxford University Press, 2000.

[226] M. Le Bellac and J. M. Lévy-Leblond. Galilean electromagnetism. IL NUOVO CIMENTO, 14 B(2):217–233, 1973.

[227] E. S. Santos, M. de Montigny, F. C. Khanna, and A. E. Santana. Galilean covariant Lagrangian models. J PHYS A-MATH THEOR, 37(41):9771–9789, 2004.

[228] G. Rousseaux. Lorenz or Coulomb in Galilean electromagnetism? EUROPHYS LETT, 71(1):15–20, 2005.

[229] M. de Montigny and G. Rousseaux. On some applications of Galilean electrodynamics of moving bodies. AM J PHYS, 75(11):984–992, 2007.

[230] J. A. Heras. The Galilean limits of Maxwell's equations. AM J PHYS, 78(10):1048–1055, 2010.

[231] G. Rousseaux. Forty years of Galilean electromagnetism (1973–2013). EUR PHYS J PLUS, 128(81):1–14, 2013.

[232] R. M. McMeeking and C. M. Landis. Electrostatic forces and stored energy for deformable dielectric materials. J APPL MECH-T ASME, 72(4):581–590, 2005.

[233] R. M. McMeeking, C. M. Landis, and S. M. A. Jimenez. A principle of virtual work for combined electrostatic and mechanical loading of materials. INT J NON-LINEAR MECH, 42(6):831–838, 2007.

[234] R.A. Toupin. The elastic dielectric. J RATION MECH ANAL, 5(6):849–915, 1956.

[235] L. D. Landau and E. M. Lifshitz. Electrodynamics of Continuous Media. Pergamon, Oxford, 1960.

[236] A. C. Eringen. On the fundations of electroelastostatics. INT J ENG SCI, 1(1):127–153, 1963.

[237] Y. H. Pao. Electromagnetic forces in deformable continua. In S. NEMAT-NASSER, editor, Mechanics today, volume 4, pages 209–305. Pergamon, 1978.

[238] G. A. Maugin. Continuum Mechanics of Electromagnetic Solids. North-Holland Series in Applied Mathematics and Mechanics. Elsevier Science Ltd, 1988.

[239] Tiersten H. F. A Development of the Equations of Electromagnetism in Material Continua. Springer, 1990.

[240] A. Dorfmann and R. W. Ogden. Nonlinear magnetoelastic deformations. Q J MECH APPL MATH, 57(4):599–622, 11 2004.

[241] A. Dorfmann and R. W. Ogden. Nonlinear magnetoelastic defiormations of elastomers. ACTA MECH, 167:13–28, 2004.

[242] A. Dorfmann and R. W. Ogden. Magnetoelastic modelling of elastomers. EUR J MECH A-SOLID, 22(4):497–507, 2003.

[243] A. Dorfmann and R. W. Ogden. Nonlinear electroelasticity. ACTA MECH, 174:167–183, 2005.

[244] R. M. McMeeking. A Maxwell stress for material interactions. J COLLOID INTERF SCI, 199(2):187–196, 1998.

[245] C. Argento, A. Jagota, and W. C. Carter. Surface formulation for molecular interactions of macroscopic bodies. J MECH PHYS SOLIDS, 45(7):1161–1183, 1997.